Factors Governing Tin Whisker Growth

by

Erika R. Crandall

A dissertation submitted to the Graduate Faculty of
Auburn University
in partial fulfillment of the
requirements for the Degree of
Doctor of Philosophy

Auburn, Alabama

August 4, 2012

Keywords: tin whiskers, mitigation, prevention, lead-free, Pb-free, reliability

Approved by

Chair: Michael Bozack, Professor of Physics
Minseo Park, Associate Professor of Physics
John Williams, Professor Emeritus of Physics
George Flowers, Professor of Mechanical Engineering

Abstract

Tin (Sn) whiskers are electrically conductive, single crystal eruptions that can grow from surfaces where tin is deposited on a substrate surface. They present reliability problems for the electronics industry due to the formation of stable, bridging shorts in low voltage, high impedance circuits. Due to legislation in the EU, Japan, and the U.S. which mandates a gradual shift from lead (Pb)-based to lead-free solders and board finishes, there has been a re-emergence of Sn whiskers. Continuing reports of Sn whisker induced failures coupled with the lack of an industry-accepted understanding of tin whisker growth and/or test methods to identify whisker-prone products has made blanket acceptance of pure tin plating a risky proposition in high reliability systems.

This research is designed to clarify and control the mechanisms that govern whisker formation. An ultimate objective is to discover how to impede and/or prevent whisker growth, either by surface coatings or by modifications of the thin film properties. While tin whisker growth is believed to be largely mechanical, there is currently no general agreement on the mechanism governing the growth of tin whiskers. In whiskering, multiple material and processing variables interact to create whiskers which makes it difficult to produce effective mitigation schemes and develop a comprehensive picture of whisker growth. While there are some commonly accepted factors that impact whisker growth (residual stress, externally-imposed stress, intermetallic formation, Sn diffusion, scratches, corrosion, CTE mismatches, etc.), controlled laboratory experiments demonstrating which ones are most important are

lacking. Further, many previous investigations of whiskers involve electroplated thin film systems on brass or copper which, although complying with industry practice, introduce several uncontrolled variables into the whiskering event. A more optimum model system to study whiskering is needed. A final motivation for this work is the existence of considerable "common lore" in the whisker community that is contradicted by recent experiments in several laboratories (including ours). Tightly designed and controlled experiments whose goal is to generate a broad experimental whisker database is necessary to aid evolving mechanistic and theoretical efforts that describe whiskering.

Progress has recently been made by use of high-performance analytical tools such as focused ion beam (FIB) microscopy and EBDP (electron backscatter diffraction), which allows for whisker morphology and whisker root/grain orientation examinations respectively. However, considerably more fundamental work is needed to develop a detailed understanding of the physical, chemical, and materials mechanisms leading to initiation and growth of tin whiskers and to reduce and/or eliminate it in Pb-free electronic components. This thesis seeks to clarify some of the key questions by studying several important factors involved with whisker incubation and growth.

Our work takes several novel approaches to the whisker problem: 1) We focus on a limited set of focused research objectives using "laboratory" created whiskers, as opposed to archival, industrial, and/or anecdotal specimens; 2) We use a reproducible method of growing whiskers in a reasonable (weeks) time by using magnetron sputtering techniques rather than electrochemical deposition; 3) We produce tailor-made films with known "dialed-in" degrees of intrinsic thin film stress (tensile, none, compressive) to investigate the role of net film stress; 4) We eliminate the role of interfacial stress by growing whiskers on substrates that do not form

intermetallic compounds with Sn; 5) We examine whisker growth in near-real time using field-enhanced, high current density methods that grow whiskers in hours rather than weeks and months; 6) We study whisker growth from considerably thinner (submicron) films than most other researchers, which has enabled us to observe the uniform depletion of the Sn feedstock during whisker growth, which provides further evidence for the importance of long-range Sn diffusion during whisker growth; 7) We address the question of whisker prevention by studying why certain topside metal films (Ni, Pt) appear to prevent whisker growth while others (Cu, Pb) do not. Special attention has been devoted to measurements of whiskering under a variety of rigorously controlled environmental factors such as substrate roughness, gas environment, and humidity, which are known to play a significant role in whisker production. Generally, we find that whisker densities are higher for smoother substrates (such as semiconductors) and, by using accurate humidity exposures (generated by calibrated vapor pressure solutions), we show that Sn whiskers favor relative humidity values ~ 85%. Generating whisker growth from films which contain no native and/or surface oxides (such as Au) shows that a surface Sn oxide layer is not a necessary requisite for whisker production. Sluggish whisker growth from small, micron-dimensional patterned Sn deposits implies that large lateral films of tin are optimum for whisker growth.

Ideally, it is desirable to mitigate and/or prevent whisker growth failures before they occur. We show that whisker prevention is possible by a variety of impenetrable topside hard metal films, which prevent Sn whiskers from penetrating through the capping barriers. In particular, Ni (700 Å or thicker) was found to successfully block all Sn whiskers for time periods of greater than one year. Pt films (325-1360 Å) also appear to be successful, preventing whisker penetration for over three months. In contrast, Au (875-3000 Å) and Cr (250-1400 Å) cap films

are penetrated by Sn whiskers within a couple of months. Penetrating whiskers have been observed to carry up a fractured piece of the metal cap layer during the puncture process, which helps explain why only certain metal caps block whiskers while others do not. Cap metals with high shear moduli are likely to block whiskers since cap penetration appears to be a metal punching process. Shear modulus values for the pure elemental cap films approximately follows the trend for whisker prevention by metals, with the exception of Cr, which oxidizes considerably during thin film formation. The true situation is more complex than this simple mechanical picture, however, owing to the formation of intermetallic compounds and/or diffusion between the Sn and cap film layers.

In memory of one of the greatest role models,
Steve Irwin

"*I have no fear of losing my life - if I have to save a koala or a crocodile or a kangaroo or a snake, mate, I will save it.*"

-Steve Irwin

"All we have to decide is what to do with the time that is given to us."

-Gandalf

Acknowledgements

There is really no measure of thanks adequate to express how grateful I am for all of those who have painstakingly guided, supported and encouraged me throughout my doctoral work. Nevertheless, I would like to try to say a few words.

First, I thank my advisor, Dr. Michael Bozack, for taking me on as a research assistant. All of the many great tips and tools of knowledge I have gained will stick with me forever. I thank him for all the research experienced I've accumulated over the years. Having the opportunity to work under Dr. Bozack taught me to become an independent researcher, excellent multitasker, a project leader, great outsourcer, and probably most of all, how to practice the ever simple, but impossible to follow saying: " do not let things get to you that you cannot control".

I must also thank the faculty and industrial members of AU/NSF Center for Advanced Vehicle and Extreme Environment Electronics ($CAVE^3$) for financial support of my research throughout the years. An extended thanks goes out to Dr. George Flowers, who always helped and supported me and my work, from small pep talks before $CAVE^3$ review presentations to large contributions such as conference attendance and future paths.

A special thanks to Auburn University faculty and staff who have taught, trained, and helped me through my work. I couldn't be more grateful and appreciative for the pleasure of working with Tami Isaacs-Smith. She is one of the hardest working, busiest people I know, yet always provided endless help, insightful counsel, along with her genius tips and suggestions, which really made the world of difference (weather she realized it or not). I also had the

pleasure of working with Dr. Michael Miller, who always brought his wonderful personality with him to work and was always more than willing to help in any situation. Along the years I received generous help and support from Dr. Robert Jackson, Dr. John Williams, and Dr. Minseo Park, and thank them for sharing their immense knowledge. I would also like to thank Max Cichon and Dr. Claude for always putting up with all my questions along the way and assisting me no matter how small the task.

Extraordinary thanks to the two people who influenced me the most throughout my life must be, of course, my parents, Roland and Jana. They instilled in me the qualities that got me where I am today, and continually support me no matter where my foolish ambition leads me. I thank them for their genuine interest in my research, being more than happy to sit and listen to me talk about my work for as long as I needed, though understanding barley any of it. They have always encouraged me through every step of the way, and I could not ask for better parents.

Last but not least, I want thank the kindness person I have ever met and the love of my life, Dr. Joshua Williams. I couldn't be more thankful and grateful for his presence along my concluding endeavors. No matter how silly, trivial and insignificant my inquiries, he set aside all else, considerately providing honest advice, along with teaching and sharing all tidbits of knowledge possible to help. He has been the most encouraging, supporting and motivating individual throughout everything and continues to be. There is no amount of thanks commendable when it comes to Joshua, I am forever indebted.

Table of Contents

List of Tables

List of Figures

CHAPTER 1

WHISKERS AND THEIR ROLE IN COMPONENT RELIABILITY

"*Quantum Physics means anything can happen at any time for no reason.*"
- Professor Hubert Farnsworth

1.1 What Are Whiskers?

Metallic whisker formation first arose as a component reliability issue as early as the 1940's. A metallic whisker is a single crystal filamentary eruption from a metal surface. Multiple single crystalline filaments can join together and form a single whisker. Most high-aspect whiskers are cylindrical in shape with average diameters about a micron with lengths up to several millimeters. Whiskers are usually generated on thin metal films (0.5 to tens of microns) which have been deposited on a substrate material, though whiskers have also been observed infrequently to grow from bulk materials. Whiskers can be straight, kinked, or even curved. Metallic film deposits can also have other types of eruptions that are quite different in appearance from the high aspect ratio whisker eruptions. These are commonly referred to as flowers, extrusions, hillocks and volcanoes. Generally, they are of lower academic interest when compared to the longer, high aspect ratio whiskers this thesis addresses.

Most of the work presented here will focus on Sn whiskers, since they are the dominant whiskering problem for electronic components today. Sn, however, is not the only existing whisker-forming material, for cadmium, zinc, indium, aluminum, gold, lead, and silver have also been observed to produce whiskers.

1.2 History of Whiskering

Metallic whisker formation first became a problem and a subject of interest as early as the 1940s, right after World War II. Electroplated cadmium was the first to grow whiskers long enough to short out adjacent capacitor plates in electronic components, first reported by Cobb in 1946 [1]. In 1948, Bell Telephone Corporation experienced failures on channel filters used to maintain frequency bands in multi-channel telephone transmission lines. Failure analysis quickly showed that Cd whisker formation was the root cause of the channel-filter failures. Bell Laboratories then initiated a series of long-term investigations into the general topic of whisker formation, which was first reported in 1951 by Compton et al. [2]. The research established that whisker formation occurred spontaneously, but not only on Cd electroplating. Whisker growth was also found on electroplated zinc, Sn, silver and even on Al casting alloy. The Compton et al. paper provided the first summary statements that would be used as a guide to future whisker research. The conclusion was that whisker growth is not limited to electrodeposited coatings and may also be found on solid metals. Much of the research since the 1951 Compton paper has focused on electroplated Sn and Sn-alloys on various substrates, since Sn and Sn-alloy electroplating became the plating of choice for electronic components due to the favorable combination of contact resistance, corrosion resistance, low cost, and solderability.

In 1959, Arnold published a paper [3] detailing the beneficial whisker mitigation effect observed when alloying Sn plating with Pb. He noted that, while Sn-Pb alloys will whisker if subjected to high compressive stresses (a conclusion we have also found), it is rare otherwise. After his article, the predominant mitigation strategy for Sn plating in the

US electronics industry for the next 50 years became the co-deposition of Pb into the Sn electroplating process. A few years later (1964) this result was reinforced by Pitt and Henning [4], who observed whisker growth due to clamped-pressure environments on hot-dipped Sn and 50%Sn-50%Pb deposited on copper (Cu) and steel substrates. The observed whisker densities decreased with increasing Pb content.

In 1974, a review article [5] was published by Britton of the Tin Research Institute (now known as the International Tin Research Institute (ITRI) Ltd.) in collaboration with Bell Labs, which stated that Sn-Pb deposits at least 8µm thick (either matte or bright) are probably safe and suitable for most purposes where whisker growth may be a hazard. It claimed that a Pb content of 1% is sufficiently effective to prevent whiskers but better to select a Sn-Pb process with a larger developed Pb content, which again supported Sn-Pb alloy as the recommended alloy of choice.

In 1975-1976, a set of publications by Dunn [6], [7] of the European Space Agency strongly recommended that surfaces which are prone to stress-induced whisker growth (such as Sn, Cd, and Zn) be excluded from spacecraft design. The alternative finish suggested, of course, was a Sn-Pb alloy of 60Sn/40Pb. Dunn was the first to suggest that pure Sn plating should not be used for critical applications, such as spacecraft. However, no mandated or regulatory position was taken relative to Dunn's recommendations, which proved to be very unfortunate in future years, as several significant reliability failures occurred in US Air Force equipment which were attributed to Sn whiskers.

In 1986, Nordwall and Capitano el al. [8], [9] discussed the US military's first experience with whiskers growing from Sn-plated hybrid circuits. The whiskers were

breaking off, falling into active circuitry and causing intermittent operation. The USAF discovered the problem while screening 12 yr old failed radar systems. Analysis showed numerous bridging whiskers (up to 2.5 mm long, some of the longest whiskers observed in electronic circuits) which had shorted out the circuitry. A few years later, in 1989, Corbid [10] of Hi Rel Laboratories examined the use of Sn in miniature electronic packages. He claimed that reflowing did not prevent whisker formation as previously noted in earlier studies on assembled circuits. The question of whether reflowing (melting solder during circuit assembly) helps to prevent whiskers remains a research topic and is still debated today.

In 1990, Cunningham and Donahue [11] of the Raytheon Company presented a paper at the SAMPE Conference on Sn whiskers, which compared whisker growth from Sn and Sn-Pb alloy films subjected to mechanical stresses at elevated temperatures. The results showed that the process which produced the fewest whiskers was 60/40 Sn/Pb with reflow, which again, combined an elevated temperature with Pb-containing Sn. The first published paper from a connector company that dealt with reliability problems involving Sn whiskers was a 1993 work by Diehl [12] from Burndy Connector Corporation. Diehl also concluded that the addition of Pb was necessary to insure that Sn electroplating would not produce whiskers. His directive was subsequently adopted by all of Burndy Corporation's Sn plated connector products.

In 1999, whisker problems arose in ultrafine pitch circuits, reported by Ishii et al. [13]. The ultrafine circuits referred to a pitch of 50 μm, corresponding to a lead-frame spacing with gaps of 20 μm or less between adjacent leads. The pure Sn lead-frames

were experiencing a high incidence of shorting due to whiskers (the problem was reported to be mitigated by annealing at 150^{o}C for 2 hrs).

At the beginning of the 21st century, General Electric [14] issued a service bulletin stating that whisker problems had been found on certain GD relays in field service for over 10 years. The recommended corrective action was to brush off and vacuum up the removed whiskers. Around the same time (2001), in a different case study, Stevens [15] of the Foxboro Company reported whisker-induced relay failures (used in nuclear facilities). After eight years in service the relays failed due to Sn whiskers. The relay finishes where originally Sn-Pb, but due to cost savings the finishes had been switched to pure Sn in 1983. Since the failed relays were used in nuclear facilities, a total field replacement action was initiated immediately.

In 2002, the Government-Industry Data Exchange Program (GIDEP) issued an Agency Action Notice on Sn whiskers authored by Khuri [16] from the Department of the Navy to remind the electronics industry of the potential risks associated with the use of pure Sn-plated finished on electronic assemblies. The notice recommended that pure Sn finishes be avoided at all costs and that the use of Sn-Pb solders be utilized. Due to current mandated regulations involving use of Pb in electronic assemblies, it has become more difficult to solve the whisker problem by use of Pb-containing alloys. We discuss this subject in the next section.

1.3 Impact of the Lead-Free Movement

We have shown that, since the late 1940's when Sn and Sn-alloys were chosen for use in electronic circuits (instead of Cd), there have still been several reported incidents of Sn whisker failures in electronic systems containing pure Sn plating. Further, it was

clear from the early work on whiskers that one of the best and most reliable solutions to mitigate Sn whiskers was to use a Sn-Pb alloy instead of pure Sn. Enter governmental regulations involving the use of Pb in electronics products. The European Union legislation "Restriction of the use of Certain Hazardous Substances (RoHS) in Electrical and Electronic Equipment" required the elimination of Pb (less than 0.1 wt%) from electronic devices by July 2006 [17]. The most non-disruptive and economical way of complying with the RoHS directive was to replace Sn-Pb with pure Sn [18,19]. This led to the need for higher confidence in high Sn content plating, since the generally accepted whisker prevention method (additives of Pb) was to be flushed out.

The rationale behind RoHS was the exponential sales growth in consumer electronics such as computers and cell phones. Along with the explosive growth of electrical units in the field was the problem of how to dispose of them at their end-of-lifetime. Electronics are thrown away and replaced with the newest and latest versions with increasing frequency. Millions of Pb-containing circuit boards from disposed electronics are dumped into landfills. The RoHS concern was that Pb in the buried electronics could migrate into municipal water supplies, which in turn spawned the worldwide Pb-free movement, culminating in the RoHS regulations. The Pb-free regulations currently affect nearly all electronic products (an exception is granted for certain high-reliability military use devices). Sn whiskers have therefore re-emerged as a major reliability concern in electronic systems. The problem has further been exacerbated by the continued industry demands for smaller and faster devices, with higher packing densities and smaller critical dimensions. Under these conditions, whiskers pose even more of a threat.

1.4 Reported Sn Whisker Failures

There are a variety of ways whiskers can lead to electronic device failure. Numerous failures have been attributed to short circuits caused by tin whiskers that bridge closely-spaced circuit elements maintained at different electric potentials. Whiskers can typically conduct a current of ~ 10 mA before melting. If the current through the whisker is less than this threshold value, then the failure mode is usually a permanent short. However, but if the current is greater than the threshold, the whisker melts and create an intermittent short. Applications with very high levels of current and voltage may cause whiskers to vaporize into a conductive plasma of metal ions. These plasmas are capable of carrying hundreds of amperes, which can lead to catastrophic damage. The arcs can be sustained for several seconds until interrupted by circuit protection devices. It has been shown [20] that, as the air pressure is reduced, less power is required to initiate and sustain a whisker-induced metal vapor arc. Metal vapor arcs in vacuum have blown fuses on several commercial satellites, rendering the spacecraft non-operational. The small diameter and long length of many whiskers also make the whisker susceptible to fracture. If fracture occurs, then the whisker can drop onto neighboring portions of the circuitry and interfere with the operation of devices that weren't growing whiskers. Clearly, whiskers can lead to device failures in many ways including but not limited to these discussed above.

Sn whiskers have been observed in numerous electronic assemblies. Figure 1 illustrates a few representative cases. Figure 1(a) shows Sn whiskers on pure Sn-plated connector pins, observed after ~10 years old in 2000 [14]. In Figure 1(b) whisker growth appears on matte Sn-plated microcircuit leads (2002), which created failures in the

electric power utility industry for over 20 years [21]. Sn whiskers have also been observed on the exterior surface of Sn-plated electromagnetic relays (Figure 1(c)), creating shorts between terminal-to-terminal, terminal-to-header, case-to-another component, and even whisker-to-whisker. Whisker growth has also occurred on the interior surfaces of electromagnetic relays, seen in Figure 1(d). In this case, whisker growth up to 3 mm in length was found on the Sn-plated steel armature (observed on ~14 year old parts). In 2001, whiskers were seen sprouting from pure Sn-plating over Ni terminals on ceramic chip capacitors, shown in Figure 1(e). The capacitor was mounted by conductive epoxy inside a hermetically sealed hybrid and subjected to ~ 200 thermal cycles (-40/90°C). Whiskers can also be found inside the lid of the Sn-plated microcircuit packages, shown in Figure 1(f), found in 1998. Sn whiskers up to 2mm long were observed growing toward the inside of the package and several were reported to break loose, creating intermittent shorts leading to field failures. These are just a few of many examples where whiskers are terrorizing electronic devices. Whiskers have also been responsible for failures in critical applications involving heart pacemakers, space capsules, missile control systems, satellites, medical devices, aircraft radar, nuclear and electrical power plants and much more. Table 1 lists a few of the reported whisker-related problems in various electronic applications.

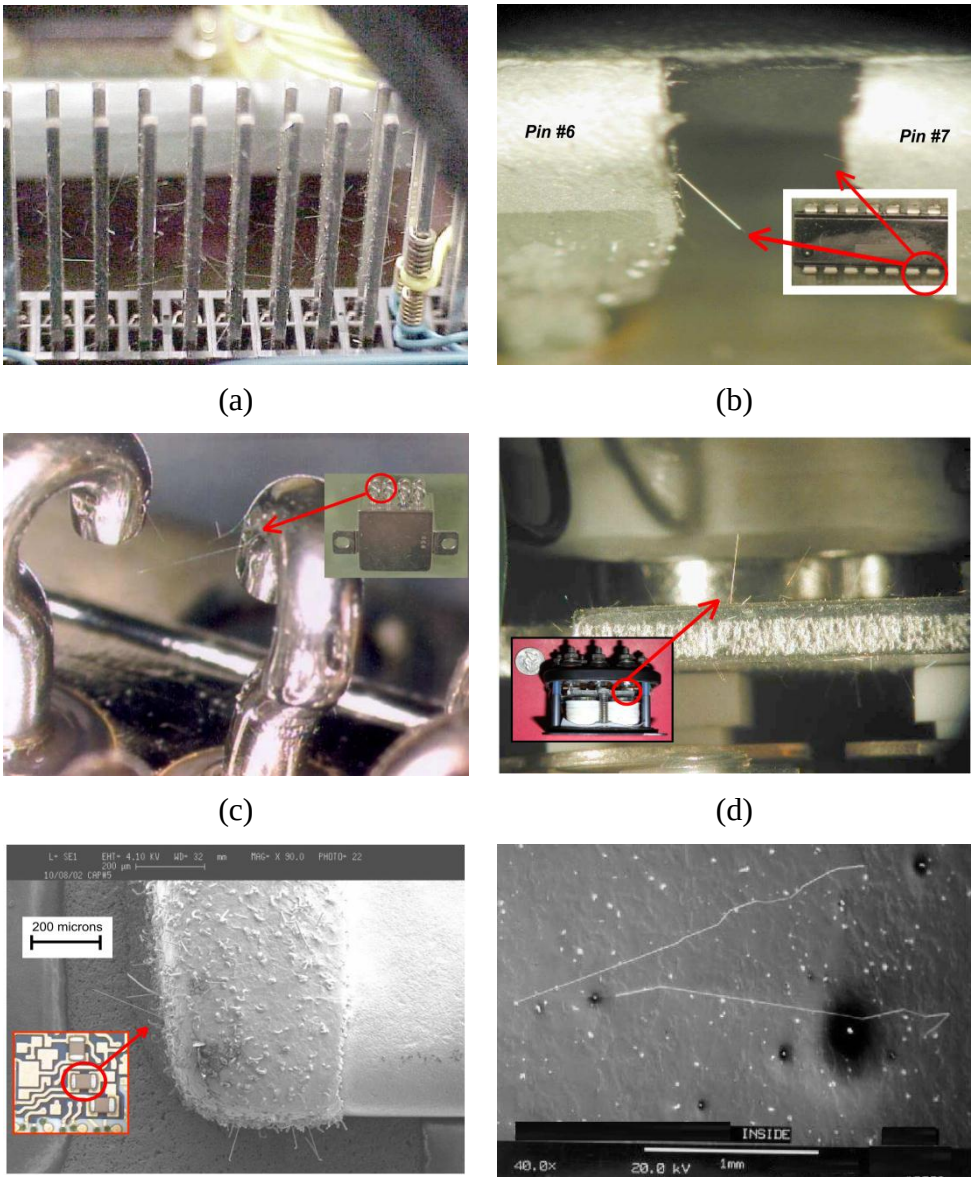

(a) (b)

(c) (d)

(e) (f)

Figure 1: Examples of whisker growth in electronic assemblies.

(a) Sn-plated connector pins; (b) Sn-plated microcircuit leads; (c) Exterior surface of Sn-plated electromagnetic relays; (d) Sn-plated steel armature on interior of electromagnetic relay, (e) Sn-plating over Ni terminals on ceramic chip capacitor, and (f) Inside lid of Sn-plated hybrid microcircuit package ((b)-(f) from [21]).

Table 1: List of Various Reported Whisker Problems (1986 – 2003) [21]

Year	Application	Industry	Whiskers on?
1986	Heart Pacemakers	Medical (RECALL)	Crystal Can
1986	MIL Aircraft Radar	Military	Hybrid Package Lid
1987	MIL/Aerospace PWB	MIL/Aerospace	PWB traces
1988	Missile Program “A”	Military	Relays
1989	Missile Program “B”	Military	Electronics Enclosure
1992	Missile Program “C”	Military	Xsistor Package +Standoff
1993	Govt. Electronics	Govt. Systems	Transistor, Diode, Lug
1996	MIL Aerospace	MIL Aerospace	Relays
1998	Aerospace Electronics	Space	Hybrid Package Lid
1998	Commercial Satellite #1	Space (Complete Loss)	Relays
1998	Commercial Satellite #2	Space	Relays
1998	Commercial Satellite #3	Space	Relays
1998	Military Aerospace	Military Aerospace	Plastic Film Capacitor
2000	Missile Program “D”	Military	Terminals
2000	Commercial Satellite #4	Space (Complete Loss)	Relays
2000	Commercial Satellite #5	Space (Complete Loss)	Relays
2000	Power Mgmt Modules	Industrial	Connectors
2001	Commercial Satellite #6	Space	Relays
2001	Nuclear Power Plant	Power	Relays
2001	Hi-Rel	Hi-Rel	Ceramic Chip Caps
2002	Commercial Satellite #7	Space	Relays
2002	Military Aircraft	Military	Relays
2002	Electric Power Plant	Power	Microcircuit Leads
2002	GPS Receiver	Aeronautical	RF Enclosure
2002	MIL Aerospace	MIL Aerospace	Mounting Hardware (nuts)
2003	Commercial Electronics	Telecom	RF Enclosure
2003	Telecom Equipment	Telecom	Ckt Breaker
2003	Missile Program “E”	Military	Connectors
2003	Missile Program “F”	Military	Relays

1.5 Literature Survey of Factors Influencing Whisker Growth

There is currently no general consensus on the underlying mechanism(s) of whisker incubation and growth. The science of whiskering is still being worked out. A great deal of controversy and contradictory information regarding the key factors that affect whisker formation still exists. Several attempts have been undertaken/currently running to develop accelerated test methods to determine the propensity of a particular system and its environment to form whiskers. To date, however, there are no universally

established test methods for evaluating whisker susceptibility. In fact, much of the experimental data compiled throughout the years has produced contradictory findings regarding which factors accelerate or even retard whisker growth.

That said, there are a number of commonly agreed upon variables that influence whisker formation. Most researchers agree that compressive stress in the Sn film is the fundamental driving force behind whisker growth [22]. This stress may be intrinsic stress, which is stress distributed in the as-plated Sn film with its associated texture (grain size and crystallographic orientation) [23, 24] or, extrinsic stress, arising from chemical reactions between the Sn-film and the substrate alloy (intermetallic compound formation), uneven diffusion between the substrate material and tin film, mechanical processes such as bending, forming, and thermo-mechanical stresses (CTE mismatch induced), plating chemistry (bright tin) and/or impurities introduced during film deposition, oxygen diffusion and/or oxide formation on the surface, and even storage or operating environment conditions (such as corrosion possibilities). Figure 2 displays a multitude of factors that can influence whisker growth.

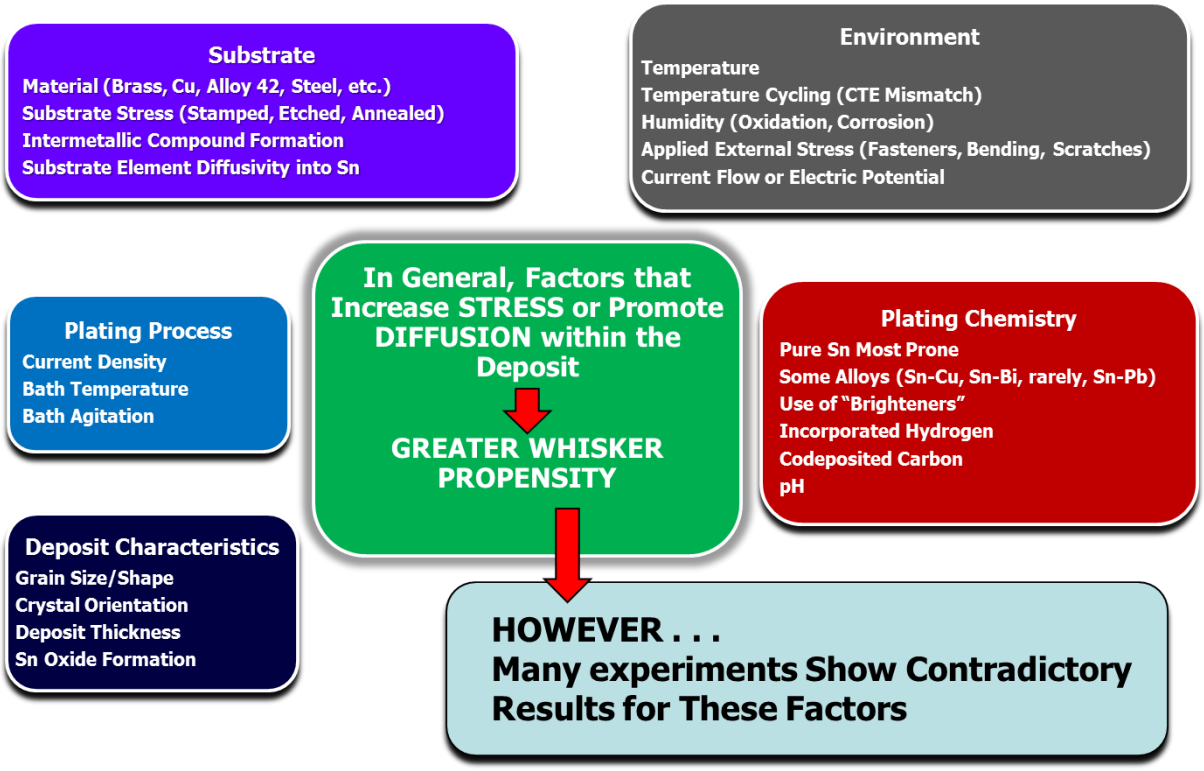

Figure 2: The multitude of factors that can influence whisker growth.

If the film stress is maintained at high levels for a sufficiently long period of time, there is strong likelihood of a whisker growth event as a means to relax the stress within the film beyond the extent possible by competing stress reduction schemes. It is commonly thought that tensile stress retards whisker formation, while compressive stress accelerates whisker formation. We offer additional data on this question below, but it is likely that stress is not sufficient in itself to initiate whiskers. The factors that affect whisker growth are conveniently grouped into a few major categories: plating chemistry and process, deposit characteristics, substrates, and environment.

When it comes to plating chemistry and the plating process there are many concerns. First is the plating material. Pure Sn is the most commonly used whisker

prone plating material, but other Sn alloys (such as Sn-Cu and Sn-Bi) can also generate whiskers. In fact, even the rare whisker producer, Sn-Pb, has been observed to create whiskers under suitable circumstances. The use of "brighteners" during plating can also greatly effect whisker growth. In general, bright Sn films are more prone to whisker formation and growth than the so-called matte Sn films. A matte tin film is a tin film that contains lower internal stresses and larger grain sizes (typically of 1 μm or greater) with a carbon content < 0.050%, while a bright tin film has higher internal stresses and smaller grain sizes (typically 0.5 to 0.8 μm) with a carbon content of 0.2 to 1.0% [25]. Impurities in the plating bath which get incorporated into the Sn film as defects may also enhance the possibility of whisker formation. It is not completely known which impurities (and concentrations) are the primary culprits, but Cu and C appear to be impurities that make the tin film stress increasingly compressive [26]. Incorporated H or co-deposited C during plating may also influence whisker growth [27]. The current density, bath temperature, and degree of bath agitation during the plating process also affect whisker development.

Once deposition is complete, the deposited film characteristics play a role in whisker formation. The grain size and shape along with the crystal orientation in the microstructure of the film affect whisker growth [28]. Typically, the smaller the grain size the higher the internal stresses in the film [29]. The grain size and shape in turn become important when taking into account the grain boundaries. Increasing the grain size of a deposited Sn film reduces the number of grain boundaries, which slows both the self- and inter-diffusion rates in the film. Fewer grain boundaries also mean fewer places for non-uniform intermetallic compound (IMC) growth, which can reduce the stress in

the system. The migration of substrate atoms into the film usually act to increase stress in the film, enhancing whisker growth. The self-diffusion of Sn along grain boundaries to the root of a whisker supplies Sn atoms to push the growth upwards from the base of the whisker. The predominant diffusion mechanism affecting whisker growth is expected to be grain boundary diffusion [30]. However, in many cases, grain boundaries are pinned within films so the diffusion rate is limited by the available flux of vacancies with the film. Finally, the thickness of the deposited film can influence whisker growth. Thicker layers of Sn (~ 7 μm or greater) have greater volumes and lower overall stresses which result in longer whisker incubation times.

There are currently two principal whisker models that are thought to describe whisker growth. Vianco's [31] whisker model proposes that the underlying process behind whisker growth is dynamic recrystallization (DRX). Numerous researchers have considered the possibility that whisker growth results from recrystallization, but not specifically DRX [63, 32, 33]. The idea is that time-dependent, creep deformation caused by compressive stress is the mechanism which initiates DRX and then provides the mass transport necessary to sustain the grain growth phase of DRX. Here the compressive stress does not explicitly cause whisker growth by the bulk movement of material, but rather, the compressive stress generates inelastic deformation, increasing strain energy, which initiates DRX. Whisker growth from the surface is the result of the DRX.

DRX is an enhancement of static recrystallization. Static recrystallization occurs when the strain energy of defect structures is reduced without additional deformation occurring at the same time. In contrast, DRX is caused by the simultaneous occurrence

of deformation. The slower the strain rate, the more likely it is for the deformation (strain energy build-up) and recrystallization (strain energy loss) processes to overlap, thereby giving rise to DRX. Mechanistically, the DRX process begins with the build-up of defects. The resulting increase of strain energy provides the added driving force that initiates recrystallization either sooner or, at a lower temperature, than would occur under static recrystallization. Once the strain energy has exceeded a limit, the DRX process proceeds with the nucleation of new grains (smaller than original grains). These new grains grow under the driving force generated by the annihilation of the dislocation pile-ups and tangles, which removes strain energy from the material. Soon, the growing grains, like the pre-existing grains, become susceptible to an increased defect density at their boundaries under the applied stress. Dislocations pile-up and tangle at these recently created grain boundaries causes them to become sites of new grain initiation for possible whisker growth. This cycle continues until the stress has been removed from the material.

Therefore, whisker development, as a form of DRX (Figure 3), is a serial process comprising of deformation that raises the strain energy, new grain initiation and then grain growth (which is responsible for the whisker formation). The sustained deformation under compressive stress drives the mass transport mechanism. The compressive stress creates dislocations that pile up at pre-existing grain boundaries and the resulting strain energy increases to the point where new grains are initiated. In this model the whisker does not grow from a pre-existing grain, which is similar to the model proposed by Smetana [35], who offers a second current principal whisker model.

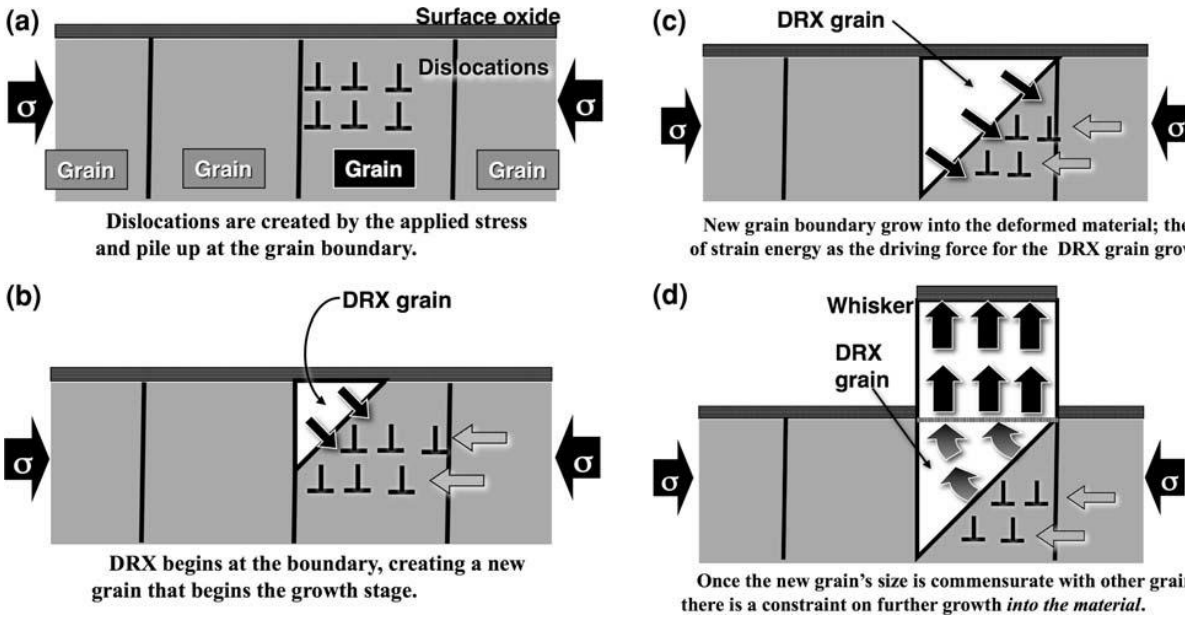

Figure 3: Schematic showing whisker growth under the DRX model [31].

In Smetana's model, the atoms at the whisker grain boundary at the base of the whisker are shown to be (on average) at lower energy levels (compressive stress levels) than surrounding areas. This aids in the movement of Sn atoms without requiring that they go to a higher energy state. The base of the whisker is the grain boundary interface of the whisker with other whisker grains (not the surface of the tin deposit in the area of the whisker grain). In this model, recrystallization is necessary and there must be vacancies at the base of the whisker grain boundary; otherwise, Sn atoms cannot move there.

Figure 4 (a) shows columnar grain boundaries under compressive stress (mechanical, CTE mismatch, IMC growth, etc.). After recrystallization (Figure 4 (b)), oblique angled grain boundaries are created, which results in lower stress grain boundaries than the vertical grain boundaries. This is the source of the stress gradient. Since grain boundaries are high vacancy sites with a low degree of atom packing density,

they may act as a source or sink for vacancies. Figure 4 (c) demonstrates diffused Sn atoms that have been driven into the oblique angle grain boundaries due to the stress gradient. Since the grain boundaries are not fixed, grain boundary sliding (creep) can occur along the boundaries. As more Sn atoms diffuse into the grain boundaries (lower packing density), some atoms in the grain boundary move into the whisker grain. One possible example of this is displayed in Figure 4 (d), which produces whisker growth directed upward, resulting in a simplified schematic of the whisker growth model in Figure 4 (e). Depending on where the Sn atoms are introduced into the whisker grain and if there are any pinned grain boundaries deciphers how the whisker protrudes out from the surface (straight, bent, kinked, etc.).

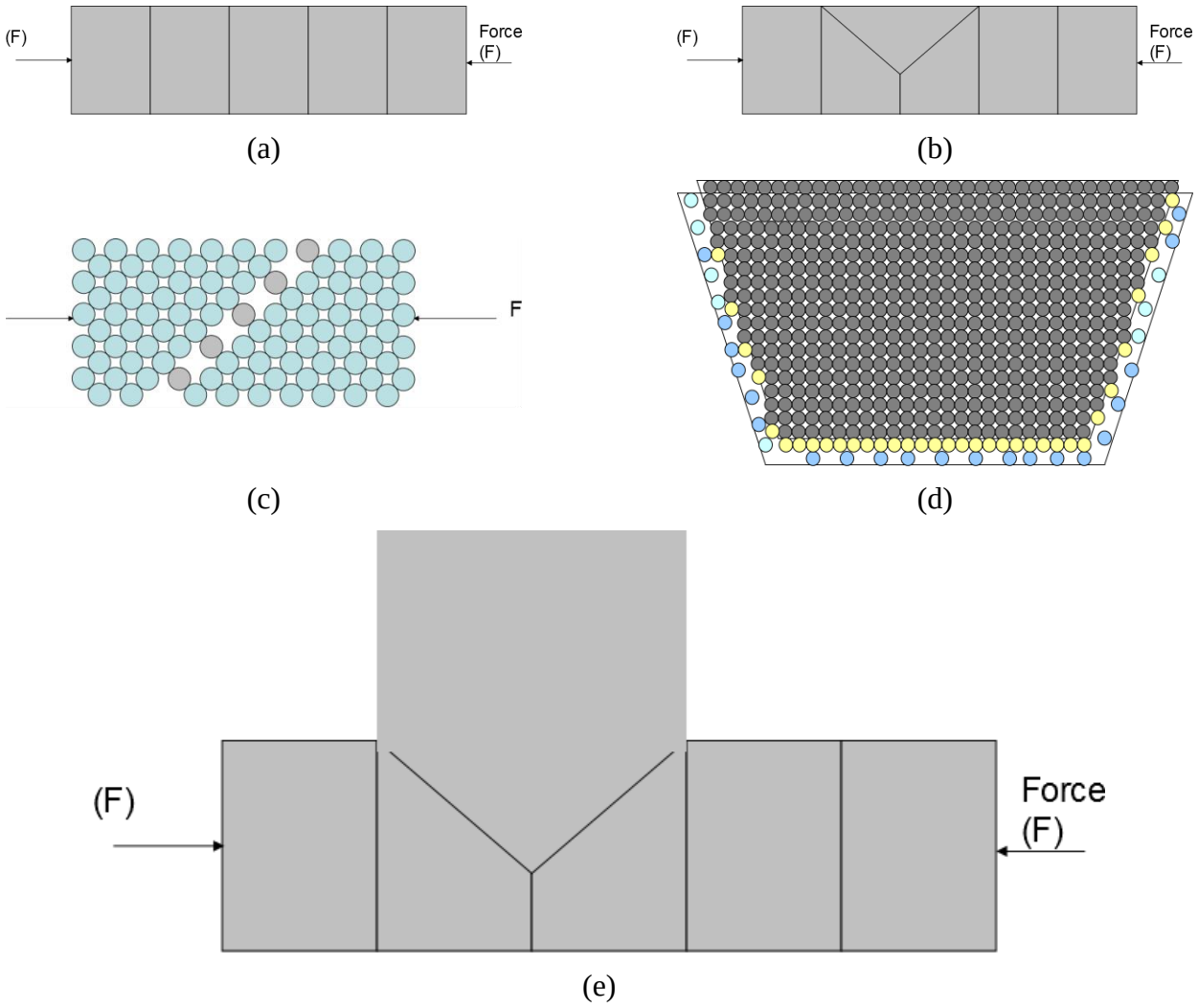

Figure 4: Schematic of Smetana whisker model [35].

Once Sn is deposited, it oxidizes. Sn oxide formation is thought to play a significant role in whisker growth. In one theory, localized breaches in the surface Sn oxide layer can provide a path for vacancies to diffuse into the film from the ambient air, but only for a limited time (depends on the rate of re-oxidation of the surface of the Sn film where the oxide was breached) [34]. Excess Sn present in the system under any kind of compressive stress can move along grain boundaries that are not pinned, such as in the vicinity of the oxide breach. The Sn can then reach a nucleation site and begin to grow at that location and form whiskers.

Sn oxides can contribute to whisker production in other ways. It has been seen that Sn oxide growth can be non-uniform [35,36,37], meaning there are holes in the oxide or regions where the oxide is weaker, which favors whisker penetration through the Sn oxide layer. Sn oxidation also may affect whisker growth by creating extra stress in the film. As oxygen diffuses into the film and combines with Sn atoms to form SnO or SnO_2 it can create extra stress in the film due to the relative volume of Sn/SnO_x within the film space. This extra stress contributed by oxygen incorporation is expected to affect thin films more than thick films since the thicker films have a larger volume over which to dissipate the stress. Generally, the role of oxygen is complicated and not well understood, with many theories describing ways in which oxygen contributes to whisker formation. The role of oxidation in whiskering is a controversial topic. Some go as far to say that the surface oxide layer is a *necessary* condition for whisker formation [38] while others believe that a surface oxide has minimal effect on whisker growth [39]. Our work reported below on Au whiskers favors the latter perspective.

The substrate under the Sn film can greatly affect whisker growth. Different substrate materials react differently with Sn or various Sn alloys in many ways. Certain film/substrate combinations are likely to form interfacial intermetallic compounds while other film/substrate combinations lack intermetallic compounds. For example, Sn films on brass or Cu lead to concerns with unwanted stress created by the formation of intermetallic layers. Cu_6Sn_5 is a common intermetallic interfacial compound which forms at a Sn-Cu boundary at ambient room temperature. It is the dominant IMC between Cu and Sn [40] and is known to grow faster with increasing temperature. The intermetallic layer is formed by Cu diffusion into the Sn film through grain boundaries.

Though IMC's grow faster at elevated temperatures, they can actually pose more of a threat at room temperature, since grain boundary diffusion is higher than bulk diffusion near room temperature, creating locally limited Cu migration routes. This leads to the characteristic, highly irregular Cu-Sn IMC, which creates localized, compressively stressed regions within the Sn film. At elevated temperatures, bulk diffusion increases and results in a more uniform IMC and less stress.

Molar volume differences can contribute to film stress and enhanced whiskering. If six parts of Cu are mixed with five parts of Sn, the resultant Cu_6Sn_5 has a larger molar volume (10.6 cm^3/mol) [41] than the molar volume of Sn. This can lead to compressive stresses in interfacial areas. IMC effects become more complicated at elevated temperatures where a neighboring intermetallic layer of Cu_3Sn may also form, though Cu_3Sn intermetallic layers have lower molar volumes (8.6 cm^3/mol) [42] than Cu_6Sn_5 and are not expected to create as much extra stress within the film.

A host of environmental conditions have a major impact on Sn whiskering. Everything from assembly line processes to storage conditions has been found to influence whisker growth. Some variables of concern include the specific plating process, temperature, temperature cycling, relative humidity, applied external stress, current flow or electric bias, and even pressure since whiskers grow in vacuum as well as under atmospheric pressure. Elevated temperatures and temperature cycling affect whisker formation due to CTE mismatches and IMC formation. Some studies report that thermal cycling increases the growth rate of whiskers [43, 37], while others report no effects due to thermal cycling [44,45]. Heat treatment processes include procedures of annealing, fusing, and reflow. Annealing refers to a heating and cooling process typically

intended to soften metals and make them less brittle. According to studies, annealing should be performed within 24 hours of plating in order to be effective in mitigating whiskers due to irregular IMC growth. Dittes and Olberndorff [46] have shown that Cu based lead-frames should be heated to 150°C for 1 hour directly after plating. Due to bulk diffusion at the elevated temperature, a less irregular and more continuous IMC layer forms, which results in less compressive stress. The grain boundaries of the Sn can shift, resulting in larger grains and fewer grain boundaries [47]. The more regular IMC layer results in a continuous diffusion barrier for further IMC growth, which slows the formation of irregular growth by grain boundary diffusion at ambient conditions [48].

Fusing and reflow act similarly since they both melt and resolidify tin plating under relatively slow cooling conditions. Fusing is a reflow procedure usually done by dipping the tin-plated surface in a hot oil bath. By fusing Sn plating shortly after deposition, whisker formation may be mitigated [49]; however, when IMC layers form, the effectiveness of the fusing is reduced. In contrast to fusing, reflow, which is done as part of the printed circuit board assembly process, has not always been shown to be a successful whisker mitigation practice. In fact, some studies report an increase in whisker growth [50,51] during reflow without flux. These are just some examples of the widely varying effects temperature can have on whisker formation.

Relative humidity has been shown to play a complicated role in whisker development. Some reports claim that moisture is not a contributing factor in whisker growth while others observe that whiskers form more readily under high humidity (≥85% RH) [52,53,54]. Humidity is thought to introduce stresses due to the diffusion of oxygen from the surface into the film [55]. High humidity then affects the thickness of the oxide

film on the Sn leading to compressive stress [56]. High relative humidity is also thought to increase the rate of grain boundary or surface diffusion, and can also lead to corrosion, which introduces additional stress within the film [52]. Corrosion-assisted whisker growth caused by water condensation during high-temperature humidity testing or by water droplet exposure has been observed [57]. Excessive localized surface corrosion leads to non-uniform oxide growth, which imposes differential stress states on the Sn film. Whiskers have been found to nucleate in the corroded regions and continue to grow even after removal of the condensed moisture. It is clear that humidity plays a significant role in whisker production. Humidity and its frequently produced offspring, corrosion, are still very much confounding factors in whiskering requiring a great deal of careful work. We report below the results of a highly controlled experiment on the effects of relative humidity on Sn whiskering.

Finally, the presence of an electric field or voltage bias has been found to affect whisker growth in multiple ways. The extent and impact of electrical potential is not fully understood [58] at the present time. However, NASA workers have demonstrated that whiskers can bend due to the forces of electrostatic attraction, which increases the likelihood of Sn whisker shorts [59]. A few studies have shown that electrical currents accelerate Sn whisker growth [60] but this remains a controversial subject; we report our study of the influence of current density on whiskering below. More work is required to fully confirm and understand the effects of electric field on whiskering.

In summary, there are multiple factors that play a role in whisker growth on any given system and, unfortunately, a quantitative relationship between these variables and whisker growth does not yet exist. Over nearly a half century after the first observation

of whiskers, there is still no generally accepted consensus for the root causes of whiskers or a protocol for mitigation that is universally applicable over all electronic assemblies. In spite of this, there have been several attempts by the electronic industry to develop practices for whisker prevention and mitigation. After the RoHS regulations effectively banned the use of lead in electrical products, the National Institute of Standards and Technology (NIST) became active in Sn whisker research. NIST was one of the first agencies to specify whisker mitigation practices by the reduction of internal compressive stresses created by IMC formation. In 2001, iNEMI also embarked on a series of experiments to find accelerated tests (e.g., high temperature, humidity and thermal cycling) for tin whiskers, where it quickly became clear that standard accelerated test conditions were insufficient to provide a clean-cut, simple set of tests that would predict whisker growth. As the industry continued its march toward Pb-free electronics, the need to insure the reliability of tin coatings became all the more necessary, so iNEMI was determined to produce a set of accepted industrial test procedures to monitor and minimize whisker reliability exposure. The plan of attack was to first define a set of test conditions that would promote Sn whisker growth and then to recommend a protocol for inspecting the whisker growth and recording the data. The next step was to gain a sufficient understanding of whisker formation to allow for development of accepted test criteria and mitigation practices which would provide a methodology to minimize whisker reliability exposure for long life, high reliability electronics systems. iNEMI published the acceptance test requirements in July 2004 [61] which were submitted as a formal standard in the JEDEC standard JESD 201, “Environmental Acceptance Requirements for Tin Whisker Susceptibility of Tin and Tin Alloy Surface Finishes” in

2006. However, the documents provide only recommended guidelines to reduce the risk of whisker-related problems. They do not describe specific methods that can be used to eliminate whisker-related failures.

1.6 Challenging Aspects of Whisker Studies

One of the complications when studying whiskers is the issue of time. Whiskers have been observed to grow within days in some cases, but may take up to years and even decades before growing long enough to cause failures in electronic systems. This means that an electronic component that is whisker-free one day can be whisker prone the next day, creating a reliability nightmare scenario. It is this dormancy, commonly known as the incubation period, that distinguish whiskers from other surface plating defects such as nodules or dendrites, which may be roughly similar in appearance to whiskers but present on the surface immediately after plating. This attribute of whisker growth is particularly frustrating since, in order to complete any kind of meaningful experiment, very long time periods may be necessary to create whiskers.

It is important not to take the incubation period lightly. Sn plated electronic systems that may seem fine and functional for many years remain under the threat of whisker growth. In 1976, Dunn (of the European Space Agency) released a set of publications strongly recommending that surfaces susceptible to whisker growth (such as Sn) be excluded from spacecraft design [6,7], but not all satellite manufacturers followed his suggestion and, over a decade later, in 1990, several commercial spacecraft failed due to Sn whisker problems. The U.S. military first become aware of the incubation of Sn whiskers and their potential problems when the USAF was inspecting failed circuits in 12 year old radar systems and found whiskers up to 2.5 mm in length growing on Sn-plated

lids of hybrid circuits [8]. Another incident where whiskers arose after a long period of dormancy was found in March 2000 in 10 year old General Electric relays [14].

A second frustrating factor in whisker studies is the highly variable growth rate of whiskers. Whisker growth rates range from 0.03 to 9 mm/yr [62] which means their growth is highly variable and unpredictable. For example, in 1954, Fisher et al. [63] reported a Sn whisker growth rate of 10,000 Å/s under a clamping pressure of 7500 lbf/in^2 on Sn plated steel. The growth rate was essentially linear which at some point in time went to zero. He also reported (private communication) growth rates for spontaneous Sn whisker growth (no clamping pressure) at ~ 0.1 to 1.0 Å/s [64]. However, in 1964, Pitt and Henning, also using clamp pressure on hot-dipped tin deposited on Cu and steel, reported the highest whisker growth rate at 593 Å/s with 8000 lbf/in^2 of pressure, with whisker growth rates that decreased with time [4]. The wide range of variation in whisker growth rates makes whisker studies difficult, as one never knows how long to wait to see whiskers, how fast whiskers grow, and when whiskers will stop growing. Other contributing complications include the fact that not all of the variables affecting whisker growth are known and the known variables are not always reported accurately when data is published. Further, current test methods cannot correlate whisker growth in test conditions to actual field conditions; therefore, test results cannot be used to predict whisker growth in other environments or for longer durations. There is a need to compare whisker growth data derived in controlled, short-term environmental tests to long-term field exposures in order to quantify whisker-reliability predictions for electronic devices.

Since Pb was used as the main mitigation method for whiskers up until the implementation of the RoHS legislation, the literature on whisker growth mechanisms pertaining to Pb-free solder alloys and assembly of Pb-free electronics is sparse. For example, the Pb-free sessions and workshop of the 2006 annual meeting of the Materials, Minerals and Metals Society (TMS) had only four papers on Sn-whiskers but more than 200 papers dealing with different aspects of Pb-free solders. Furthermore, the 2005 and 2006 IEEE Electronics Components Technology Conference (ECTC) had more than 200 papers each year dealing with Pb-free solders in electronic packaging, but when including the 1-day Sn-whisker workshops held in each of these years, there were less than 25 combined Sn-whisker papers. Over the last 60 years, there have been only a few hundred publications on whisker growth but in the past 10 years alone, there have been thousands of papers dealing with Pb-free solders. One of the primary reasons for the lack of published work on whiskers involves the experimental difficulties in carrying out the time-consuming, long-range experimental studies, which are best done in academic environments. The difficulties are not due to the allowance in whisker growth time alone, but also factor in the time associated with the identification of whiskers by labor-intensive optical and scanning electron microscopes.

One of our goals in this work was to minimize the time to whiskers by developing a quick and reproducible method for growing whiskers in a timely (weeks) fashion. Electroplating is the current thin film method of choice in industrial processes; however, whisker growth can take up to years and even decades in many electroplated Sn films. It is advantageous to devise a faster method to grow whiskers. We found that the key to producing fast whisker growing Sn films was to look backwards. In 1989, Hoffman and

Thornton [65] studied sputter deposition under argon plasma for many different metal films and compiled a simple system of "dialing in" various amounts of intrinsic thin film stress by changing the background gas pressure in the sputtering system. For the case of Sn films (see Figure 5 from Hoffman and Thornton's results), compressive stress results by using a background Ar pressure ranging from ~1-6 mT and tensile stress results when using 10-100 mT. Even a "no stress" state can be produced by the Thornton approach, but it has a fairly narrow, 7-9 mT, gas pressure range which is difficult to achieve and control without practice.

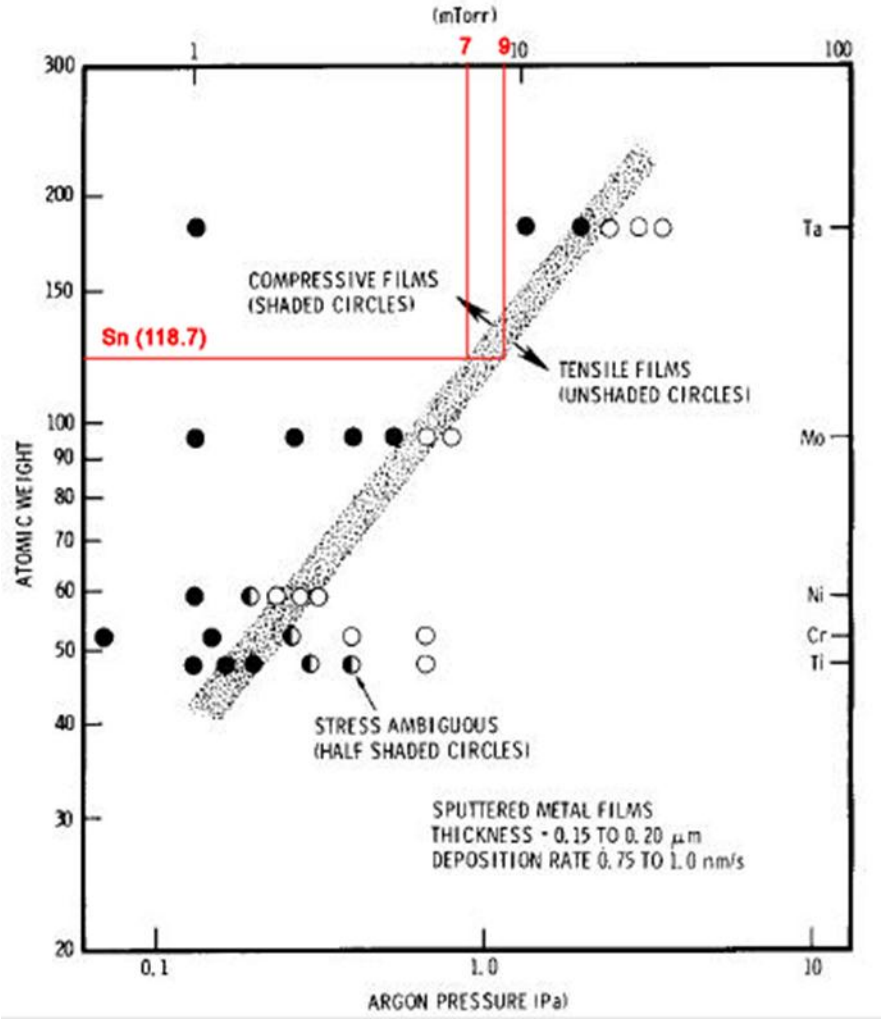

Figure 5: Plot from Hoffman and Thornton [65] showing the range of background argon pressures needed to produce various stress states in thin films.

Figure 6 illustrates the underlying mechanism responsible for creating the stress states during sputter deposition. Sputtering at high Ar pressure leaves the depositing Sn atoms with low kinetic energy (due to multiple Sn/Ar atom interactions during the Sn atom's travel from sputter target to substrate), which produces a low packing density in the film. This leaves the deposited atoms far apart, creating a net force of attraction between them, which shrinks the film and produces a concave curvature in the substrate. However, sputtering at low Ar pressure gives the depositing Sn atoms high kinetic energy

(since there is minimal energy loss due to Sn/Ar atom interaction during deposition), which leaves the deposited atoms packed tightly. This causes them to exert a force of repulsion against each other (due to overlapping electron orbitals). As a result, the film expands and produces a convex curvature in the substrate. This approach has allowed us to "dial in" high values of compressive stress in order to decrease the incubation period associated with whisker growth to days and weeks rather than months and years.

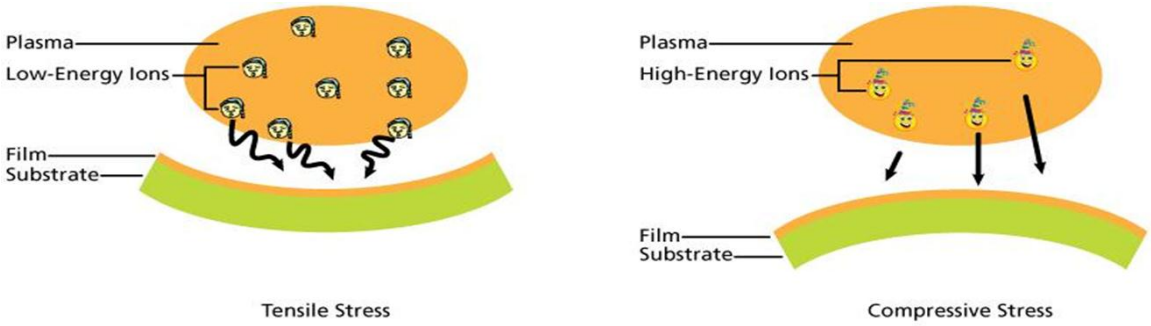

Figure 6: Creation of stress states due to varying sputtered argon pressure.

Another challenge in whisker research arises from the limited whisker statistics available when manually counting whiskers and measuring their lengths. In this study all whisker lengths are measured "as observed" from the SEM screen, when the thin film surface is perpendicular to the incident electron beam. This method is chosen for simplicity and time maintenance, due to the large volume of experiments and whisker measurements conducted throughout the work. We note that, although practical for our experiments, this method does not account for foreshortening angles of the protruding whisker. A second, common whisker measuring technique (provided by JESD22-A121A [66]) measures the straight line distance from the point of emergence of the whisker to the most distant point on the whisker, as shown in Figure 7. In this case, the system used

for measurement must have a stage that is able to move in three dimensions and rotate, such that whiskers can be positioned perpendicular to the viewing direction for measurement.

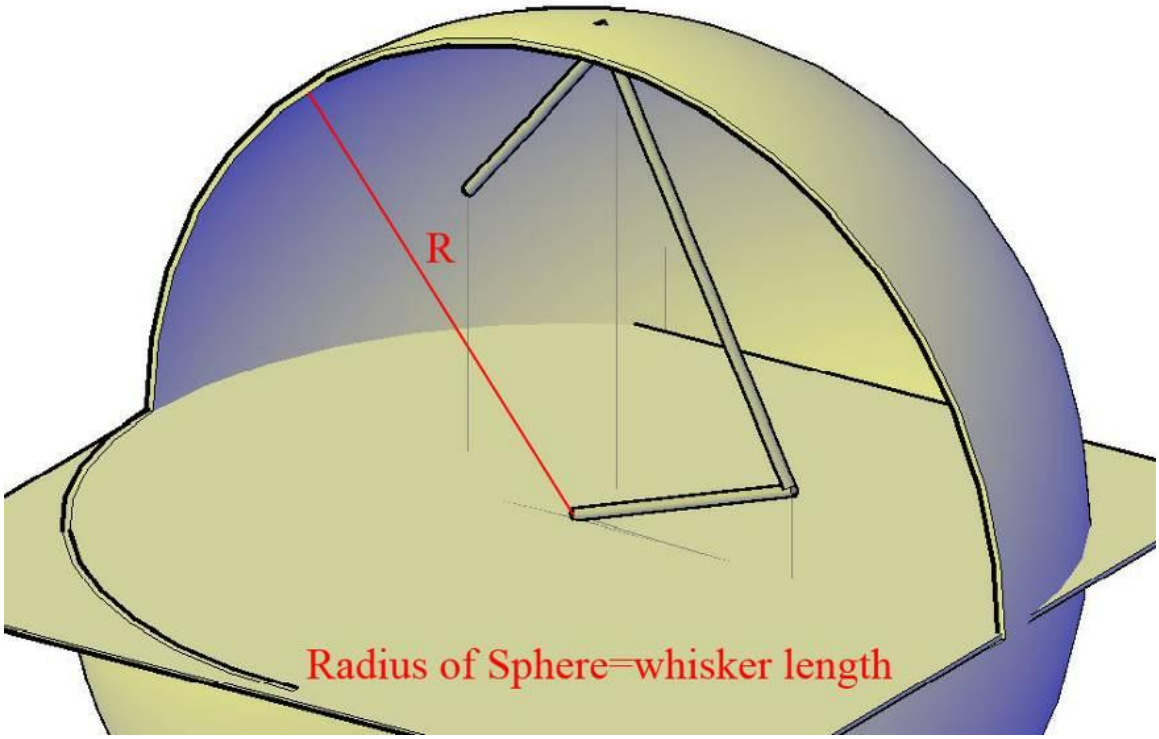

Figure 7: Whisker length measurement technique provided by JESD22-A121A.

The best, most accurate whisker measurement scheme has been proposed by Panashchenko [67], where foreshortening angles are taken into account. The measurement is made by using two images offset by a known tilt, as shown in Figure 8. The whisker length, L_{ab}, can be calculated using:

$$L_{ab} = \sqrt{\frac{{L_{cd}}^2 + {L_{ce}}^2 - 2L_{cd}L_{ce}cos\theta}{sin^2\theta} + (L_{cd}tan\beta)^2}$$

where the axis along L_{ac} is the tilt axis, L_{cd} is the projection of whisker length on axis perpendicular to tilt axis Plane 1, L_{ce} is the projection of whisker length on axis

perpendicular to tilt axis in Plane 2, θ is the tilt angle between Plane 1 and 2, and β is the angle between L_{cd} and L_{ad} in Plane 1.

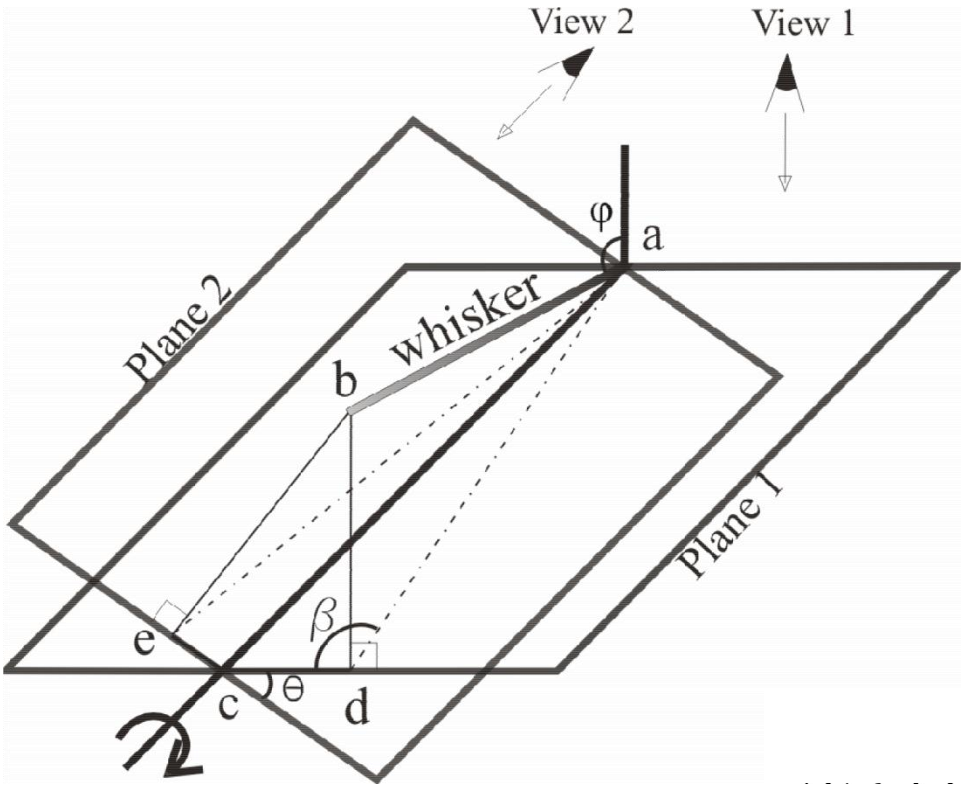

Figure 8: Whisker length measurement method given by Panashchenko [67].

The statistics issue is a never ending battle in whisker studies, with researchers constantly asking themselves "is this measurement of whiskers statistically significant." It is a challenge to achieve such significance for the low numbers and manual counting schemes involved with whisker studies. Further, the modeling of whisker lengths requires a statistically significant number of whiskers to be measured, and a given measurement method has a % error associated with it. By measuring the whisker length from a single image as conducted here, we define the % error as:

$$\%error = (1 - cos\alpha) * 100\%$$

where α is the angle of the whisker from the surface. The error associated to the JESD22-A121A method is ~ 20 ±11% and ~ 7±3% for Panashchensko's methods [67]. It has also been observed by Panashchenko [67] and Fukuda [68] that whisker lengths generally follow a log-normal distribution.

Whisker counting needs to be considered as well. Just as with measuring whisker lengths, there are various whisker counting approaches used. Some studies incorporate whisker statistics from mass produced, high volume sample sets, while others use well controlled test environments with fewer specimens. The technique used to count whiskers can also play a role in whisker statistics. Whisker can grow up to millimeters long and can even be seen with the naked eye under the right conditions. However, since whiskers can also be observed as small as a couple microns long, an SEM is ideal for viewing them. Some optical microscopes can be used, but the limited depth resolution of most optical microscopes can lead to false identifications of whiskers. There is also an element of skill necessary when using any microscopic technique and the associated skill to recognize when something is a whisker and something is debris. This becomes important when comparing whisker statistics from study to study. In some studies (due to imaging technique or extensive number of whisker count) whiskers are only counted if they exceed a given length (such as 10 µm or greater).

Throughout the experiments herein, we have used a SEM to count whiskers, accounting for all whisker lengths ranging from 2 µm and greater. Unless otherwise stated, the whisker densities are determined by manually counting whiskers in the SEM over ten equal areas (~275 µm x 275 µm) representative of the surface in question as a whole. Each whisker counted is also measured for length from a single, top-down view.

Being able to produce whisker growth within reasonable time periods, through laboratory specimens in well-controlled environments, large numbers of whisker statistics were observed in the majority of our studies. As with any large statistical count, the "random error" becomes the statistical error associated with sampling or counting, which goes as $\sim \sqrt{N}$ exists, where N is the number of counts.

1.7 Unique Features of the Investigative Plan

Our research program takes several novel approaches to the whisker problem by focusing on a limited set of focused objectives using "laboratory" created whiskers as opposed to archival, industrial, and/or anecdotal whisker specimens. Here are the key features which have governed our experimental strategy:

- We have used a reproducible method of growing whiskers in a reasonable (weeks) time by using magnetron sputtering techniques rather than electrochemical deposition.
- We have produced tailor-made films with known "dialed-in" degrees of thin film stress (tensile, none, compressive) to investigate the role of net film stress.
- We have eliminated the role of interfacial stress by growing whiskers on substrates that do not form intermetallic compounds with Sn.
- We have examined whisker growth in near-real time using field-enhanced, high current density methods that grow whiskers in hours rather than days, weeks, months.

- We have addressed the question of whisker mitigation/prevention by studying why certain topside metal films (Ni) appear to prevent whisker growth while others (Cu, Pb) do not.

The last approach reflects our philosophy to attack the whisker problem along parallel paths. The first path recognizes the need for carefully designed and highly controlled whisker experiments which attempt to isolate the key variables affecting whisker growth. The goal of this work is to uncover the key scientific principles which govern whisker phenomena. The second path is designed to help solve the practical whisker problem by identifying the critical engineering steps needed to dramatically increase the reliability of contemporary electronic devices that are affected by whiskers. The dual approach recognizes a common experience in technology whereby the solution often precedes the science.

For each investigation reported below, we began by posing a single key question involving whiskers which we believed could be answered by a well-designed and controlled experiment, doable using the instruments within the surface science and condensed matter group at Auburn University. Here is an outline of the key questions we have sought to answer:

Film/Substrate Effects:

1) Sn film thickness
    - Are thinner/thicker films more prone to whiskering?
    - Is a maximum whisker length produced depending on film thickness?

2) Sn film volume/depletion

   - Where is the Sn in the Sn whiskers originating from (feedstock issue)?
   - Is there a minimum amount of Sn needed to produce whisker growth?

3) Sn/substrate combinations

   - Are certain film/substrate combinations more prone to whiskering?
   - Is an intermetallic layer (IMC) necessary for whisker growth?
   - If not, how does whisker growth compare to Sn film/substrate combinations with and without an IMC layer?

4) Film stress

   - The consensus is that compressive stress enhances whisker growth, but what about tensile stress? How does it compare?
   - By sputter depositing intrinsic macroscopic film stresses, can the stress state be varied (and what is the film stress value)?
   - How does the average net film stress affect whisker growth?

5) Sn alloy films (SAC 305 and eutectic SnPb)

   - Can whiskers grow from Sn alloy films?
   - If so, how does the whisker growth compare to whisker production from pure Sn films?
   - Does a Sn alloy pose whisker reliability risks in our electronics?

Environmental Effects:

1) Oxygen & Humidity
    - What effect does oxygen have on whiskering?
    - How do various humidity exposures affect whisker growth?
    - How does the effects of ambient room temperature/humidity exposure compare to pure oxygen and humidity on whisker growth?
2) Sn oxides
    - What types of Sn oxide(s) are created under ambient room temperature/humidity exposures? How thick are they?
    - What type and how thick of an oxide is created when exposed to a dry oxygen environment, and even oxygen exposure at elevated temperatures?
    - How does the dry oxidation of Sn compare to wet oxidation (steam exposure at elevated temperature)?
    - Is a surface oxide layer a necessary condition for whisker production?
3) Electric bias
    - Is whisker growth affected by electric fields, and if so how?
    - How does the current density through a Sn film affect whiskering?
    - Can Sn migration be observed by an electrical bias?

The remainder of the dissertation addresses each of these questions in detail.

CHAPTER 2

FILM/SUBSTRATE EFFECTS ON WHISKER GROWTH

"I think physicists are the Peter Pans of the human race. They never grow up and they keep their curiosity."

-I.I. Rabi

2.1 The Influence of Film Thickness on Sn Whiskering

The thickness of the deposited film has been thought to effect whisker growth. Since is it commonly agreed that compressive stress plays an important role in whisker formation, thicker Sn layers (~ 7 μm or greater) are thought to distribute the film stress over a larger volume, resulting in lower net stress values within the film.

Oberndorff et al. [69] studied electroplated Sn films deposited on typical lead-frame materials with varying thicknesses between 1.5 to 15 μm. In order to influence the whisker growth, several heat treatments and storage conditions were used. It was observed that increasing film thicknesses produced shorter whiskers. The whisker incubation time was also longer for thicker layers and ambient room temperature/humidity samples grew the longest whiskers. All whiskers from Sn film thicknesses of ~5-10 μm were < 50 μm long (most suggest Sn film thicknesses of ~7μm or greater). However, thicker films cannot be considered as a countermeasure to prevent whisker growth since eventually whiskers will still grow. In a second, related study, Oberndorff et al. [70] observed no whisker growth on electroplated Sn films > 11.6 μm in thickness incubated under ambient room temperature/humidity after ~ 325 days.

Do the trends observed by Oberndorff hold for films < 2 μm? Can one expect similar results for sputtered Sn films? Whence, we have investigated the role of film

thickness on Sn whisker growth for sputtered Sn on electro-polished brass over a thin Sn film regime ranging from 375Å - 20,000Å (0.0375 μm to 2 μm). Two classes of brass substrates were utilized for this experiment. One class was brass "out of the box," meaning a purchased, unpolished specimen supplied in sheet form. The other class was brass that had been commercially electropolished. In both cases, the starting material was a commercial [71] thin sheet of muntz brass having composition Cu (63 wt %) and Zn (37 wt %), cut into several square pieces each of approximate dimensions 1 cm x 1 cm x 0.25 cm.

Sn films were deposited on the brass by using a standard magnetron sputtering system operating at an Ar gas pressure of 2-3 mTorr. The Sn target was 99.99998% pure (Kurt Lesker). The Sn film thicknesses investigated were 375, 750, 1125, 1500 Å, along with slightly thicker films of 3000, 6000, 12000, and 20000 Å. All deposited film thicknesses were measured using a stylus profilometer on a sputter-deposited Sn on Si wafer under identical deposition conditions. This procedure was necessary due to the difficulty in accurately measuring film thicknesses on (rough) brass.

In early thin film work using a similar magnetron sputter deposition system, Thornton and Hoffman [72] determined the critical pressures for the compressive-to-tensile stress transition in thin films as a function of atomic mass. This plot, shown in Figure 9, was used to determine the sputtering pressures necessary to produce thin Sn films under states of compression, tension, and zero stress. All Sn films thicknesses were deposited under a compressive stress state. After deposition, the samples were stored at ambient pressure and room temperature for several weeks until long, high aspect ratio Sn

whiskers were generated. A Cambridge Stereoscan 200 scanning electron microscope (SEM) enabled observation of the whisker growth in time.

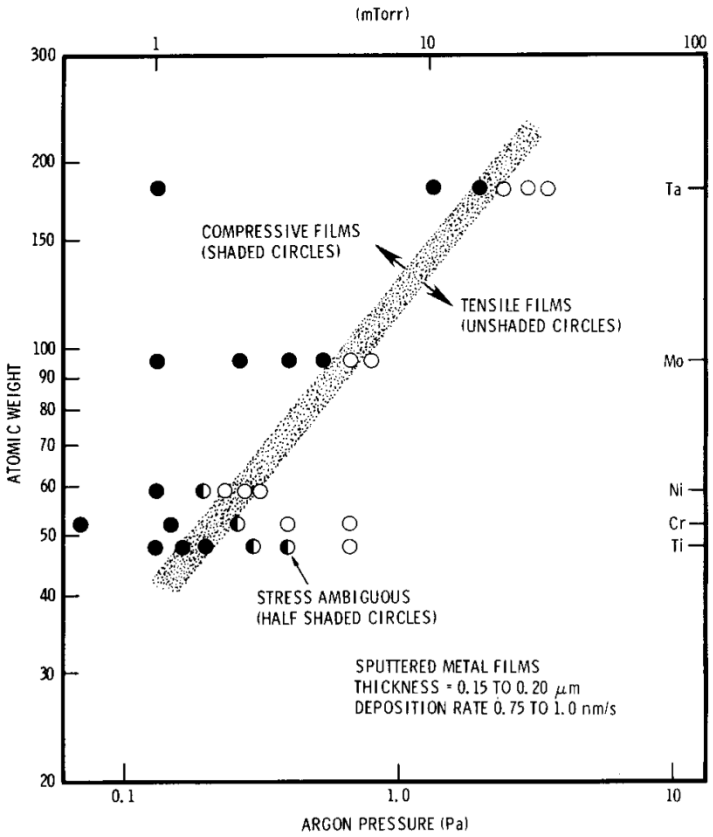

Figure 9: Atomic mass vs. working Ar pressure dependence for compressive and tensile sputter deposited metal films [72].

2.1.A Ultra-Thin Film Whiskering

After a few months of incubation in ambient room temperature/room humidity (RT/RH) the ultra-thin Sn films (375, 750, 1125, and 1500 Å) on brass were observed in the SEM, with corresponding whisker statistics shown in Table 2. It is evident that rough brass substrates produce fewer whiskers than polished brass substrates. After less than 5 months of incubation all ultra-thin Sn films on polished brass produced whiskers densities between 5,000 – 7,000 cm^{-2}, with the exception of the 1500 Å thickness with a

whisker density of only ~ 1700 cm^{-2}. Table 3 and Table 4 show the whisker statistics after further incubation periods. It is evident that all samples (polished and unpolished substrates) are producing more whiskers over time. After ~ 1.4 years of incubation, the 1125 Å film is producing the most whiskers (~ 26,000 whiskers/cm^2) and the 1500 Å film is producing the fewest whiskers (~9300 whiskers/cm^2). Figure 10 shows representative SEM photographs of the whiskers formed on the various ultra-thin Sn films.

Table 2: Whisker Statistics on Ultra-Thin Sn Films after 140 Days of Incubation

Sn Film Thickness (Å)	**Polished (P) Unpolished (U)**	**Whisker Density (cm^{-2})**	**Average Whisker Length (µm)**	**Standard Deviation (µm)**	**Mode**
375	P	5,868	73.5	112.4	14
	U	0	0	0	0
750	P	6,758	36.8	74.5	5
	U	1,048	16.5	16.4	5
1125	P	6,339	18.7	20.5	5
	U	1,938	7.6	4.4	7
1500	P	1,729	14.2	23.7	5
	U	0	0	0	0

Table 3: Whisker Statistics on Ultra-Thin Sn Films after 211 Days of Incubation

Sn Film Thickness (Å)	Polished (P) Unpolished (U)	Whisker Density (cm^{-2})	Average Whisker Length (μm)	Standard Deviation (μm)	Mode
375	P	8,225	61.6	110.2	10
	U	1,048	8.8	10.8	4
750	P	8,749	22.1	39.0	6
	U	4,768	9.0	12.8	2
1125	P	10,216	17.3	22.1	4
	U	3,824	4.8	3.5	2
1500	P	3,563	6.5	10.4	4
	U	419	4.1	1.5	3

Table 4: Whisker Statistics on Ultra-Thin Sn Films after 470 Days of Incubation

Sn Film Thickness (Å)	Polished (P) Unpolished (U)	Whisker Density (cm^{-2})	Average Whisker Length (μm)	Standard Deviation (μm)	Mode
375	P	13,885	45.5	87.9	3
	U	2,620	5.4	5.1	3
750	P	19,780	10.3	25.4	2
	U	12,837	5.6	6.0	2
1125	P	26,199	13.0	29.8	4
	U	9,956	3.6	2.5	2
1500	P	9,301	4.3	6.7	2
	U	655	2.6	0.5	3

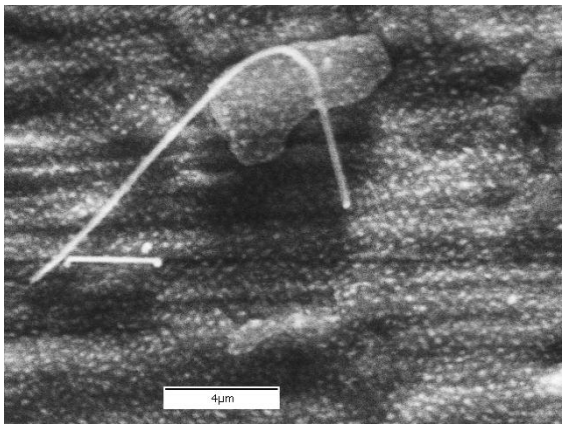

(a)

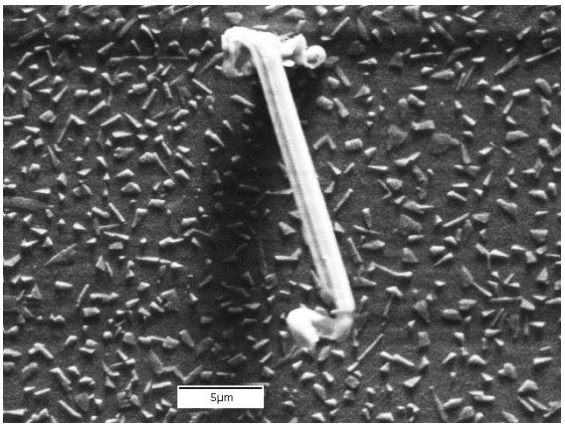

(b)

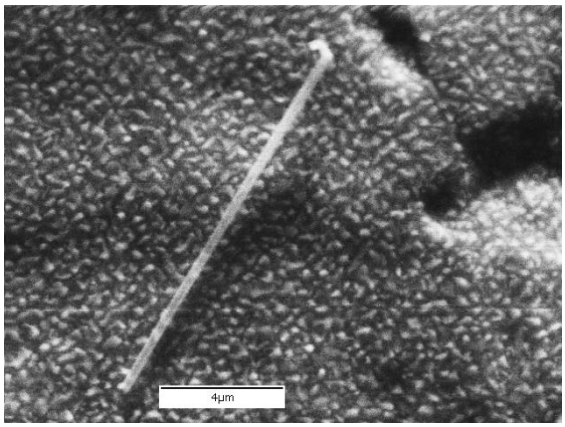

(c)

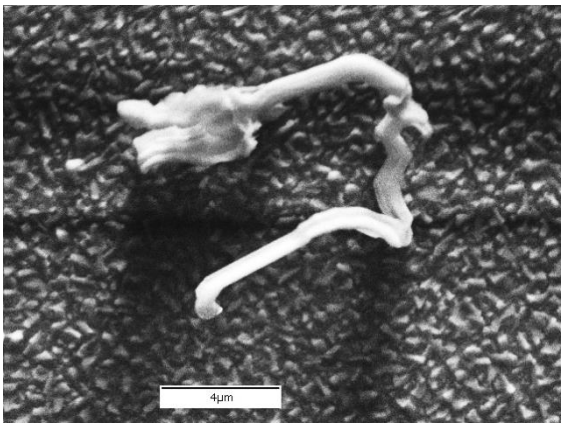

(d)

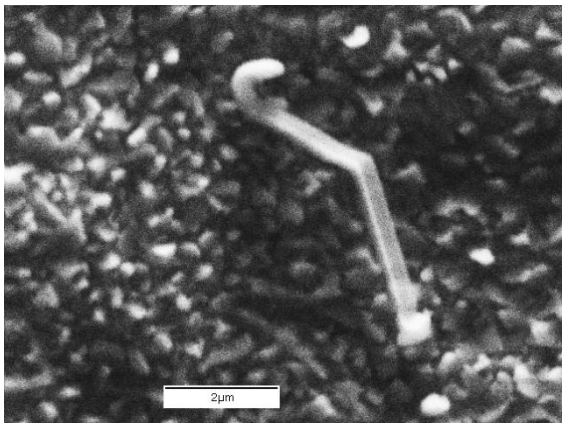

(e)

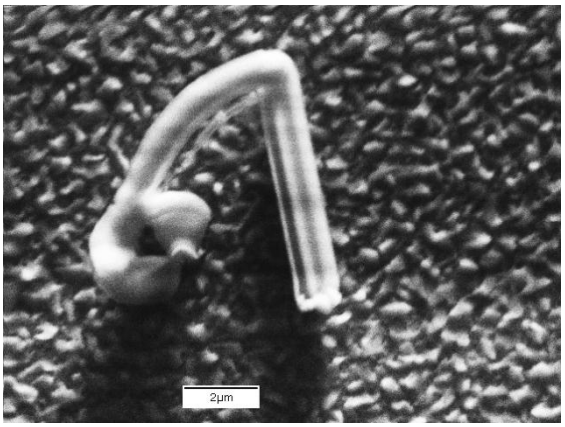

(f)

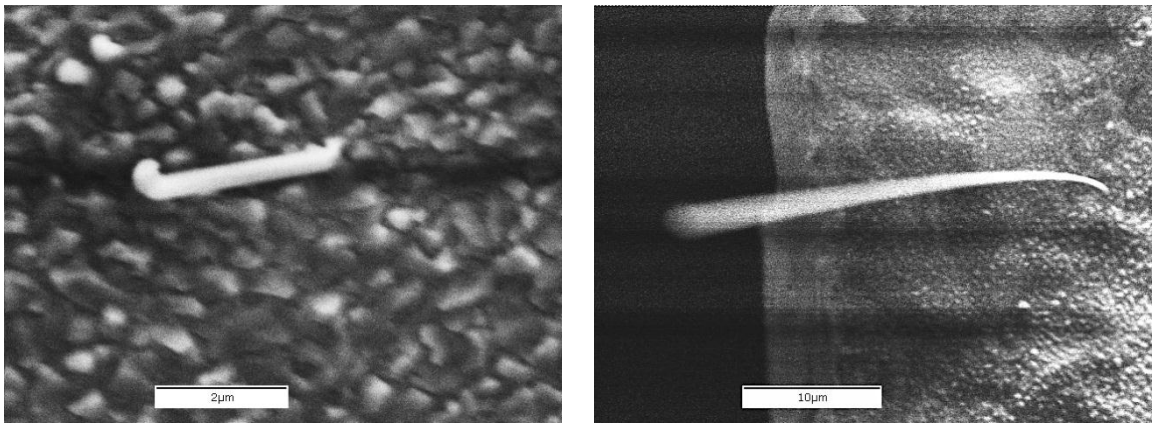

(g) (h)

Figure 10: SEM whisker images from ultra-thin Sn films on polished (P) and unpolished (UP) brass; (a) 357 Å on UP, (b) 357 Å on P, (c) 750 Å on UP, (d) 750 Å on P, (e) 1125 Å on UP, (f) 1125 Å on P, (g) 1500 Å on UP, and (h) 1500 Å on P.

In Figure 11, the whisker growth rate is plotted, which allows us to determine if we are approaching an asymptotic whisker density. Observing no plateau in the whisker density vs. time plot suggests there is still a sufficient amount of Sn feedstock left on the surface. By the use of Auger electron spectroscopy (AES) depth profiling it is possible to measure the thickness of the Sn film left after whisker growth. The depth profile was performed by successive manual sputter/spectra cycles to carefully observe when the brass substrate was reached for an accurate thickness. AES spectra in Figure 12 shows the existence of Cu and Zn at a depth of 300 Å below the free Sn surface after 211 days of incubation for the 1125 Å film, suggesting Sn film depletion during whisker growth and/or increasing Cu-Sn IMC growth during the incubation period, but still enough feedstock left to continue producing whiskers. The AES data was acquired from four evenly spaced positions over the surface of the sample, all giving the same results, which implies that the film is consuming Sn uniformly over the surface. The AES spectra in

Figure 13 on the 750 Å sample shows a Sn thickness of 25 Å after 360 days of incubation, which also appears to be depleting the Sn feedstock uniformly.

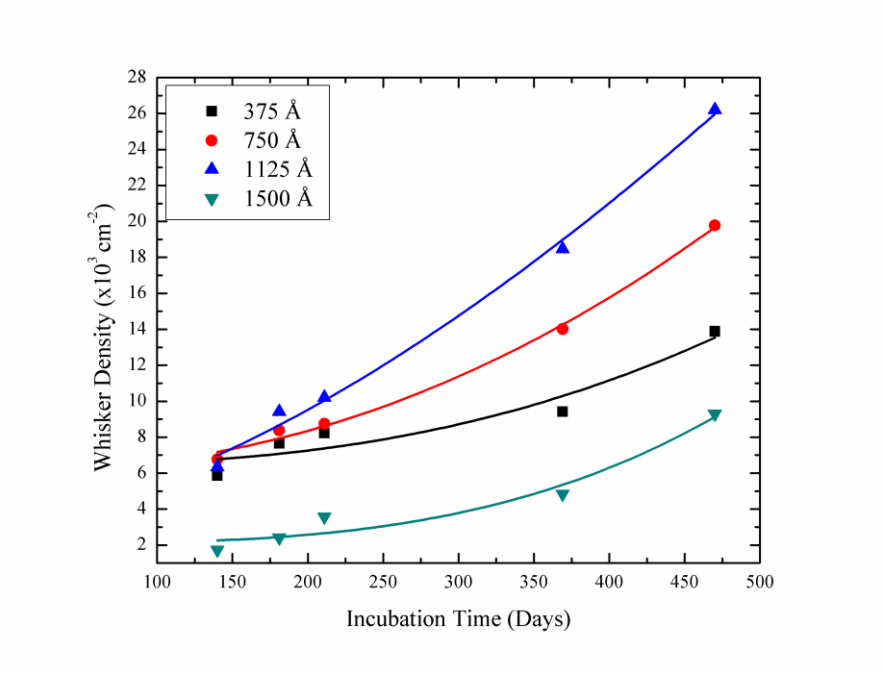

(a)

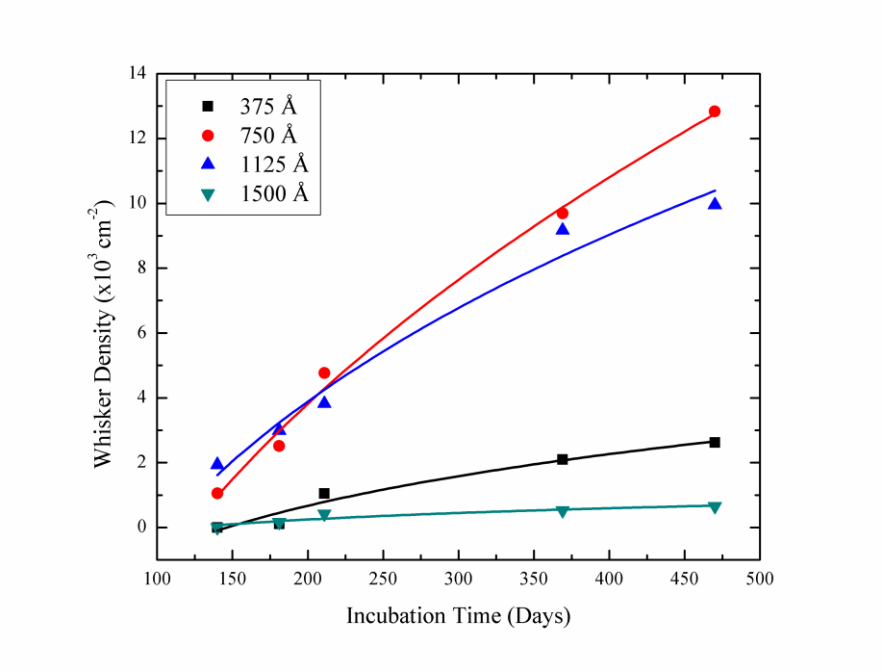

(b)

Figure 11: Whisker density vs. incubation time for Sn on (a) polished brass and (b) unpolished brass.

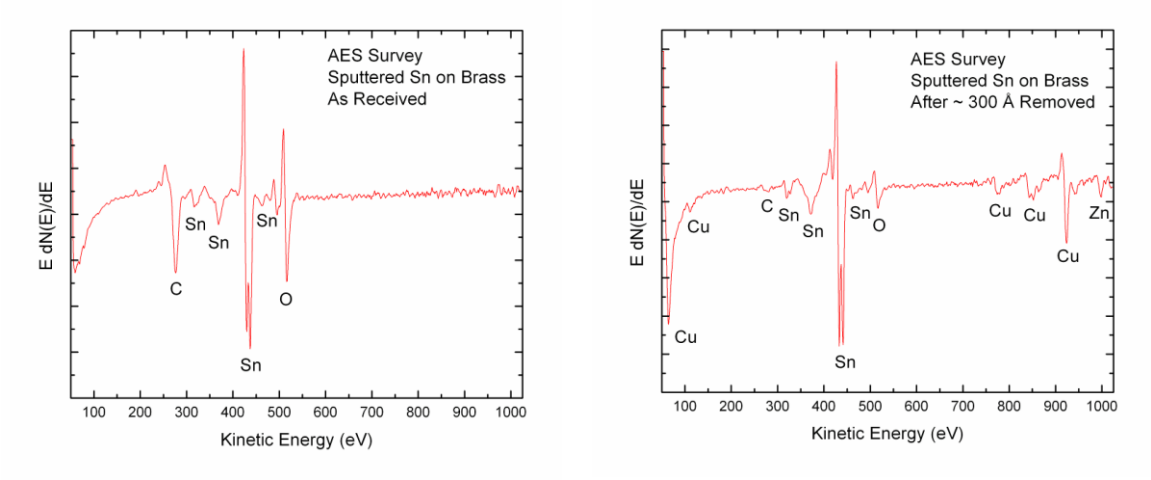

(a) (b)

Figure 12: AES survey taken after 211 days of incubation for the case of 1125 Å Sn on polished brass (a) as received and (b) after ~300 Å removed.

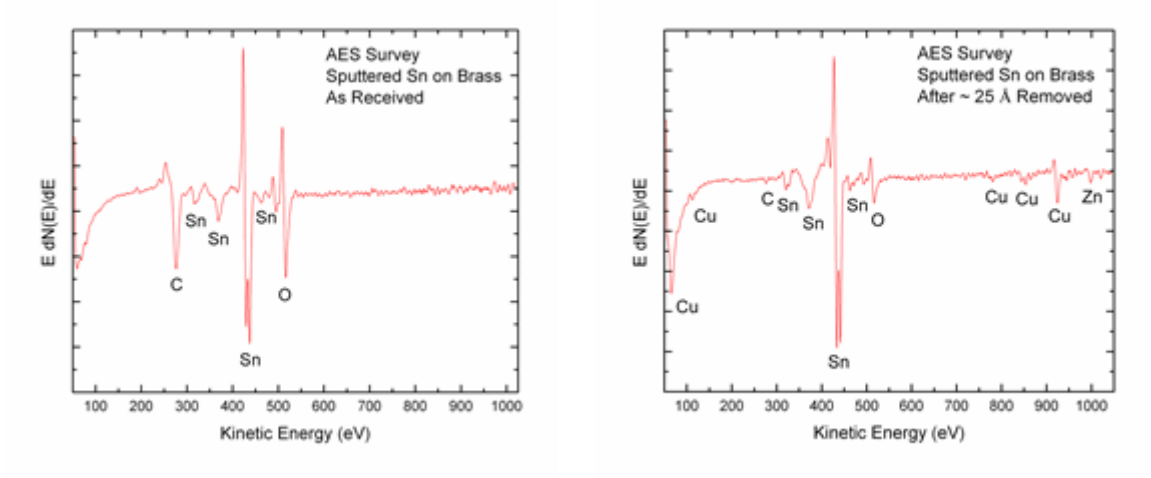

(a) (b)

Figure 13: AES survey taken after 360 days of incubation for the case of 750 Å Sn on polished brass (a) as received and (b) after ~25 Å removed.

Since we 1) observe uniform film thickness decreases during the whisker growth period and 2) do not observing local Sn depletion immediately surrounding the whisker root, a reasonable conclusion is that the Sn used to grow whiskers originates from a large range of proximity on the film. Woodruff [74] also reported data using tracer elements

and secondary ion mass spectroscopy (SIMS) showing that Sn can migrate over large distances within the film. That we see the Sn pond draining uniformly additionally supports the notion of long-range Sn migration during whisker growth. Further, we generally find that, for the case of ultra-thin Sn films, thicker Sn films produce higher whisker densities for polished brass substrates (the exception is the thickest, 1500 Å film), while for Sn on unpolished brass, the thinner films produce the highest whisker densities (the exception is the thinnest, 375 Å film). Sn film thicknesses between 750 – 1125 Å produce the highest whisker densities for polished and unpolished brass substrates. We also find that polished substrates and thinner films tend to grow the longest whiskers. This is in agreement with Oberndorff et al. [69].

2.1.B. Thicker Sn Film Whiskering

In this experiment, Sn films were sputter deposited on electro-polished brass (only) with thicknesses of 0.3, 0.6, 1.2, and 2.0 μm under compressive stress conditions. The samples were incubated at ambient room temperature/humidity and periodically observed in the SEM for whisker growth. The whisker statistics after ~ 4 months of incubation is shown in Table 5. At this point in time, the highest whisker density (~ 11,800/cm^2) is found on the 1.2 μm Sn film. However, the lowest whisker producer (6000 Å film, ~ 5,600 whiskers/cm^2) grew the longest average whiskers (~ 44 μm) compared to the thicker 1.2 and 2 μm films, with average whisker lengths around 13 μm.

Table 6 and Table 7 show the whisker growth after an extended incubation period, up to ~1.2 years. The highest whisker density is found on the thinnest 0.3 μm Sn film (~33,300 whiskers/cm^2). The 0.6 μm film is producing the lowest whisker density (~19,000 whiskers/cm^2); however it is still growing the longest whiskers, with an average

whisker length of ~ 21 μm, which is about twice the average whisker length of the next longest whisker producing specimen (the 2.0 μm film, producing an average whisker length of ~ 10 μm). SEM images of some representative whiskers from these specimens are shown in Figure 14.

Table 5: Whisker Statistics on Various Sn Film Thicknesses after 123 Days of Incubation

Sn Film Thickness (μm)	Whisker Density (cm^{-2})	Average Whisker Length (μm)	Standard Deviation (μm)	Mode
0.3	7,531	21.5	43.2	5
0.6	5,566	43.5	69.6	6
1.2	11,788	13.5	13.4	4
2.0	8,404	13.2	12.0	5

Table 6: Whisker Statistics on Various Sn Film Thicknesses after 268 Days of Incubation

Sn Film Thickness (μm)	Whisker Density (cm^{-2})	Average Whisker Length (μm)	Standard Deviation (μm)	Mode
0.3	20,959	11.0	30.3	3
0.6	9,060	33.4	92.2	3
1.2	20,522	10.1	15.8	4
2.0	16,047	9.1	10.7	4

Table 7: Whisker Statistics on Various Sn Film Thicknesses after 434 Days of Incubation

Sn Film Thickness (μm)	Whisker Density (cm^{-2})	Average Whisker Length (μm)	Standard Deviation (μm)	Mode
0.3	33,272	7.5	24.4	3
0.6	18,994	20.6	78.6	4
1.2	32,093	9.6	10.0	5
2.0	27,378	10.1	13.2	5

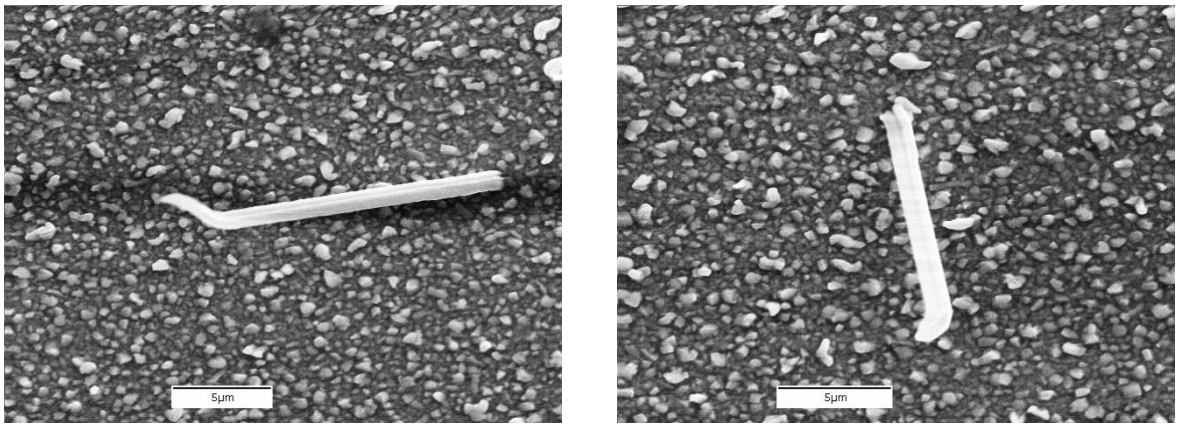

(a)

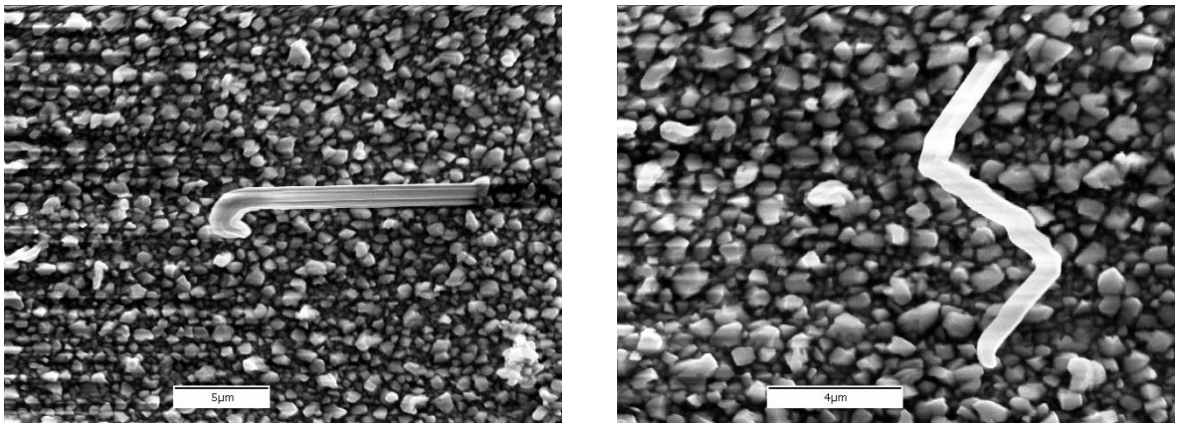

(b)

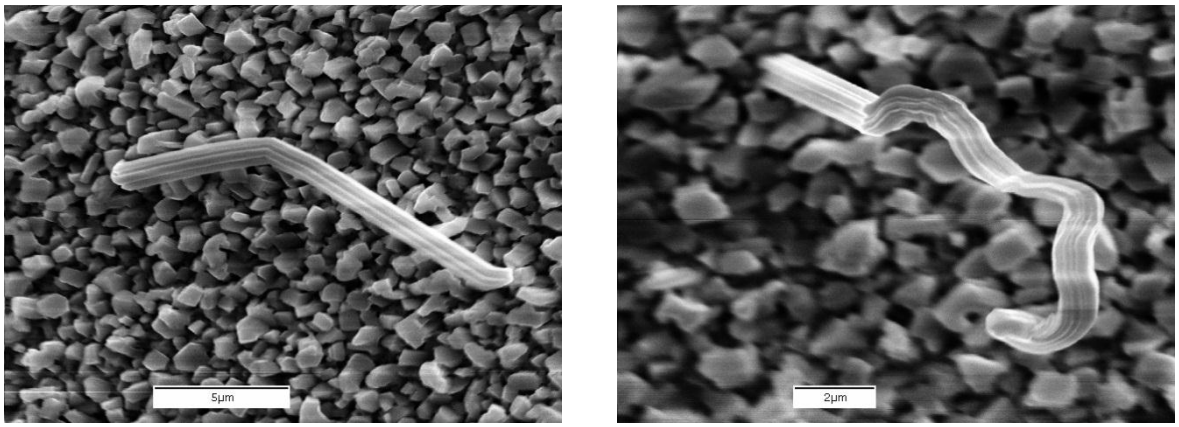

(c)

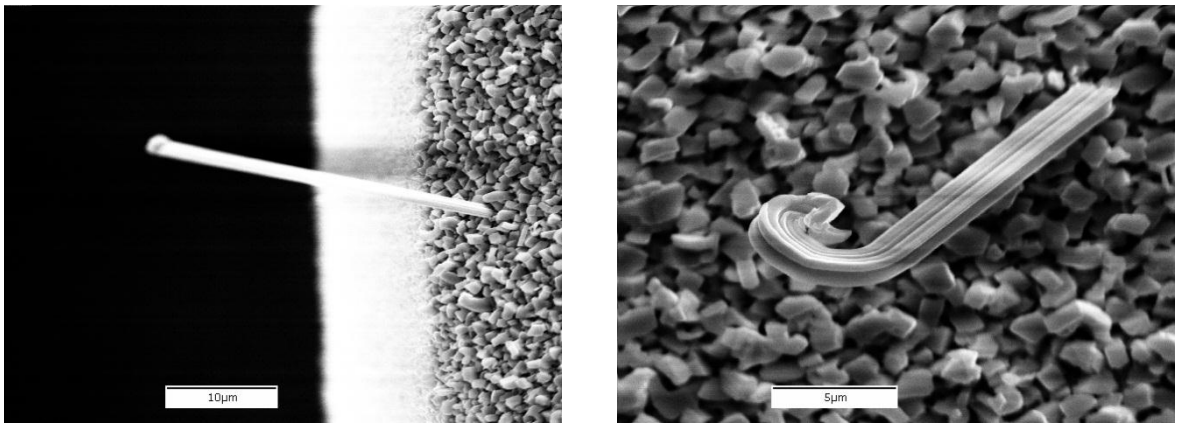

(d)

Figure 14: SEM whisker images from sputtered Sn film thicknesses (a) 3000 Å, (b) 6000 Å, (c) 12000 Å, and (d) 20000 Å on polished brass.

The whisker growth rate for each sample is shown in Figure 15. All samples are continuing to produce whiskers with no sign of a whisker density plateau. This is corroborated by AES data taken in Figure 16 on the 0.3 μm film, the thinnest of these films, which shows there is plenty of Sn feedstock remaining (existence of Cu and Zn at a depth of 625 Å below the free Sn surface after 125 days of incubation and a depth of 500 Å below the Sn surface after 165 days). The depth profiles were recorded at four widely spaced positions on the surface with similar results, which again indicates that the "Sn pond" is draining uniformly as whiskers incubate and grow.

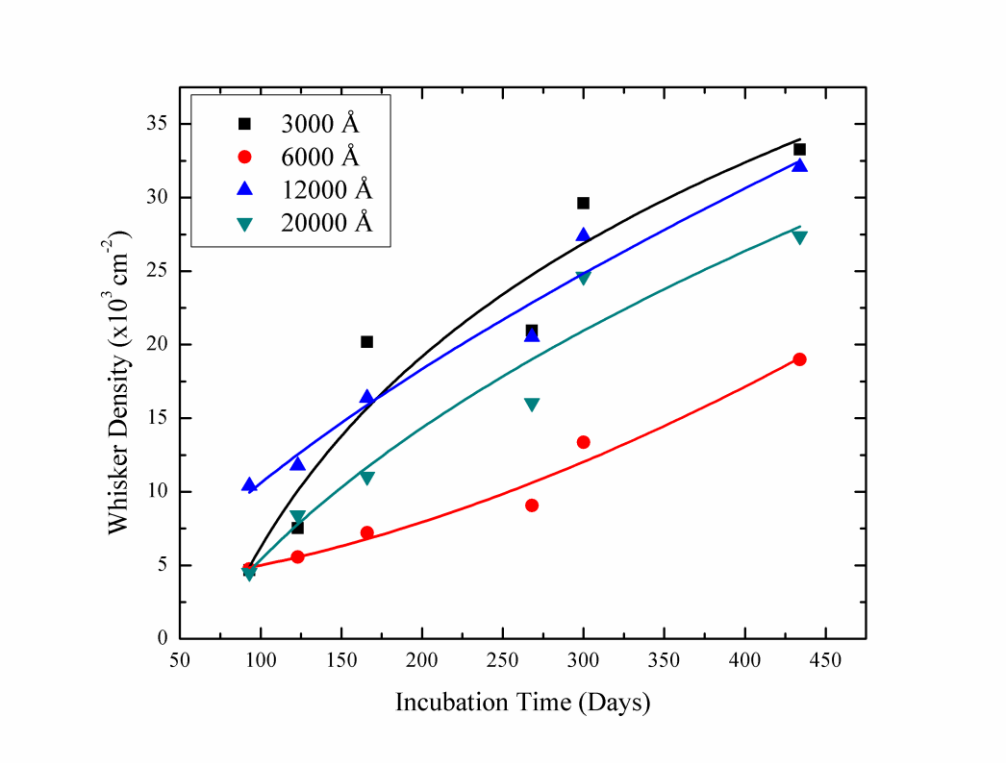

Figure 15: Whisker density vs. incubation time for sputtered Sn on polished brass.

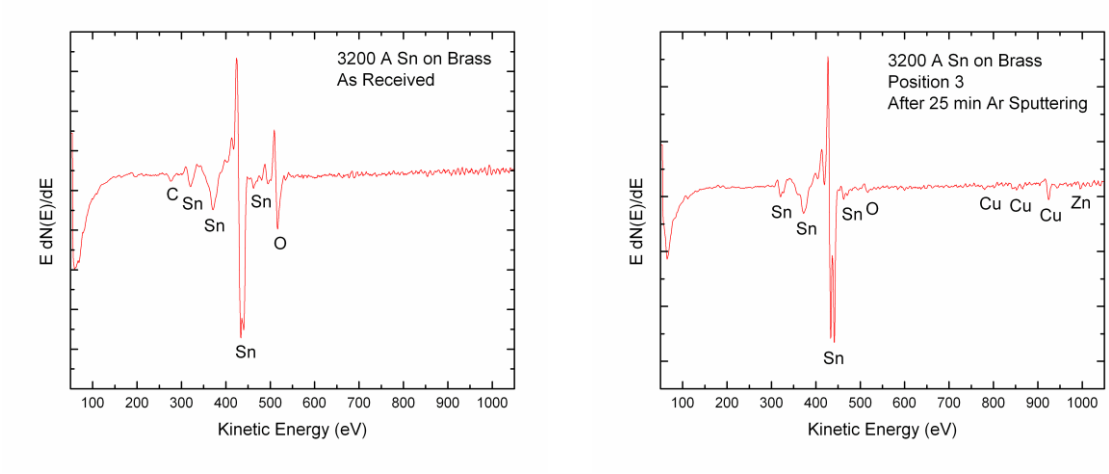

(a) (b)

Figure 16: AES survey taken after 125 days of incubation for 0.3 μm Å Sn on polished brass (a) as received and (b) after ~25 min of Ar^+ sputtering.

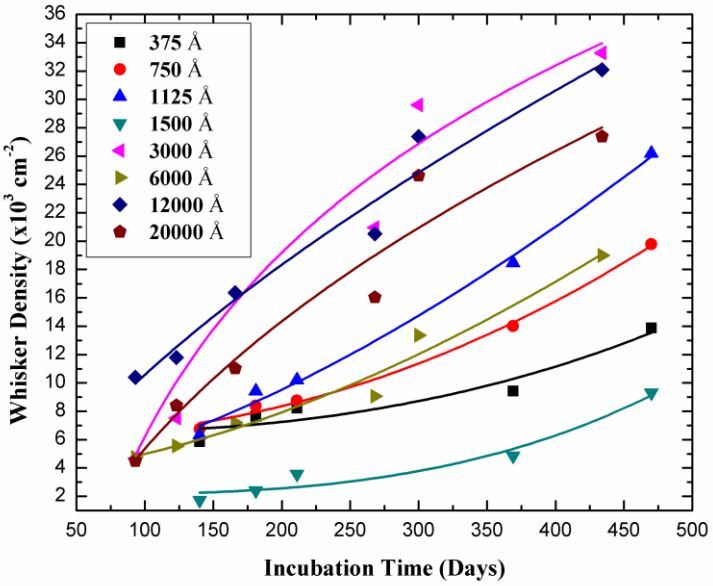
375 Å
750 Å
1125 Å
1500 Å
3000 Å
6000 Å
12000 Å
20000 Å
Whisker Density (x10^3 cm^-2)
Incubation Time (Days)

(a)

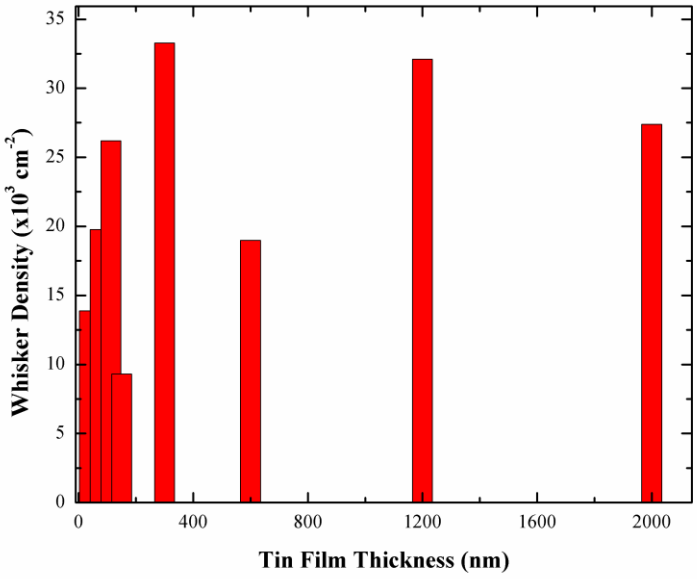
Whisker Density (x10^3 cm^-2)
Tin Film Thickness (nm)

(b)

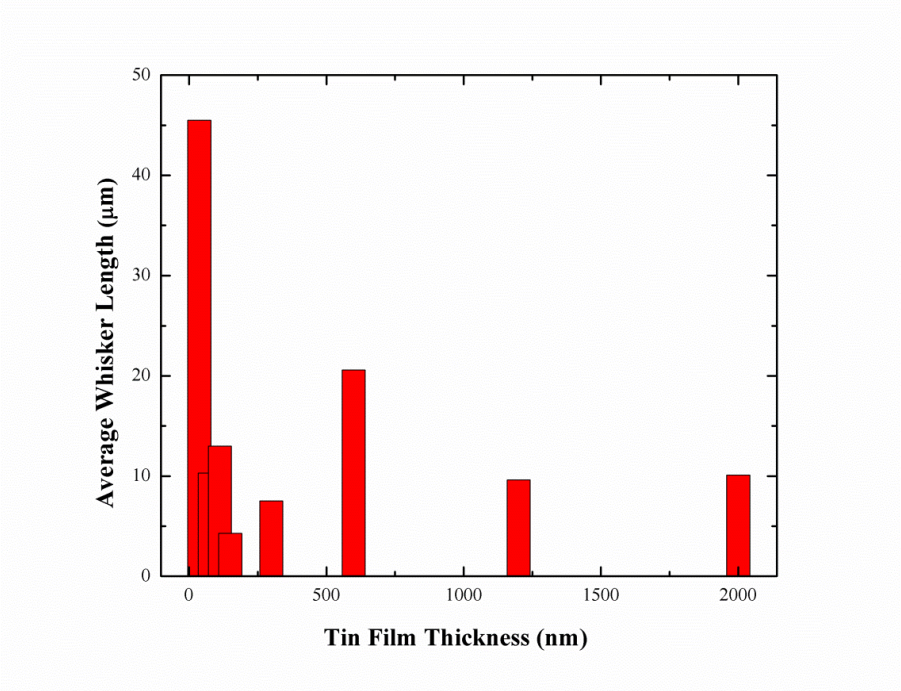

(c)

Figure 17: Comparison of whisker growth vs. film thicknesses on polished brass (a) whisker density vs. incubation time, (b) whisker density vs. Sn film thickness, and (c) average whisker length vs. Sn film thickness (up to ~ 450 days).

Figure 17 compares the whisker density and whisker length vs. film thickness for the full range of Sn film thicknesses. On polished brass, we find that thicker films produce higher whisker densities, with an optimum of film thickness of 3000 Å. The case of polished brass is different from a wide variety of other whisker growth experiments reported in this thesis, which characteristically show that thinner films produce more whiskers. It is not clear at the moment what is causing this variation, except to note that brass suffers from the complication of the Su-Cu intermetallic compounds at the interface which, for the thin films studied here, may be dominating the interfacial mechanics. From Figure 17(c), the thinnest, 375 Å film produced the longest whiskers (one whisker up to 577 μm long) and the thickest (12,000 and 20,000 Å) films grew the shortest (with one exception in the 1500 Å Sn film). This trend largely follows

the results seen by Oberndorff et al. [69], where thinner films grew longer whiskers and the thicker films produced shorter whiskers.

2.2 Whisker Growth from Patterned Arrays of Deposited Sn

By use of high lateral resolution AES measurements on Sn whiskers grown on brass, it has been shown by Bozack et al. [73] that a whisker is 100% Sn at all locations along the whisker shaft, including the growing blunt end of the shaft and with depth (~ 1000 Å) into the whisker, with no observation of brass pull-up in the whisker. Since Sn whiskers are composed entirely of Sn, with no indication that the deposition substrate is pulled up into the whisker, an important question to address is the origin of the Sn in the whisker, known as the feedstock issue. We addressed this issue above in our earliest whisker experiments and report further nuances on it here.

The fact that brass was not observed in the whisker shaft supports the notion that whisker formation is accompanied by material mass transport through interfaces and grain boundaries which causes stress (usually compressive) relief. Direct evidence of lateral diffusion of Sn during whisker growth was reported in elegant tracer experiments performed by Woodrow [74]. The existence of substantial lateral mass transport during whisker growth is also supported by one of the most remarkable aspects of whisker growth; namely, that high aspect ratio Sn whiskers ~ 100-500 μm in length containing no brass can be grown from **submicron** thin films of Sn. In this section, we explore this fact in more detail by asking whether a minimum amount of deposited Sn is necessary to produce whisker growth. We have done this by studying Sn whisker growth on ultra-thin (< 2000 Å) *patterned arrays* of Sn on brass, where it may be possible to observe a maximum growth length and, in addition, determine if the surrounding Sn in the array

element is *used up* during the whisker growth. The ideal result we anticipated was that, over a sufficiently long growth period, the patterned array of Sn would *disappear* as the surrounding Sn was consumed during whisker growth. Further, by studying Sn whisker growth on variously sized square and circular areas of Sn, we surmised that it may be possible to directly observe lateral surface diffusion by examining the region between the deposited features, which would be initially devoid of Sn. Last, since whisker growth is connected to high stress, we anticipated that we may observe more whiskers at the corners of rectangular shaped array elements than for circular array elements. While the final results of this experiment proved to be disappointing, one valuable observation gleaned was that optimum whisker growth seems to be favored by a large lateral supply of Sn.

Two deposition substrates were selected for the experiment. The substrates were polished and unpolished brass of composition Cu (63 wt %) and Zn (37 wt %). The patterned Sn films were deposited by sputtering through open apertures in various grid structures [75,76] laid atop the growth substrate. The grids are commonly used in transmission electron microscopy for calibration purposes. The Sn deposition was carried out at a chamber Ar gas pressure of 2-3 mTorr, which produces compressive stress in the Sn films. The deposited Sn thicknesses were 1200 and 2000 Å for Sn on brass. Due to the difficulty in measuring film thicknesses on (comparatively rough) brass, the deposited film thicknesses were measured using stylus profilometry on a Sn on Si wafer sputtered under identical conditions. After deposition, the samples were stored at ambient room temperature/humidity and monitored periodically for whisker growth. The grid structures are shown in Figure 18 with details in Table 8. Images of the

resulting deposited Sn patterns are shown in Figure 19. The colored boxed regions in Figure 19 indicate the specimen location where whisker statistics were gathered.

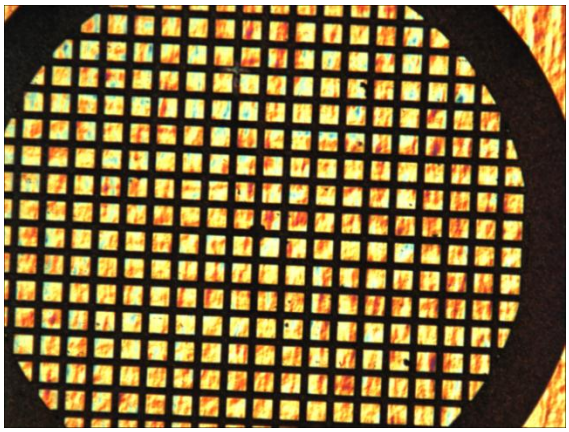

G200

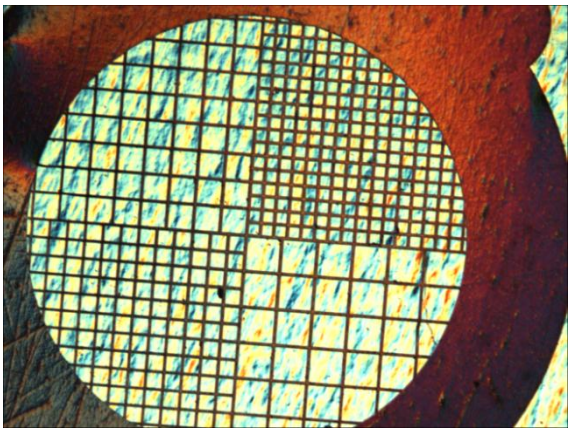

TVM

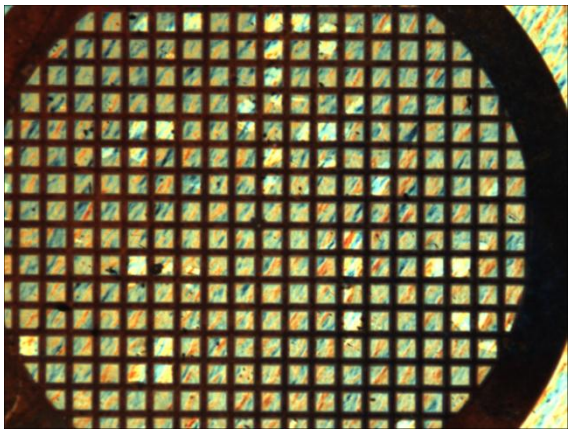

CF-MH-2C

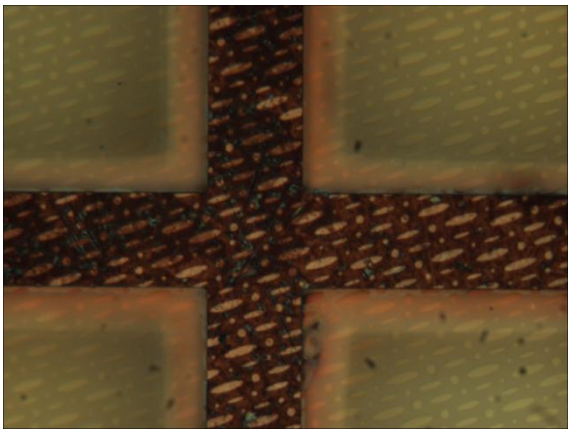

CF-MH-2C (higher mag)

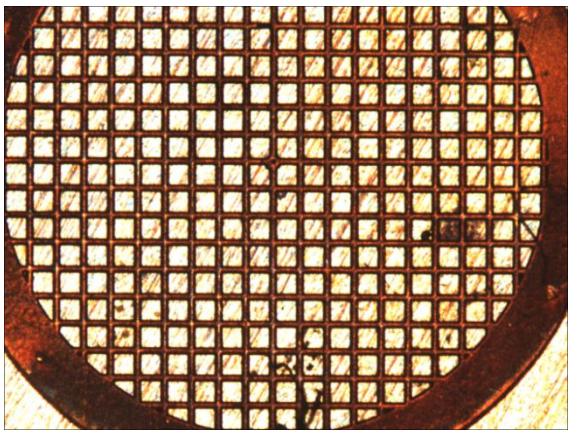

CF-4/2-2C

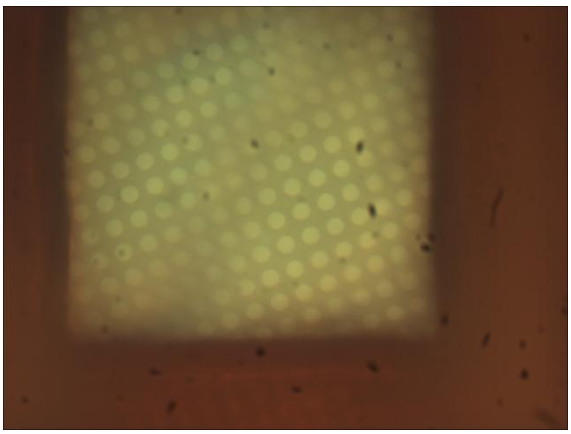

CF-4/2-2C (higher mag)

Figure 18: Normarski (optical) microscope images of patterned grid structures used for patterned Sn deposition.

Table 8: Pattern Dimensions for Grid Structures

Fixed Aperture Grids		**Corresponding Pattern Size**
G75		285µm x 285µm square, w/ 55µm spacing
G100		205µm x 205µm square, w/ 45µm spacing
G150		125µm x 125µm square, w/ 40µm spacing
G200		90µm x 90µm square, w/ 35µm spacing
CF-MH-2C		Multi hope, ellipse, and spacing
CF-4/2-2C		4µm hole, w/ 2µm spacing
CF-1/1-2C		1µm hole, w/ 1µm spacing
TVM: Combination Grids	A	153µm x 153µm square, w/ 13µm spacing
	B	113µm x 113µm square, w/ 12µm spacing
	C	73µm x 73µm square, w/ 10µm spacing
	D	54µm x 54µm square, w/ 8µm spacing

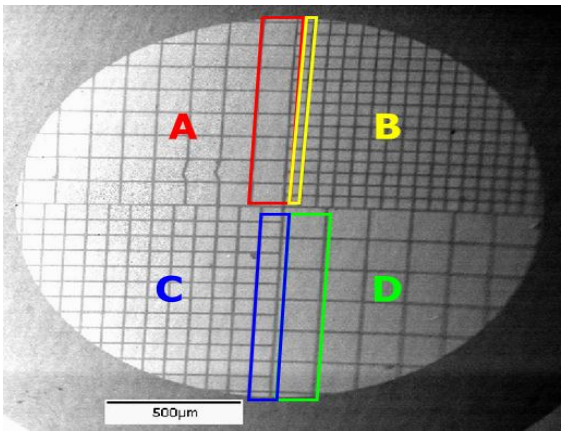

TVM

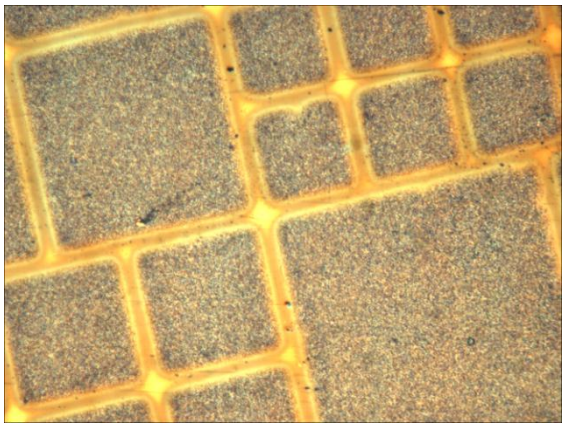

TVM (Nomarski)

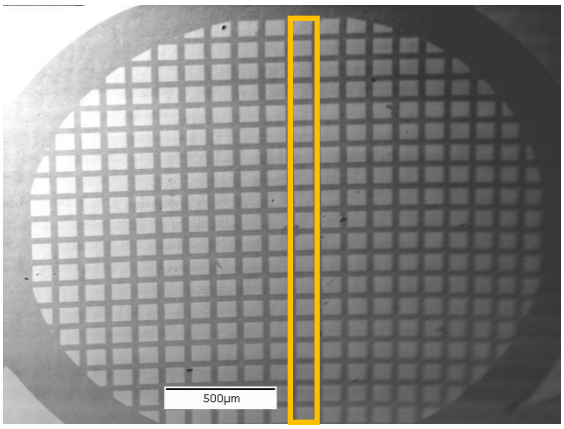

Example of Representative Grid Layout

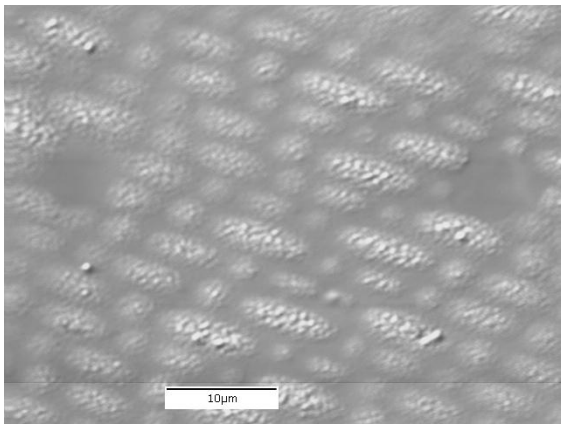

CF-MH-2C

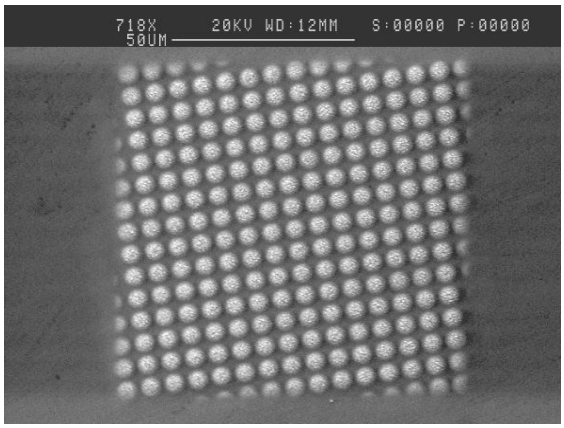

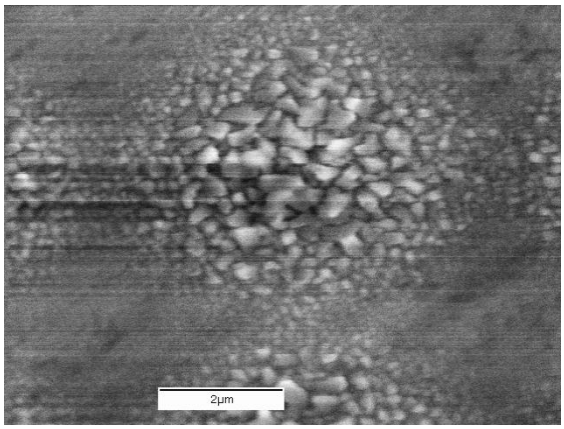

CF-4/2-2C

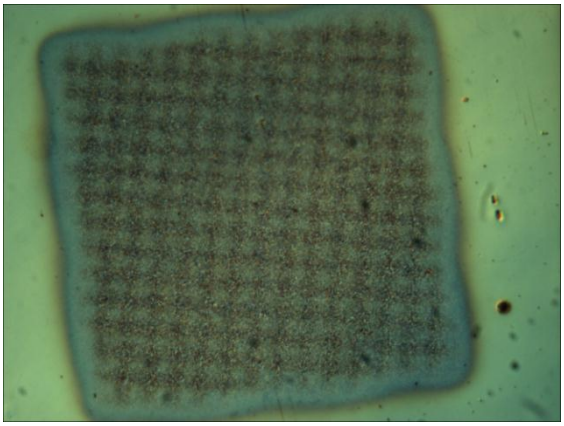

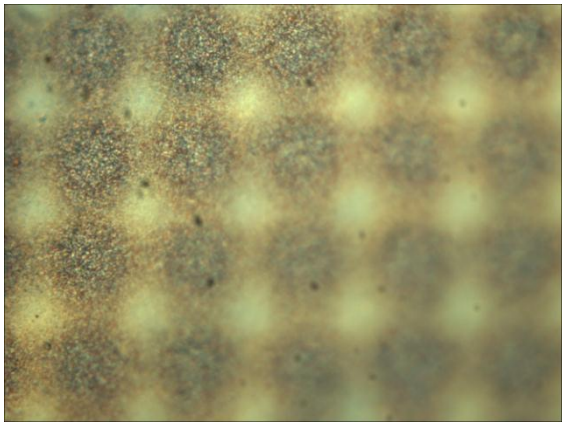

CF-4/2-2C (Nomarski)

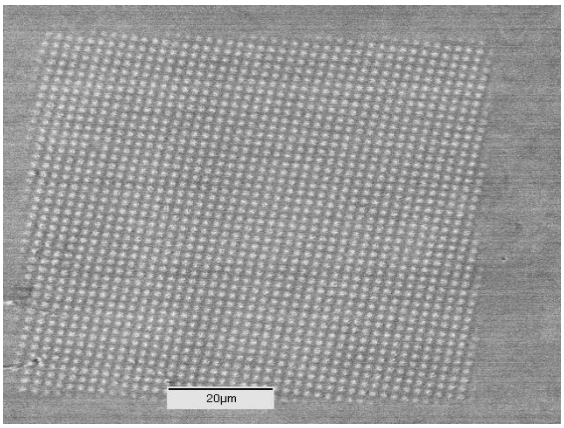

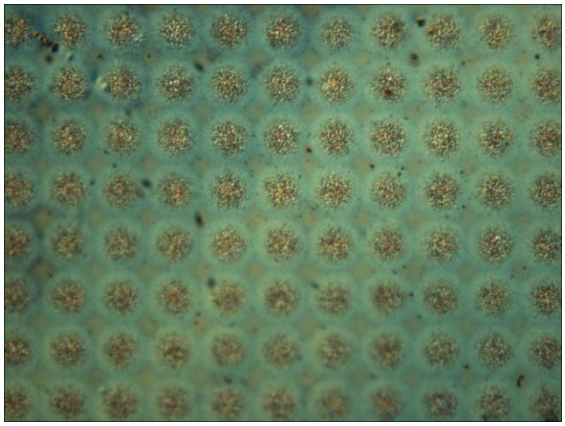

CF-1/1-2C CF-1/1-2C (Nomarski)

Figure 19: SEM and Nomarski images of deposited Sn patterns.

Table 9 shows the whisker statistics after a few months of incubation for the Sn on brass case. Most patterned areas show some signs of whiskering within the first ~ 105 days. The G75 screen (largest patterned area) has produced the most whiskers and, on the opposite end, the smallest patterns (CF-4/2-2C and CF-1/1-2C) show no whisker growth. At this incubation time, no firm conclusions can be made apropos to whisker density vs. substrate roughness. However, with further incubation up to ~ 415 days (Table 11) the polished brass produces more whiskers than the unpolished brass in nearly all cases. This agrees with our previous results. Generally, we see that the larger the patterned area, the greater the whisker growth, with the largest Sn features, G75 and G100, producing the greatest number of whiskers. The smallest, CF-4/2-2C and CF-1/1-2C, patterns are still not producing whiskers after almost 1.2 years of incubation.

In general, the overall trend in whisker growth on patterned Sn features is *significantly l*ower than the whisker numbers on un-patterned (~ 1 cm^2) Sn films deposited under similar stress conditions and incubation times. The very low whisker numbers from the smallest deposited features leads to the supposition that a minimum

size/volume of Sn may be necessary for optimum whisker growth. Table 12 shows the whisker growth after ~ 2.6 years, where there is an increase in whisker numbers from some of the larger Sn features. However, even after over 2.6 years, whisker growth is *pitifully low* from the majority of Sn patterns and *zero* on the smallest features. Further, we are not seeing any depletion zones around the whisker roots or within the patterned Sn features, nor are we observing (at least from microscopy images) any gross lateral Sn diffusion between the Sn features. Figure 20 shows some representative whiskers growing from the various patterns of Sn.

Table 9: Whisker Statistics for Sn on Brass Patterns after ~ 105 Days of Incubation

Pattern	Polished (P) Unpolished (U)	Total # of Whiskers	Average Whisker Length (µm)	Standard Deviation (µm)	Mode
G75	P	54	5.1	4.7	3
	U	28	4.6	2.3	5
G100	P	9	2.4	0.5	2
	U	1	4	N / A	N / A
G150	P	8	3	1.4	2
	U	0	N / A	N / A	N / A
G200	P	7	2	0	2
	U	8	2.5	0.76	2
CF-MH-2C	P	0	N / A	N / A	N / A
	U	3	2	0.51	2
CF-4/2-2C	P	0	N / A	N / A	N / A
	U	0	N / A	N / A	N / A
CF-1/1-2C	P	0	N / A	N / A	N / A
	U	0	N / A	N / A	N / A
TVM	P (A)	9	3.1	1.4	2
	P (B)	4	2.25	0.5	2
	P (C)	3	2.7	0.6	3
	P (D)	6	2.5	0.8	2
	U (A)	12	6.3	9.8	3
	U (B)	1	2	N / A	N / A
	U (C)	4	2.75	0.5	3
	U (D)	6	2.83	0.75	3

Table 10: Whisker Statistics for Sn on Brass Patterns after ~ 150 Days of Incubation

Pattern	Polished (P) Unpolished (U)	Total # of Whiskers	Average Whisker Length (µm)	Standard Deviation (µm)	Mode
G75	P	115	3.9	3.0	2
	U	22	3.6	0.9	3
G100	P	17	2.9	1.2	2
	U	2	2.5	0.7	N / A
G150	P	13	2.6	0.8	2
	U	0	N / A	N / A	N / A
G200	P	8	2.2	0.5	2
	U	7	2.3	0.5	2
CF-MH-2C	P	0	N / A	N / A	N / A
	U	7	2	0.51	2
CF-4/2-2C	P	0	N / A	N / A	N / A
	U	0	N / A	N / A	N / A
CF-1/1-2C	P	0	N / A	N / A	N / A
	U	0	N / A	N / A	N / A
TVM	P (A)	8	3.9	2.4	2
	P (B)	5	2	0	2
	P (C)	5	2.4	0.54	2
	P (D)	11	2.4	1.21	2
	U (A)	22	3.6	6.0	2
	U (B)	4	1.8	0.5	2
	U (C)	7	2.4	0.5	2
	U (D)	16	2.3	0.8	2

Table 11: Whisker Statistics for Sn on Brass Patterns after ~ 415 Days of Incubation

Pattern	Polished (P) Unpolished (U)	Total # of Whiskers	Average Whisker Length (µm)	Standard Deviation (µm)	Mode
G75	P	154	6.9	6.5	3
	U	35	3.9	1.7	4
G100	P	83	3.6	3.4	2
	U	7	2.4	0.5	2
G150	P	58	3.0	1.4	2
	U	1	2	N / A	N / A
G200	P	14	3.0	1.0	3
	U	2	3.0	1.4	N / A
CF-MH-2C	P	4	4.0	2.8	2
	U	8	2	0	2
CF-4/2-2C	P	0	N / A	N / A	N / A
	U	0	N / A	N / A	N / A
CF-1/1-2C	P	0	N / A	N / A	N / A
	U	0	N / A	N / A	N / A
TVM	P (A)	21	5.8	4.1	2
	P (B)	10	2.5	1.0	2
	P (C)	15	3	1.3	2
	P (D)	27	3.3	1.9	2
	U (A)	25	3.0	1.7	2
	U (B)	4	2	N / A	2
	U (C)	10	2.8	1.0	2
	U (D)	18	3.2	1.2	3

Table 12: Whisker Statistics for Sn on Brass Patterns after ~ 955 Days of Incubation

Pattern	Polished (P) Unpolished (U)	Total # of Whiskers	Average Whisker Length (µm)	Standard Deviation (µm)	Mode
G75	P	358	6.2	6.8	3
	U	38	2.7	1.0	2
G100	P	94	4.0	3.8	2
	U	7	2	0	2
G150	P	61	3.4	2.2	2
	U	1	2	N / A	N / A
G200	P	51	3.2	1.7	2
	U	4	2.3	0.5	2
CF-MH-2C	P	11	3.0	1.2	3
	U	8	2	0	2
CF-4/2-2C	P	0	N / A	N / A	N / A
	U	0	N / A	N / A	N / A
CF-1/1-2C	P	0	N / A	N / A	N / A
	U	0	N / A	N / A	N / A
TVM	P (A)	76	4.6	3.9	2
	P (B)	36	2.8	1.5	2
	P (C)	47	3.5	2.5	2
	P (D)	85	4.6	5.0	2
	U (A)	27	2.5	1.3	2
	U (B)	5	2	0	2
	U (C)	11	2.3	0.6	2
	U (D)	21	2.4	0.8	2

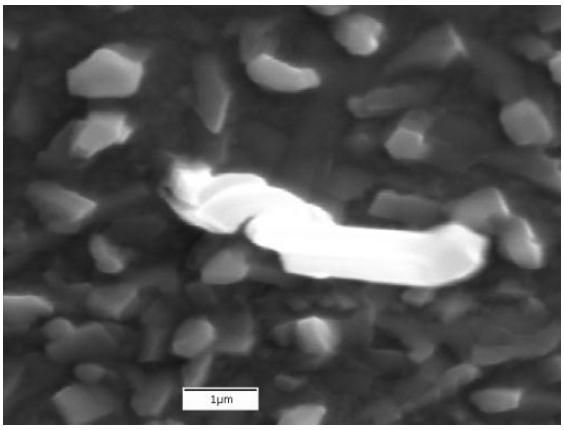

(a) G75 UP

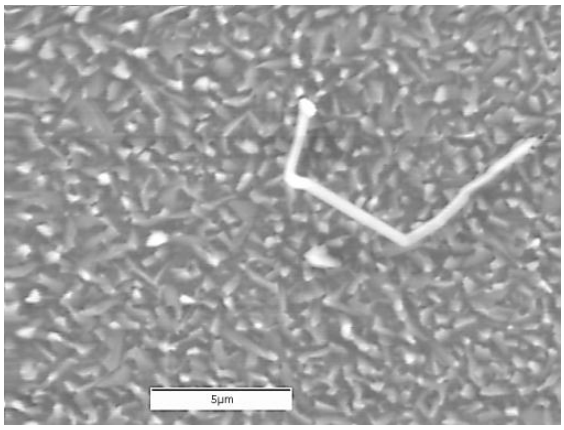

(b) G75 P

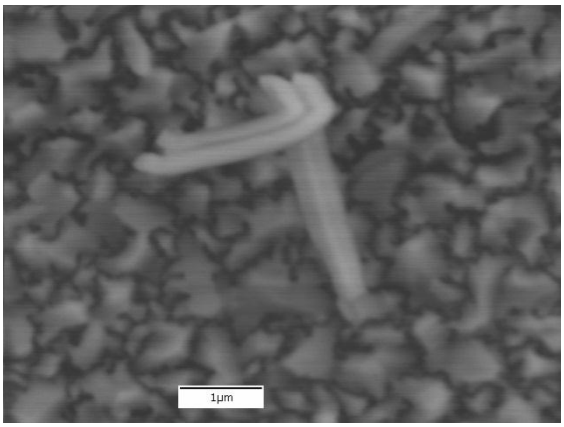

(c) G100 P

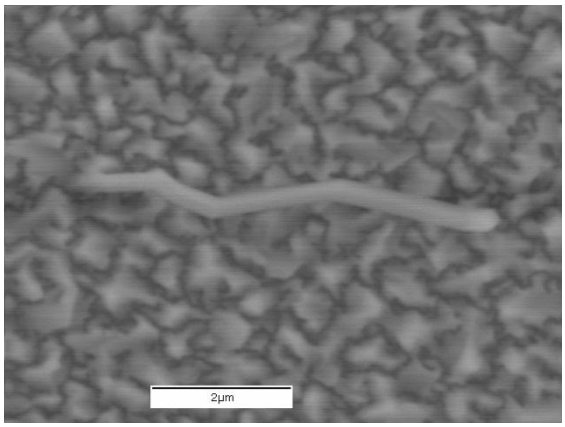

(d) G150 P

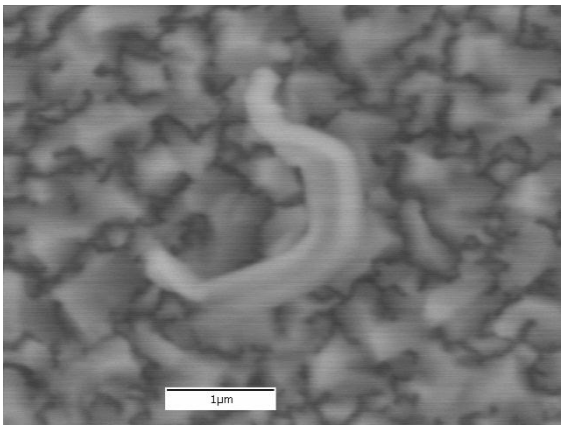

(e) G 200 P

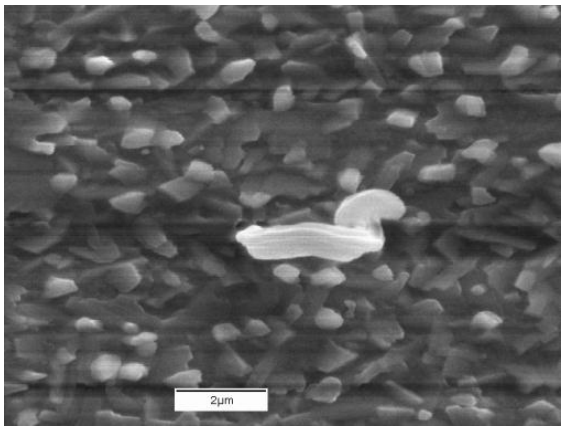

(f) TMV-A

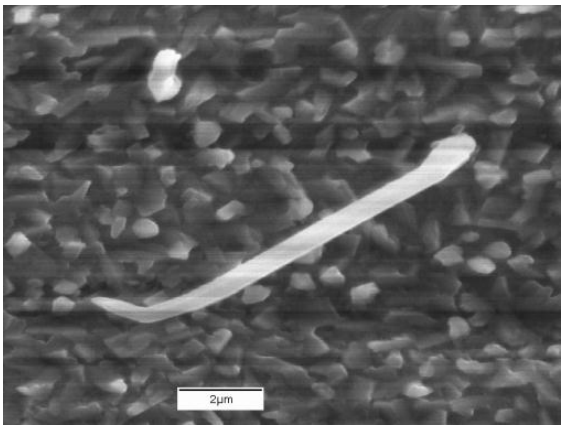

(g) TMV-B

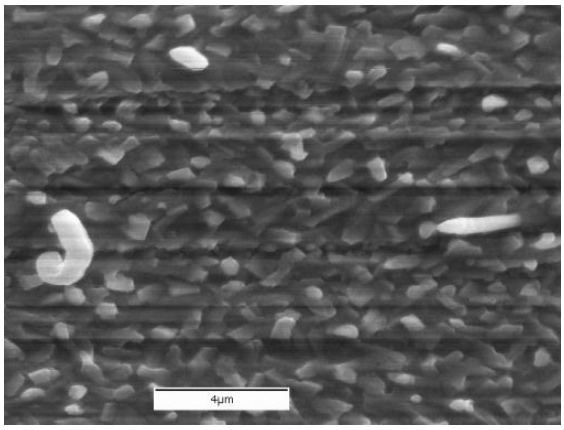

(h) TMV-C

Figure 20: SEM images of various whiskers from polished (P) and unpolished (UP) brass substrates with Sn features (a) G75 UP, (b) G75 P, (c) G100 P, (d) G150 P, (e) G200 P, (f) TMV-A UP, (g) TMV-B UP and (h) TMV-C UP screens.

2.3 A Spectacular Case: Whisker Growth from Sn on Ag Substrates

During an early search (unpublished) for fast whisker growing systems, experiments in our laboratory showed that the Sn/Ag combination was capable of producing extremely high (~ 0.25 million/cm^2) whisker densities. After several subsequent years, the Sn/Ag still holds our internal lab record for prodigious whisker growth. This subsection documents a more recent attempt to quantify this incredible whisker system. Sn films were deposited onto Ag substrates at thicknesses of 1200 and 2000 Å under compressive stress conditions. The Ag substrate was a commercial thin sheet of Ag foil [71] cut into square pieces of dimensions 1cm x 1cm x 0.25mm.

Whisker data after 3 months of incubation is given in Table 13. There is significant Sn whisker growth on both specimen thicknesses, but the thinner Sn film specimen (characteristically) has the higher whisker density. For example, the thinner 1200 Å Sn film produces a much greater number of whiskers (~116,000 whisker/cm^2) having a (slightly) longer average whisker length (10.7 μm). After 426 days of

incubation (Table 15), however, the 2000 Å Sn film grew the longest whiskers (11.5 µm). The longest whisker produced by the 2000 Å film was 394 µm long, showing again that submicron thin films of Sn can grow exceedingly long (hundreds of microns) whiskers. And then, equally amazing, is the extent of whisker growth on the 1200 Å Sn film on Ag, with over one million whiskers/cm^2 (see Figure 21). Sn on Ag is a remarkable whisker producer!

Table 13: Whisker Statistics for Sputtered Sn on Ag after ~ 90 Days of Incubation

Sn Film Thickness (Å)	**Whisker Density (cm^{-2})**	**Average Whisker Length (µm)**	**Standard Deviation (µm)**	**Mode**
1200	116,132	10.7	15.2	4
2000	66,143	8.2	6.8	3

.

Table 14: Whisker Statistics for Sputtered Sn on Ag after ~ 265 Days of Incubation

Sn Film Thickness (Å)	**Whisker Density (cm^{-2})**	**Average Whisker Length (µm)**	**Standard Deviation (µm)**	**Mode**
1200	689,023	7.5	10.3	2
2000	161,121	5.8	6.2	2

Table 15: Whisker Statistics for Sputtered Sn on Ag after ~ 425 Days of Incubation

Sn Film Thickness (Å)	**Whisker Density (cm^{-2})**	**Average Whisker Length (µm)**	**Standard Deviation (µm)**	**Mode**
1200	1,303,505	8.4	12.6	3
2000	578,989	11.5	24.9	3

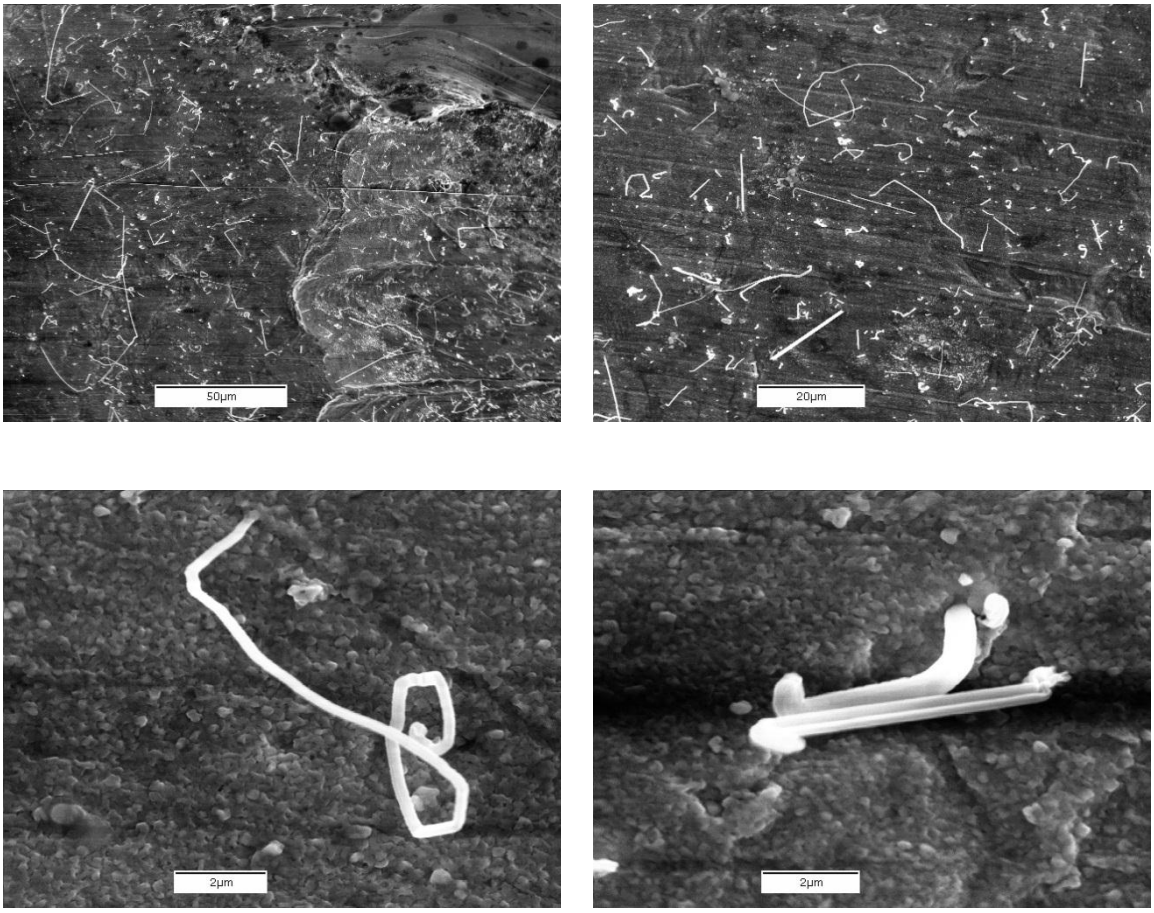

(a)

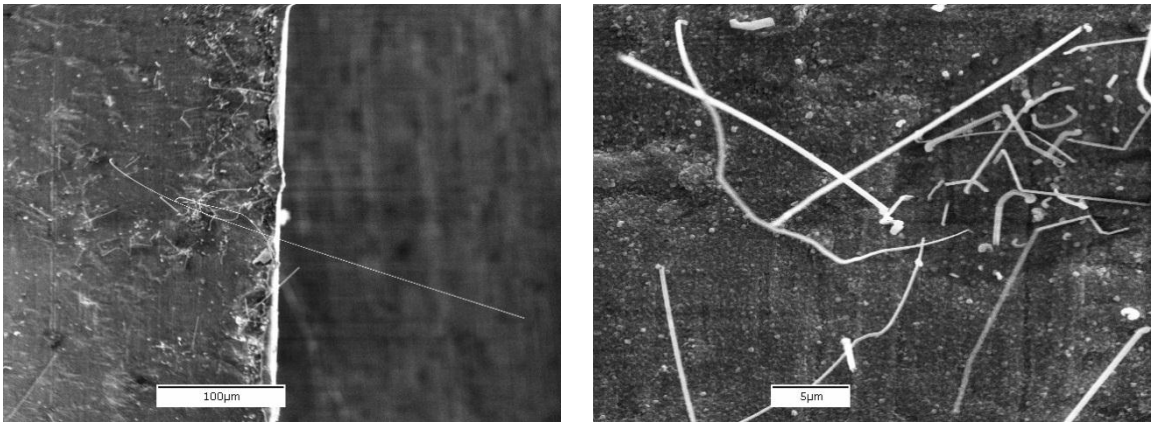

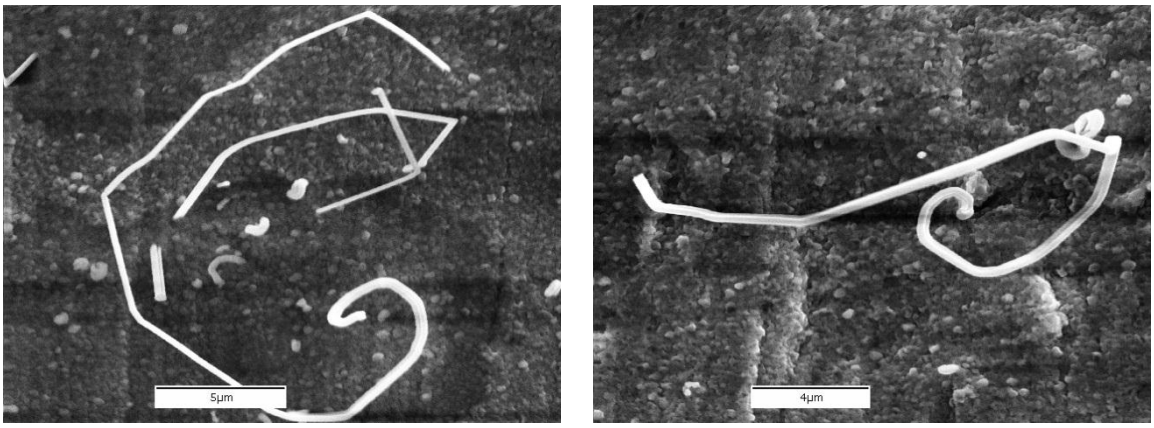

(b)

Figure 21: SEM images of whisker growth from Sn films of (a) 1200 Å and (b) 2000 Å on Ag substrates.

A plot of whisker density vs. time is shown in Figure 22. Even at the end of one year, Sn on Ag continues to form whiskers at high rates, with no sign of a plateau or even a decrease in whisker growth.

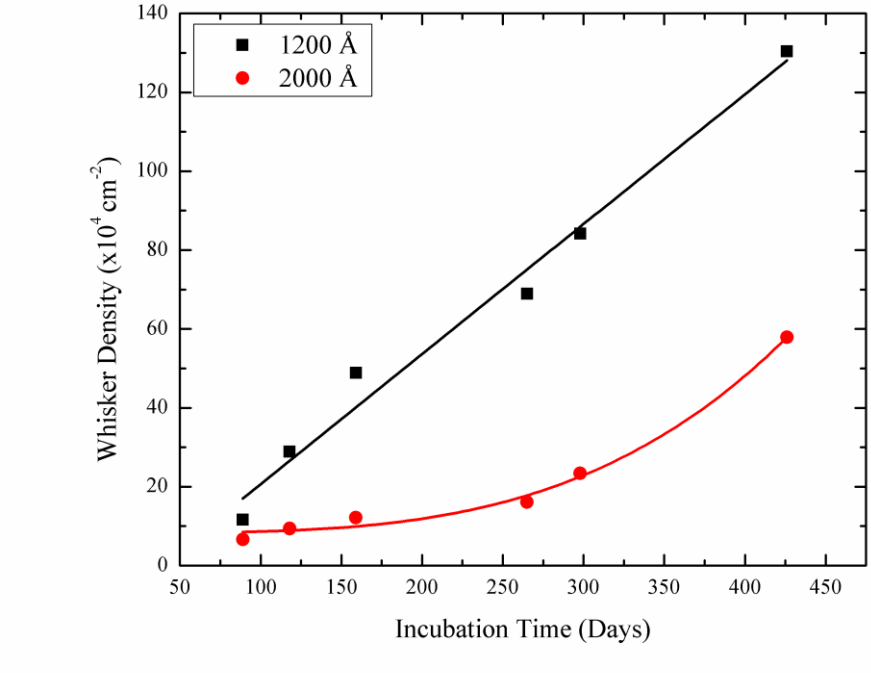

Figure 22: Whisker density vs. incubation time for Sn on Ag.

Such a fast growing whisker system offers an optimum test bed to investigate how the "Sn swamp" is draining during whisker growth. Whence, AES depth profiling was carried out on the 1200 Å film. Figure 23 shows the results of drilling ~ 600 Å (12 min of AES depth profiling at ~50 Å/min) into the Sn film after 120 days of incubation. The height of the Ag Auger feature at this depth in the Sn film shows that roughly half of the Sn remains after 4 months of whisker growth. By repeating the measurement at four widely spaced areas on the specimen (Figure 24) similar results suggest once again that the Sn feedstock is draining uniformly during whisker growth. We will show data later in the thesis which investigates the feedstock drain idea more carefully using Rutherford backscattering spectroscopy.

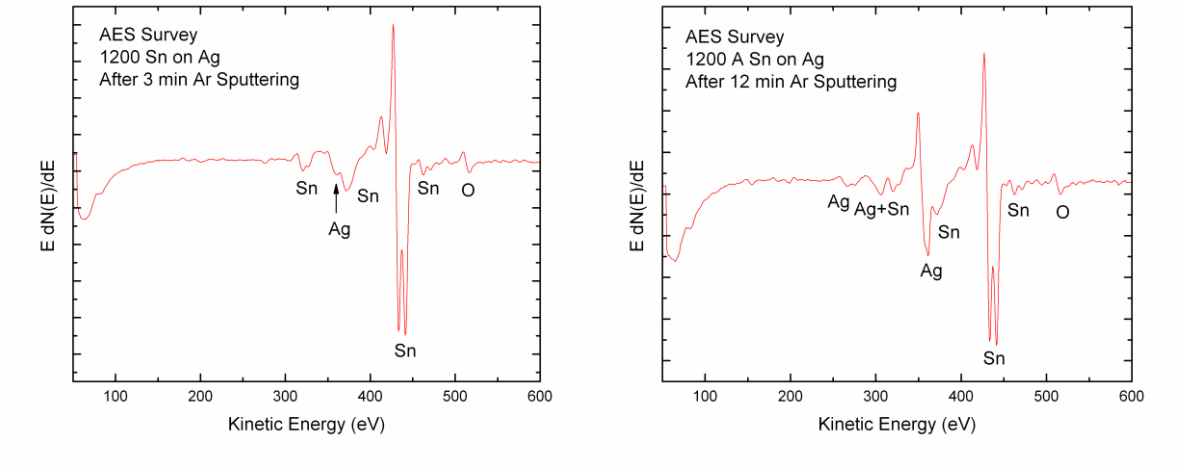

(a) (b)

Figure 23: AES survey taken after 120 days of incubation on 1200 Å during sputter depth profiling of (a) 3 min and (b) 12 min.

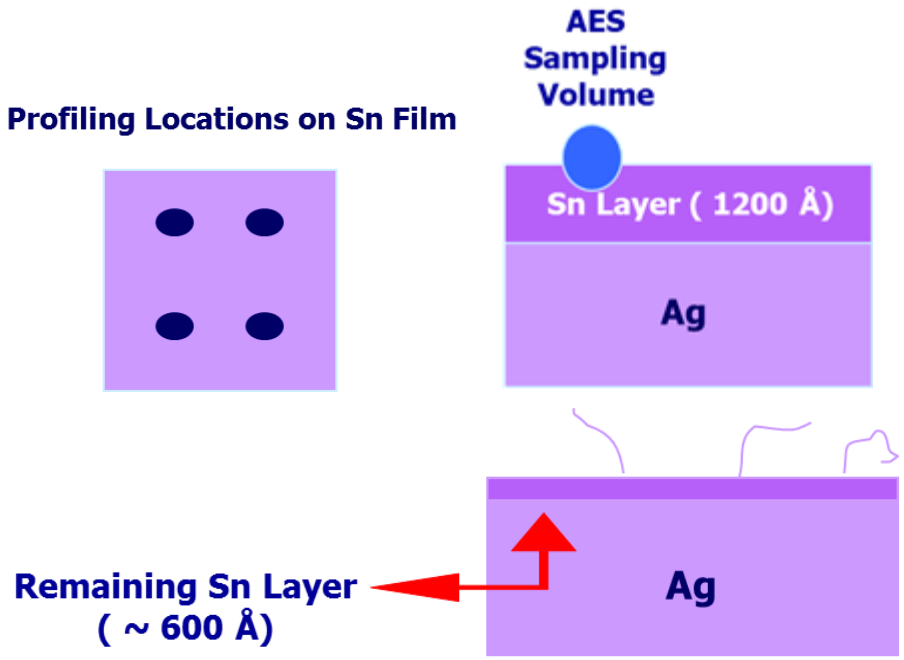

Figure 24: Cartoon of AES depth profiling into the 1200 Å Sn film on Ag.

2.4 Sn/Substrate Combinations Which Eliminate the Influence of Intermetallic Formation

Many studies of Sn whiskers have emphasized the role of intermetallic compound formation at the tin-substrate interface, which is believed to induce a high compressive stress state in the film [77,43]. The increased compressive stress in high tin plated components (on Cu) is thought to be a major contributor to Sn whisker growth. The goal of the work in this subsection is to characterize whisker growth from sputtered Sn films where intermetallic compounds (IMC) are **absent** and compare to sputtered Sn films where IMC's are known to exist. A corollary purpose of our studies was to see whether differences in whisker production *between* the chosen substrates could be attributed to coefficient of thermal expansion (CTE) mismatches, which invariably exist when different materials are mated as a bimetallic strip. While CTE effects on whisker growth are expected to be small for material systems maintained at isothermal temperatures, it is

nonetheless useful to be aware of possible effects owing to CTE variations between film and substrate. For the record, Table 16 shows a substantial CTE mismatch between Sn and the various substrates in this study (Si, Ge, GaAs, InP, InAs, and glass), but very little mismatch between the substrates *themselves*.

Table 16: Comparison of Linear Coefficients of Thermal Expansion

Substrate	**CTE[#] (10^{-6} K^{-1})**	**ΔCTE***	**%ΔCTE***
Sn	23.4	0	0
Si	5.1	18.3	78.2
Glass (pyrex)	4	19.4	82.9
InP	4.6	18.8	80.3
GaAs	5.7	17.7	75.6
InAs	4.5	18.9	80.8
Ge	6.1	17.3	73.9

#Refs. [78,79]; *Compared to Sn

A pure Sn sputter target (99.999%, Kurt Lesker Co) was used to deposit 1600Å Sn films on a variety of semiconductor and insulator surfaces (Si, Ge, GaAs, InP, InAs, and glass) in a magnetron sputtering system. The film thickness was verified by stylus profilometry over a step edge in the deposit. The semiconductor and glass substrates were commercial, wafer thickness specimens. The Sn films were sputtered at argon pressures of 2-3mT which produced an intrinsic compressive stress in the Sn films [65]. The samples were then incubated under ambient room temperature/humidity (RT/RH) conditions followed by periodic whisker counts for many months using a Cambridge scanning electron microscope (SEM). After four months (120 days) of incubation and

whisker growth, the Sn films were examined using Auger electron spectroscopy (AES) and Rutherford back scattering (RBS) techniques in order to measure the Sn film thickness as a function of growth time.

After ~ 50 days of incubation in ambient room temperature/humidity conditions, the growth of Sn whiskers on the various film combinations was recorded by SEM. The whisker densities were determined by manually counting whiskers over ten equal representative areas (~275 µm x 275 µm) on the surface. Table 17 shows the whisker growth statistics. All Sn film/substrate combinations produced whiskers after 54 days of incubation. Si and Ge substrates yielded the largest whisker densities of 15,195 and 19,911 whiskers/cm^2 respectively. Si and Ge also produced the longest average whisker lengths, with 6.6µm for Si and 7.5µm for Ge. The Sn on glass substrate shows the lowest density of whiskers (262 whiskers/cm^2) along with the shortest average whisker length of 2.5µm.

Table 17: Whisker Statistics after 54 Days of Incubation

Substrates (1600 Å Sn film)	**Whisker Density (cm^{-2})**	**Average Whisker Length (µm)**	**Standard Deviation (µm)**	**Mode***
Si	15,195	6.6	9.1	2
Glass	262	2.5	0.7	N/A
InAs	655	6.0	3.5	N/A
GaAs	7,074	4.2	3.8	2
InP	3,668	3.3	1.6	2
Ge	19,911	7.5	7.6	2

*Mode is defined as the most frequently observed whisker length

Table 18 shows the whisker statistics after another two months of incubation (total of 116 days). The Sn on Si and Ge specimens are still producing the largest whisker densities, surpassing 35,000 whiskers/cm^2; however, Sn on InAs, GaAs, and InP are producing the longest average whisker lengths (InAs leads with an average whisker length of 8.3μm). Further, during the additional two months of incubation, Sn on InAs, GaAs, and InP combinations show sudden increases in whisker growth, resulting with 21,000-28,000 whiskers/cm^2. In contrast, Sn on glass still lags in whisker density (1,703 whiskers/cm^2) with an average whisker length (2.5μm) compared to the other semiconductor and insulator substrates. Though high whisker densities are produced over the various Sn/substrate combinations, the average whisker lengths for all the samples are only in the single digits. A representative sample of the high aspect ratio whiskers produced on the various films is shown in Figure 25. Figure 26 illustrates the whisker density vs. incubation time for each sample.

Table 18: Whisker Statistics After 116 Days of Incubation

Substrates (1600 Å Sn film)	**Whisker Density (cm^{-2})**	**Average Whisker Length (μm)**	**Standard Deviation (μm)**	**Mode***
Si	38,512	6.5	7.9	2
Glass	1,703	2.5	0.7	2
InAs	23,710	8.3	5.8	6
GaAs	27,378	6.9	6.5	2
InP	21,221	6.9	6.2	2
Ge	39,167	6.6	6.8	2

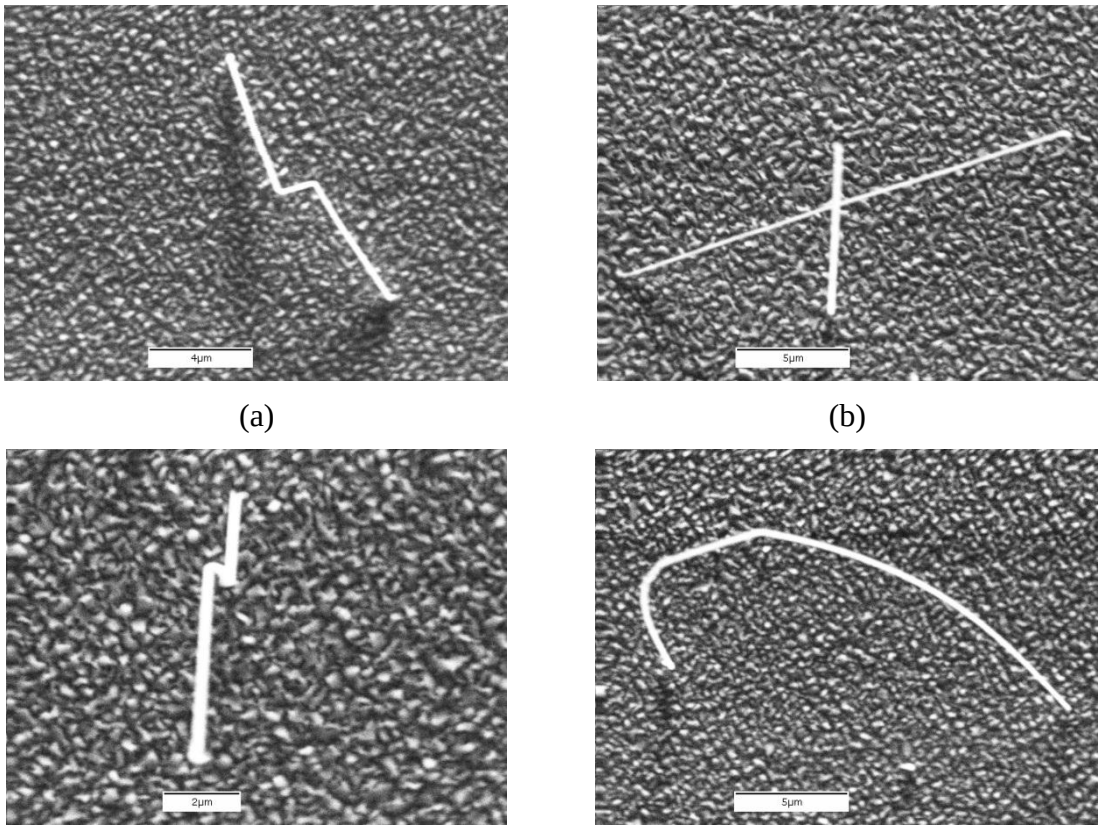

(a) (b)

(c) (d)

Figure 25: Representative whisker morphologies produced on various Sn/semiconductor combinations (a) Sn on GaAs @ 4270X, (b) Sn on InP @ 3760X, (c) Sn on Si @ 6350X, and (d) Sn on GaAs @ 3760X.

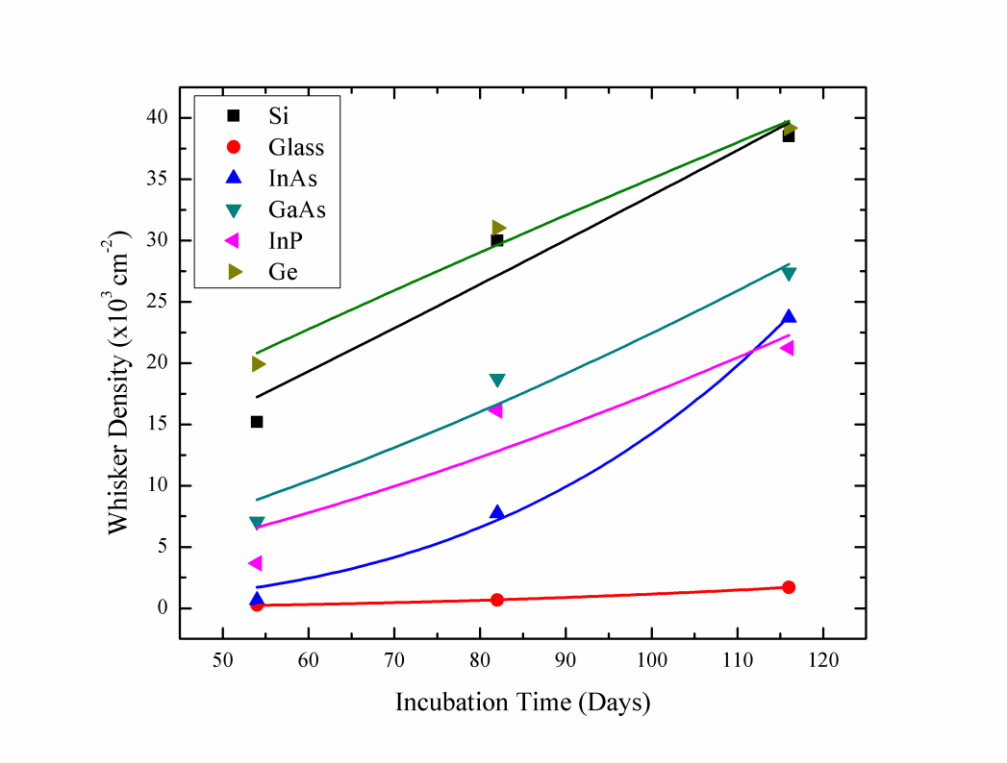

Figure 26: Plots of whisker density vs. incubation time for the 1600 Å Sn film on various semiconductors/insulators exposed to RT/RH conditions.

Table 19: Whisker Density Change between 54-116 Days of Incubation

SUBSTRATES (1600 Å SN FILM)	**WHISKER DENSITY CHANGE (CM^{-2}) (116 - 54 DAYS)**
Si	23,317
Glass	1,441
InAs	23,055
GaAs	20,304
InP	17,553
Ge	19,256

It is interesting that the substrates yield markedly different whisker densities over the first 54 days of incubation but, between 54-116 days, the *increases* in whisker density are *similar* (glass is a notable exception). This means that the various surfaces initially produce quite different whisker densities but then begin to produce similar whisker densities, ranging between 18,000-23,000 whiskers/cm^2. This may suggest a critical nucleation step or activated process operating after the initial incubation period. There have been several activated growth mechanisms in complex whisker-producing thin film systems suggested, ranging from critical strain relief levels, recrystallization to form oblique grain boundaries, oxygen diffusion kinetics into grain boundaries, stress-assisted Cu and Sn diffusion, the work necessary to puncture the tin oxide surface, creep and plastic deformation levels, and so on.

Rutherford backscattering spectroscopy (RBS) was used to observe any noticeable change in the Sn film thickness during whisker incubation and growth on the various semiconductor/insulator substrates. In RBS, an incident 2 MeV α-particle beam is scattered from the film and film/substrate interface. The energy loss by the α-particles during scattering from the front and back surface of the Sn film (the a – b distance in the RBS spectrum in Figure 27) yields the Sn film thickness.

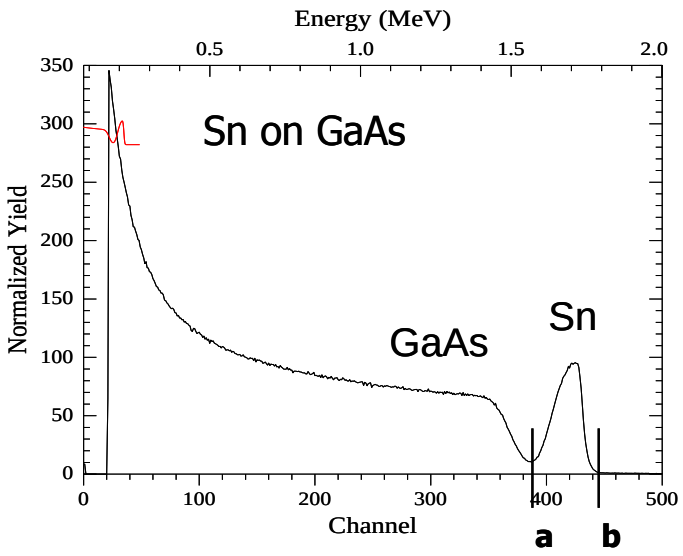

Figure 27: Sn films thickness determination on GaAs measured by RBS.

Figure 28 shows the RBS-determined Sn film thickness vs. incubation time for three substrates. For each sample the RBS data was taken at widely spaced positions, producing similar results. While it is difficult to measure such small incremental variations (~ 100 Å) in film thickness with most analytical techniques (including RBS), there is a general trend toward decreasing Sn thickness with incubation time. Notice further that, in some samples, there is an apparent increase in Sn film thickness at the end of the incubation time. We believe this is attributable to two factors; first, that a non-uniform sputtered film thickness may exist over the broad extent of our specimen sizes (1 cm x 1 cm); and, second, that the RBS particle beam "sees" the whiskers formed at the top of the surface, which effectively makes the film "look" thicker. The second explanation is more likely since we have only rarely observed non-uniform film deposits in our sputtering system. The RBS thickness measurement is difficult because of the large lateral size of the specimens needed for RBS. What is needed optimally is a large amount of whisker growth over ~ 120 days of incubation to significantly "thin" the Sn

feedstock. Values of ~ 100-150 Å of film depletion for the films push the depth resolution of RBS for this class of interfaces. RBS works best on semiconductor film stacks which approach atomic flatness. Sputtered tin, on the other hand, has a very rough top surface which limits the accuracy of thickness measurements in RBS.

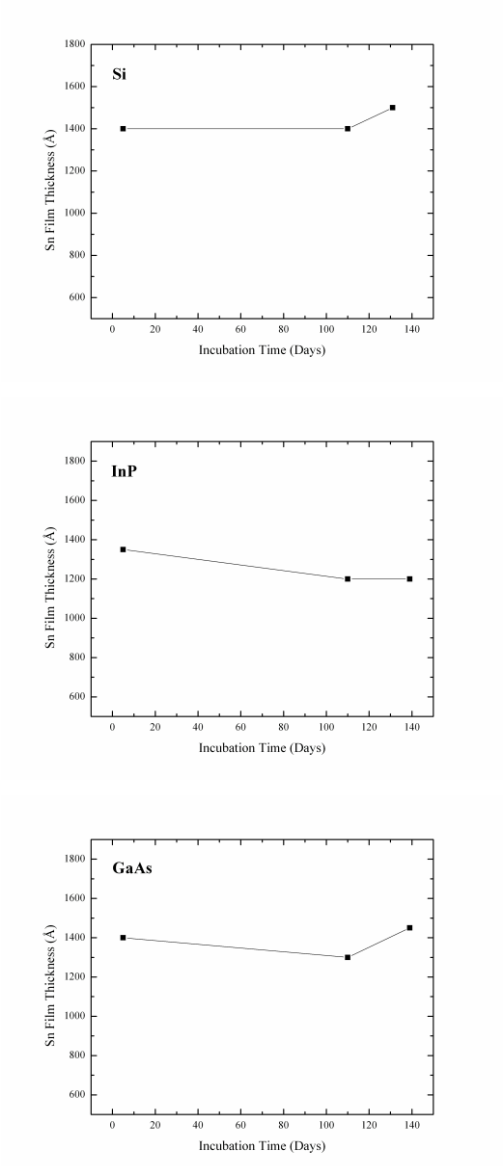

Figure 28: Representative plots of the Sn film thickness vs. incubation time for the substrates Si, InP and GaAs, determined by RBS.

In Figure 28, the RBS results indicate that the Sn on GaAs sample has depleted ~100 Å of Sn film during ~120 days of whisker growth. Is the amount of film diminution consistent with the expected mass balance as the depleted film ends up as Sn whiskers? Table 20 shows several calculated mass balance possibilities for whisker density and length assuming that 100 Å of Sn is depleted due to whisker growth. The numbers in **bold** correspond to the whisker density and average length values measured here for the Sn on GaAs sample. The numbers correlate favorably to the RBS-derived ~ 100 Å of Sn film consumption reported in Figure 28. For the case of InP, the RBS measured ~ 150 Å decrease in film thickness corresponds to an average whisker length of ~ 10 μm for the measured whisker density of 21,221 whiskers/cm^2 while the measured average whisker length was ~ 7 μm.

Table 20: Whisker Growth Possibilities for Sn Film Depletion on GaAs

	Whisker Density (cm^{-2})	**Average Length (μm)**
100Å of Sn depletion on GaAs corresponds to . . .	5,000	28.29
	10,000	14.15
	15,000	9.43
	20,000	**7.07**
	27,378	5.17
	30,000	4.72
	40,000	3.54

It is best to view the mass conservation calculations as a "sanity check" of the RBS results. They turned out better than expected given the approximations cited above and limited statistics when manually counting and measuring whiskers in an SEM. One other major approximation is that we typically do not measure the thickness of the

whiskers, which varies slightly from surface-to-surface and whisker-to-whisker. The whisker radius used for all mass conservation estimates was 1.5 microns, which is a reasonable average.

Finally, Auger depth profiling was used to ascertain the film composition with depth after 130 days of incubation (Figure 29). The Sn on Si and Sn on Ge samples (largest whisker producers) were selected for this purpose. Two observations are noteworthy; first, the AES derived Sn film thickness (1600 Å) agrees well with the deposited film thickness measured by both RBS, stylus profilometry, and through familiarity with the Sn sputter deposition rates generated by our magnetron sputter system; second, there is evidence of diffusion between the Sn and Si and Ge during the incubation period at ambient room temperature/humidity. This was surprising, as we expected minimal diffusion and a sharper interface under room temperature conditions. The depth resolution of our AES depth profiling system is insufficient to detect the ~ 100 Å of film depletion observed by RBS.

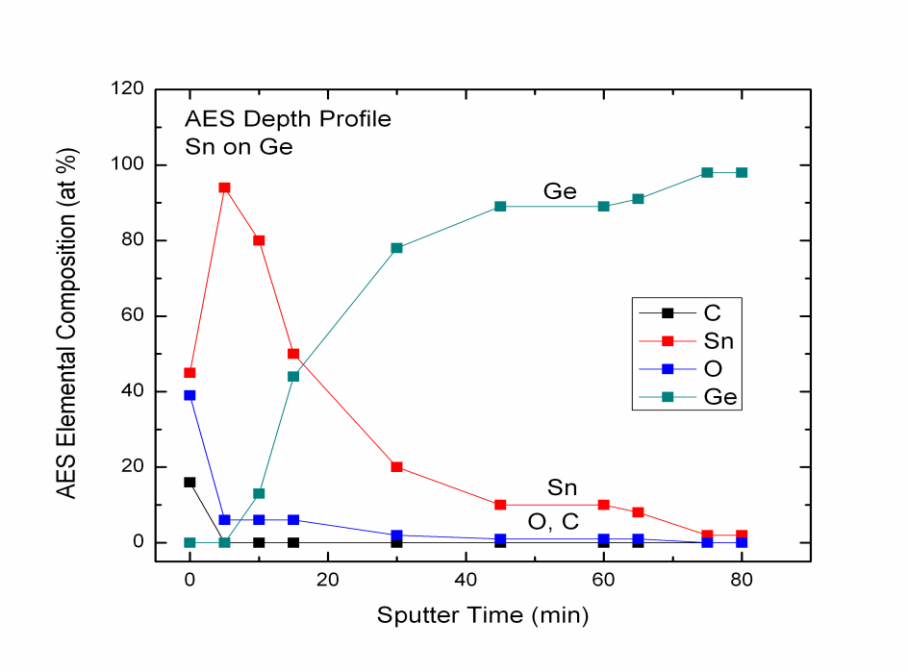

(a)

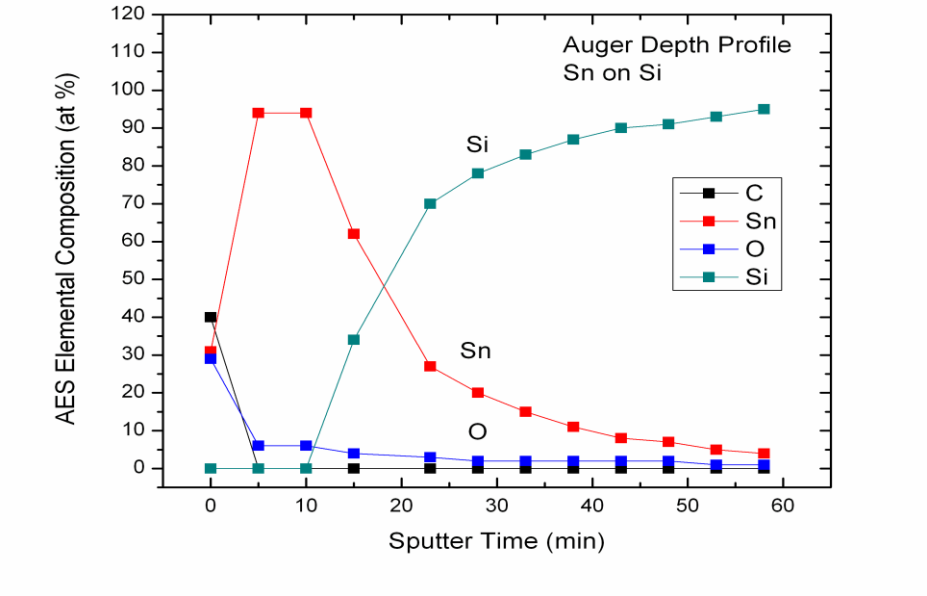

(b)

Figure 29: Depth compositions of (a) Sn on Ge and (b) Sn on Si from the film surface to the substrate as measured by Auger depth profiling. The Ar^+ sputter rate used during profiling was measured to be ~27 Å/min on a standard thin film of SiO_2, commonly used for sputter rate determinations in AES.

In conclusion, it is clear that Sn whiskers grow readily on thin, sputter-deposited Sn films on semiconductor and insulator substrates under internal compressive film stress conditions where intermetallic layers are absent. The fact that Sn on semiconductor surfaces grows copious amounts of whiskers is consistent with our earlier work on surface roughness, which showed that smoother surfaces grow more whiskers [80]. Semiconductor surfaces are some of the smoothest surfaces that can be technologically manufactured.

For the case of Sn on semiconductors/insulators, the highest whisker density after 116 days of incubation occurs for the Si and Ge substrates (38,512 and 39,167 whiskers/cm^2 respectively). Glass produced the fewest amount of whiskers (1,703 whiskers/cm^2). InP, InAs, and GaAs have similar, intermediate whisker densities (~ 21,000-27,000 whiskers/cm^2). The substrates yield markedly different whisker densities over the first 54 days of incubation but from 54-116 days the *increases* in whisker density are *similar* (glass is a notable exception). The largest whisker producers in this study, Si and Ge, have whisker densities over 22X of 1500 Å Sn on brass exposed to RT/RH after similar incubation periods. Though the Sn on Ag produced significantly higher whisker numbers than on Si or Ge, it is clear that an IMC is not necessary to produce large numbers of whiskers.

Most of the Sn/semiconductor combinations produced similar average whiskers lengths (6.5-8.3μm). By comparison to previous cases studied in our laboratory, this length is just slightly shorter than Sn on Ag (~8.5μm), but much less than Sn on brass exposed to RT/RH (14.2μm) after similar incubation periods. Sn on glass was an exception, producing an average whisker length of only 2.5μm.

RBS studies show evidence of the slight Sn film depletion expected during whisker growth, owing to the mass balance that must occur when forming Sn whiskers. We observe a decrease of ~ 100 Å in the thickness of the deposited Sn film during the incubation period (130 days), which roughly agrees with previous Sn depletion studies of whisker growth from Sn on Ag using AES depth profiling. The fact that identical RBS results were obtained over two widely separated analysis positions on the film surface support the notion of long-range lateral movement of Sn to the whisker shaft during whisker growth. As stated above, direct evidence of such lateral diffusion of Sn during whisker growth was reported in elegant tracer experiments performed by Woodrow [74] and explains why smoother surfaces tend to produce larger whisker numbers, even when IMC formation is absent.

AES depth profiling studies indicated diffusion between the deposited Sn film and semiconductor/insulator substrates during the incubation period at room temperature and humidity conditions. No simple correlation due to CTE mismatches was found between the various semiconductor substrates (having similar CTEs) and Sn whisker growth.

2.5 Whisker Growth Under Different Film Stress Conditions

Most investigators agree that compressive stress in Sn films is the primary driving force behind whisker growth [22], yet little has been reported about the possible, more controversial role of tensile stress [43,19]. The goal of the work reported here is to produce measurable intrinsically induced thin film stress states (tensile, no stress, and compressive) in Sn and study the effects on whisker growth under the different stress conditions. Our motive for investigating sputter-deposited (rather than electroplated) Sn

films is due in part to the relative ease in fabricating films with various stress states in sputtered films (shown below). Further, control of the film stress and prudent selection of film systems which do not grow intermetallic compounds and have minimal CTE mismatches allows for easier elucidation of the fundamental mechanisms impacting whisker growth.

Numerous studies of Sn whiskers have emphasized the role of intermetallic compound formation at the tin-substrate interface, which typically induces a high compressive stress state in the film [43,23]. To eliminate the complications of intermetallic compound (IMC) formation, all Sn films in this study have been deposited on Si, since the binary phase diagram for Sn-Si shows that Sn-Si IMCs do not form at room temperature. We produce the various stress states through sputter deposition. By controlling the background argon pressure during sputtering, the desired stress state can be dialed into the film [65].

A pure Sn sputter target (99.999%, Kurt Lesker Co) was used to deposit 2000 Å Sn films on Si wafer substrates (~1cm x 1cm) in our magnetron sputtering system. The film thickness was verified by stylus profilometry over a step edge in the deposit. The Sn films were sputtered with background argon pressures of 2-3mT, 8mT, and 19mT to produce intrinsic compressive stress, no stress, and tensile stress states respectively in the Sn films. After depositing the sputtered Sn films, the samples were incubated under ambient room temperature/humidity (RT/RH) conditions followed by periodic whisker counts for many months using a Cambridge scanning electron microscope (SEM).

In early work on thin film stress, Hoffman and Thornton [65] specified regions of compressive, no stress, and tensile stress states depending on the background Ar gas

pressure in the sputter system. For the case of Sn films, compressive stress results when using a background Ar pressure from ~1-6mT and tensile stress is produced with 10-100mT. The "no stress" state has a very narrow (7-9mT) gas pressure range, which creates difficulties in duplicating the "zero" stress state determined in the original Hoffman work due to gauge pressure variations. In our sputter system, the Ar pressure is measured using a Convectron gauge, which measures the heat loss from a sensor wire that is maintained at constant temperature. The heat loss is converted into gas pressure, but it varies with the gas and results in varying gauge sensitivities which can be adjusted in modern gauges. Since the method of pressure measurement in the Hoffman system was not reported, it is not surprising that the critical zero stress pressure may vary slightly between sputter systems depending on the geometry and pressure gauge.

The stress states were examined/verified by curvature measurements using a Veeco Dektak diamond-tipped stylus profilometer. By taking 8mm line scans across the surface (along perpendicular directions) and measuring the radius of curvature, R, of the specimen, Stoney's equation can be used to determine the stress in the Sn film. To obtain R, each profilometer scan was fit with a 5^{th} order polynomial by the method of least squares [81] to obtain y(x), the vertical displacement (μm) of the stylus as a function of the lateral displacement (μm). The radius of curvature, R, was then calculated by:

$$R(x) = \frac{(1+y'^2)^{\frac{3}{2}}}{y''}$$

where y' = dy/dx and y'' = d^2y/dx^2, which are then evaluated at x = position of maximum curvature in profilometer scan to obtain a value for R. The radius of curvature was then used to calculate the stress by Stoney's equation [81], assuming an initially flat substrate:

$$\sigma = \frac{1}{6R}\frac{E_s}{1-\upsilon_s}\frac{t_s^2}{t_f}$$

Here σ is the film stress, E_s is Young's modulus (160 GPa), υ_s is the Poisson ratio (0.27) [82], t_s is the substrate thickness (500 μm) and t_f is the film thickness. A more general form of Stoney's equation that accounts for the effect of intermetallic (IMC) growth [26] on curvature is unnecessary for films which do not form IMCs.

After a month (28 days) of incubation at ambient room temperature/humidity conditions, the growth of Sn whiskers on the stressed film specimens was evaluated by SEM. The whisker densities were determined by manually counting whiskers over ten equal representative areas (~275 μm x 275 μm) on the surface. Table 21 shows the whisker growth statistics. Each stress state condition produced whiskers after 28 days of incubation. High whisker densities are observed for both the compressive and tensile states (4,585 and 7,991 whiskers/cm^2 respectively). The observation of whiskering in both tensile and compressive states is in agreement with earlier work in our laboratory with "imposed" external stress states formed by deliberate coupon curvature [83]. There are also whiskers observed for the "zero" stress state, but the density is comparatively low (< 1,000 whiskers/cm^2). The tensile stressed film produced the longest average whisker length (16.5 μm) while the compressive (4.3 μm) and "zero" (2.3 μm) stress states created much smaller average whisker lengths.

Table 22 shows the whisker statistics after an additional two months of incubation (total of 96 days). All samples show increases in whisker density and average whisker length. Films under compression and tension continue to produce the highest whisker densities. However, the Sn films under compression are now producing more whiskers than the films under tension. During the additional two months of incubation, the zero

stress specimen retains the smallest whisker density (1/3 and 1/4 the densities observed in the tensile and compressive stressed films respectively) and the shortest average whisker length (3.4μm).

Table 21: Whisker Statistics after One Month of Incubation for Sn Stress States

Sn Film State	**Whisker Density (cm^{-2})**	**Average Whisker Length (μm)**
Compressive	4,585	4.3
Zero	786	2.3
Tensile	7,991	16.5

Table 22: Whisker Statistics after Three Month of Incubation for Sn Stress States

Sn Film State	**Whisker Density (cm^{-2})**	**Average Whisker Length (μm)**
Compressive	15,850	5.3
Zero	4,061	3.4
Tensile	12,051	26.8

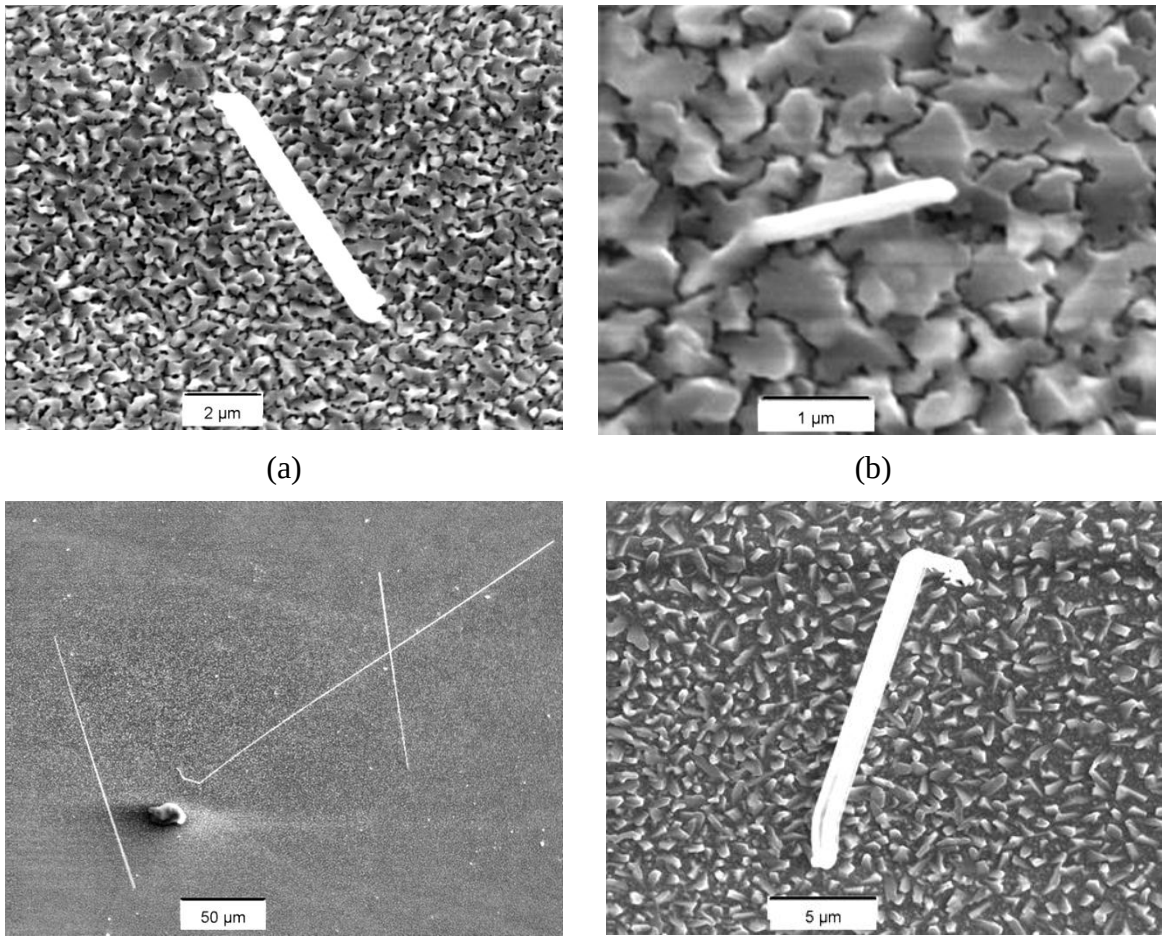

(a) (b)

(c) (d)

Figure 30: Representative SEM photographs of whiskers produced on Sn films under (a) compressive stress, (b) "zero" stress and (c,d) tensile stress.

Representative high aspect ratio whiskers produced on the various films is shown in Figure 30. The photograph in Figure 30(c) shows much longer whiskers than in (a) or (b), representing the significant increase in average whisker length observed on films under tension.

Experimental verification of the sputtered film stress states are shown in Figure 31, measured after three months of incubation. Negative stress values represent compressive stress (convex surface) and positive values mean tensile stress (concave surface) [81]. The stress values were calculated to be -1.85×10^{11} dyn/cm^2

(compressive); 9.8 x 10^9 dyn/cm^2 (tensile); and the "unstressed" stress state was 9.83 x 10^8 dyn/cm^2. The stress values signify the average stress in the film at the three month time marker and do not give any indication of the existence of stress gradients in the film, which would require more exhaustive, time-dependent measurements.

The "unstressed" state appears to have no curvature in Figure 31(a), but when a higher resolution vertical scale factor is used, there is a *slight* curvature. We believe the "zero" stress value is not precisely zero due to 1) the difficulty when trying to "hit" the narrow argon pressure range needed to attain zero stress; and, 2) pressure gauge variations and slight geometrical differences between Hoffman's magnetron sputtering system and ours; 3) the fact that we are observing whisker production. It is common when measuring stress in Si wafers using profilometry to expect a measurement uncertainty of the order of 1 x 10^8 dyne/cm^2 [84].

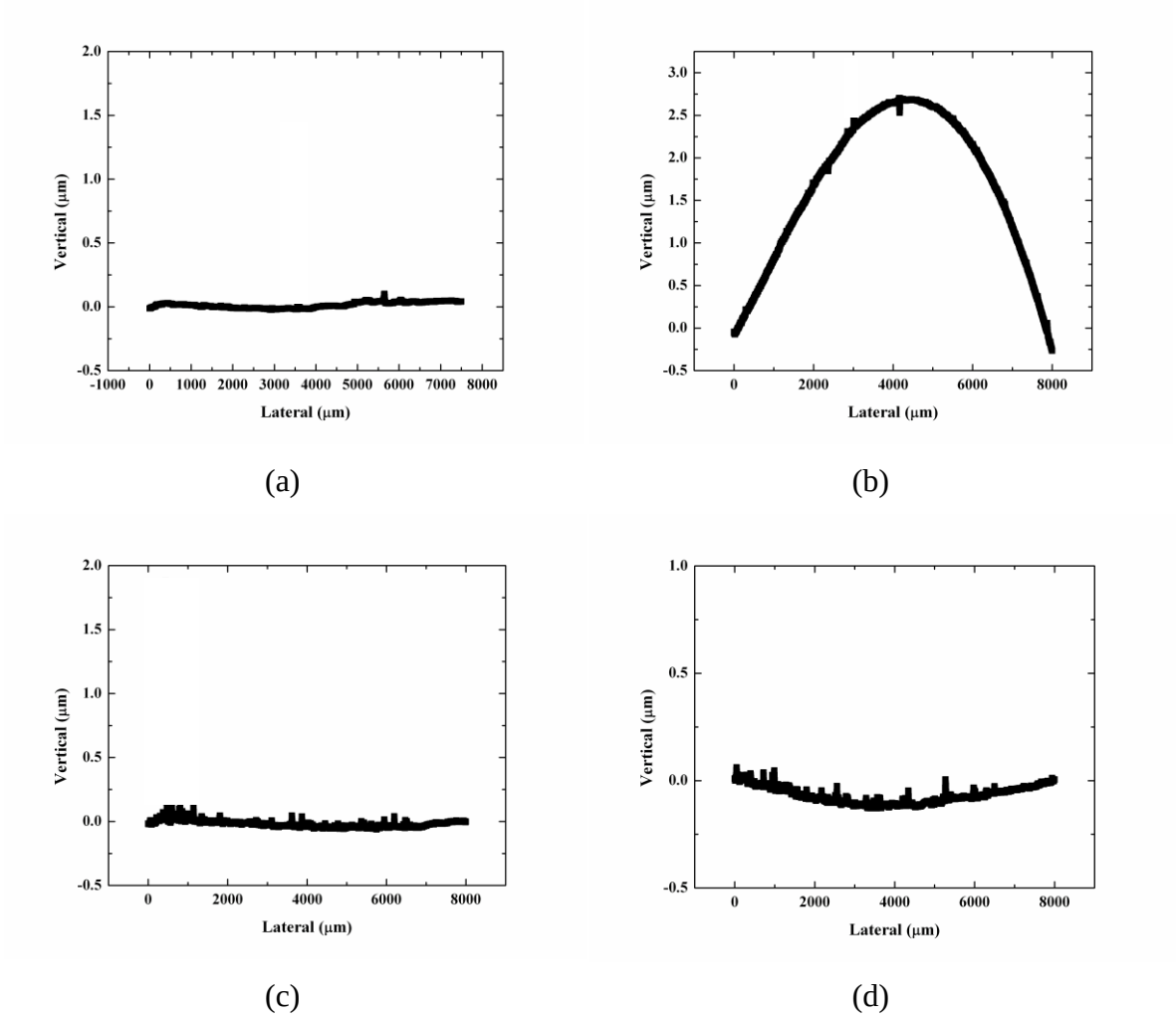

Figure 31: Stylus profilometer topography scans (a) Si substrate only (no sputtered Sn film); (b) Sn film under compression; (c) Sn film with "zero" stress; and (d) Sn film under tension.

Figure 32 illustrates the measured whisker density vs. incubation time for each sample. All samples show increasing whisker growth with time, regardless of whether they are producing large or small quantities of whiskers. After ~100 days of incubation, there is no evidence of a plateau in the whisker density vs. incubation time graphs.

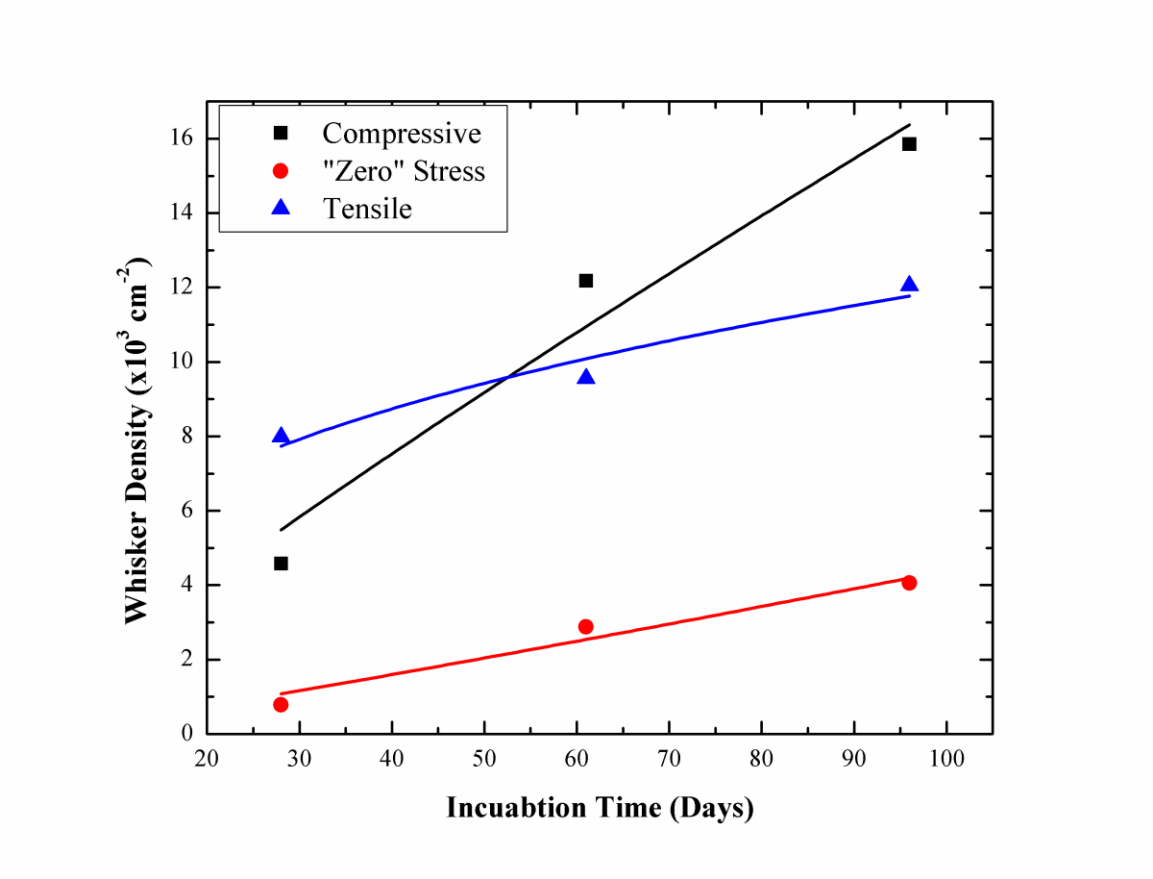

Figure 32: Plot of whisker density vs. incubation time for Sn film stress states exposed to RT/RH conditions.

This work gives evidence of whisker growth from sputter-deposited Sn films under *both* compression and tension. While there are questions about how the film stress evolved over time since deposition, the curvature results give some level of confidence that the initial "dialed" up stress states still existed three months later. At that time, the films under compression had produced ~ 15,000 whiskers/cm^2 and the films under tension had produced ~ 12,000 whiskers/cm^2. In contrast, the "unstressed" film had generated ~ 4,000 whiskers/cm^2 after three months. The lower whisker numbers on the unstressed film is better understood after verifying that the *actual* stress in the "unstressed" Sn film had a comparatively low, but nonzero, (tensile) value of 9.83 x 10^8

dyn/cm^2. In contrast, the compressive and tensile stress values were an order of magnitude higher than the "unstressed" film.

While films under compression produced the largest whisker densities after three months, the films under tension grew the longest whiskers (average whisker length of ~27 μm) compared to the film under compression (~5 μm). The "zero" stress film had an average whisker length of only ~ 3.5 μm. The longest whisker was produced under tension and reached 338 μm! The stress values calculated using Stoney's equation were in the expected range for Si substrates and in accordance with the desired compressive film state (negative stress value) and tensile film state (positive stress value).

Although rare, the literature shows that whiskers can be produced under tensile stress. Xu et al. [19] observed whisker production in electroplated Sn films on Cu, aged at 50°C for up to ten months. The specimens were subjected to externally imposed compressive and tensile stress. The tensile specimens started producing whiskers after four months and, after ten months; there were more than 45,000 whiskers. The films under compression produced greater whisker numbers than films under tension, although no actual stress values were reported in that work. Studies in our laboratory [83] using sputtered Sn on brass under imposed tension and compression also showed whiskers under both stress states. The whisker densities under each condition of stress increased as the magnitude of the tensile and compressive forces increased.

2.6 Whiskering from Sn Alloy Films

Since the Pb-free movement mandated the removal of Pb entirely from the electronics supply chain, there has been an emergence of SAC solder alloys. The

question is whether SAC alloys having high mole fractions of Sn are whisker-prone. The answer is yes. Handwerker et al. [85] from Purdue University found whisker growth on electroplated SAC405 soldered surfaces. The whiskers were observed on the leads of a MOSFET device, both after life testing (20 days at 65°C/25%RH with a 40CFM blower) and under normal storage conditions. Whiskers have also been observed [86] on hot dipped SAC305 surface mount resistor terminations after 500hrs @ 85C/85%RH plus 500 temperature cycles from -55°C to 125°C, and from SnCu [87] and SnAg [88] electrodeposits.

In fact, even eutectic Sn-37Pb alloys can produce whisker growth under the right stress conditions. Chason et al. [89] observed whiskering from electrodeposited Sn-10%Pb alloy films on multilayer samples fabricated on Si substrates. The layer structure was created by electron beam deposition with a 15nm Ti adhesion layer followed by 600nm Cu and a 1200nm Sn alloy film. NASA and the QSS Group [90] has observed SnPb alloy whiskers which have created electrical shunts. In a 2003 evaluation of GaAs laser diode arrays at NASA Goddard Space Flight Center, whiskers were observed emanating from reflowed eutectic Sn-37Pb solder die attach material. The maximum whisker lengths ranged from 25-30 µm while the shunting distance (heat sink to laser diode) was only 2.5-3.0 µm. Whiskering within 30 min has been witnessed from a coating layer of Sn60/Pb40 hot air solder leveling under compressive stress conditions [91]. Thick electroplated films of 3, 7, and 16 µm have shown no whiskering from the incorporation of only 2% Pb (Sn98/Pb2) after a month of incubation [26]. Electrodeposited films of 10 µm (> 83 X thicker than our 1200 Å film, described below)

produced no whiskering after 6 months with the incorporation of only 5% Pb in the Sn film [92].

In our experiments involving whiskering on alloyed materials, we were asked by a CAVE3 client to determine if *sputtered* films of SAC305 and Sn-37Pb were whisker prone. This posed a challenge, as sputter targets of these materials do not exist, so we had to make our own targets. The solution was to make a round glass mold with dimensions matching our sputter target size (2 in dia. x 1/8 in thick). Bulk specimens of SAC 305 and Sn-37Pb were then melted and poured into the glass mold, followed by water quenching. The glass mold was then broken, the target was removed, and then sanded down for a smooth distinct shape compatible with our sputter system. The custom sputter target is shown in Figure 33.

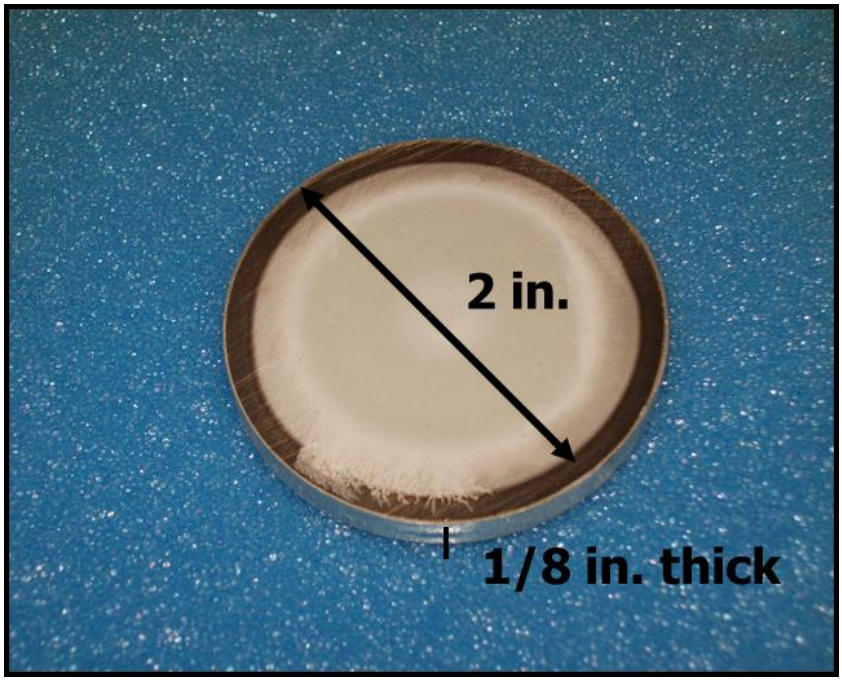

Figure 33: Custom made sputter target.

SAC305 and Sn-37Pb thin films were subsequently sputter-deposited under compressive stress conditions onto electrochemically polished brass (Cu63/Zn37). The resulting film thicknesses were ~2400 Å (SAC305) and ~750 and ~1200 Å (Sn-37Pb), measured by RBS. When doing sputter deposition of alloy films, the issue of congruency arises. Congruency means that the deposited film contains the same ratio of elements as the sputter target. Incongruent sputtering, by contrast, occurs when one element (e.g., Sn) is sputtered preferentially, which results in a film composition which differs from the target composition. To verify congruency, it is necessary to determine the mole fraction of elements in the sputtered film. For this purpose we used energy dispersive X-ray spectroscopy (EDX), under two precautions. First, since the SAC was deposited on brass, the EDX Cu peak is a superposition of Cu in SAC305 and Cu in the brass substrate. This forced the test to be done with SAC305 deposited on a silicon wafer instead of brass. Second, there is a problem when doing EDX on thin films having to do with the signal sampling volume. Specifically, EDX is more properly a volume materials technique, not a surface analysis technique. The difference is important when analyzing thin films. Shown in Figure 34, the X-ray signals generated during a standard EDX analysis originate from a pear-shaped volume ~ 1-3 μm under the surface, which is problematic when doing analyses on submicron thin films. The EDX data obtained from a submicron film is dominated by the signal from the substrate signal and not from the desired thin film. It was therefore necessary to deposit thicker layers than typical and to utilize glancing-angle EDX to maximize the fraction (cos θ dependence) of X-ray signal from the film. The conclusion (Table 23) from EDX was that both SAC305 and Sn-37Pb had been sputter deposited congruently.

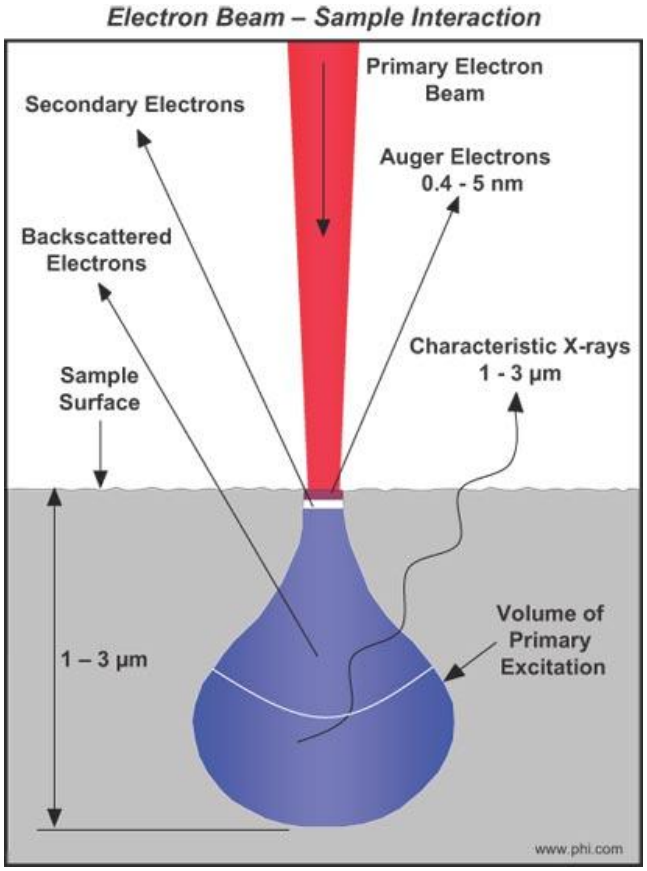

Figure 34: The signal categories emanating from a surface during electron beam excitation. The signal from EDX typically originates from 1-3 microns below the surface.

Table 23: EDX Element Composition Sputtered (a) SAC and (b) SnPb Films

Element	Weight	Atomic
Cu	0.16	0.29
Ag	3.02	3.30
Sn	96.83	96.40

(a)

Element	Weight	Atomic
Sn	67.04	78.02
Pb	32.96	21.98

(b)

After sputter deposition, the SAC 305 and Sn-37Pb films were incubated under ambient RT/RH. Whisker statistics recorded after a month of incubation are shown in Table 24. At this time, the thinnest, 750 Å Sn-37Pb alloy film was producing the greatest

number of whiskers (~3,500 whiskers/cm^2) while the 1200 Å Sn-37Pb film produced no whiskers. The SAC film grew ~1,050 whiskers/cm^2 over a one month period with an average whisker length ~ 2 µm. After 190 days of incubation (Table 25), the rate of SAC whisker production has increased greatly (> 33,600 whiskers/cm^2). In contrast, the thinner Sn-37Pb film has only slightly increased whisker growth while the thicker Sn-37Pb film is still void of any whiskers. The average whisker lengths are low on both films, with SAC 305 producing the greatest average whisker length of 4.6 µm.

Table 24: Whisker Statistics for Sn Alloy Films after 36 Days of Incubation

Film	**Thickness (Å)**	**Whisker Density (cm^{-2})**	**Average Whisker Length (µm)**	**Standard Deviation (µm)**	**Mode**
SAC 305	2400	1,048	2.3	0.7	2
SnPb	750	3,537	2.2	0.4	2
	1200	0	NA	NA	NA

Table 25: Whisker Statistics for Sn Alloy Films after 190 Days of Incubation

Film	**Thickness (Å)**	**Whisker Density (cm^{-2})**	**Average Whisker Length (µm)**	**Standard Deviation (µm)**	**Mode**
SAC 305	2400	33,665	4.6	5.8	2
SnPb	750	4,454	3.9	1.9	2
	1200	0	NA	NA	NA

Table 26: Whisker Statistics for Sn Alloy Films after Over a Year of Incubation

Film	Thickness (Å)	Whisker Density (cm^{-2})	Average Whisker Length (µm)	Standard Deviation (µm)	Mode
SAC 305 (590 Days)	2400	147,498	5.0	5.3	2
SnPb (407 Days)	750	7,991	3.4	2.0	2
	1200	524	2.3	0.5	2

Table 26 shows whisker statistics after a year of incubation. We finally see whisker growth (albeit, near-zero) from the 1200 Å Sn-37Pb film (524 whiskers/cm^2), corresponding to only 5 whiskers for every square millimeter of surface. The thicker 750 Å Sn-37Pb film has modest whisker numbers after one year, while SAC has produced > 147,000 whiskers/cm^2. The data highlights the ability of incorporated Pb to suppress whiskers and shows that, under specific stress conditions, both Sn-37Pb and SAC305 will form whiskers. Figure 35 and Figure 36 show representative whisker morphologies from SAC and SnPb films respectively.

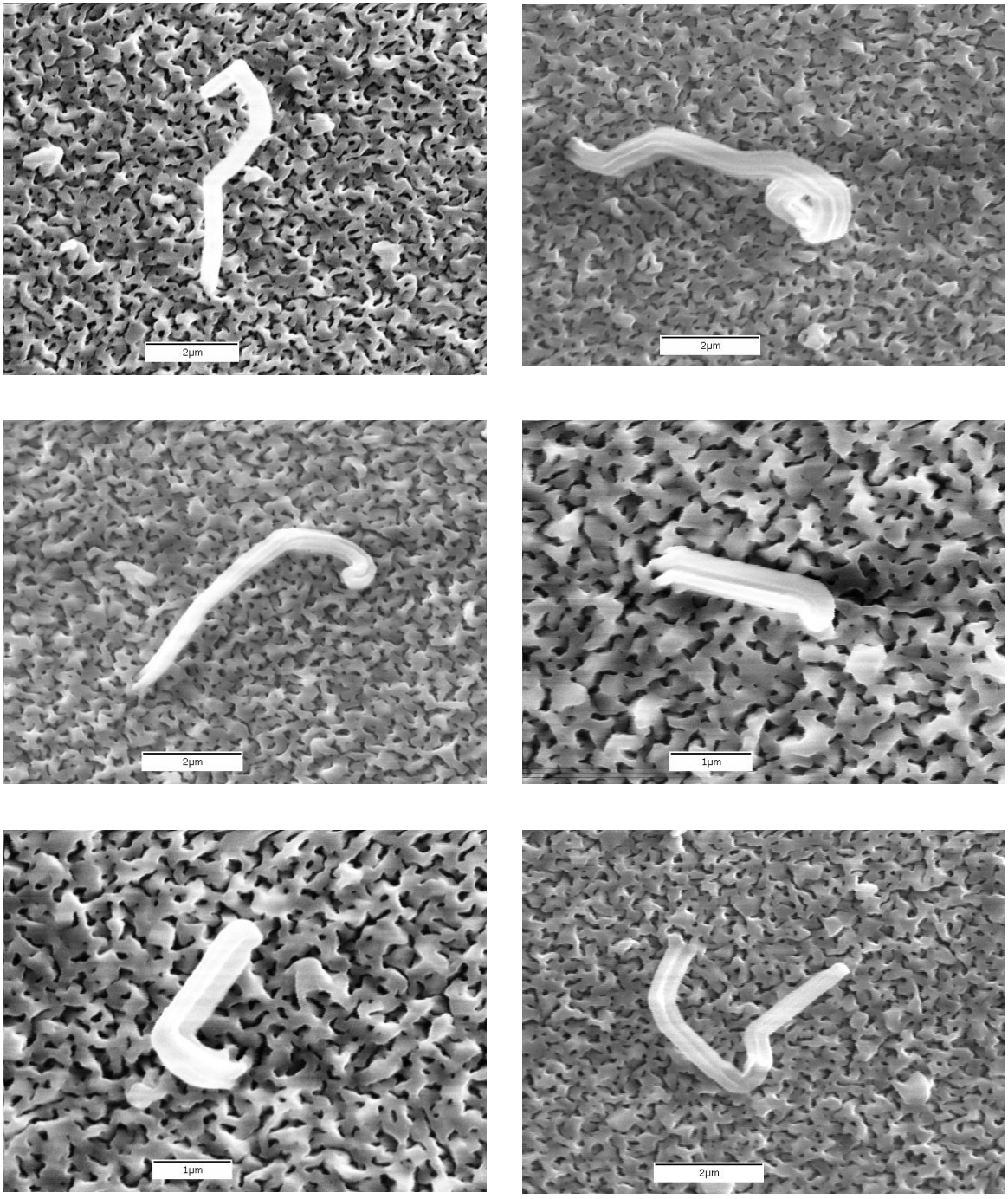

Figure 35: SEM images of whiskers growing from SAC 305 film.

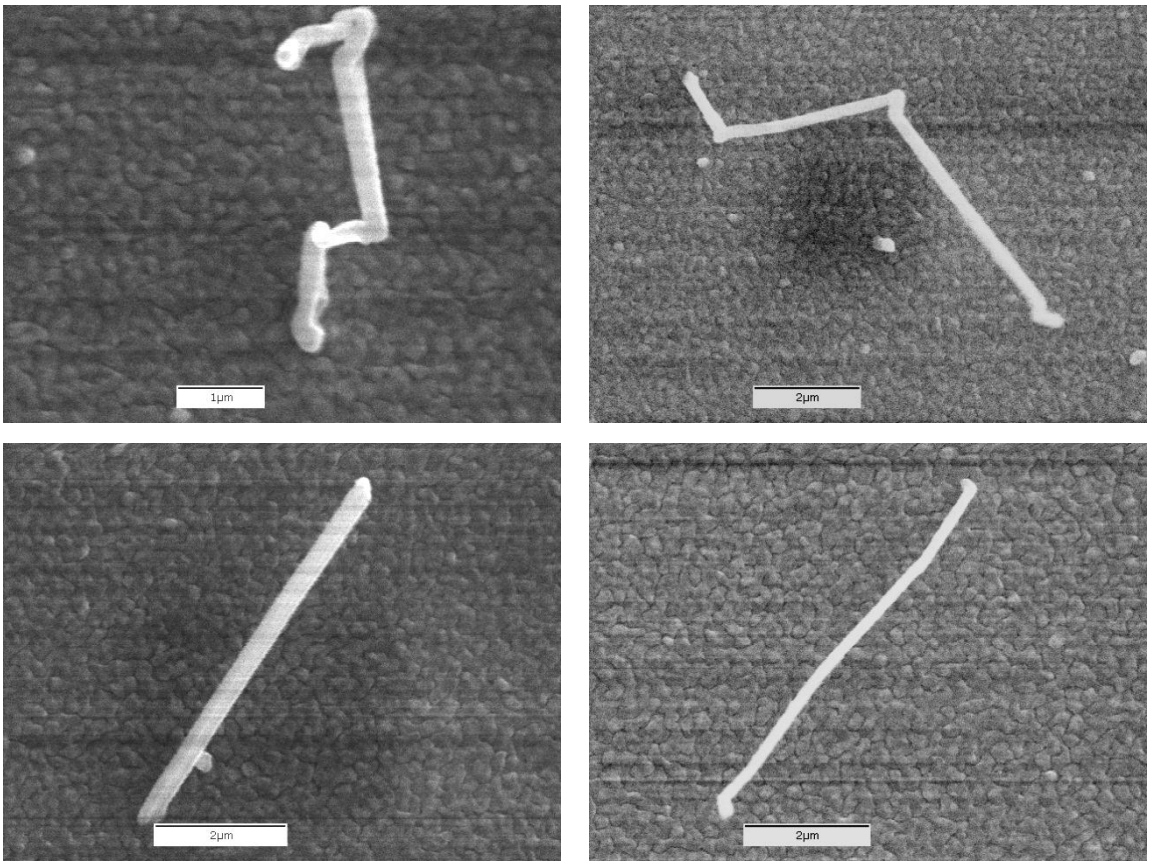

(a)

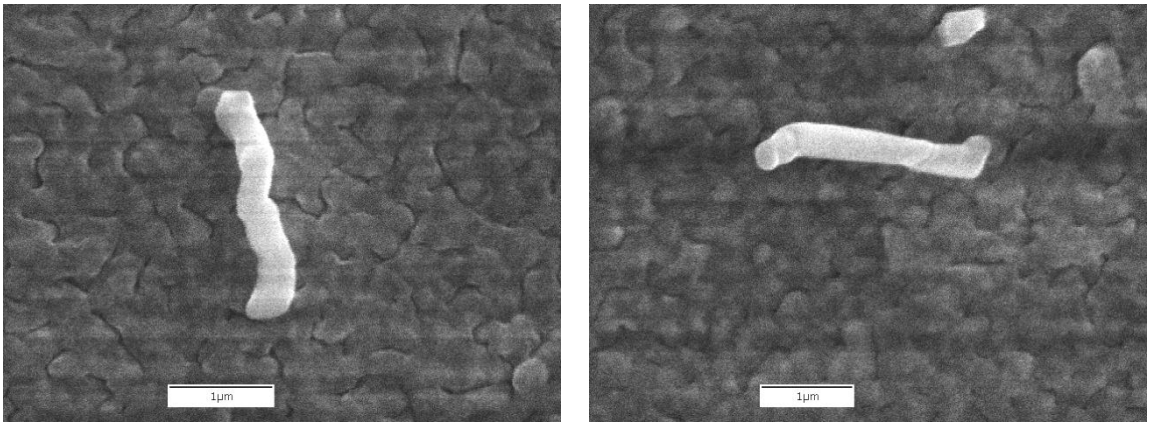

(b)

Figure 36: SEM images of whiskers growing from SnPb films (a) 750 Å and (b) 1200 Å.

The whisker density vs. incubation time for sputtered SAC305 and Sn-37Pb films are compared in Figure 37. It is clear that the SAC film is producing much larger whisker numbers than the SnPb films. The thinner, 750 Å, SnPb film is producing some

whiskering in time, but the 1200 Å SnPb film is barely producing any whisker growth (even after a year of incubation).

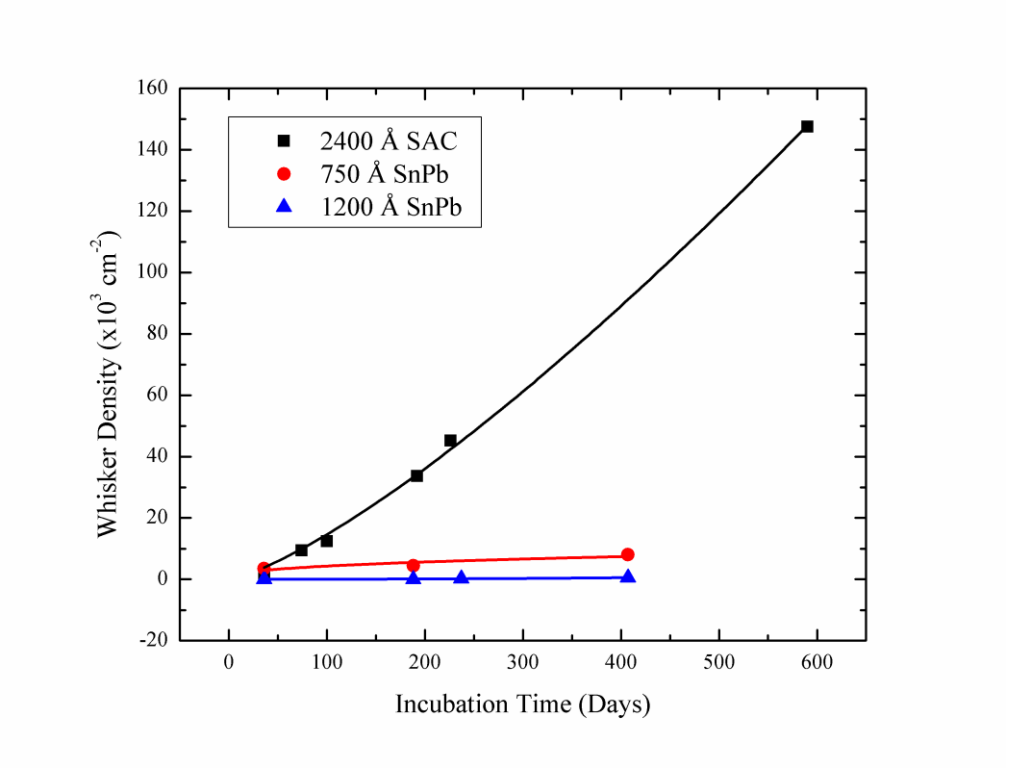

Figure 37: Whisker Density vs. Time plot for Sn alloy films.

In conclusion, it is apparent that whisker growth can occur on Sn alloyed deposits such as SAC. After 407 days of incubation in ambient RT/RH, we find over 7900 whiskers/cm^2 on the 750 Å Sn-37Pb specimen. Comparing this to 750 Å of pure Sn on brass after similar incubation periods, the Sn film produced ~ 1.75X the whisker density of the Sn-37Pb film, with > 5 X the average whisker length. This is not surprising, since the corporation of Pb in Sn is known to mitigate whisker growth. In fact, Chason et al. [89] observed whiskering from electrodeposited Sn-10%Pb alloy films and found that the stress developed in the SnPb film was much less than that in the pure Sn films. This is in agreement with the whisker statistics above.

CHAPTER 3

ENVIRONMENTAL EFFECTS ON WHISKER GROWTH

"Do you have the patience to wait until the mud settles and the water is clear? Can you wait until the right action arises by itself?"

-Lao Tzu

3.1 Effects of Oxygen Exposure on Sn Whiskering

Since Sn oxidizes readily once deposited, oxygen exposure and the subsequent Sn oxides formed play a significant role in whisker growth. Many studies have demonstrated that Sn whisker growth is enhanced by exposure to oxygen and high relative humidity conditions [53,93], especially near regions of surface corrosion. In a study by Oberndorff et al. [54], all whiskers produced on Sn films (> 7.5 μm) after 2000 hrs of 60°C/93%RH exposure were found near regions of surface corrosion. The diffusion of oxygen into the thin film results in lattice expansion when metal oxide phases form [94], which places the film under compressive stress. The increased stress is relieved in part by the growth of Sn whiskers. The reaction between oxygen and Sn is also thought to influence where whiskers form on a surface due to non-uniform oxide formation [36]. In order to clarify the role of oxygen on whisker production, in this work we exposed thin sputtered Sn films on brass to 99.999% pure oxygen gas.

Pure Sn films were deposited onto brass substrates using magnetron sputtering techniques. The thicknesses of the films were 1400 and 2000 Å, measured by stylus profilometry over a step edge in the deposit. The brass (Cu63/Zn36) substrates were commercially-purchased [71] metal foils which we cut into coupons of dimension 1 cm x 1 cm. The coupon surfaces were subsequently electrochemically polished due to

previous work in our laboratory which showed that smoother substrate surfaces enhance whisker growth [80]. The Sn films were sputtered in an argon plasma at pressures of 2-3 mT, producing intrinsic compressive stress in the films [65]. Subsequently, the coupons were transferred to a controlled environmental chamber under 1 atm pressure of pure O_2. The environmental chamber (Figure 38) was built onto the sidewall of an ultrahigh vacuum, multi-technique surface analytical system. The pure O_2 environment was achieved by first pumping the environmental chamber down to ~10^{-6} torr using the ion- and turbo-pumping system of the surface analytical chamber, followed by backfilling with pure O_2 (99.999%) to a pressure of 1 atm, measured by a Bourdon gauge.

To assess the whisker growth, the samples were periodically removed and transferred to a scanning electron microscope, where whisker observation and counting occurred. Afterwards, the samples were subsequently returned to the pure-O_2 environment for further incubation. After a ~ 6 month incubation period the Sn film surfaces were also studied using Auger electron spectroscopy (AES) and X-ray photoelectron spectroscopy (XPS). By recording high resolution XPS features around the $Sn3d_{5/2}$ peak, the oxidation states of the surface Sn oxides could be determined and compared to a similar Sn film on polished brass exposed to ambient room temperature/humidity conditions. AES depth profiling was also utilized to determine the film composition at the top, middle, and bottom regions of the incubated Sn film.

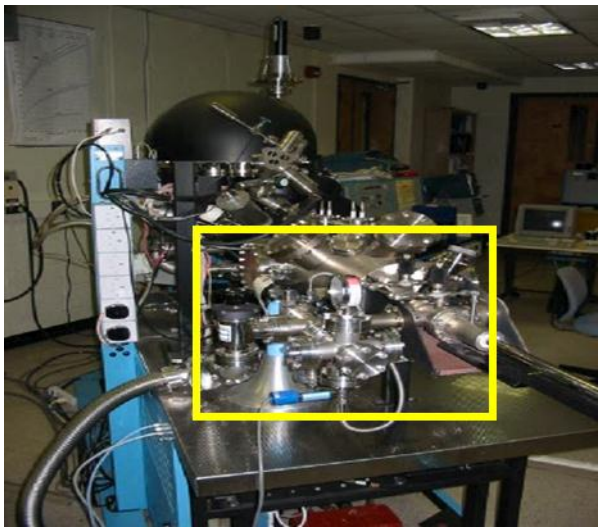

Figure 38: Pure O_2 environmental chamber (boxed inset) attached to the sidewall of a UHV surface analysis system.

After 50 days of 1-atm pure O_2 exposure, the 1400Å Sn film produced 5,895 whiskers/cm^2 and the 2000 Å film produced 873 whiskers/cm^2, shown in Table 27. The thinner film also grew longer whiskers. The average whisker length on the 1400 Å film was 7.5µm compared to 5.3µm on the 2000 Å film.

Table 27: Whisker Statistics after 49 Days of Pure O_2 Exposure

.

Sn Film Thickness (Å)	Whisker Density (cm^{-2})	Average Whisker Length (µm)	Standard Deviation (µm)	Mode
1400	5,895	7.5	5.5	3
2000	873	5.3	2.3	6

Table 28: Whisker Statistics after 147 Days of Pure O_2 Exposure

Sn Film Thickness (Å)	Whisker Density (cm^{-2})	Average Whisker Length (µm)	Standard Deviation (µm)	Mode
1400	15,588	5.7	6.3	2
2000	7,598	3.2	1.8	2

Table 29: Comparative Whisker Statistics for RT/RH Atmospheric Exposed Sn on Brass (~150 Days of Incubation)

Sn Film Thickness (Å)	Whisker Density (cm^{-2})	Average Whisker Length (μm)	Standard Deviation (μm)	Mode
1500	1729	14.2	23.7	5

After ~ 150 days the 1400 Å Sn film produced > 2.5 X higher whisker density than 100 days earlier, as seen in Table 28. During the same time, the 2000 Å film produced > 8.5 X more whiskers per area, indicating a longer incubation time was necessary for the thicker film before significant whisker growth. While there is a rise in the whisker density for both thicknesses, the average whisker length for both has decreased to 5.7 and 3.2 μm respectively over the extended incubation period. The whiskers have not shortened over time, but more short whiskers have grown, which contributes to a shorter average whisker length.

Compared to similar thicknesses of Sn on brass incubated at ambient room temperature/humidity (RT/RH) conditions over similar incubation times, pure O_2 exposed samples produced ~ 9X more whiskers (Table 29). However, the average whisker length under O_2 exposure is less than half (6 μm) compared to atmospheric-exposure (14 μm). Figure 39 displays representative SEM images of typical whiskers grown from Sn on brass exposed to pure O_2. Figure 40 shows the whisker density as a function of time.

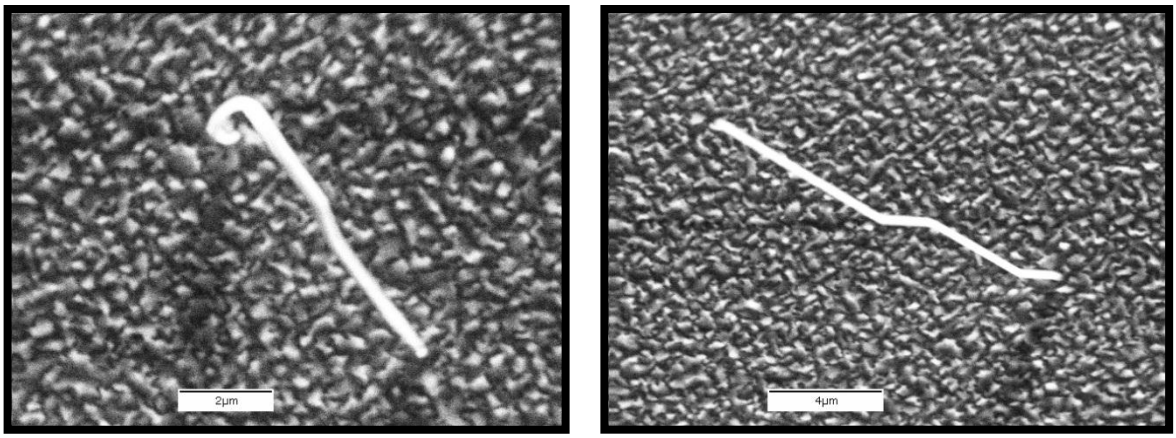

(a)

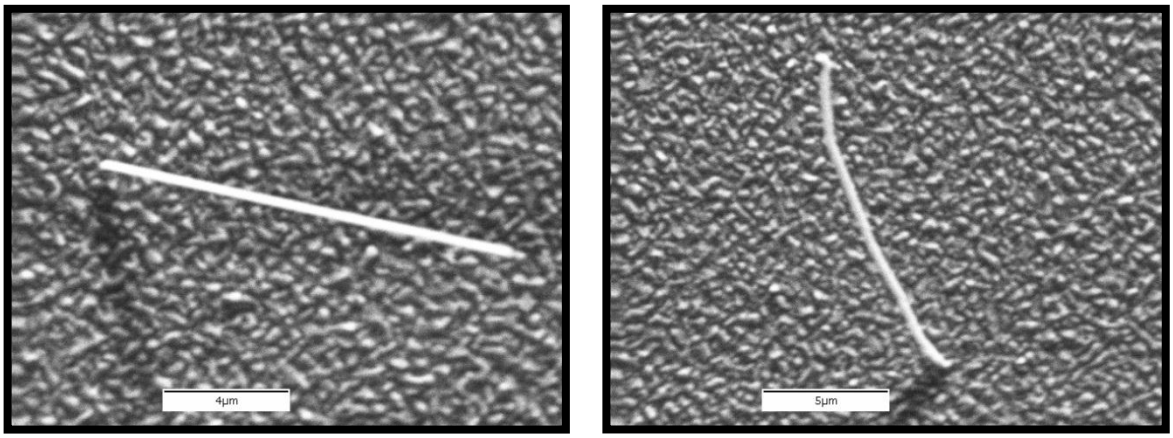

(b)

Figure 39: Whisker morphologies formed in a pure-O_2 environment (a) 2000 Å and (b) 1400 Å Sn film.

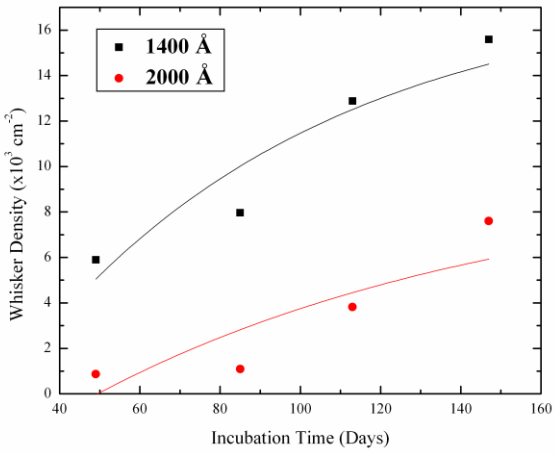

Figure 40: Whisker density vs. incubation time for 1400 and 2000 Å Sn films on brass exposed, to 1 atm of pure O_2.

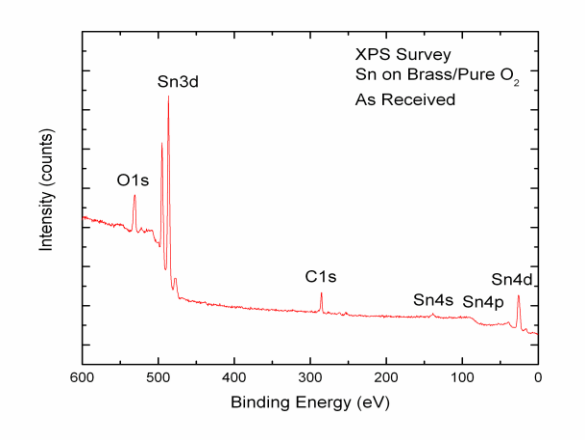

(a)

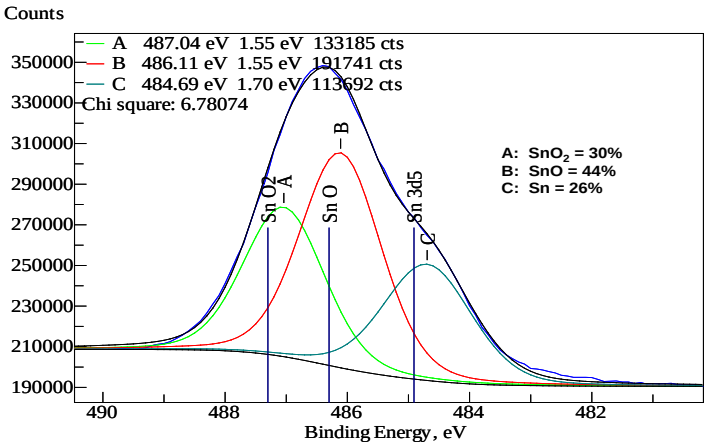

(b)

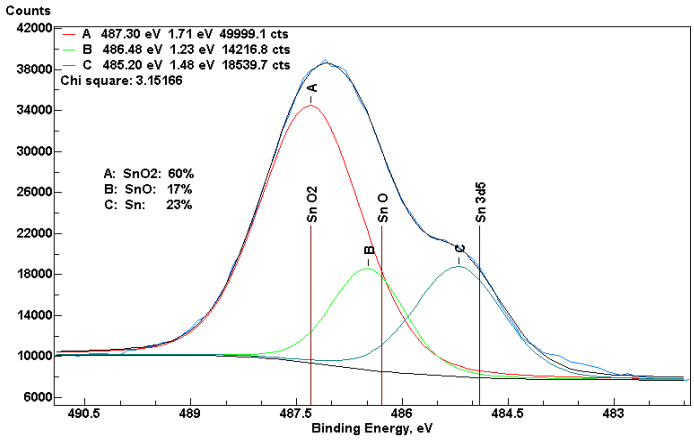

(c)

Figure 41: (a) XPS survey spectrum of 1400 Å Sn on brass exposed to pure O_2 after 150 days of incubation; (b) High resolution XPS scan over the $Sn3d_{5/2}$ peak for Sn on brass exposed to pure O_2; (c) High resolution XPS scan over the $Sn3d_{5/2}$ peak from Sn on brass exposed to RT/RH.

It is useful to compare the oxidation state of Sn surfaces exposed to pure oxygen and atmospheric oxygen. Figure 41(a) shows an X-ray photoelectron spectroscopy (XPS) survey spectrum from the 1400 Å pure O_2 exposed sample, showing the surface composition of the Sn on brass sample. A high resolution (480-490eV) scan over the $Sn3d_{5/2}$ peak is given in Figure 41(b). The best fit of component peaks to the broad spectral envelope reveals that the pure O_2 exposed surface consists of a combination of two oxidation states (SnO_2=30%, SnO=44%) and elemental Sn. Comparison to the atmospheric-exposed case in Figure 41(c) shows that the pure O_2 exposed Sn film has a larger fraction (1.5) of SnO/SnO_2 than the atmospheric-exposed sample (0.3). Theoretical calculations of the Gibbs free energy of formation for SnO and SnO_2 shown in Figure 42 show that both oxides are energetically favorable under equilibrium conditions near room temperature, although SnO_2 is slightly more thermodynamically stable than SnO. The peak deconvolution includes a peak due to elemental Sn which shows that the Sn oxide coverage is exceedingly thin for both oxygen exposures. We infer this from the information volume probed by XPS, which is from 0 – 50 Å below the surface. The fact that Sn in the elemental state is observed in the high resolution XPS spectra shows that the Sn oxides formed are thinner than 50 Å.

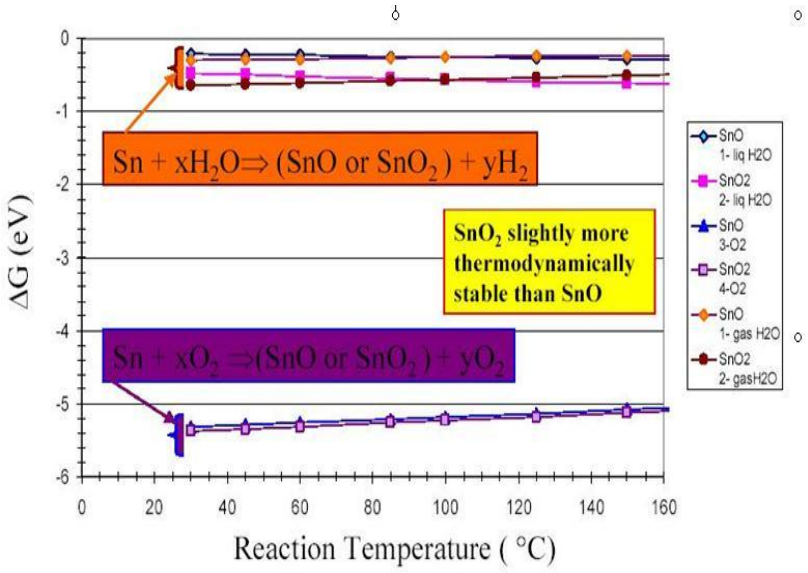

Figure 42: Theoretical Gibbs free energy of formation vs. reaction temperature for Sn oxides [93].

An Auger (AES) depth profile on the pure-O_2 exposed 1400 Å Sn film on brass case as a function of depth is given in Figure 43. The specimen had been incubated in pure O_2 for 150 days. The spot size of the incident AES electron beam had a diameter of ~ 0.1 mm, covering a surface area large enough to potentially intercept ~ 5 whiskers which would minimally contribute to the Sn and O Auger signals. The profile was accomplished by manual successive sputter/spectra cycles (instead of by automated machine setup) in order to follow the peak ratios with film depth. The AES surface composition of the "as-received" O_2 exposed sample (no sputtering) is shown in Figure 43(a), showing the expected Sn, O, and C on the surface. As the profile proceeds, the results indicate a significant amount of film/substrate diffusion during the whisker incubation period. A small amount of Cu is found after 5 min of sputtering (~ 100 Å depth into the Sn film) and after 25 min (~ 675 Å depth), Zn begins to appear. This was surprising, as we expected minimal diffusion and a sharper interface under room temperature conditions. We presume the Cu near the free surface after incubation is due

to Cu diffusion rather than formation of a Cu-Sn intermetallic (IMC) since the AES peak ratio Cu/Sn would be different had a true IMC been formed. During the incubation period, O_2 has not penetrated into the bulk of the Sn film since the O signal nearly vanishes after 5 min of sputtering (the small amount of oxygen observed at all depths in the film is due to oxygen rebuilding on the surface during spectral acquisition). We will have more to say about this later in the dissertation. The thickness of the SnO/SnO_2 layer is < 100 Å, similar to the native SnO/SnO_2 oxide thickness formed under normal atmospheric conditions. The total Sn film thickness measured by AES is ~ 1500 Å, in good agreement with the profilometric-determined value (1400 Å) on the starting film before whisker growth. The AES/XPS results concur that, even in a pure O_2 environment at room temperature, the oxide formed on Sn is *exceedingly* thin.

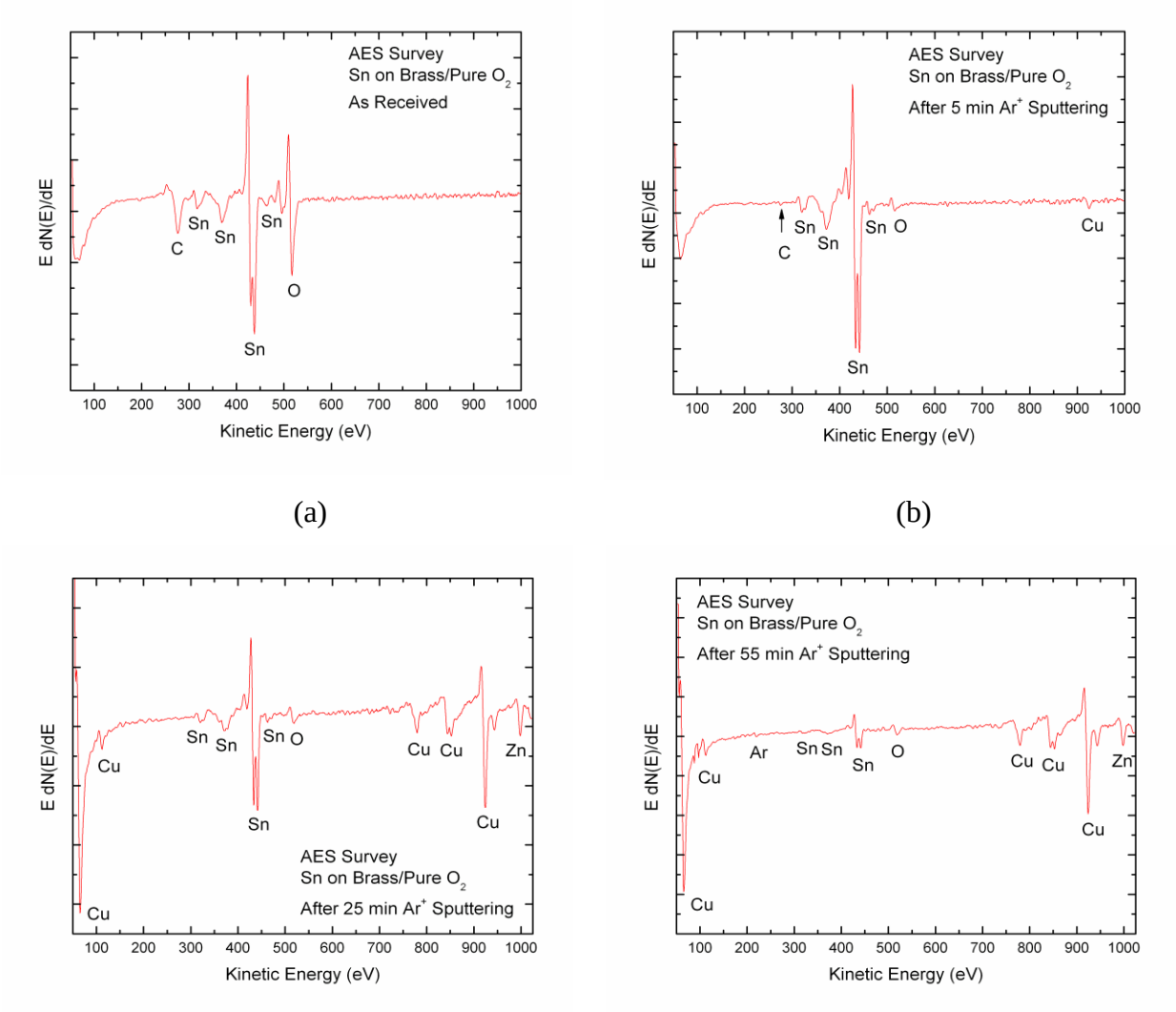

Figure 43: Auger depth profile for the O_2-exposed 1400 Å Sn on brass specimen. AES survey spectra vs. depth (a) as received; (b) after 5 min (c) 25 min, and (d) 55 min of Ar^+ sputtering The sputter rate was ~ 27 Å/min, measured on a calibrated thin film of SiO_2.

3.2 The Influence of Relative Humidity on Whiskering

Several studies [53,93,52] have demonstrated that Sn whisker growth is enhanced by exposure to oxygen and high relative humidity, especially near regions of surface corrosion. Oberndorff et al., e.g, have observed whiskers within 125 µm of corrosion products on electroplated Sn on Cu-alloy exposed to 2500 hours of 60°C/93%RH. Peng Su et al. studied whisker growth in plastic quad flat packages electroplated with a matte

Sn finish (60°C/93%RH) and found that whiskers grew in corroded portions of leads. These and related results suggest that Sn corrosion due to high-temperature/high humidity exposure is a major driving force in whisker growth. A suggested mechanism is that, during corrosion, oxygen displaces Sn atoms in the Sn film but, due to pinned grain boundaries, the excess Sn atoms are constrained to the original volume of the Sn film, creating localized stress in the film. When the pinning constraint is removed, the Sn atoms can diffuse to nucleation sites to decrease the localized stress. As we saw in the previous section, there is a marked increase in whisker growth when a Sn film is exposed to pure O_2 compared to ambient room temperature/humidity. The goal of the current study is to further investigate the role of oxygen in the whiskering process by exposing sputtered Sn films to various controlled relative humidity environments.

Pure Sn films were sputter deposited on brass and Si substrates using a 99.999% pure Sn (Kurt Lesker Co) target. The thickness of the deposited films was 1500 Å, measured by stylus profilometry over a step edge of the deposit. The brass (Cu63/Zn36) substrates were commercial metal sheets which we cut into coupons of dimension 1 cm x 1 cm. To observe whisker growth within a reasonable time period, the brass coupon surfaces were electrochemically polished, since previous work showed enhanced whisker growth on smooth surfaces [80]. The Si substrates were (100) oriented, n-type commercial wafer specimens, snap cleaved to 1 cm x 1 cm dimensions. Si was chosen due to its atomically smooth surface and because Si and Sn do not create intermetallic compounds (IMC), which eliminates the stress contribution due to IMC growth. The Sn films were sputtered at Ar gas pressures of 2-3 mT, producing intrinsic compressive stress in the films [65]. Subsequently, the coupons were transferred to highly controlled

environments containing the desired relative humidity. The humidity environments were created within air tight beakers sealed with rubber stoppers. The specimens (Figure 44) were laid on a stainless steel platform connected to the bottom of the beaker's stopper, which was suspended over the various saturated aqueous salt solutions (Table 30) used to maintain the relative humidity environments [95] at room temperature.

Figure 44: Sputtered Sn film coupons exposed to saturated aqueous salt solution.

Table 30: ASTM Saturated Salt Solutions Used to Create Accurate Relative Humidity Environments

Saturated Salt Solutions	**Calibrated Relative Humidity (RH)**
Magnesium Chloride	33.1 ± 0.2
Potassium Carbonate	43.2 ± 0.4
Potassium Iodide	69.9 ± 0.3
Sodium Chloride	75.5 ± 0.2
Potassium Chloride	85.1 ± 0.3
Potassium Sulfate	97.6 ± 0.6

The samples were periodically removed from their humidity environments and transferred to a scanning electron microscope (SEM) where whisker observation and counting occurred. The whisker densities were determined by manually counting whiskers over ten equal areas (~275 µm x 275 µm) representative of the surface. The whisker lengths were estimated using the calibrated micron marker of the SEM and, as indicated above, no attempt was made to correct for length foreshortening due to the observation angle [96]. Before the samples were placed back into their humidity environments, each beaker was emptied, cleaned, and fresh solutions were used to continue the RH exposure.

After one month, whisker growth is observed on every sample at every relative humidity. The 69.9% RH produced the most whiskers for both substrates at 29,080 (brass) and 14,409 whiskers/cm^2 (Si), shown in Table 31. The longest average whisker lengths were observed on the 75.5% RH samples (8.6 µm for brass and 3.7 µm for Si). The 75.5% RH Sn on brass specimen grew the longest whiskers, but it also produced the lowest whisker density (3,668 whiskers/cm^2). The smallest whisker density observed for Sn on Si was at the lowest humidity, 33.1% RH (2,620 whiskers/cm^2).

Table 31: Whisker Statistics after 30 Days of Incubation for RH Exposed Specimens

Humidity (RH)	**Substrate**	**Whisker Density (cm^{-2})**	**Average Whisker Length (μm)**
33.1 ± 0.2	Brass	5,764	2.5
	Si	2,620	3.6
43.2 ± 0.4	Brass	5,502	2.5
	Si	3,668	2.9
69.9 ± 0.3	Brass	29,080	2.8
	Si	14,409	3.3
75.5 ± 0.2	Brass	3,668	8.6
	Si	11,134	3.7
85.1 ± 0.3	Brass	4,716	4.8
	Si	4,978	2.3
97.6 ± 0.6	Brass	8,646	2.6
	Si	10,610	2.3

Table 32: Whisker Statistics after 137 Days of Incubation for RH Exposed Specimens

Humidity (RH)	Substrate	Whisker Density (cm^{-2})	Average Whisker Length (μm)
33.1± 0.2	Brass	40,870	5.4
	Si	24,365	9.1
43.2 ± 0.4	Brass	25,806	4.7
	Si	22,662	5.7
69.9 ± 0.3	Brass	93,136	6.1
	Si	82,788	9.3
75.5 ± 0.2	Brass	81,740	3.7
	Si	110,296	7.1
85.1 ± 0.3	Brass	96,280	3.6
	Si	164,527	3.7
97.6 ± 0.6	Brass	13,492	4.0
	Si	94,446	4.7

Whisker statistics after ~ 140 days is shown in Table 32, where an increase in whisker growth is observed in all samples, with some Sn/Si samples exceeding100,000 whiskers/cm^2. The highest whisker density occurs for 85.1% RH (96,280 whiskers/cm^2 for brass and 164,527 whiskers/cm^2 for Si). After a month of incubation the highest whisker densities were found on the samples exposed to 69.9% RH, but after an additional ~100 days of incubation, the 69.9% RH samples now show the longest average whiskers for both the brass and Si substrates, at 6.1 and 9.3 μm respectively. After ~ 140 days, the average whisker lengths are longer on Si at every humidity level. While there is a rise in the whisker density for all samples with time at humidity, the average whisker length does not increase in every case. For example, the whisker length for Sn on brass at 75.5% RH goes from 8.6 to 3.7μm over 150 days. More short whiskers have grown,

contributing to a shorter average whisker length. The lowest whisker densities were observed for 43.2% RH (Si) and 97.6% RH (brass).

Figure 45 illustrates the whisker densities as a function of humidity after ~140 days. Relative humidity in the 65 - 90% range produces the highest whisker numbers on both substrates. The maximum whisker densities occurred for ~ 77% (Sn) and ~ 85% (brass).

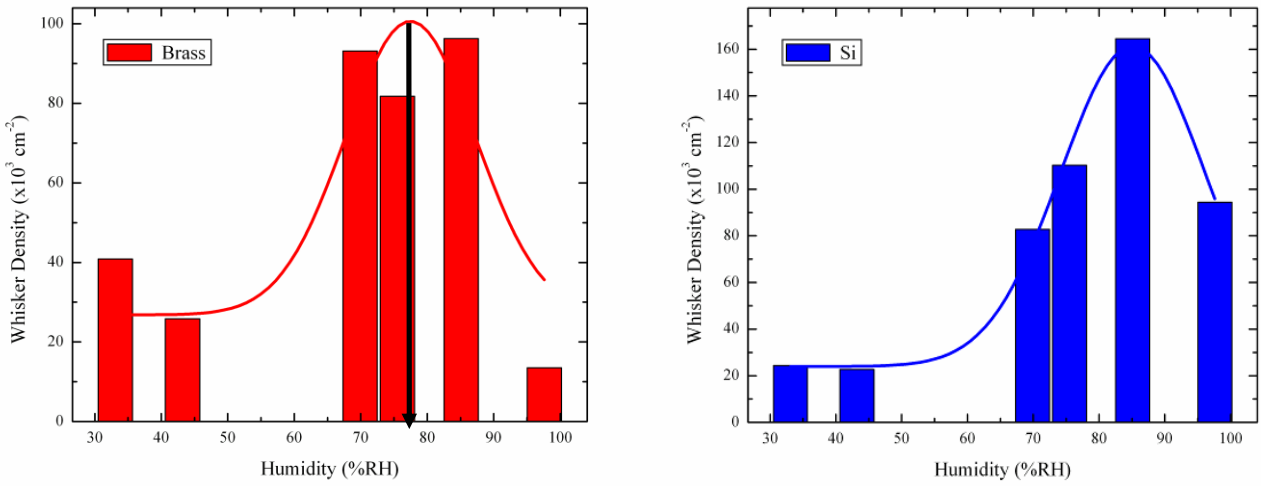

(a) (b)

Figure 45: Whisker densities produced in various humidity environments for the case of Sn films on (a) brass and (b) silicon.

Table 33: Comparative Whisker Statistics for Sn on Brass (~ 145 Days of Incubation)

Specimen	**Sn Film Thickness (Å)**	**Whisker Density (cm^{-2})**	**Average Whisker Length (μm)**
Sn (pure O_2)	1400	15,588	5.7
Sn (85% RH)	1500	96,280	3.6

To summarize (Table 33), the average whisker length for pure O_2 exposed Sn/brass is ~ 1.5X the average whisker length for the highest whisker producing case of Sn on brass (85.1% RH) based on humidity. However, the longest average whisker length for Sn on brass exposed to humidity (69.9% RH) is about the same for the O_2 exposed case. After similar incubation times, Sn on brass exposed to 85.1% RH produced >6X the whisker density of pure O_2 exposed Sn/brass. Representative SEM images of typical whiskers grown during ~140 days of exposure to each RH environment from the deposited thin Sn/brass films is displayed in Figure 46 and similarly for Sn/Si in Figure 47.

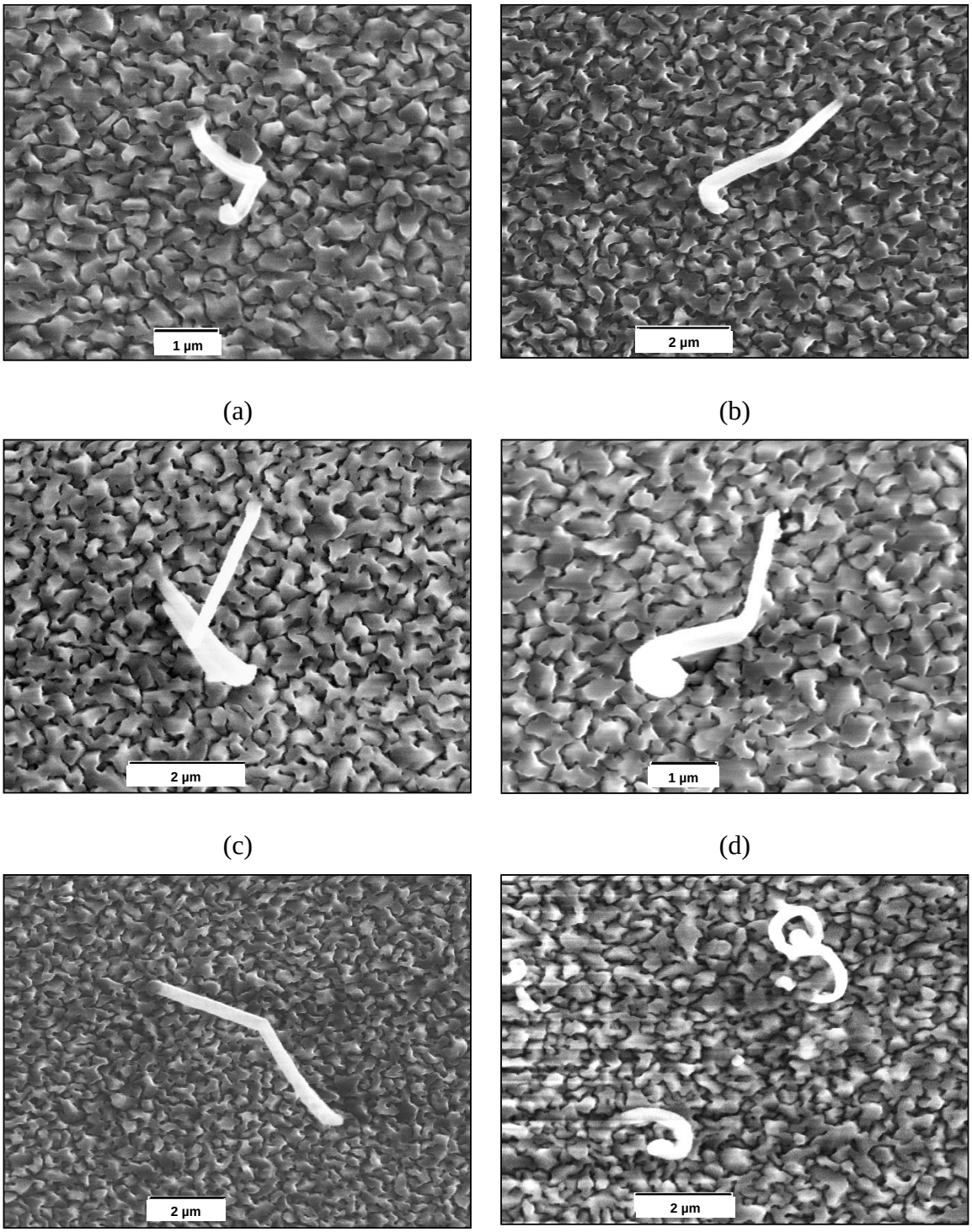

Figure 46: Whiskers formed in humidity environments for 1500 Å Sn films on brass (a) 33% RH (b) 43% RH (c) 70% RH (d) 76% RH (e) 85% RH (f) 98% RH.

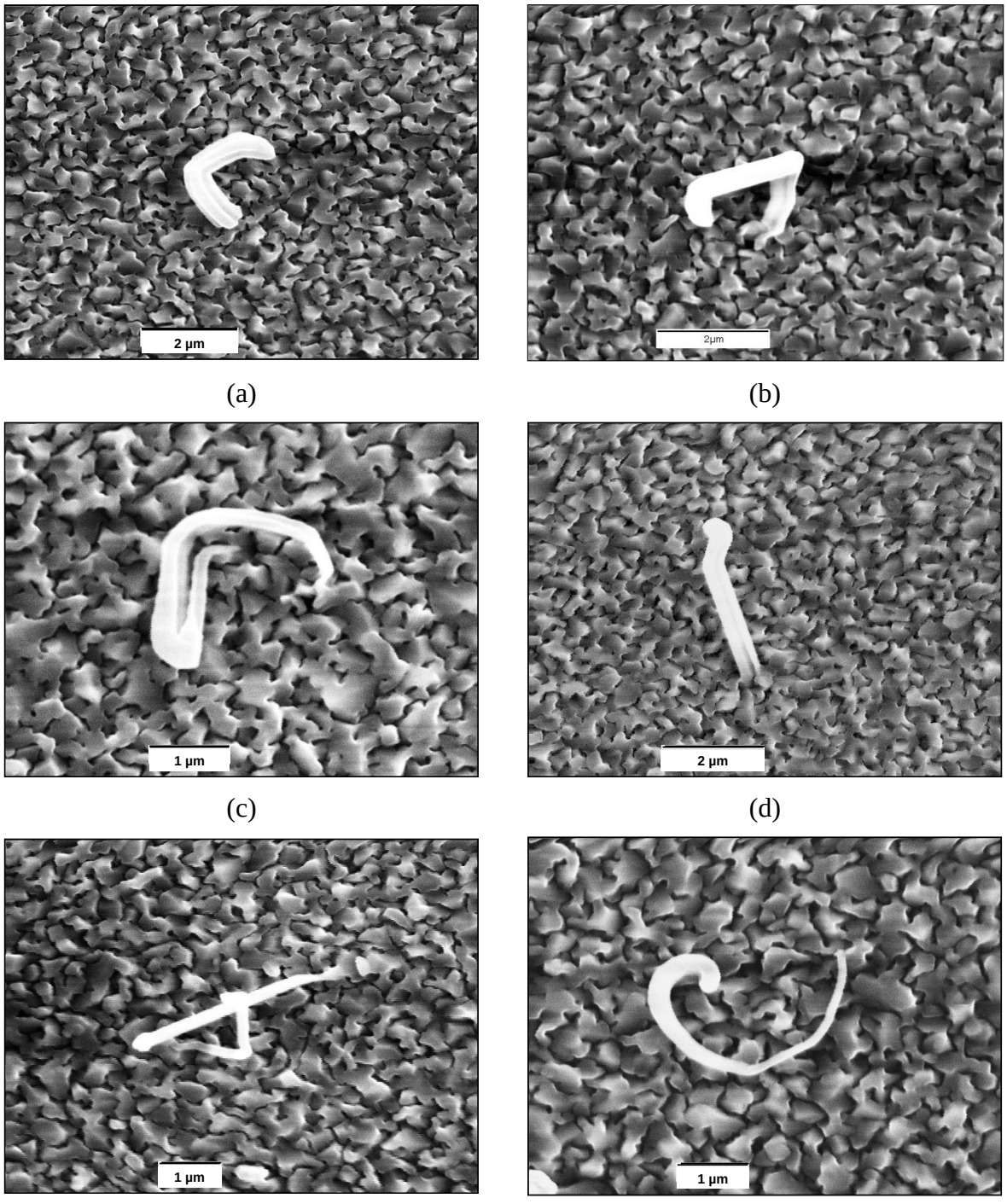

Figure 47: Whiskers formed in humidity environments for 1500 Å Sn films on Si (a) 33% RH (b) 43% RH (c) 70% RH (d) 76% RH (e) 85% RH and (f) 98% RH.

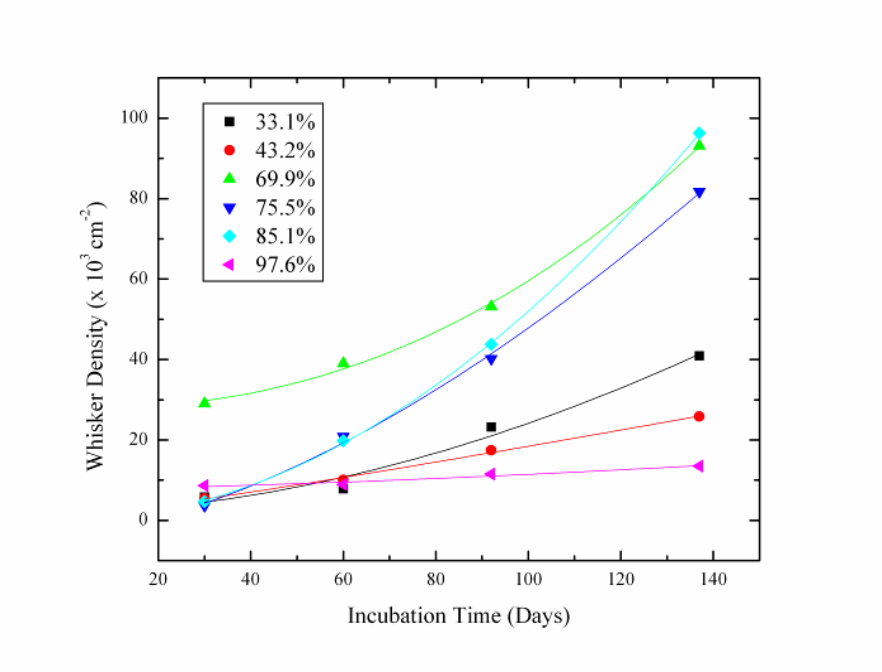

(a)

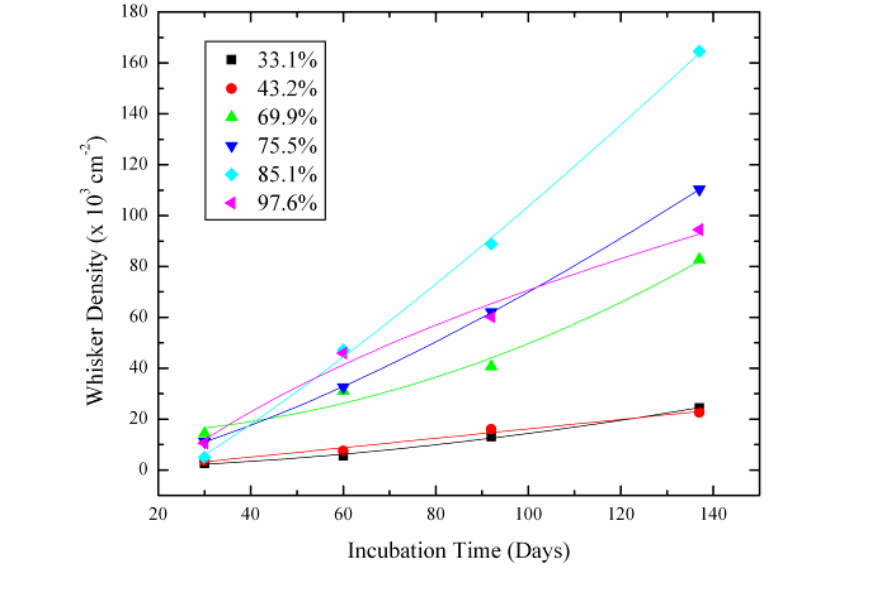

(b)

Figure 48: Whisker density vs. incubation time for 1500 Å Sn film deposited on (a) brass and (b) Si exposed to relative humidity environments.

Figure 48 shows the whisker density as a function of time over the full range of humidity environments, 33-98% RH. The highest slope is for 85% RH, which agrees with previous studies concerning the effect of humidity on whiskering, where it was found that ~85-93% RH produces the higher whisker densities [97]. After only two months of incubation, corrosion features/products are observed on the exposed specimens (Figure 49) and, in many cases, whiskers were found protruding from the corroded surface, as seen in Figure 50. Though corrosion was observed on all specimens, the corrosion didn't always occur before whisker growth.

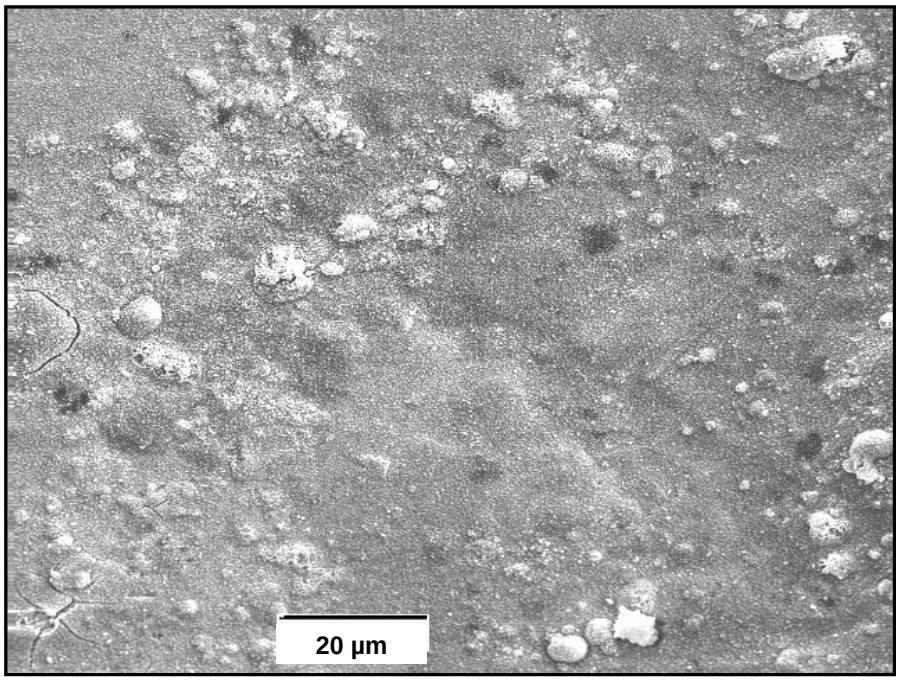

(a)

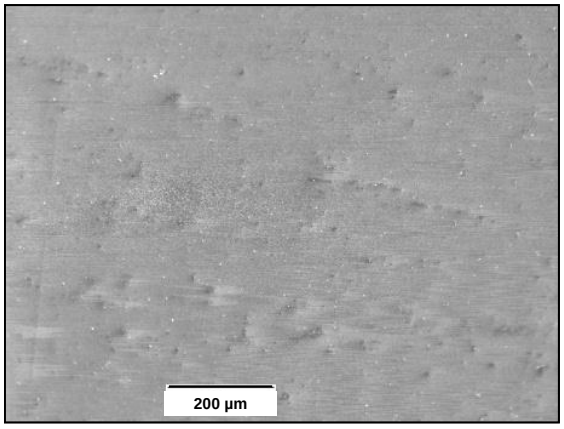

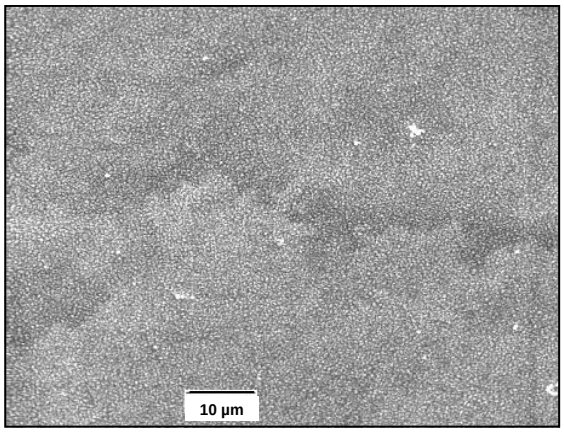

(b)

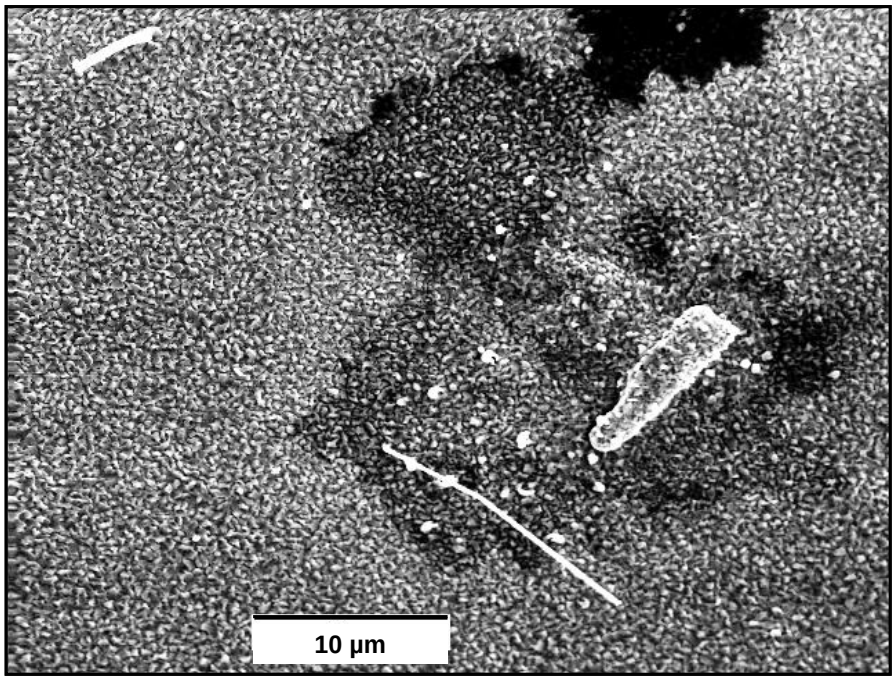

(c)

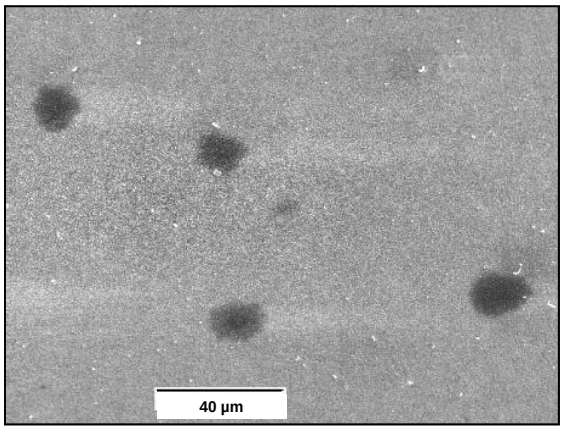

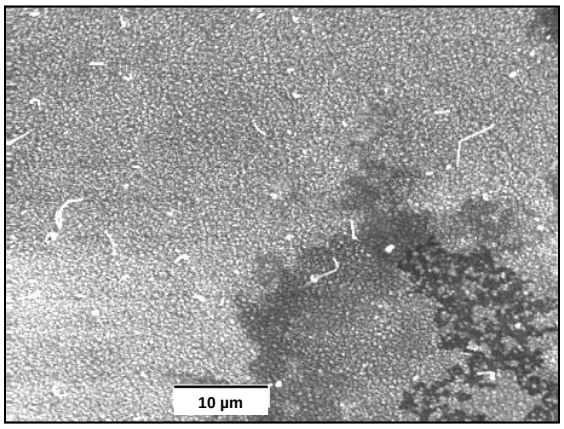

(d)

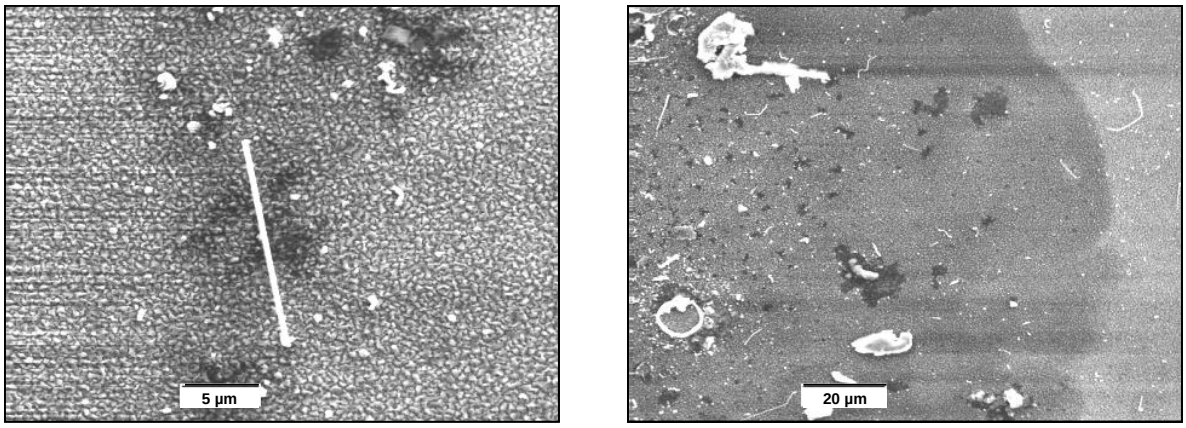

(e)

Figure 49: Corrosion features observed on the different humidity environments: (a) 33 % RH on brass; (b) 70 % RH on brass; (c) 76% RH on Si; (d) 85 % RH on Si; and, (e) 98% RH, (left) on brass and (right) on Si.

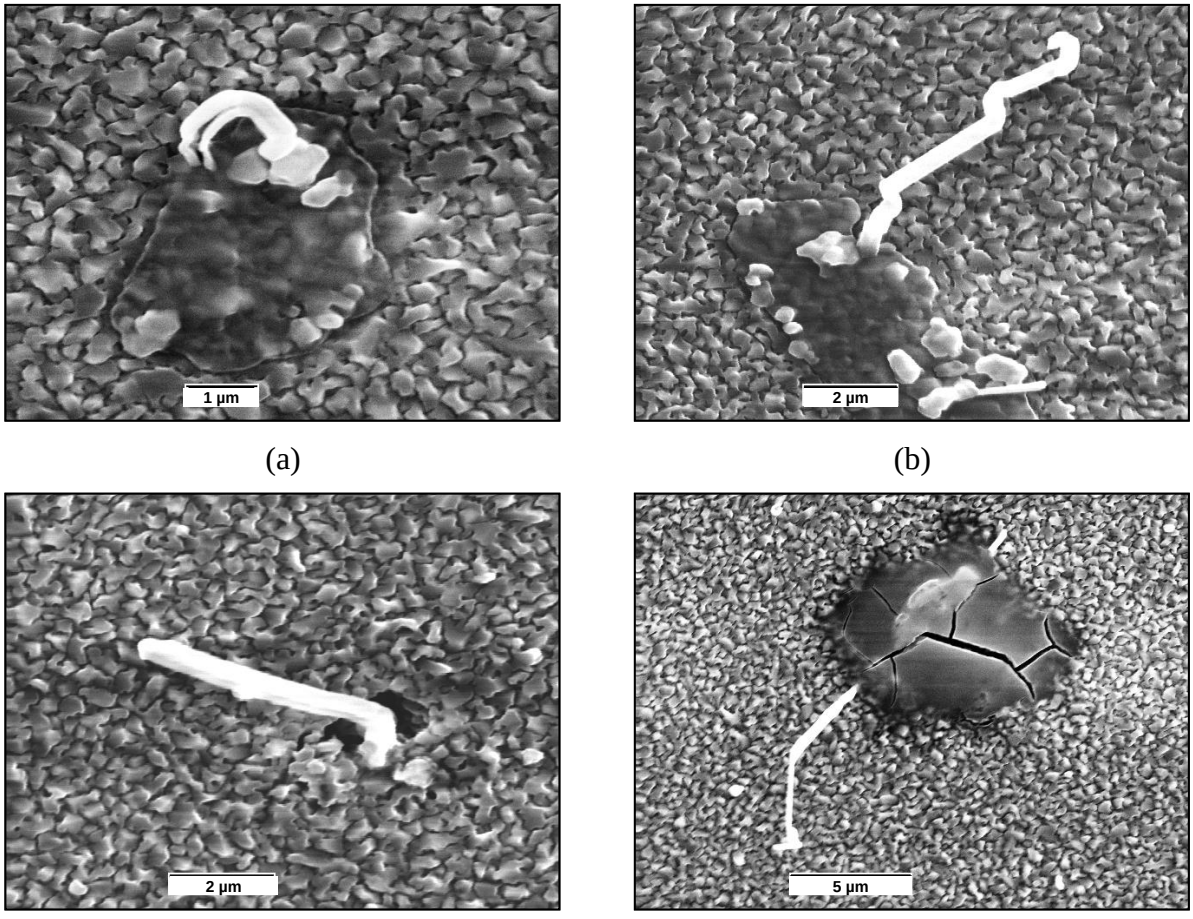

(a) (b)

(c) (d)

Figure 50: Whisker growth from corrosion regions due to humidity exposure (a) 33% RH on brass (b) 76% RH on brass, (c) 98% RH on brass and (d) 98% RH on Si.

3.3 The Role of Sn Oxide Formation on Whisker Growth

In the previous two sections we saw that oxygen/humidity significantly affects whisker growth. Surface oxidation, diffusion of oxygen into Sn, and formation of bulk Sn oxides are all thought to play important roles [98,99] in the whisker process. This section details some preliminary studies we have done which address Sn oxide formation and growth. To truly understand the role of oxygen in whiskering it is important to understand Sn oxide products formed in various environments.

Surprisingly, little is currently known/been reported on Sn oxide growth. It is clear from our studies here that a surface oxide of two to five monolayers (~ 30-50 Å) in thickness is formed on Sn films exposed to oxygen at temperatures ~ 25^{o}C. Also, electron diffraction work has indicated that when Sn foil is thermally oxidized in air, an amorphous oxide layer is formed at temperatures up to 130°C. Above 130°C, one study has reported that only crystalline SnO and SnO_2 are formed [100].

In our work here, pure Sn films were sputter deposited on Si substrates. The thickness of the deposited films was 2000 Å and 2μm, measured by stylus profilometry over a step edge of the deposit. The Si substrates were commercial, (100) oriented, n-type wafer specimens, snap cleaved to 1 cm x 1 cm dimensions. The Sn films were sputtered at Ar gas pressures of 2-3 mT, producing intrinsic compressive stress in the films [65]. For comparison, commercial bulk Sn substrates [71] were carried along in the design of experiments. After deposition, the coupons were transferred to wet and dry oxidation environments (shown in Figure 51). The wet oxidation environment was produced by a medical autoclave where the specimens were exposed to H_2O steam at 121°C for 12-15

hrs. Dry oxidation was provided by a furnace with continual pure O_2 flow (~0.5 sccm) at varying temperatures and exposure times. Table 34 describes the matrix of samples for this study.

(a) (b)

Figure 51: (a) Medical autoclave and (b) semiconductor furnace environments.

Table 34: Matrix of Samples in Sn Oxide Growth Study

	Sn Specimen	Temperature (°C)	Exposure Time (hr)
Wet Oxidation (Autoclave)	0.2 µm	121	15
	2µm		12
	Bulk Sn		12
Dry Oxidation (O_2 Furnace)	0.2 µm	100	1
			5
			10
			20
		150	1
			5
			10
			20
		200	1
			5
			10
			20
	Bulk Sn	175	10
			20
			30
			40
		200	10
			20
			30
			40
		215	10
			20
			30
			40
	2µm	215	10
			20
			30
			40

The Sn film surfaces were examined for oxide growth using Auger electron spectroscopy (AES), X-ray photoelectron spectroscopy (XPS), Rutherford backscattering (RBS), and Raman spectroscopy. By recording high resolution XPS features around the $Sn3d_{5/2}$ peak, the oxidation states of the surface Sn oxides could be determined and compared to each other and to ambient room temperature/humidity oxide conditions. AES/RBS depth profiling was utilized to determine the elemental trend of the incubated Sn film as a function of depth.

Wet Oxidation @ 120^{o}C

The 2000 Å Sn/Si films exposed to H_2O steam at 121°C in an autoclave for 15 hr were examined with XPS depth profiling. XPS (Figure 52) shows that the best fit of the $Sn3d_{5/2}$ peak (Table 35) at the very top surface yields ~55% SnO_2 and 45% SnO and 100% SnO at roughly 100 Å into the film.

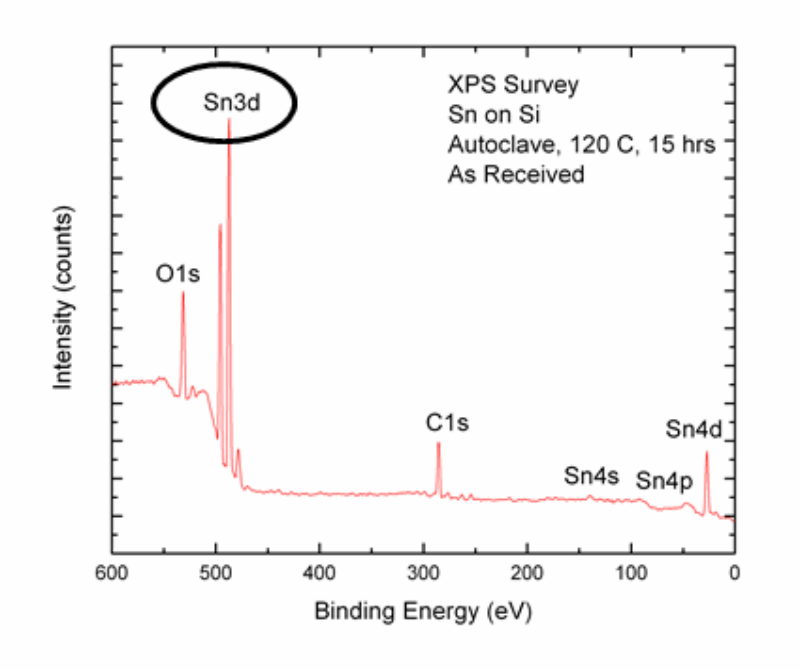

Figure 52: XPS survey for the "as received" autoclave-exposed, 2000 Å Sn surface.

Table 35: XPS Best Fit of $Sn3d_{5/2}$ Peak

Surface Analysis Depth (Å)	**% SnO_2**	**% SnO**
Very Top	55	45
~ 100	-	100

Next, bulk Sn and the 2 µm Sn/Si film were exposed to H_2O steam at 121°C for 12hrs. The oxide products were elucidated by RBS since AES depth profiling would have required prohibitively long time periods for such thick materials. RBS spectra in Figure 53 show oxygen throughout the entirety of both specimens; the sputtered Sn film has a larger O/Sn ratio (0.45) than the bulk Sn (0.30). This is probably explained by the microstructure of the bulk and sputtered Sn (Figure 54). The sputtered Sn contains a

much finer grain structure, allowing for more opportunities for oxygen to diffuse into the Sn and react with Sn atoms.

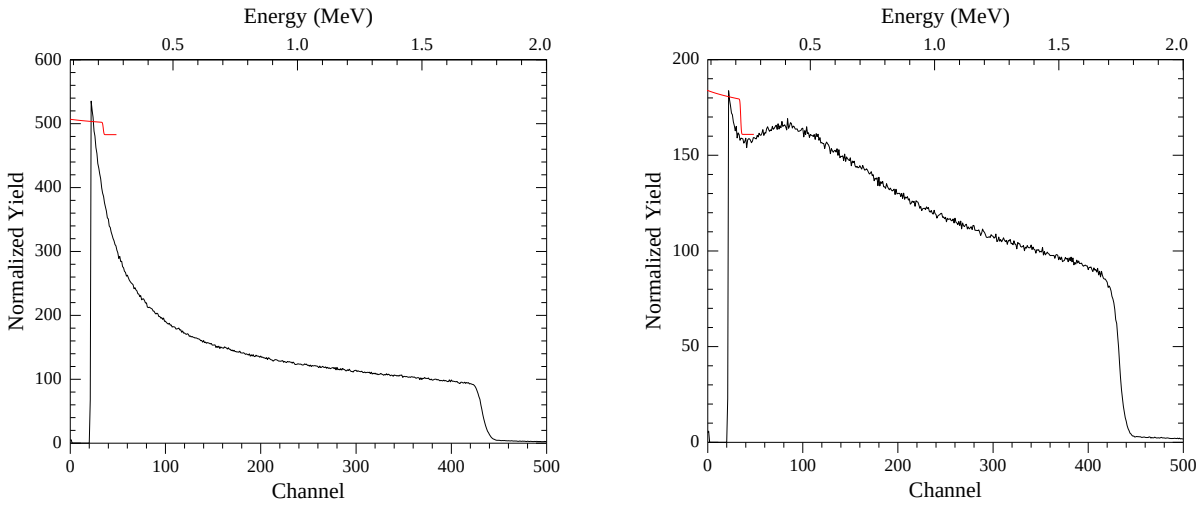

(a) (b)

Figure 53: RBS spectra of (a) bulk Sn and (b) 2 µm Sn film on Si after steam exposure.

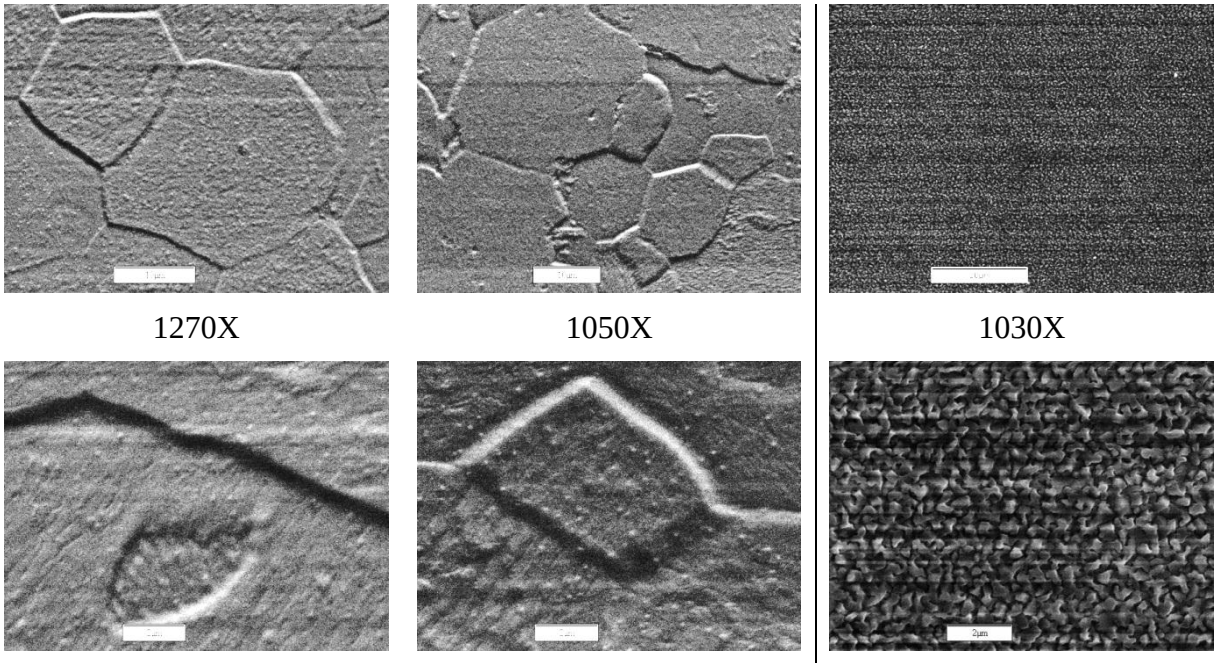

1270X 1050X 1030X

4890X 4980X 5120X

(a) (b)

Figure 54: SEM images of (a) bulk polycrystalline and (b) sputtered Sn surfaces.

Dry Oxidation

Sn/Si films (2000 Å) were exposed to continuous flow of pure O_2 (~ 0.5 sccm) in a semiconductor-grade oxidation furnace at temperatures of 100, 150, and 200°C for times of 1, 5, 10, and 20 hrs. RBS analysis showed that the SnOx layer grown on the 100 and 150°C specimens (at all exposure times) were too thin to measure. This is shown in Figure 55(a), which shows identical RBS spectra at each exposure time for the 150°C samples, with no oxygen signal. Subsequent AES analysis showed why there seemed to be no oxides on these specimens; only a thin "native" Sn oxide formed at 150°C for all exposure times (the RBS resolution @ 2MeV incident beam energy is ~ 100 ± 50 Å).

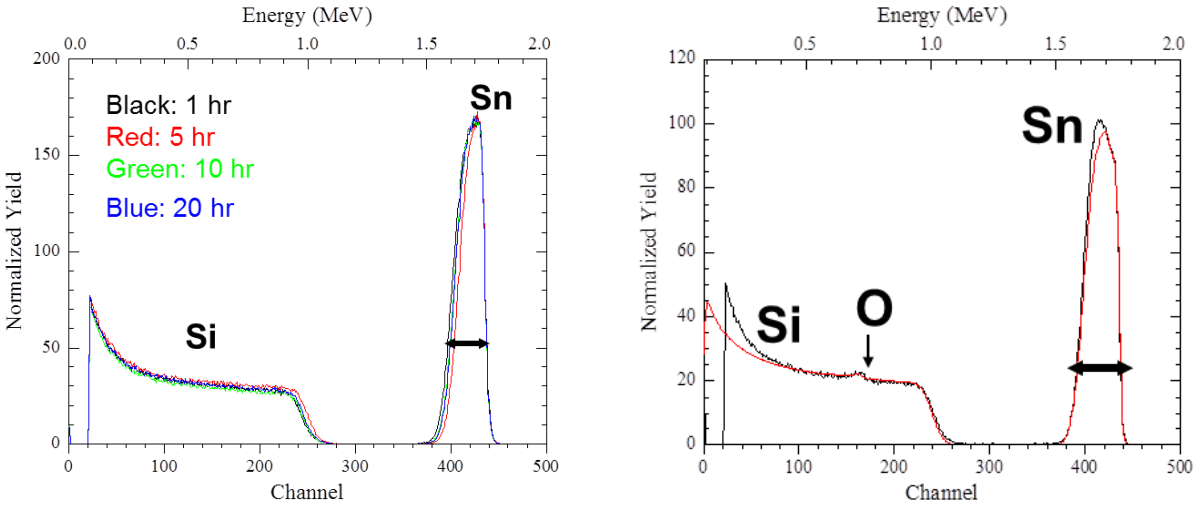

(a) (b)

Figure 55: RBS spectra of oxygen-exposed 2000 Å Sn films at (a) 150°C and (b) 200°C. (a) RBS spectra only. (b) RBS spectrum (black) with simulation (red) assuming a tin oxide surface layer (see Table 36).

Exposure to oxygen at 200°C was different. A representative RBS spectrum for 2000 Å Sn/Si exposed at 200°C is shown in Figure 55(b). A small oxygen peak has emerged. Table 36 shows the SnOx development vs. depth. The best RBS fit-to-data

yields a complex, "double SnOx" layer with less oxygen at depth in the film. The longer the exposure time, the higher the oxygen content in the film, with the longest, 20 hr, exposure specimen having an O/Sn ratio of 0.8 up to 1300 Å into the film. Also, notice that once we reach 200°C (approaching 232°C, the melting point of Sn), the ~ 2000 Å Sn films are completely penetrated by oxygen (even if the oxygen content is small towards the bottom of the film). In summary, the dry oxidation characteristics of sputtered Sn films completely changes between 150 and 200°C. At 150°C, Sn is unaffected by oxygen, while at 200°C, oxygen completely penetrates Sn.

Table 36: RBS Results for Furnace Dry O_2 Exposed Sputtered Sn Samples at 200°C

Exposure Time (hrs)	Uppermost Layer		Underlying Layer	
	Thickness (Å)	O/Sn Atom Ratio	Thickness (Å)	O/Sn Atom Ratio
1	700	0.4	1300	0.1
5	700	0.5	1350	0.2
10	700	0.5	1500	0.2
20	1300	0.8	700	0.3

An XPS survey spectrum taken on the surface of the 150°C, 1 hr exposed specimen is shown in Figure 56(a), along with the best fit of the $Sn3d_{5/2}$ peak in Figure 56(b). This was done on all 150°C/2000Å Sn samples, with SnO_2, SnO, and Sn compositions given in Table 37. We find that all samples have higher concentrations of SnO than SnO_2 with elemental Sn compositions ranging from ~25-30% (at). The fact that the SnO/SnO_2 ratios are relatively constant vs. O_2 exposure time and elemental Sn is

observed concurs with the RBS results, showing that oxidation at 150°C has little effect. No oxygen penetrates below ~ 50 Å of the Sn surface.

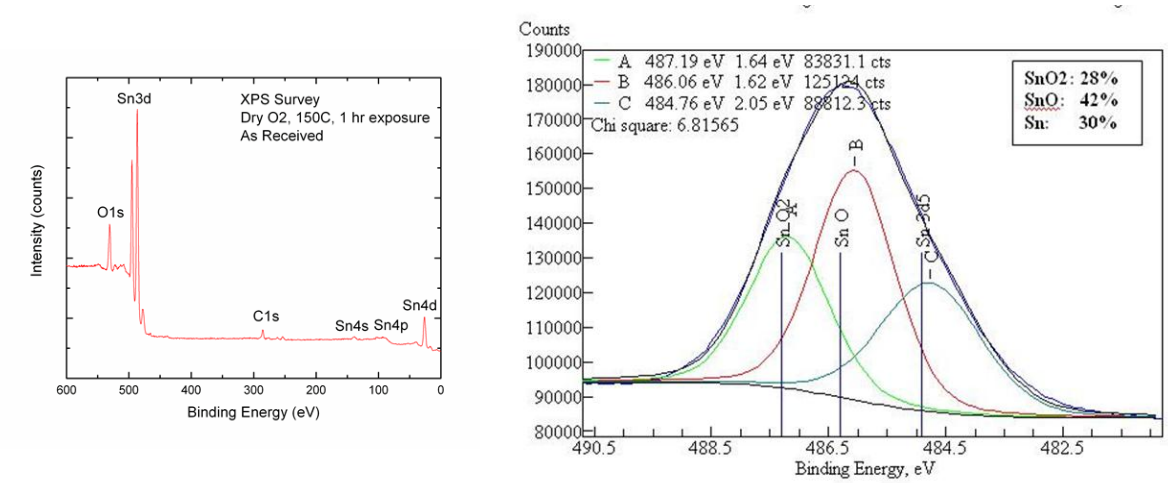

(a) (b)

Figure 56: XPS survey of 1 hr exposed 150°C specimen (a) as received surface and (b) best fit of high resolution XPS $Sn3d_{5/2}$ peak.

Table 37: Best $Sn3d_{5/2}$ Peak Fitting Results for 150°C Oxygen Exposed Samples

O_2 Furnace Exposure (hr)	**% SnO_2**	**% SnO**	**% Sn**
1	28	42	30
5	30	40	30
10	33	43	24
20	35	36	29

Finally, Raman scattering was used to determine the dominant SnOx product in the Sn oxide films. In Raman spectroscopy, incident laser light excites vibrational modes of resident molecules in a material, yielding scattered photons diminished in energy by

the amount of vibrational transition energies, depicted in Figure 57. The technique lacks depth resolution, so Raman data gives a "volume-averaged" film composition, not a composition vs. depth. Raman spectroscopy spectra are shown in Figure 58, with results in Table 38, where we see a strong signal of SnO in all 200°C exposed samples, with SnO_2 appearing in the longer, 20 hr exposed specimens.

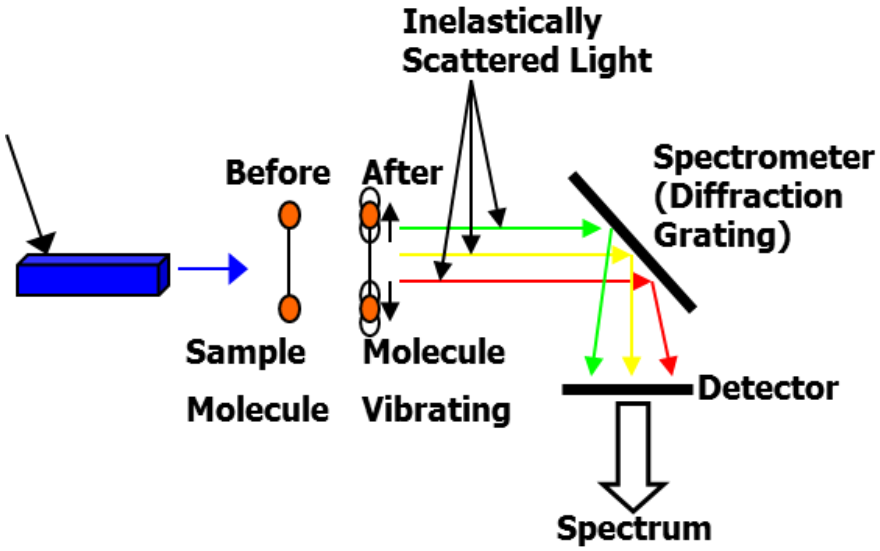

Figure 57: Simplified schematic of Raman scattering.

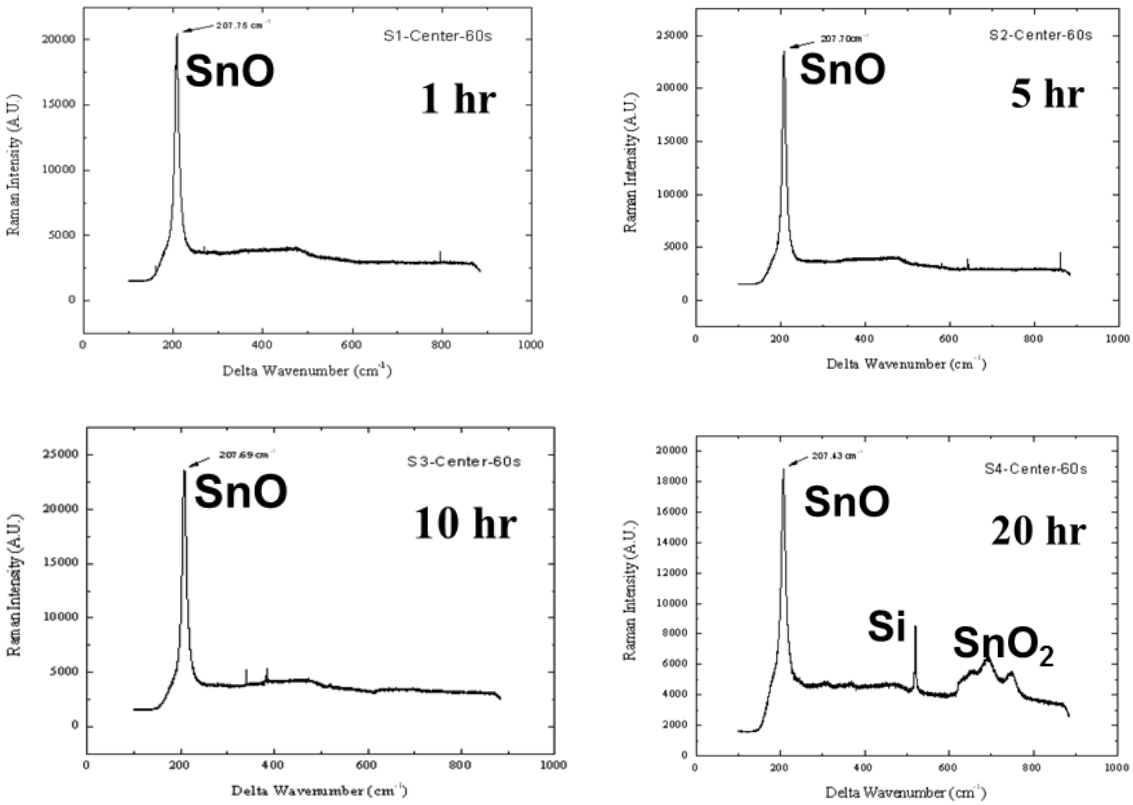

Figure 58: Raman scattering spectra on 2000 Å Sn on Si exposed to O_2 furnace at 200°C.

Table 38: Raman Scattering Results on Sn Oxide of 200°C Specimens

Exposure Time (hrs)	**SnOx Observed**
1	SnO
5	SnO
10	SnO
20	SnO, SnO_2

Bulk, Polycrystalline Sn Dry Oxidation

Here we compare oxidation of bulk, polycrystalline Sn to sputter deposited 2 µm Sn/Si films for 175, 200, and 215°C for 10, 20, 30, and 40 hrs of O_2 exposure. Figure 59 shows no discernible oxygen in any of the bulk Sn specimens. As mentioned earlier, this may be explained by the difference in grain structure of the bulk Sn compared to sputtered Sn (Figure 54). The sputtered Sn contains a much finer grain structure, alloying for more vacancy opportunities for oxygen to diffuse into the Sn and react with Sn atoms to form oxide products.

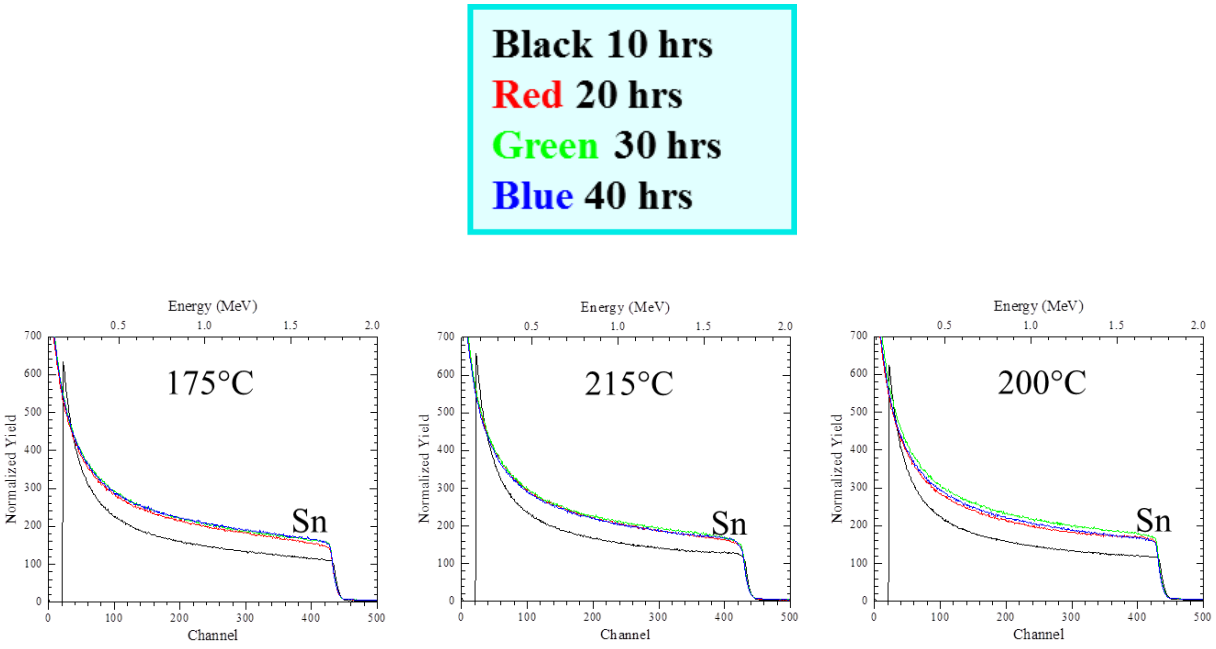

Figure 59: RBS spectra for bulk, polycrystalline Sn exposed to O_2.

Contrastingly, for the case of SnOx growth on the thicker 2 µm, sputtered Sn films exposed to pure dry O_2 at 215°C for various times, RBS sees an infinitely thick layer of Sn with oxygen penetration throughout the entire 2 µm film, just as for the 2000 Å samples. Table 39 displays the RBS O to Sn ratio. After exceeding 20 hrs of exposure

time, the O to Sn ratio is found to be roughly constant (0.4). In general, sputtered Sn films exposed to oxygen at temperatures ≥ 200°C, result in oxygen penetration throughout the entire film thickness (up to 2 µm).

Table 39: RBS Results on SnOx of 2 µm Sn Films Exposed to Dry O_2 at 215°C

Exposure Time (hrs)	**O/Sn Atom Ratio**
10	0.1
20	0.4
30	0.4
40	0.4

In conclusion, grain size and wet/dry environments make a substantial difference in Sn oxidation (Table 40). Under wet conditions, bulk oxidation is possible at 120^{o}C regardless of whether the Sn is in bulk or thin film form. Under dry conditions, however, bulk oxidation does not turn-on until temperatures near the Sn melting point. In either case, one begins to wonder about the true role of oxidation in whiskering, since this study implies that (at least pure) oxygen is not getting into the Sn bulk at temperatures near the standard operating temperature of most electronic circuitry. Understanding the details of Sn oxidation will be a fruitful line of inquiry for the next thesis student.

Table 40: Overall SnOx Growth Results for Wet Oxidation and Dry Oxidation on Sputtered Sn Film and Bulk Sn.

	Dry Oxidation (O_2 Furnace Exposure)	**Wet Oxidation (Autoclave)**
Sputtered Sn Films	No oxide growth until temperatures approach melting point of Sn (≥ 200°C) and then bulk oxidation occurs	Bulk oxidation occurs at 120°C (the only T tested)
Bulk Sn	No bulk oxide growth	Bulk oxidation occurs

3.4 Is a Surface Sn Oxide Necessary for Whisker Growth?

Our interest here is to elucidate the role of **surface** oxidation on whiskering. It is undeniable that oxidation plays an important role in the whiskering process [93,56,23,101,38,102]. The question is what role. Our studies above and others have demonstrated that Sn whisker growth is enhanced by exposure to oxygen and high relative humidity conditions [53,52,103]; however, there is a growing body of work which demonstrates that surface oxidation is not necessary for whisker growth. The evidence is fourfold: 1) In the 1950's, Brenner [104] observed Au whiskers growing from a film of condensed supersaturated gold vapor on quartz in air at about 1040°C. He concluded that it was unlikely for oxide films to play a major role in whiskering. Further, by comparing the yield strength of Au whiskers to copper and zinc whiskers, Brenner [105] established that a key mechanical property of gold whiskers (without a native oxide layer) was the same as whiskers produced with an oxide film. 2) Studies by Moon, Handwerker, et al. [39] in 2005 concluded that surface oxidation had a minimal effect on whisker growth after observing whiskers (under ultrahigh vacuum (UHV) conditions) from an electrodeposited Sn-1.5% Cu film both with and without a native oxide layer.

The oxide-free section of the film surface was generated by Ar^+ sputter cleaning; a standard in-situ cleaning method used in surface science studies. 3) At about the same time, we did a similar (unpublished) experiment using a sputter deposited Sn on brass specimen which was incubated in UHV. The two-sided specimen contained a section of native Sn oxide and a section where the oxide had been removed by sputter cleaning. Subsequently, the sample was stored in vacuum (~ 7 x 10^{-9} torr) to prevent further oxide growth during whisker incubation and growth. The results were similar to Moon and Handwerker; whisker growth was observed on both oxide and oxide free sections of the Sn film. We have since repeated this experiment with the same results; 4) At least two anecdotal reports of Au whiskers exist in the literature, discussed below.

A concern with experiments in UHV where the surface oxide has been removed has to do with the fact that, even under UHV conditions, oxygen can rebuild on many surfaces parked in vacuum due to adsorption of oxygen-containing residual gas molecules in the chamber, essentially "re-oxidizing" the surface. Figure 60 shows a mass spectrogram of residual gases inside a typical vacuum system at ~ 10^{-9} torr, where oxygen exists primarily as H_2O, CO, and CO_2. The issue is whether there is a sufficient flux of oxygen-containing species during the whisker incubation period to "rebuild" and/or "reoxidize" the Sn surface. We previously studied this in our lab using Auger electron spectroscopy (AES) and X-ray photoelectron spectroscopy (XPS) and find that there is very little (~ a few at%) buildup of oxygen on surfaces of Sn over weeks of parking under ~ 10^{-9} torr vacuum conditions. This lends credence to the prior experiments which reported that whiskers can grow from sputter cleaned, oxide-free Sn surfaces. Nevertheless, there is a desire to go a step further and determine if whiskers can

grow in an environment where native and/or "built-up" oxides are guaranteed to be absent.

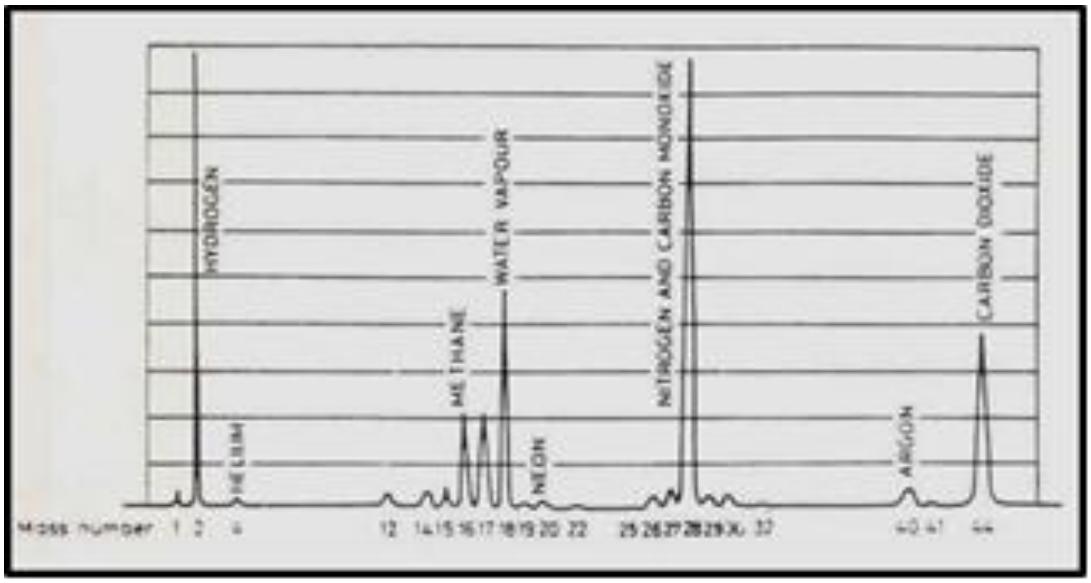

Figure 60: Mass spectrum of typical residual gases found in vacuum, ~10^{-9} torr.

This question is vital for theories of whisker growth which presume that surface oxides play a necessary role in whisker growth. Consequently, we have attempted to grow Au whiskers in our laboratory by using a compressively-stressed, sputtered-deposited Au film on Si, since Au does not form a native surface oxide layer, either in air or under vacuum (Table 41). To verify that oxygen was not rebuilding on the Au surface, the Au films were incubated in a multi-technique surface system while carefully monitoring the Au surface periodically for oxide buildup with AES/XPS. If Au whiskers are observed under these highly controlled conditions, it should put to rest theories of whiskering which rely on the necessity of a cracked or stress-modifying surface oxide in the whiskering process.

Table 41: Gibbs Free Energies of Formation Common Metal Oxides [106]

Element	Common Oxide	Gibbs Free Energy @ 25°C (kJ/mol)
Au	Au_2O_3	+50
Ag	Ag_2O	-10
Cu	CuO	-130
	Cu_2O	-150
Bi	BiO	-170
	Bi_2O_3	-460
Pb	PbO	-190
	PbO_2	-210
	Pb_3O_4	-570
Sn	SnO	-260
	SnO_2	-490
Zn	ZnO	-300

Pure Au films were deposited on Si substrates using a magnetron sputtering system using a 99.999% pure Au (Kurt Lesker Co) target. The thickness of the deposited films was ~ 1000 Å, measured by stylus profilometry over a step edge of the deposit. The Si substrates were commercial, n-doped wafer specimens, snap cleaved to 1 cm x 1 cm dimensions. Si was chosen due to its atomically smooth surface, as work discussed in Ch. 3 and earlier studies in our laboratory showed enhanced whisker growth on smooth substrate surfaces [80]. The Au films were sputtered at an Ar gas pressure of ~ 5 mT, which produces intrinsic compressive stress in the Au films [65]. Subsequently, the coupons were transferred to the UHV AES/XPS chamber for incubation and real-time assessment of oxygen buildup on the Au surface. After a few weeks of incubation, the samples were examined for whisker growth in a SEM and AES spectra were recorded on

observed whisker-like structures to verify that the whiskers were truly Au and not filamentary debris.

Figure 61 shows XPS spectra taken on the Au film immediately after deposition and after months of incubating in vacuum. There is the expected lack of oxygen buildup on the Au surface during the incubation period at ~ 10^{-9} torr. Parallel experiments on Au films parked under normal atmospheric conditions yielded similar conclusions. Oxygen does not build up on Au in either vacuum or air environments, nor is there a native Au oxide.

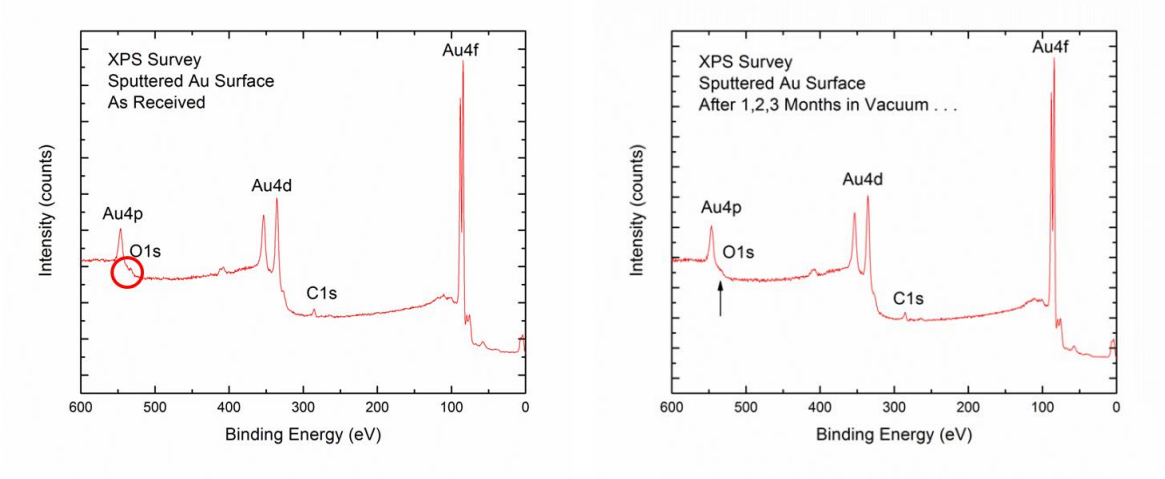

(a) (b)

Figure 61: XPS survey spectra taken on the sputtered Au surface (a) immediately after deposition and (b) during the incubation period in vacuum. The calculated oxygen surface concentration is ~ 1 at%.

After one month of incubation, whisker-like structures were observed on the Au films (Figure 62). For reference, we compare the shapes, morphologies, and dimensions of our Au whiskers with two previous instances of Au whiskering reported in the literature. In 2001, Maekawa [107] reported Au whiskers produced near Au wires after

prolonged Ar^+ ion bombardment at a few keV energy at elevated temperatures (300-400°C). In side-by-side comparisons (Figure 63), we observe (b) similar striations (c) root and whisker morphologies along with (d) a similar look to small protrusions found on the Au surface.

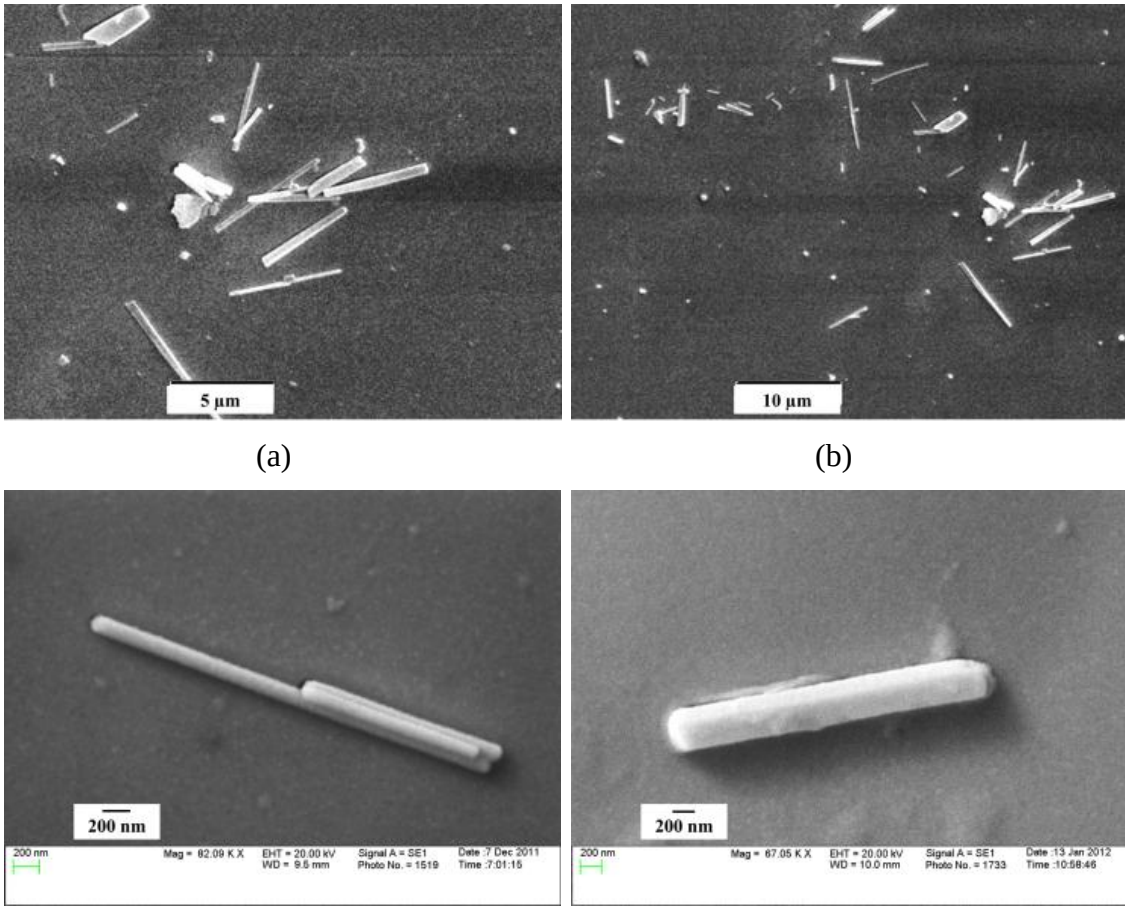

Figure 62: SEM images of whisker-like structures on the compressively-stressed, sputtered Au surface after 2 months of incubation in UHV.

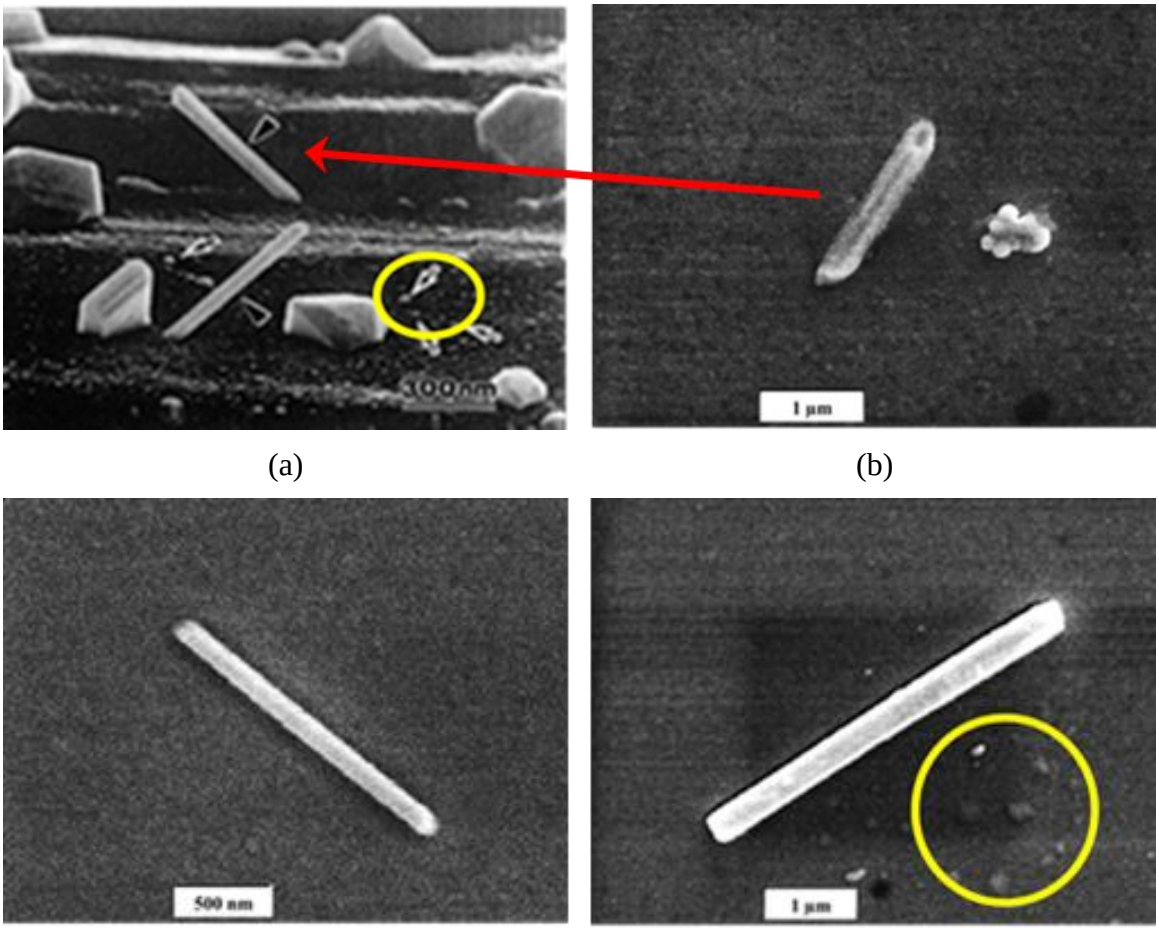

(a) (b)

(c) (d)

Figure 63: Au whisker morphological comparison (a) Au whiskers observed by A. Maekawa et al [29].; (b)-(d) Au whiskers observed in this study.

Figure 64(a)-(b) shows SEM micrographs of Au whiskers observed by A. Teverovsky [108] on electroplated Au (~2 µm) films on Ni (~20 µm) used in micro-machined relays. Figure 64 (c)-(d) shows comparative whiskers from our study, which has similar whisker characteristics. Notice that, similar to Sn whiskers, Au whiskers vary in size, shape, and diameter. Teverovsky reports needle-like, grass-root-like, and even giant, irregularly shaped, toothpaste-like Au whiskers. Figure 64 (a), (c) shows smooth cylinder shaped gold whiskers while (b), (d) demonstrate grass-root-like whiskers.

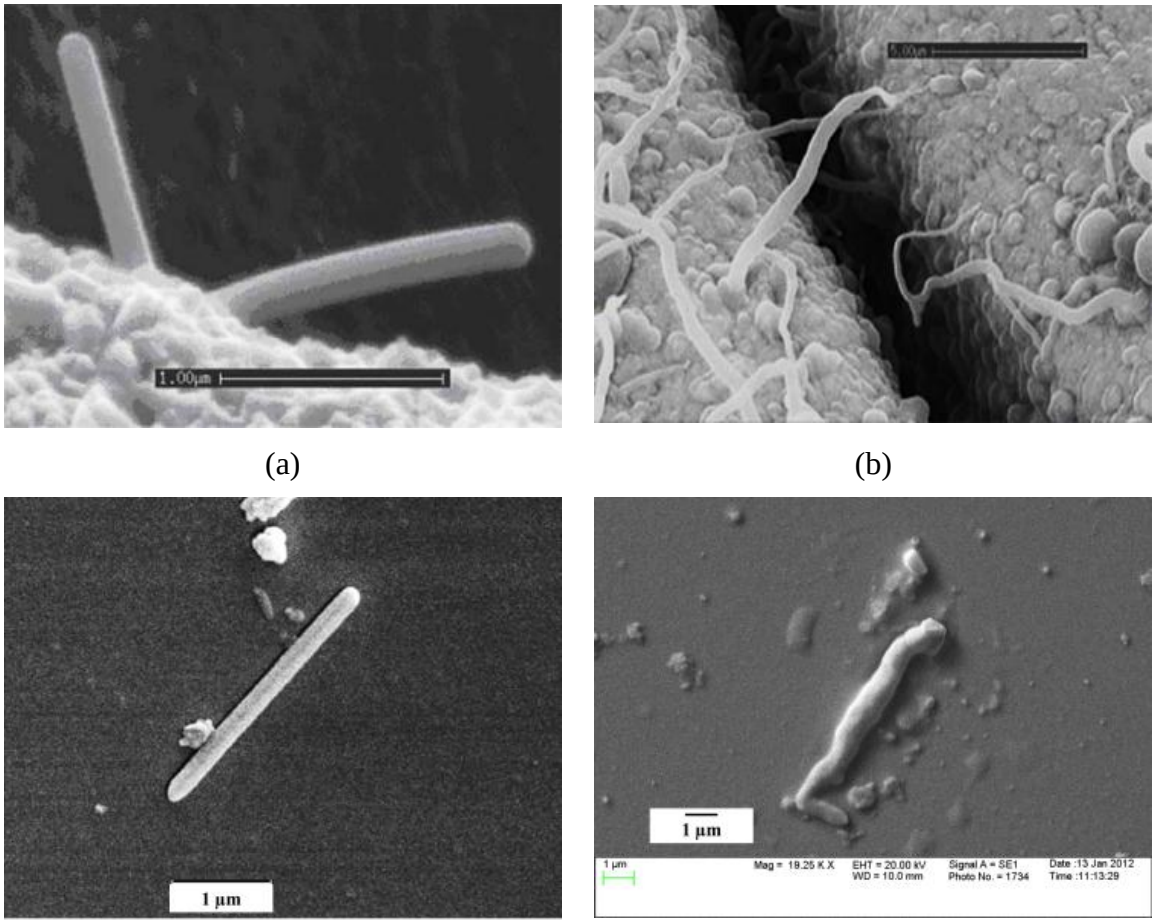

(a) (b)

(c) (d)

Figure 64: Au whisker morphological comparison. (a)-(b) Au whiskers observed by A. Teverovsky [108]; (c)-(d) Au whiskers observed in this study.

While the whisker structures grown here have similar morphologies to previously reported Au whiskers, it is necessary to directly analyze the whiskers in order to verify their composition as Au and not foreign filamentary debris on the surface. There have been few materials analyses of whiskers due to their small nano-sized dimensions. SEM/EDX techniques are usually inadequate in whisker studies due to the signal sampling depth in EDX, which is a pear-shaped volume ~ 3-4 microns below the surface for typical analysis conditions. The total X-ray signal is therefore a superposition from both the whisker and the underlying film, which confuses the analysis. Better results are

possible using high-resolution Auger spectroscopy [73]. Fig. 65(a) displays the whisker locations where AES analysis was undertaken. Point 1 was located on a whisker structure and point 2 on the adjoining Au film. Fig. 6(b) shows AES survey spectra recorded from positions on/off a whisker structure after ~ 50 Å of the surface has been removed by Ar^+ sputter cleaning. The AES signatures yield ~ 80% Au and ~ 20% C (Table 42). The large amount of (adventitious) C on the Au surface after sputter cleaning is due to the relatively "dirty" storage conditions (in air) during the incubation period (the specimen chosen for AES analysis had been incubated in air and not vacuum). Had the whisker structures been filamentary debris, the Auger signature would lack Au signals and instead consist of a large line of C after sputter cleaning.

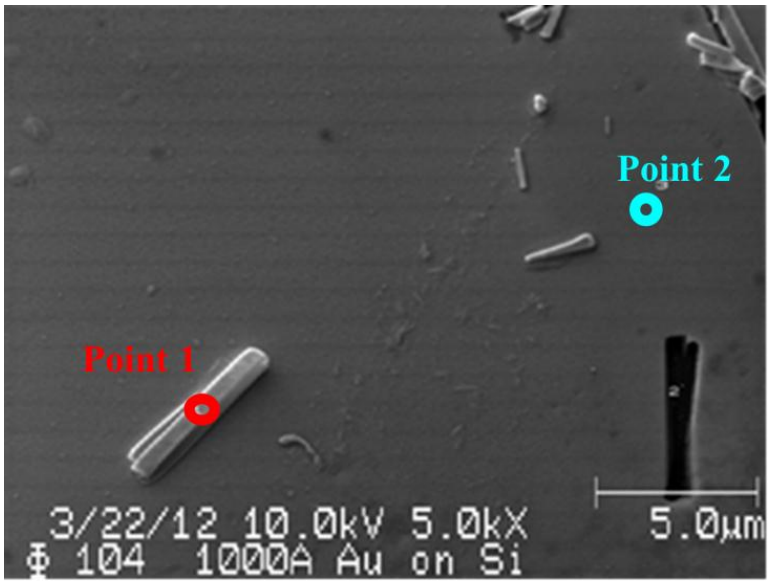

(a)

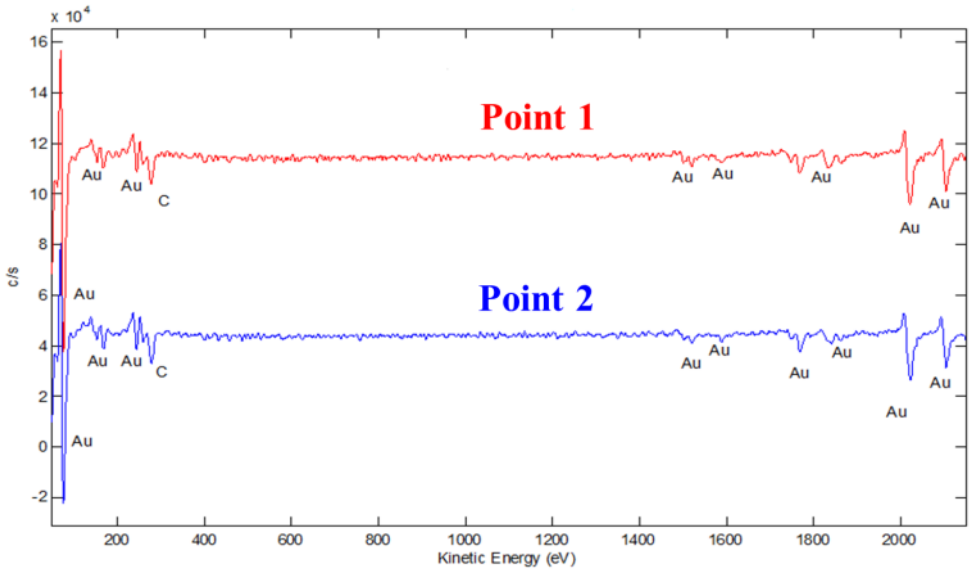

(b)

Fig. 65: High resolution AES spectra of Au whisker structures (a) surface positions where AES spectra was recorded; (b) AES spectra on/off a whisker structure after ~50 Å of Ar^+ sputter cleaning, showing that the whisker is Au and not filamentary debris.

Table 42: AES Surface Elemental Concentrations (at%)

Position	C	O	Si	Au
1	18.5	-	-	81.5
2	22.3	-	-	77.7

In conclusion, for ~ 1000 Å compressively stressed sputtered Au films on Si we observe Au whisker growth after one month of incubation under both vacuum and air conditions, verified by high resolution AES on the whisker structures. Generating Au whisker growth from films which clearly contain no native and/or surface oxide shows that a surface oxide layer is not a necessary requisite for whisker production.

3.5 The Effect of Electrical Bias on Sn Whiskering

Since Sn atoms at room temperature are fairly mobile due to the low melting temperature of Sn, there is the possibility to be highly influenced by charge flow, resulting in electromigration of Sn atoms. This could lead to defects, hillocks and/or voids within the Sn films and accelerate whiskers growth.

There has been limited work on the mechanism of Sn whisker growth driven by electrical force [109,110]. In 2004, S. H. Liu et al. [60] investigated Sn whisker growth in pure Sn due to the electromigration behavior in Sn. In that work, current densities of 7.5×10^4 and 1.5×10^5 A/cm^2 were driven through E-beam evaporated 5000 Å Sn deposited on 700 Å of Ti (used as the probing pads). Only one whisker grew due at 7.5×10^4 A/cm^2, which started growing after ~ 20 hrs of current flow. Voids were observed on the cathode and hillocks near the anode. The higher current density value produced multiple whiskers and hillocks. Whiskers ranged from 1-2 μm in diameter and grew as long as 200 μm after 260 hrs of current exposure. No whiskers were observed on the control test sample having zero current. Similar results were witnessed by Y. C. Hu et al. [111]. Electromigration was observed in fine lines of Sn foil about 30 μm in thickness, producing hillocks and voids due to 2×10^4 A/cm^2 of current density. Void

and hillock formation occurred near the cathode edge after 500 hrs of exposure. Most of the studies identify a threshold current when whisker growth increases dramatically.

Whisker growth due to electrical current differs from whiskers produced by mechanical stressing. Whisker growth by electrical currents appears to originate from the bombardment of electrons moving in the electric field from the cathode to the anode, pushing Sn atoms toward the anode. This creates voids on the cathode and results in compressive stress within the Sn film, which is relieved by whisker production throughout the film and hillocks near the anode end. We investigate Sn electromigration on whisker growth by passing current through a variety of sputter deposited Sn line thicknesses, creating current densities ranging from 0.002 A/μm^2 to 0.004 A/μm^2 (2-4 x 10^5 A/cm^2). Optical and SEM imaging were used periodically to examine the Sn lines for hillocks, voids, and whisker formation.

Sn was sputter deposited on a Si wafer using an Ar pressure of ~2-3mT, creating compressive stress in a 1 μm film. The Sn was sputtered through a mask pattern, shown in Figure 66, produced using lithography. The substrate was a scored Si slice, sandwiched between two large Cu pads, all mounted on a Teflon base (schematic and picture provided in Figure 67). The Cu provided a stable contact for the current probes connected to the patterned Sn lines. A current of 0.2 amps (probe station shown in Figure 68) through the deposited lithographic features created current densities of 0.002, 0.00267, and 0.004 A/μm^2 (2 x 10^5, 2.67 x 10^5, and 4 x 10^5 A/cm^2), shown in Figure 69. The 0.002 A/μm^2 region was near the cathode and the narrower 0.004 A/μm^2 region was near the anode. The current exposure was continuous except for brief pauses for examination by Nomarski and SEM microscopy.

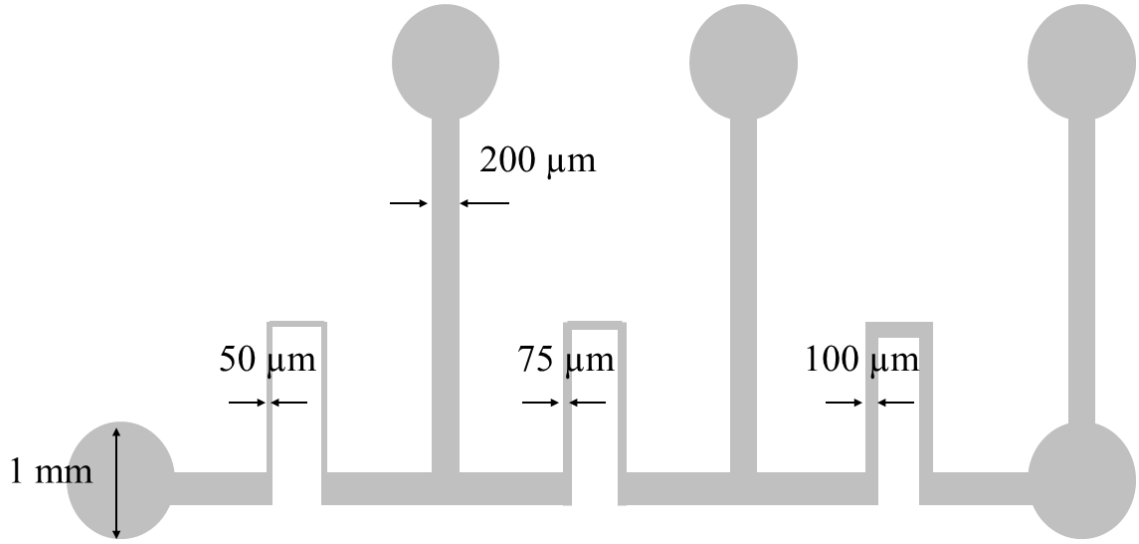

Figure 66: Lithography mask pattern used for electromigration study.

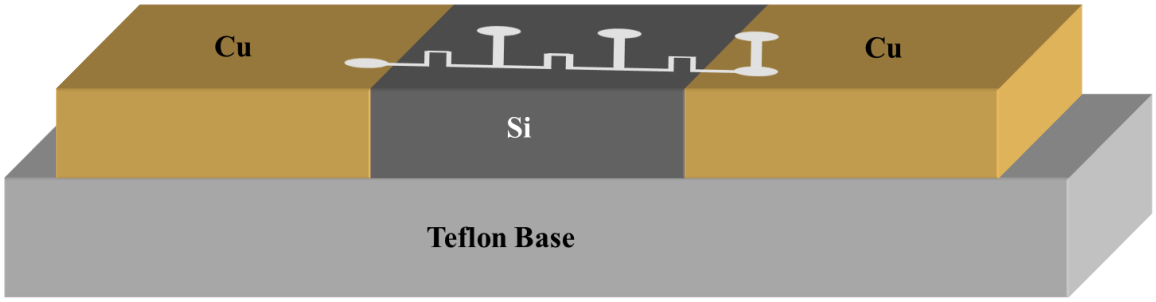

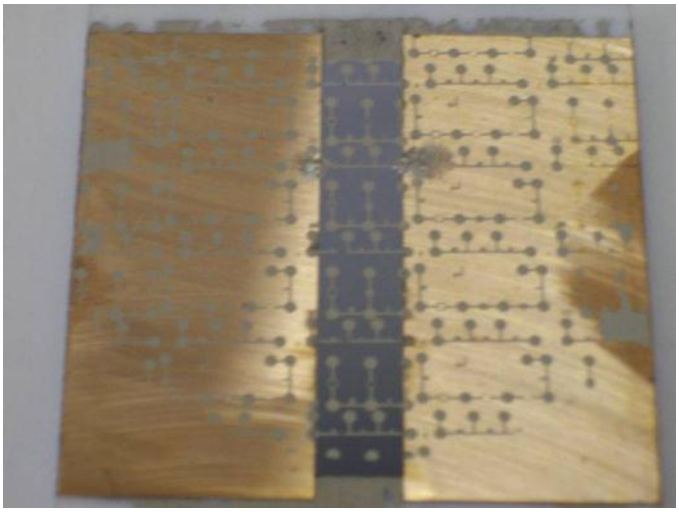

Figure 67: Schematic and picture of electromigration specimen.

Figure 68: Probe station setup for steady current exposure through Sn pattern.

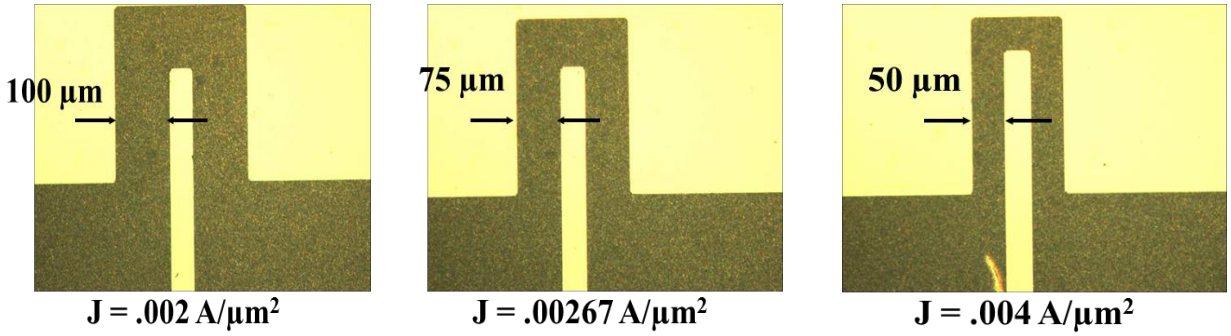

Figure 69: Nomarski microscope images of various pattern widths and corresponding current densities in each region.

The current exposure was applied for a total of 115 hrs. Table 43 displays the general trends for production of hillocks, voids and whiskers during current stressing. Hillocks and voids are created in the 0.002 A/µm^2 region, hillocks in the 0.00267 A/µm^2 region, and voids in the 0.004 A/µm^2 region. With higher the current density and longer current stress times, more whiskers grow. No whiskers were produced until 10 hrs of exposure was reached, and then whiskers were produced in the two highest current density sections. The lowest current density (0.002 A/µm^2) region did not grow whiskers

until 20 hrs of current exposure. The highest stress (0.004 A/μm^2) sections produced the greatest whiskering. No hillock formation occurred until 20 hrs of current exposure and no voids were produced until 40 hrs (both found in the 0.002 A/μm^2 section). Hillocks and voids were not found in the high current density regions until 115 hrs of exposure. The majority of the voids were found near the cathode (0.002 A/μm^2) but no hillocks were observed on the anode side after 115 hrs.

Table 43: Hillocks, Voids, and Whiskers due to Current Exposure over Time

Current Density ($A/\mu m^2$)	**0.002**			**0.00267**			**0.004**		
Current Exposure Time (hr)	**Whiskers**	**Hillocks**	**Voids**	**Whiskers**	**Hillocks**	**Voids**	**Whiskers**	**Hillocks**	**Voids**
2	**none**	**none**	**none**	**none**	**none**	**None**	**None**	**none**	**none**
5	**none**	**none**	**none**	**none**	**none**	**none**	**None**	**none**	**none**
10	**none**	**none**	**none**	**very few**	**none**	**None**	**very few**	**none**	**none**
15	**none**	**none**	**none**	**very few**	**none**	**None**	**very few**	**none**	**none**
20	**very few**	**very few**	**none**	**very few**	**none**	**None**	**Few**	**none**	**none**
40	**very few**	**very few**	**none**	**very few**	**none**	**None**	**Few**	**none**	**none**
80	**very few**	**very few**	**very few**	**very few**	**none**	**None**	**Few**	**none**	**none**
115	**very few**	**few**	**few**	**very few**	**very few**	**None**	**moderate**	**none**	**very few**

Nomarski images of observed whiskers, hillocks, and voids for 10, 20 and 40 hrs of current exposure are found in Figure 70, Figure 71, and Figure 72 respectively. Nomarski imaging was chosen since the sample could be observed in a timely fashion and quickly replaced into the probe station for near-continual current exposure. Due to the limited resolution of Nomarski microscopy, SEM images were taken for longer exposure times. SEM images of hillocks, voids, and whiskers for the different current density regions after 80 hrs of 0.2 A of current are shown in Figure 73. After the experiment was terminated (@ 115 hrs of current exposure SEM images of voids, hillocks and whiskers throughout the Sn pattern were taken. Figure 74 shows images of voids in the 0.002 A/μm^2 region (where the most voids were observed). Figure 75 displays hillocks in the 0.002 A/μm^2 and 0.00267 A/μm^2 regions, which were the only regions where hillocks were observed. Numerous whisker images from all three regions and along the intermediate paths are shown in Figure 76.

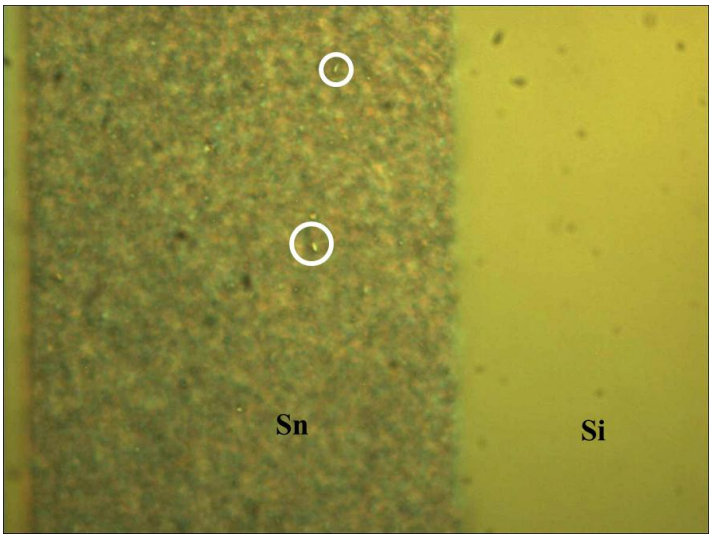

Figure 70: Nomarski image of whisker growth on .00267 A/μm^2 region after 10 hrs.

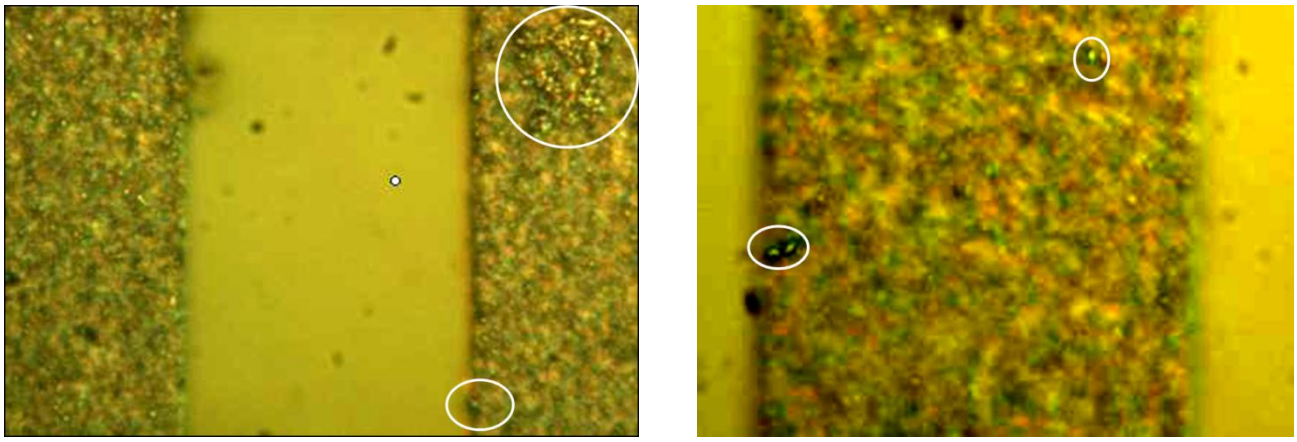

(a) (b)

Figure 71: Nomarski images of (a) hillock and whisker growth on the 0.002 A/μm^2 region (b) 0.004 A/μm^2 region after 20 hrs of current exposure.

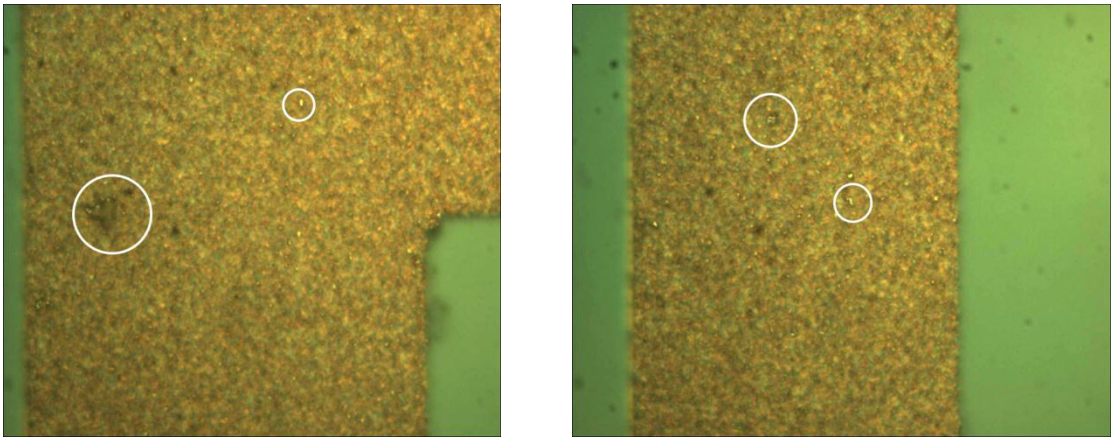

(a) (b)

Figure 72: Nomarski images of (a) hillock and whisker growth on the 0.002 A/μm^2 region and (b) the 0.00267 A/μm^2 after 40 hrs of current exposure.

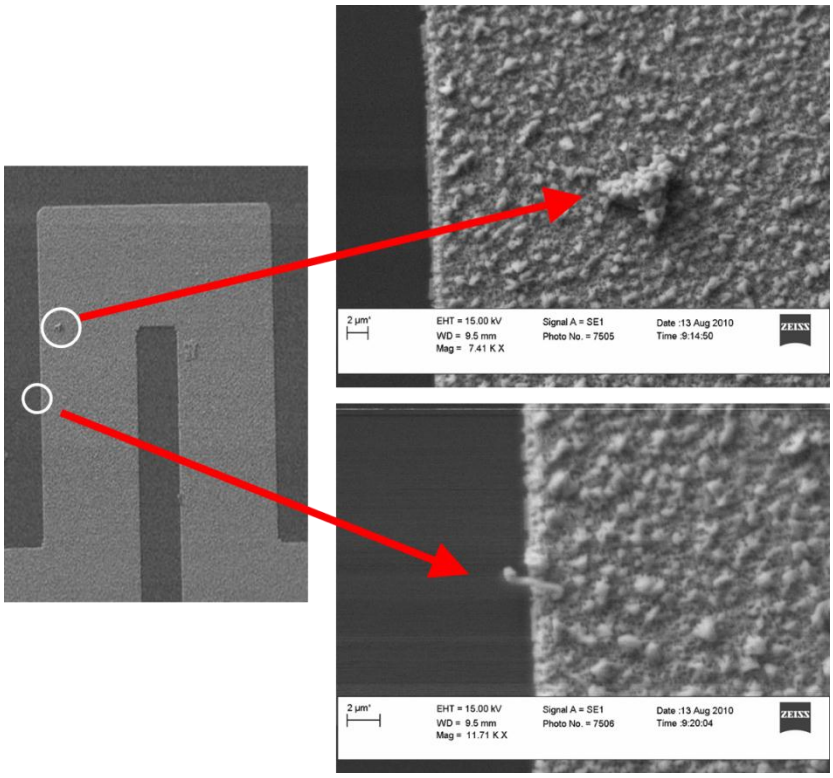
2 µm
EHT = 15.00 kV
WD = 9.5 mm
Mag = 7.41 K X
Signal A = SE1
Photo No. = 7505
Date :13 Aug 2010
Time :9:14:50
ZEISS
2 µm
EHT = 15.00 kV
WD = 9.5 mm
Mag = 11.71 K X
Signal A = SE1
Photo No. = 7506
Date :13 Aug 2010
Time :9:20:04
ZEISS

(a)

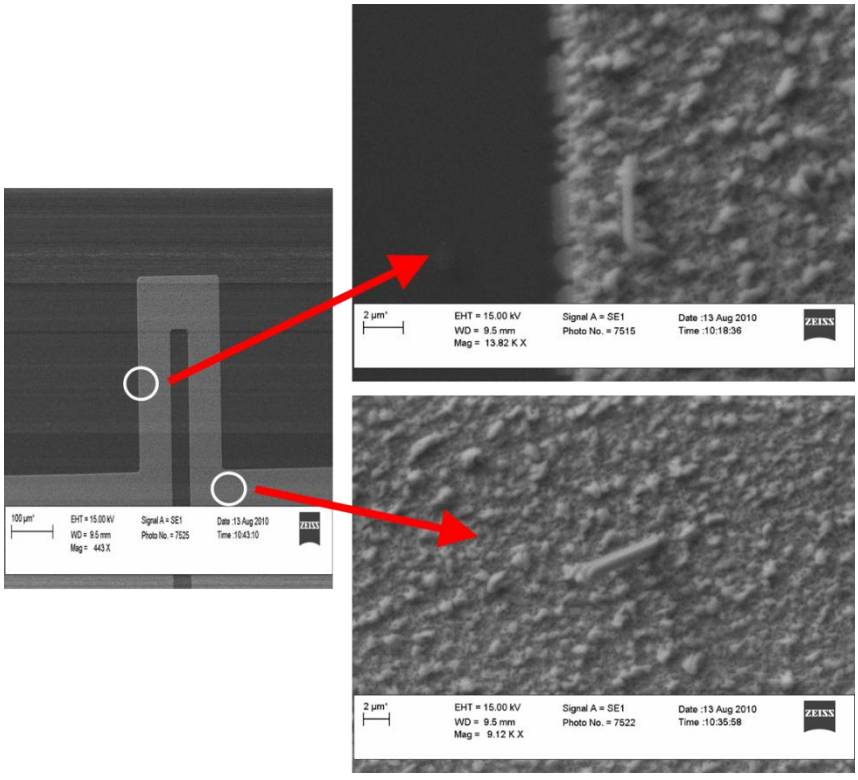
100 µm
EHT = 15.00 kV
WD = 9.5 mm
Mag = 443 X
Signal A = SE1
Photo No. = 7525
Date :13 Aug 2010
Time :10:43:10
ZEISS
2 µm
EHT = 15.00 kV
WD = 9.5 mm
Mag = 13.82 K X
Signal A = SE1
Photo No. = 7515
Date :13 Aug 2010
Time :10:18:36
ZEISS
2 µm
EHT = 15.00 kV
WD = 9.5 mm
Mag = 9.12 K X
Signal A = SE1
Photo No. = 7522
Date :13 Aug 2010
Time :10:35:58
ZEISS

(b)

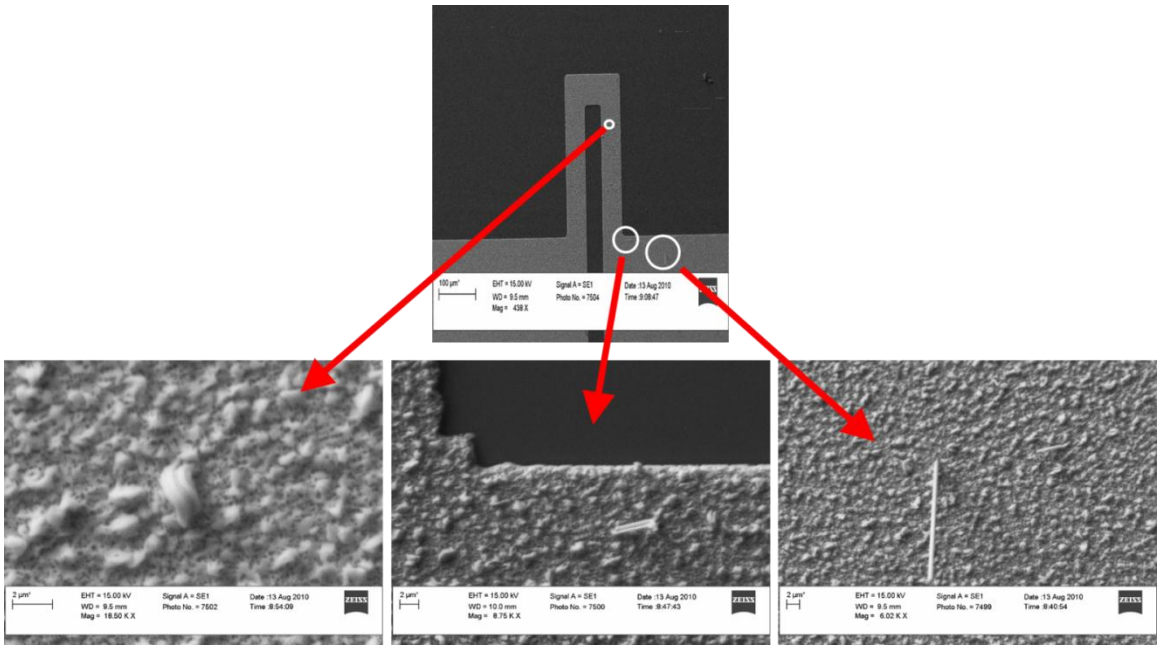

(c)

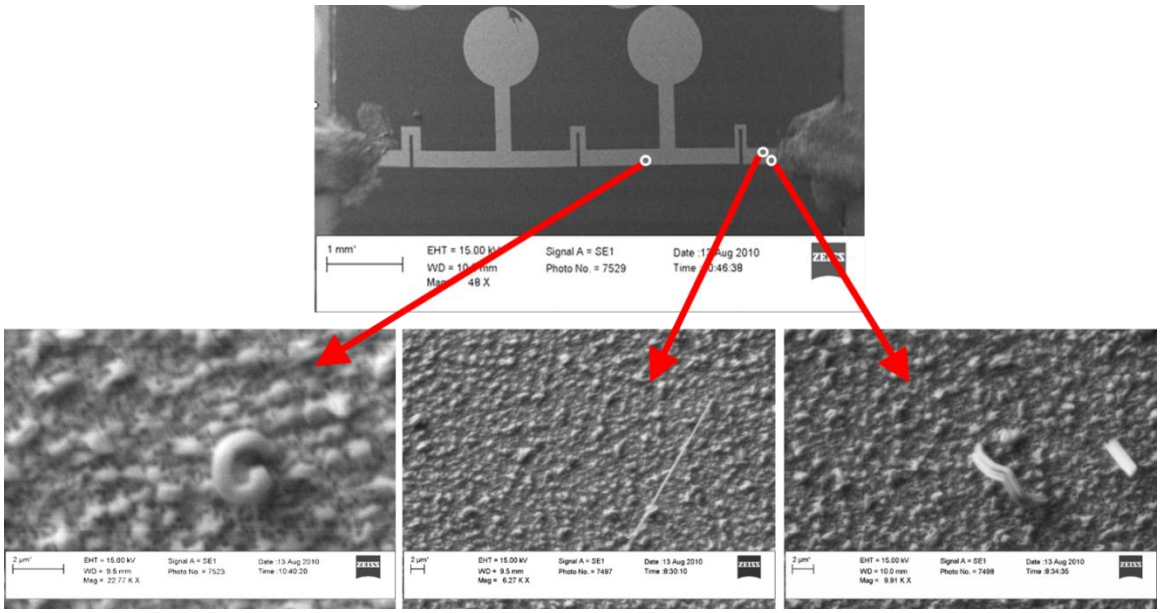

(d)

Figure 73: SEM images of the (a) 0.002 A/μm^2 region, (b) 0.00267 A/μm^2 region, (c) 0.004 A/μm^2 region, and (d) intermediate paths after 80 hr of 0.2 A current stress.

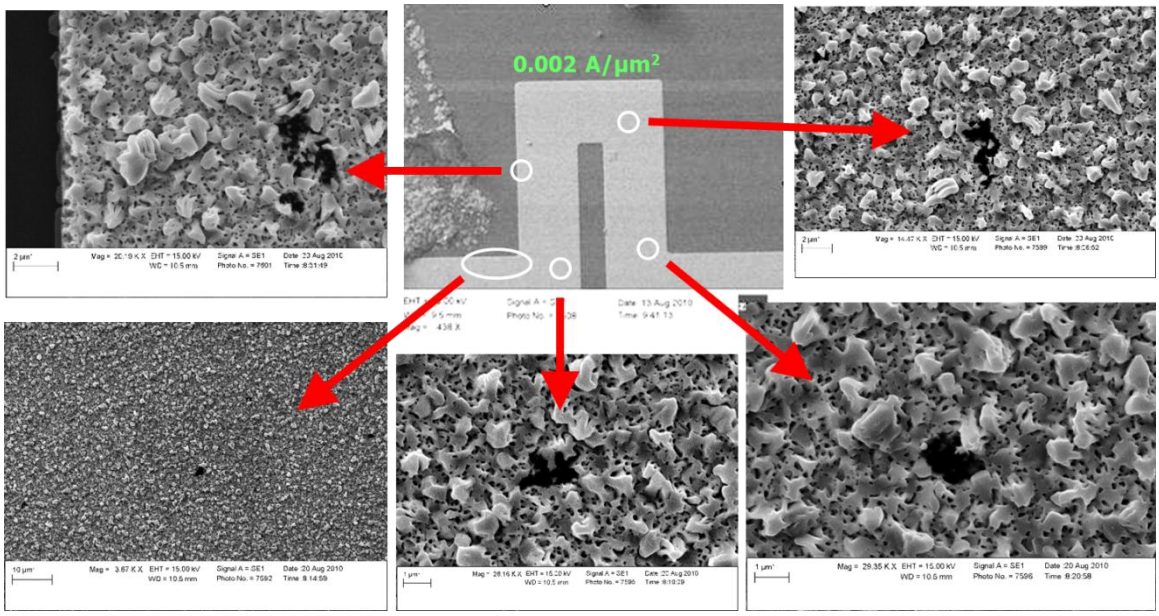

Figure 74: SEM images of voids in the 0.002 A/µm^2 region after 115 hrs of 0.2 A current stress.

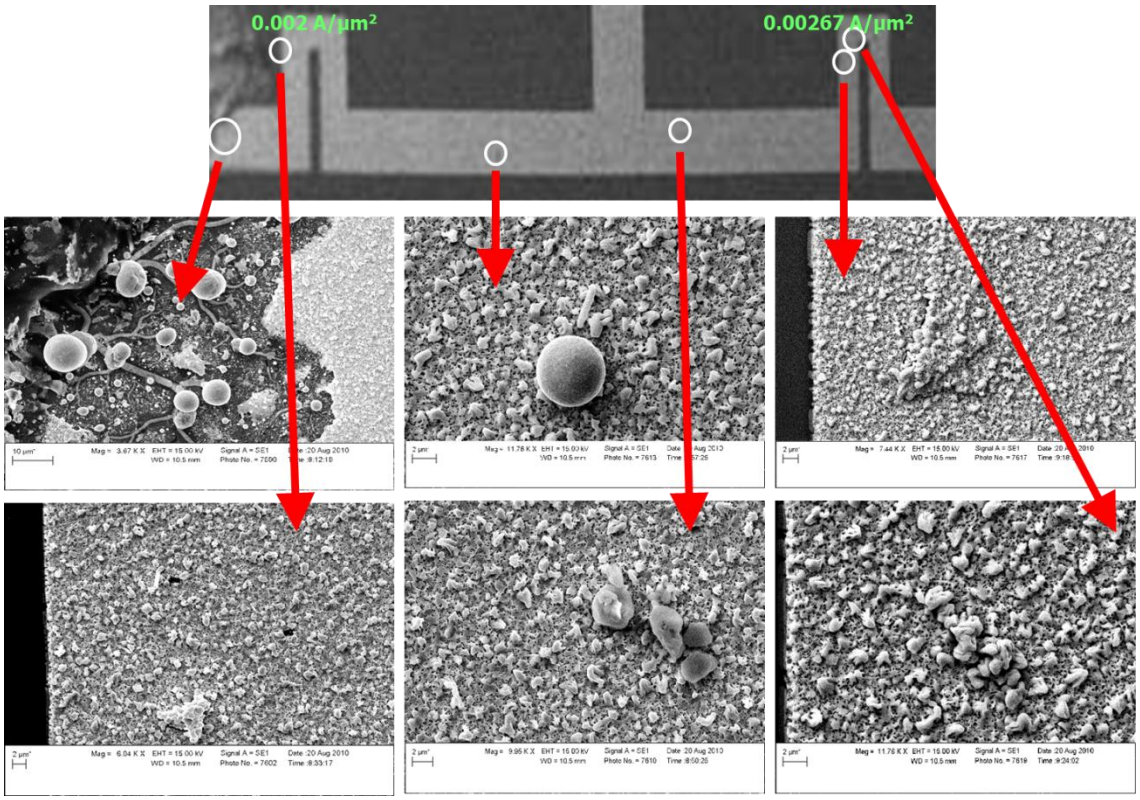

Figure 75: SEM images of hillocks in the 0.002 A/µm^2 and 0.00267 A/µm^2 regions after 115 hrs of 0.2 A current stress.

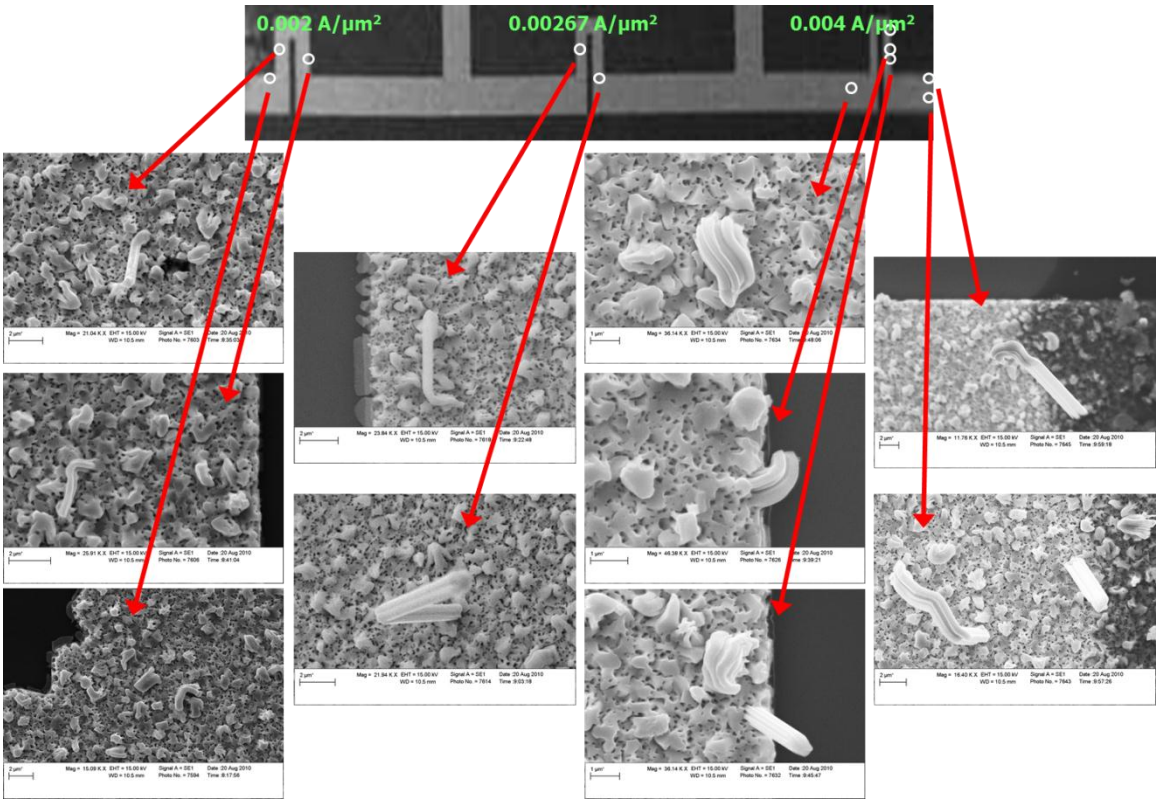

Figure 76: SEM images of whiskers grown on the Sn pattern after 115 hrs of 0.2 A of current stress.

In conclusion, exposing a 1 μm Sn film pattern to 0.2 A of current produced whiskers in hours instead of weeks or months. After only 10 hrs of steady 0.2 A current, a small number of whiskers are found on the 0.004 and 0.00267 A/μm^2 sections of the Sn pattern. Whisker production occurs on the 0.002 A/μm^2 section after another 10 hrs (total of 20 hrs) of current exposure. After 20 hrs of current exposure the 0.002 A/μm^2 section begins to form hillocks, with slight amounts of increased whiskering in all sections. From 20 hrs to 80 hrs of current exposure no dramatic changes are observed. Only in the 0.002 A/μm^2 section is a small amount of additional voids forming. After 115 hrs of current exposure, multiple voids form in the 0.002 A/μm^2 section but little whiskering. An increase in hillocks was found in the 0.002 and 0.00267 A/μm^2 sections

together with the onset of voids is the 0.004 A/μm^2 section. The only noticeable increase in whiskers is in the 0.004 A/μm^2 section.

In a similar study of Sn electromigration [112], whiskers were formed after 1 hour at 0.0036 A/μm^2 and after10 hrs at 0.0018 A/μm^2. No whisker growth occurred at current densities < 0.00045 A/μm^2, even after 100 hrs of current stress. S. H. Liu et al. [60] investigated Sn whisker growth in pure Sn due to the electromigration behavior in Sn. Only one whisker grew at 0.00075 A/μm^2 after 20 hrs of current stress. Current densities of 0.0015 A/μm^2 produced multiple whiskers and hillocks. Both works show there is a threshold current density/time for whiskering, which broadly agrees with our study.

CHAPTER 4

WHISKER MITIGATION AND PREVENTION

"In truth it matters less what we do in practice than how we do it and why we do it."
-Donna Farhi

4.1 Efficacy of POSS Conformal Coating to Block Whiskers

There is currently no effective mitigation method to reliably eliminate Sn whiskers. One promising approach is to use conformal coatings. A conformal coating refers to an insulating protective coating that conforms to the shape and contour of the coated object. The risks and benefits of conformal coatings for Sn has been studied by NASA Goddard using Uralane 5750 coating [113,114]. Electroplated Sn (~ 200 microinches) on brass was partially coated with ~25-75 μm of Uralane 5750. After 18 months, not a single whisker had broken through the coating surface and whiskers were not observed until ~ 2 years had passed. Woodrow and Ledbury [115] measured the whisker suppression of a variety of spray coatings on brass coupons (70% Cu, 30% Zn) plated with ~150 microinches of Sn. Coating thicknesses in the range 3.9-6 mils were not penetrated by whiskers (Parylene C was found to be most effective). The studies suggest that many conformal coatings are not predictably reliable for whisker mitigation in systems with long term life expectancies unless an extremely thick coating is applied.

In this work we will study the effects of POSS Short-Stop tin whisker suppressant (Figure 77). POSS is a clear and colorless polyimide applied in spray form. Whisker suppression is thought to occur in two ways: 1) the mechanically tough polyimide buckles the whiskers before penetration; 2) the thermally stable mercapto POSS cages foster stress relief near metal grains by reducing compressive stress near whisker

nucleation sites. The sulfur in the molecular structure attaches to Sn oxide and forms a good adhesive bond between the POSS and the Sn surface. We examine here if POSS effectively suppresses whisker growth on compressively stressed, sputtered Sn films.

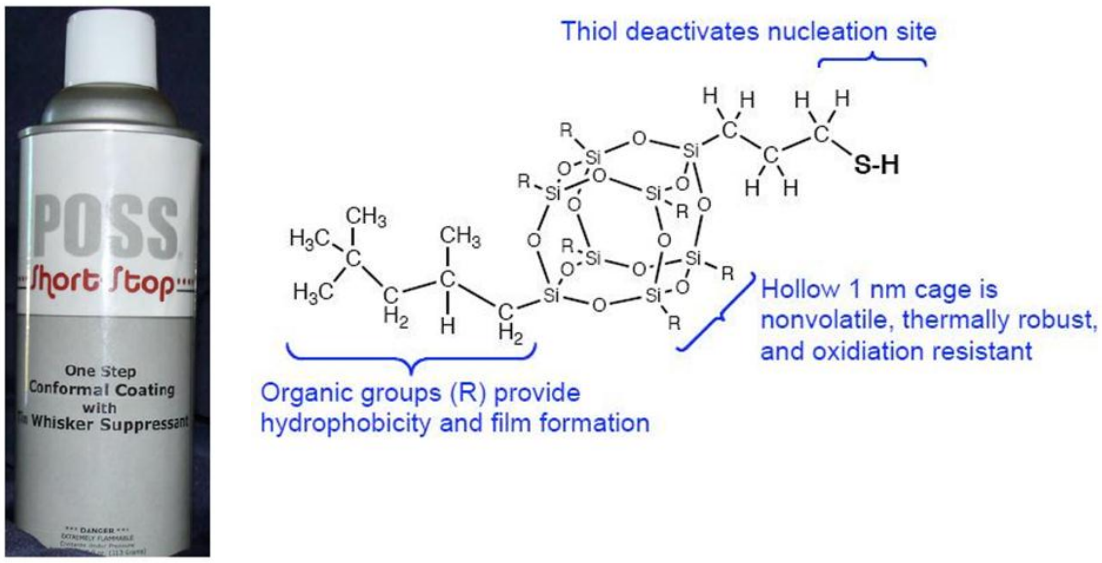

Figure 77: POSS conformal coating tin whisker suppressant and molecular structure.

Pure Sn films of ~3000 Å were sputter deposited under compressively stressed conditions (Ar pressures ~ 2-3mT) to accelerate whisker growth. Sn was deposited through a grating-like, parallel line template mask onto clean glass substrates. The deposited pattern (400 lines/in) is shown in Figure 78. The parallel Sn lines allowed for easy observation of whisker bridging. Two sets of specimens were deposited under identical conditions; one with POSS whisker suppressant (test specimen) and one without (control specimen), shown in Figure 79. The POSS was applied by following the manufacturer guidelines (spray dispenser). An estimated ~12 µm of POSS was applied which was the suggested coating to sufficiently serve as a protective barrier. The samples were incubated in RT/RH conditions and periodically observed in SEM for

whisker growth. AES and XPS analysis was carried out on the applied POSS surface to verify the elemental composition.

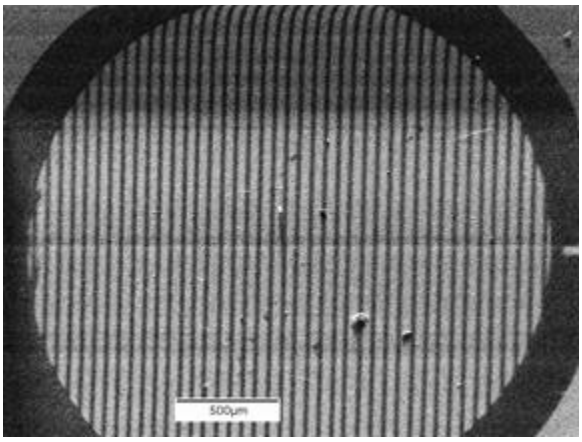

Figure 78: SEM photo of sputtered Sn lines on glass, 400 lines/inch.

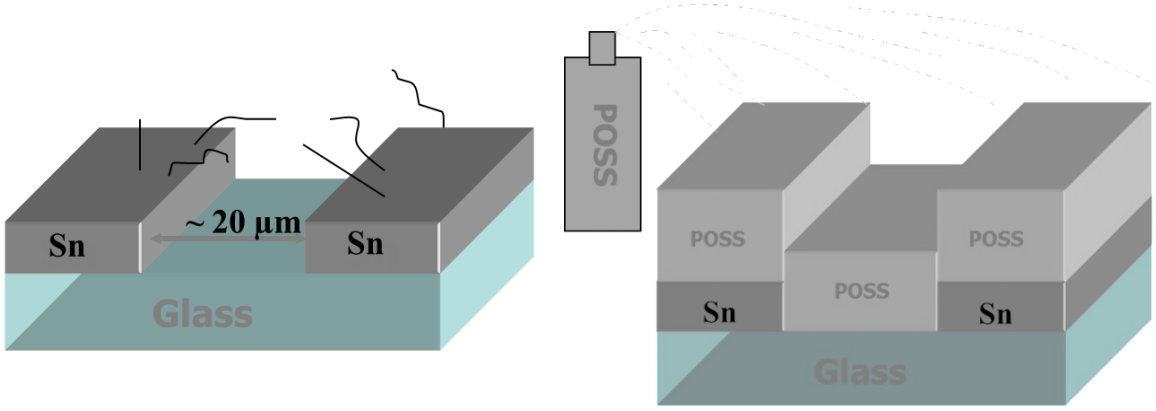

(a) (b)

Figure 79: Schematic of (a) control specimen (no POSS) and (b) test specimen (with POSS spray).

AES and XPS spectra for POSS are given in Figure 80 with calculated surface elemental compositions in Table 44. C, O, and Si are the principal elements, which conforms to the molecular structure of Fig. 79. We also find 2% (at) S on the POSS surface, touted to create the desired adhesive characteristics between POSS and Sn. The

only unexpected element was Zn, which is not is the molecular structure diagram of POSS and is not a common element found in glass.

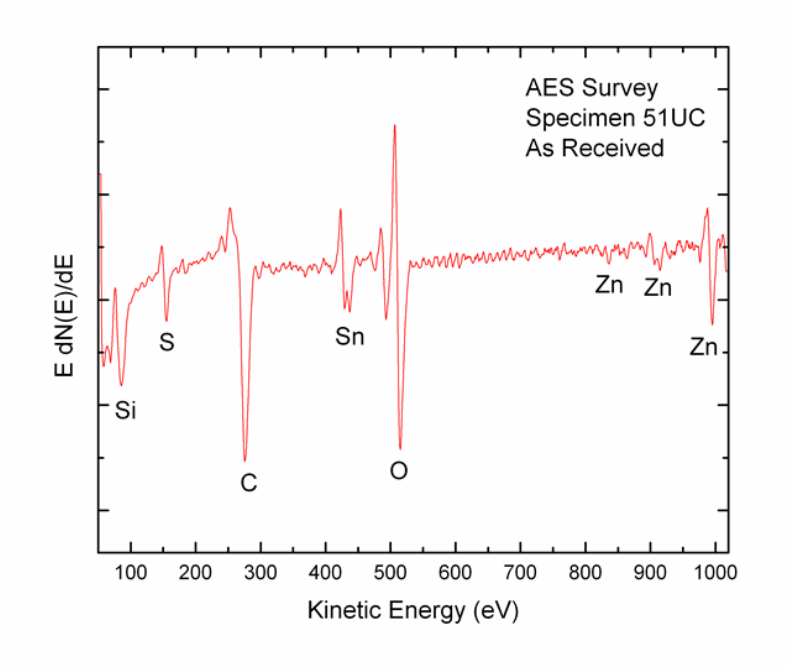

(a)

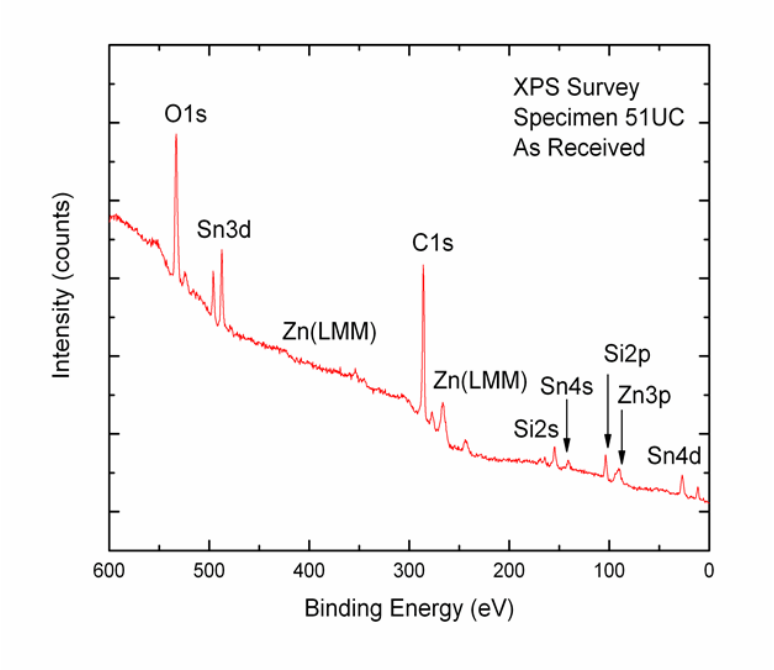

(b)

Figure 80: (a) AES and (b) XPS survey spectra of POSS conformal coating on Sn.

Table 44: XPS Surface Elemental Composition of POSS Conformal Coating

Surface Elemental Composition (at %)					
O	**Sn**	**C**	**S**	**Si**	**Zn**
19	2	60	2	11	6

After a total of ~ 2.3 years, whisker growth is observed on the control specimen (~200 whiskers/mm^2) as seen in Table 45. Whiskers from the control specimen are shown in Figure 81, which grew > 225 μm long. In contrast, the POSS coated specimen completely blocked whiskers up to 2.3 years of incubation. Figure 82 compares the whisker growth on control/test specimens, where we see complete whisker suppression up to this time. From Figure 82(a) we see multiple whiskers bridging the Sn grid lines, which would cause a dead short in electronics. The results indicate that, under the conditions of the experiment, POSS offers a potentially viable solution to the whisker problem if applied properly.

Table 45: Whisker Statistics of Control and Test Specimens after 839 Days of RT/RH Incubation

	Whisker Density (mm^{-2})	**Average Whisker Length (μm)**	**Standard Deviation (μm)**	**Mode (μm)**
Without POSS	201	16.4	43.5	6
With POSS	0	-	-	-

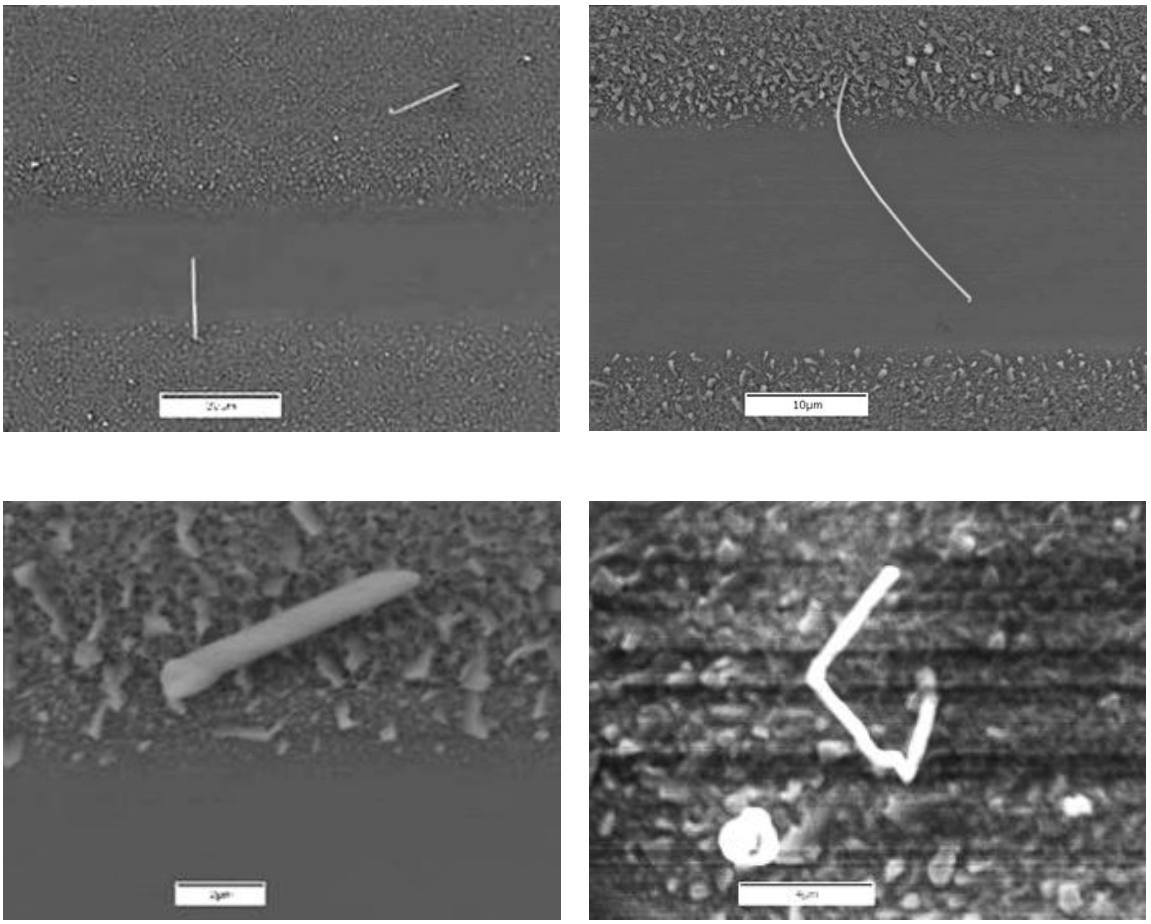

Figure 81: SEM images of whisker growth on control (no POSS) specimen.

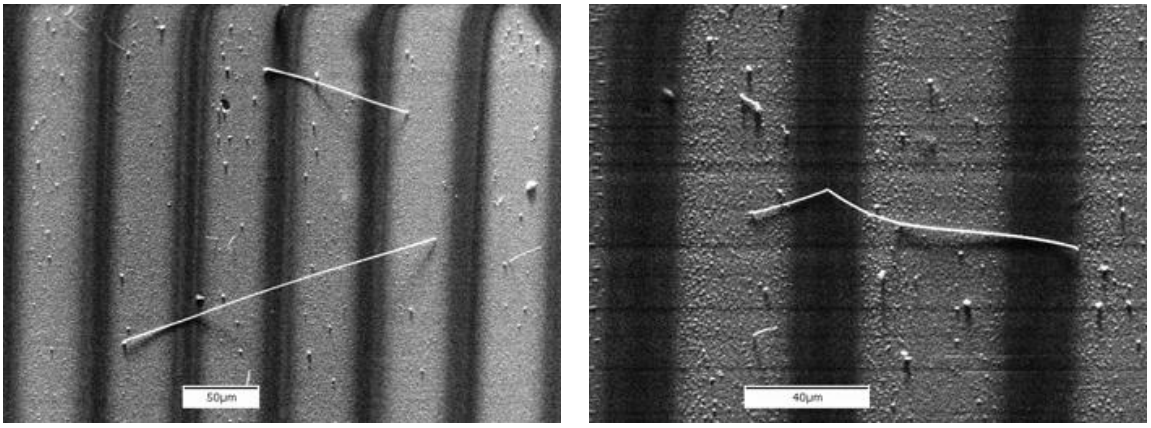

(a)

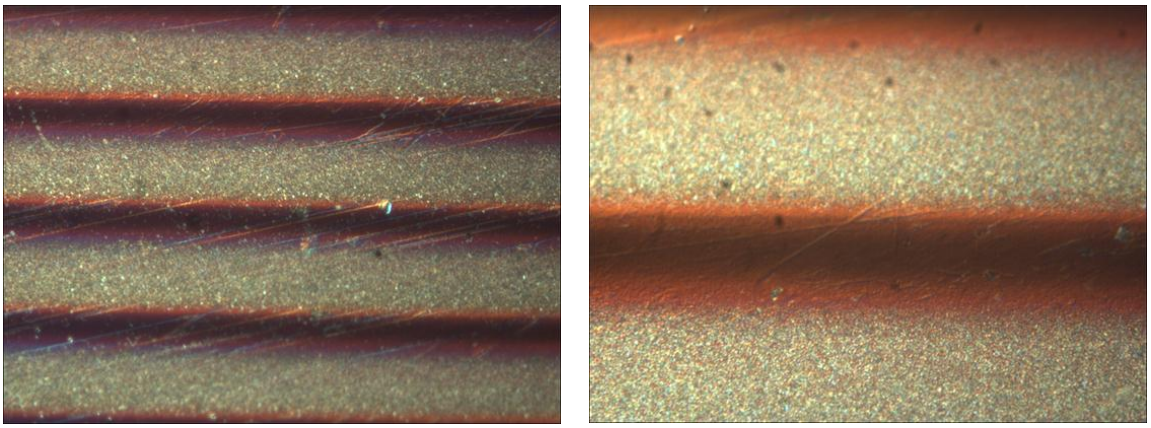

(b)

Figure 82: Comparison of (a) SEM whisker images on control (no POSS) specimen to (b) suppressed whisker growth on test (with POSS) specimen, taken with a Nomarski microscope.

4.2 Suppression of Sn Whiskering Using a Ni Under Layer

Schetty et al. [116] found that when depositing pure Sn (and Sn-10%Pb) over nickel plated copper alloy substrates, neither Sn film exhibited whisker growth. Additionally, Xu et al. [117] reported that a plated Ni layer under plated Sn films was effective in blocking whiskers after 6 months of incubation at 50°C. A control specimen without a plated Ni under layer grew whiskers after only 3 months.

Nickel is thought to reduce the initial stress between the interfaces and act as a diffusion barrier to copper, hindering the formation of Cu-Sn IMC. Application of a Ni barrier layer has been found to reduce the build-up of compressive stress in the Sn film and, over time, develop a tensile stress in the film [118]. The tensile stress in the Sn is most likely due to the interfacial diffusion between Sn and Ni. The solubility of Ni in Sn and Sn in Ni has been calculated [119] to be 0.005 at% and 11.0 at% respectively. The faster diffusion of Sn atoms into the Ni creates a material deficiency in the Sn film, leading to buildup of tensile stress in the Sn film.

There are many reports that an underlying Ni layer mitigates whisker growth, but Sn whiskers have also been produced in the presence of a Ni barrier layer. Whiskers have been found on Sn thicknesses > 7.5μm with an underlying Ni barrier after 2000 hrs of exposure at 60°C/93%RH [54]. Sn whiskers have also been observed in the presence of a Ni under layer on various passive components used in multilayer ceramic chip capacitors (MLCCs) and connectors [120]. Nevertheless, many manufacturers currently use a Ni barrier layer to mitigate whiskers.

Thus, while the use of a Ni underlayer has shown promise as a whisker mitigation method, it is not guaranteed to fully prevent whiskers. In this study, we add to the data set in the literature by investigating the use of a Ni under layer between Si and polished brass and Sn, using compressively stressed (fast whisker producing) sputtered Sn films. By periodically observing the Sn surfaces for whisker production, we determine how well a Ni under layer mitigates whisker growth and compare to (control) Sn films sputtered without a Ni barrier layer.

Pure Ni and Sn films were sputter deposited on brass and Si substrates. The Sn was sputtered at Ar gas pressures of 2-3 mT, which produces intrinsic compressive stress in the films. All Ni films were sputtered under standard Ar pressures (~18 mT). The thickness of the deposited Ni barrier was 1000 Å for Ni and 2000 Å for Sn, measured by stylus profilometry over a step edge of the deposit. The deposition sequence is depicted in Figure 83. The brass (Cu63/Zn36) substrates were commercial metal sheets cut into coupons of dimension 1 cm x 1 cm. To observe whisker growth within a reasonable time period, the brass coupon surfaces were electrochemically polished, since previous work in our laboratory showed enhanced whisker growth on smooth surfaces [80]. The Si substrates were commercial (100) oriented, n-type Si wafers, snap cleaved to 1 cm x 1 cm dimensions, chosen due it its atomically smooth surface. The samples were subsequently incubated under RT/RH conditions and periodically observed by SEM for whisker growth.

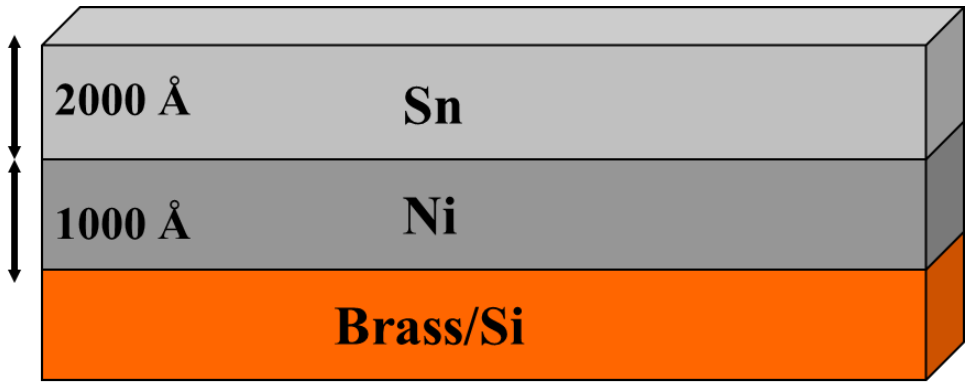

Figure 83: Schematic of Ni under layer specimens.

After ~250 days (> 8 months) of incubation, no whisker growth was observed on either the brass or Si substrate specimens. Figure 84 compares our compressively stressed sputtered Sn films on Ni to the usual microstructure appearance in our whisker

producing sputtered Sn films. We observe similar grain structure, morphology, size and shape in both Sn films, confirming that we successfully deposited our usual accelerated whisker producing Sn films. From Table 18 and Table 2 ~ 1600 Å of Sn on Si sputtered under the same conditions produced ~ 38,500 whiskers/cm^2 after ~ 120 days (< half the incubation period here) and ~ 1500 Å of Sn on polished brass grew ~ 1,700 whiskers/cm^2 after 140 days of RT/RH incubation. We find here that the Ni diffusion barrier approach is an effective whisker suppressant for sputtered Sn films. The general consensus currently seems to be that if the Ni layer is "good" it works effectively as a whisker prevention method, but if the Ni layer is "bad"; not so fast.

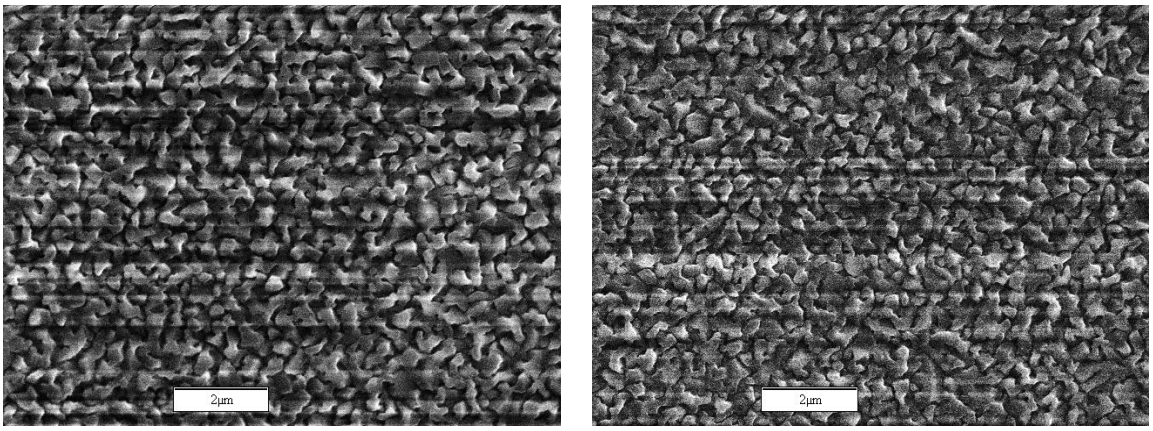

(a) (b)

Figure 84: Microstructure of (a) top Sn film in Ni under layer study and (a) usual whisker producing Sn film.

What defines a "good" vs. a "bad" deposited film include the uniformity and conformality of the Ni film, film purity, the matte/bright nature of the electrodeposits, plating bath mixture, temperature during deposition, etc. Since all our films were deposited in clean, vacuum (~ 10^{-7} torr) conditions, our deposited films contain low to minimal contamination. The films so grown have proven to be successful at suppressing Sn whisker growth for the case of compressively stressed sputtered Sn films.

4.3 Effectiveness of Hard Metal Cap Layers in Blocking Sn Whiskers

One method to deal with Sn whiskers employs hard metallic cap films deposited on top the Sn surface, which block whiskers from penetration [121,122,123]. Kim et al. [121] report, for example, that 200 nm of electroplated Ni has prevented Sn whisker growth for over five years. In contrast, Sn whiskers penetrated a 600 nm electron-beam evaporated Cu capping layer in only three days [123]. This suggests that a key distinctive property of metallic films (hardness, strength, etc.) or the intermetallic compounds they form plays a critical role in the blocking whiskers. In order to clarify the role of metal films as capping layers for Sn whisker prevention, this work addresses the thin film properties of various sputter deposited metal capping films and their ability to block Sn whiskers.

Pure Sn films of 1500 Å were deposited on commercial n-doped Si wafer substrates using magnetron sputtering techniques. The coupons were subsequently diced into specimens of 1 cm x 1 cm. Silicon was chosen as the deposition substrate. The Sn films were sputtered using an argon plasma at pressures of 2-3 mT, which produces intrinsic compressive stress in the films [65]. The specimens were then temporarily removed from the sputter system, photoresist was applied and baked on half of each sample, then metal cap layers of Pt, Au, Cr and Ni were sputter deposited with three thicknesses. Acetone was used to peel off the photoresist, which removed the cap film with from half of the coupon, leaving a Sn side (control) and a metal capped side (Figure 85). The target deposited film thicknesses were verified using RBS immediately after deposition. The coupons were then incubated under ambient room temperature/humidity conditions.

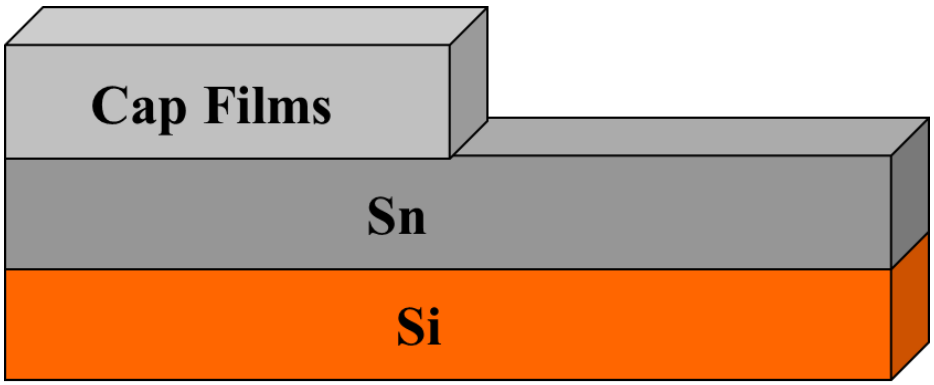

Figure 85: Design of deposited metal cap specimens.

To assess the whisker growth/penetration and/or lack thereof, the samples were periodically observed in a scanning electron microscope. The thin film characteristics and evolution over time were studied using Rutherford backscattering spectroscopy (RBS) and Auger electron spectroscopy (AES). By comparing the RBS spectra immediately after deposition and after incubation it was possible to observe cap/Sn film intermixing over time. AES depth profiling was also used to assess the degree of film diffusion at room temperature for each of the cap films.

Immediately after deposition the metal cap film thicknesses were measured with RBS (see Table 46). After ~ 100 days of incubation at RT/R the control, uncapped, Sn-sides of each specimen produced substantial whisker densities (Table 47), at the normal range for compressively stressed sputtered Sn films produced in our laboratory. Figure 86 shows SEM photographs of whiskers observed from the uncapped Sn side of the films. Since the Sn films produced whiskers, whisker penetration through the capped film sides can be compared to see which metal top layer films prevented Sn whisker penetration.

Table 46: Initial Deposited Cap Film Thicknesses

Capping Film	Attempted Film Thickness (Å)	RBS Measured Film Thickness (Å)
Au	500	875
	1000	1750
	2000	300
Cr	500	250
	1000	700
	2000	1400
Pt	500	325
	1000	685
	2000	1360
Ni	500	350
	1000	700
	2000	1500
	5000	3100

Table 47: Whisker Statistics from the Control Sn Side

Sn Thickness (Å)	Whisker Density (cm^{-2})	Average Whisker Length (μm)
350	11658	5.4
700	15981	6.3
1500	13754	5.9
3100	15719	4.5

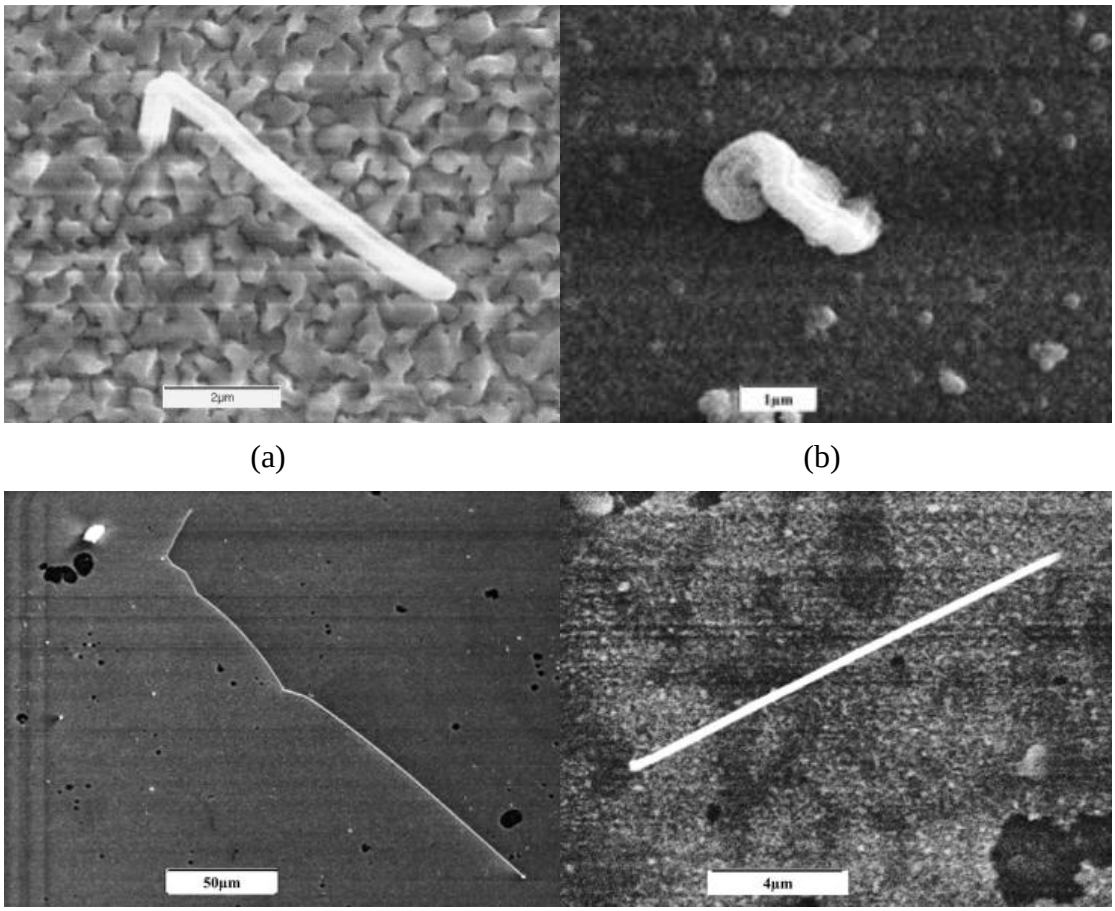

(a) (b)

(c) (d)

Figure 86: Whisker production on the control, uncapped, Sn film side (a) 1500 Å Ni film; (b) 1400 Å Cr film; (c) 875 Å Au film; (d) 1360 Å Pt film.

Whisker penetration through the cap films (Table 48) shows that after ~ 1 month of incubation all three Au cap films have been penetrated. The thinnest 250 Å Cr film has also been penetrated. All other cap films suppressed whisker growth up to this time. After ~ 2 months of incubation, however, the remainder of the Cr films showed penetration, while all Pt and Ni films have completely inhibited whisker penetration. At ~ 100 days of incubation the thinnest, 350 Å Ni cap layer has been penetrated by a single, 182 µm long whisker. The rest of the Ni films and all of the Pt films continue to block all whisker penetration at 100 days. The thickest, 3000 Å Au film was penetrated by one

whisker that grew within the first month of incubation, shown in Figure 87(a). The Ni cap films, which were incubated for an extended period (up to 510 days), have continued to block all whiskers, except for the lone penetrating whisker through the 350Å Ni cap film which has now broken from the surface, seen in Figure 87(b).

Table 48: Whisker Penetration Through Cap Films over Time

Capping Metal	**Film Thickness (Å)**	**Whisker Penetration**			
		1 Months	**2 Months**	**100 Days**	**510 Days**
Au	875	Yes	-	-	
	1750	Yes	-	-	
	3000	Yes	-	-	
Cr	250	Yes	-	-	
	700	No	Yes	-	
	1400	No	Yes	-	
Pt	325	No	No	No	
	685	No	No	No	
	1360	No	No	No	
Ni	350	No	No	Yes	-
	700	No	No	No	No
	1500	No	No	No	No
	3100	No	No	No	No

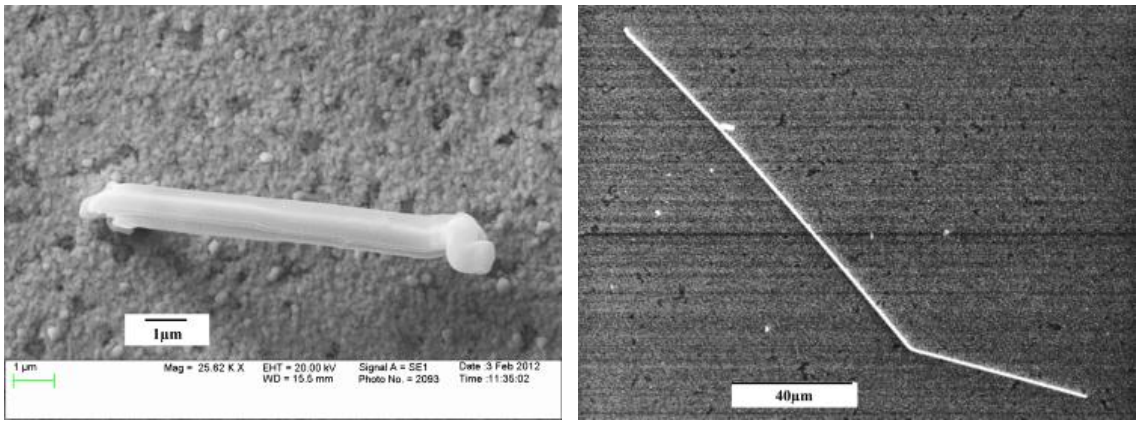

(a) (b)

Figure 87: SEM whisker images of the only Sn whisker that penetrated the (a) 3000 Å Au film and the (b) 350 Å Ni film.

Figure 88 has images of whiskers penetrating some of the other cap films. High resolution imaging of the free end of some of the penetrating whiskers (Figure 89) shows what appears to be a piece of the cap film being carried up on the whisker end during the penetration event, implying a "metal punching" process for the penetration mechanism. "Punched through" metal caps at the end of penetrating whisker tips has also been observed by Reinbold, Chason, et al. [123], shown in Figure 90. The small number of available metal penetration photographs implies that whiskers punch through the metal cap and suggests that a whisker must overcome the shear strength of the capping metal.

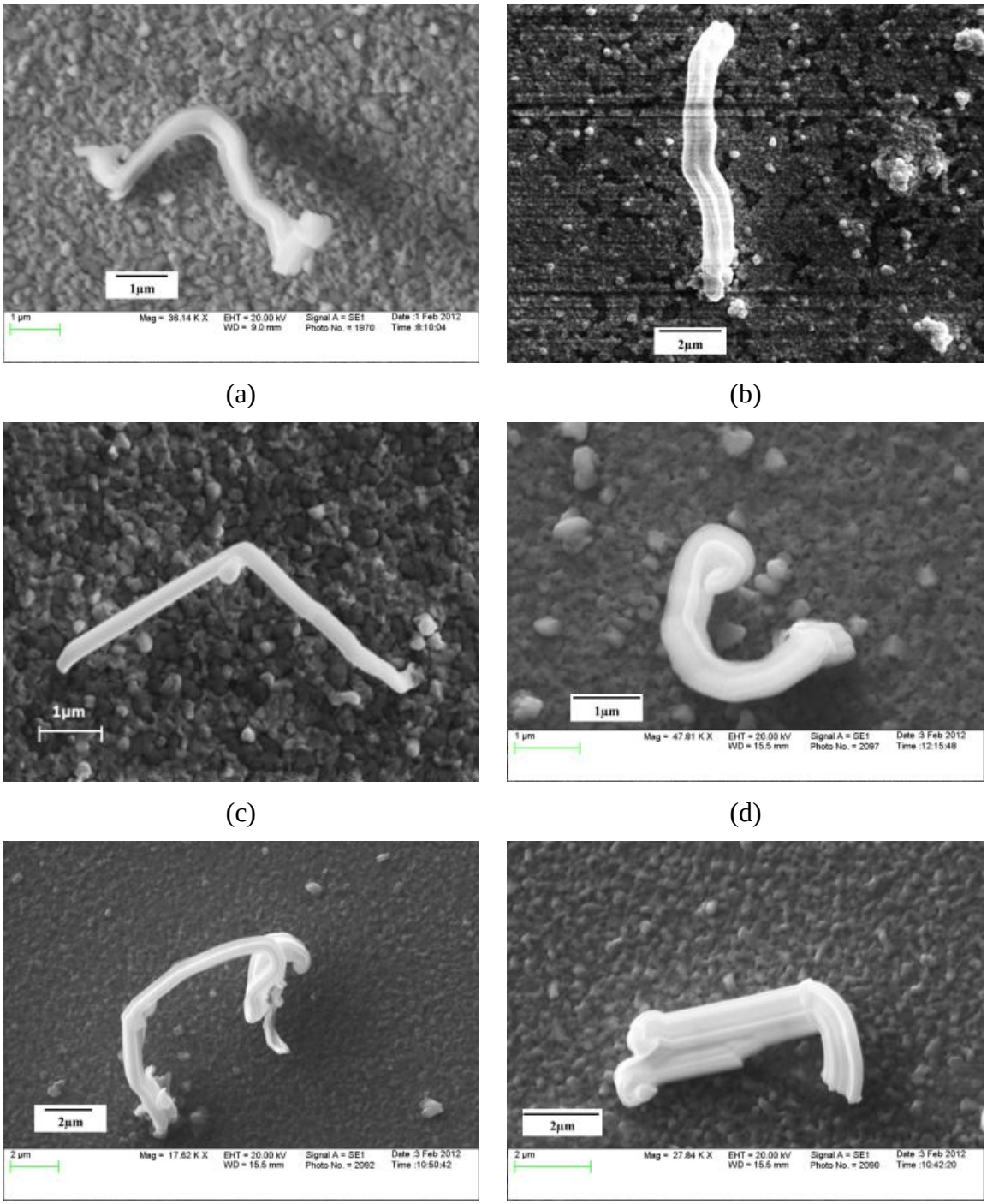

(a) (b)

(c) (d)

(e) (f)

Figure 88: SEM images of representative whiskers penetrating (a) 875 Å Au film; (b) 1750 Å Au film; (c) 875 Å Au film; (d) 250 Å Cr film; (e) 700 Å Cr film; and (f) 700 Å Cr film.

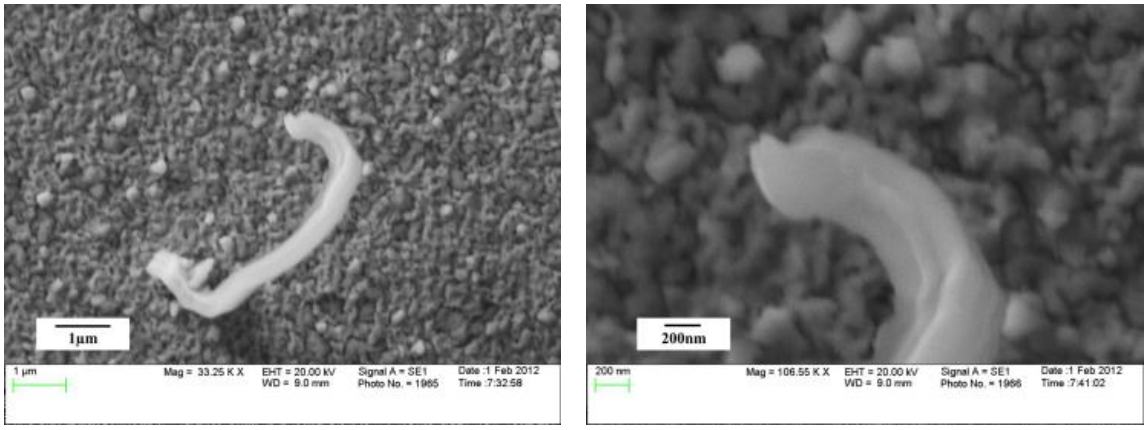

(a)

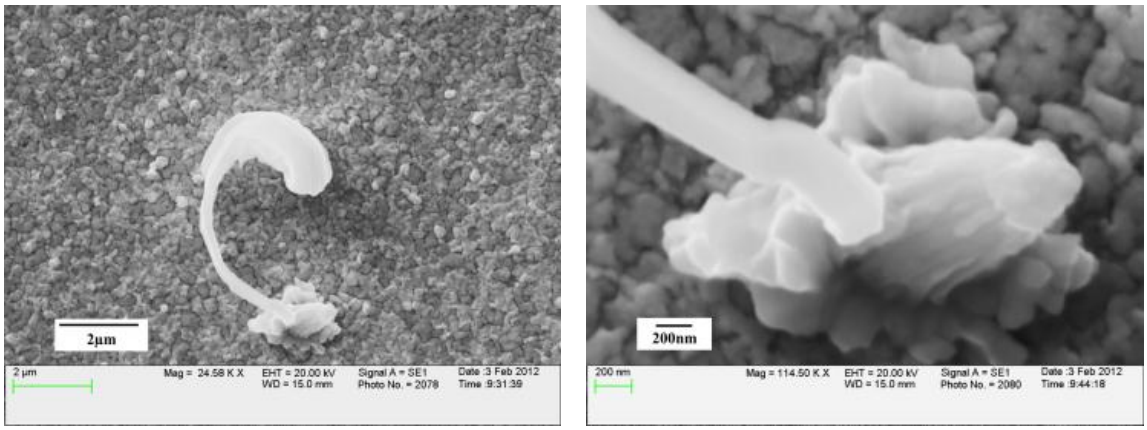

(b)

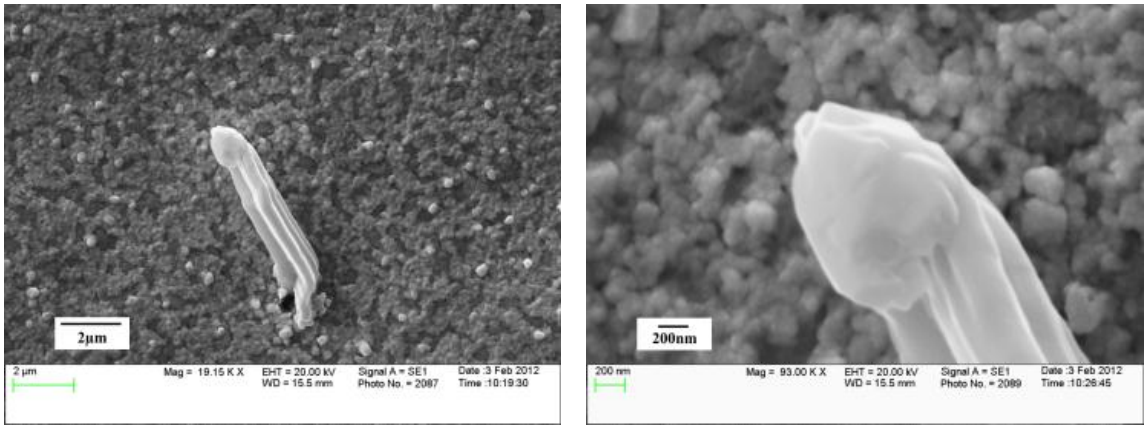

(c)

Figure 89: SEM images of penetrating whisker tips from: (a) 875 Å film; (b) 875 Å film; and (c) 1750 Å film.

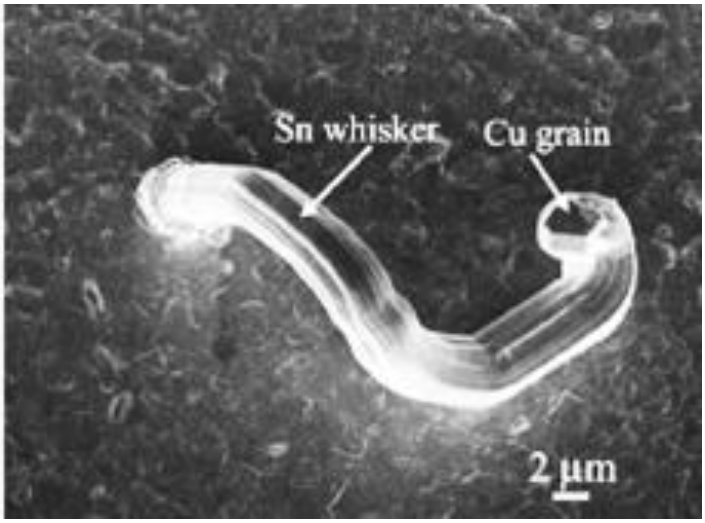

Figure 90: SEM image of Cu cap carried up atop a penetrating Sn whisker. From Reinbold, et al. [123].

The pressure P needed against a (circular) area of radius r to punch through a metal cap layer of thickness t having shear strength τ_s is readily calculated as:

$$P = 2t\,\tau_s/r$$

The puncture pressure is linearly related to the shear strength and thickness of the cap layer. For the same cap thickness and whisker radius, cap metals with larger shear strengths offer more resistance to whisker penetration. Table 49 lists a number of physical and mechanical properties of common cap metals. The shear modulus of the cap metal best fits the trends observed in the ability of various metal caps to prevent whisker penetration. The exception is Cr, which has a large shear strength, but our data shows that it is readily penetrated by Sn whiskers.

Table 49: Physical and Mechanical Properties of Metal Cap Films*

Attribute	Cr	Ni	Pt	Cu	Pd	Au	Pb
Brinell Hardness[2] (MPa)	1120	700	392	874	37.3	2450	38.3
Shear Modulus[2] (GPa)	115	76	61	48	44	27	5.6
Shear Strength (GPa)	Shear strength values are difficult to measure. It is often presumed that the shear strength depends linearly on the shear modulus, e.g., in many studies of pure metals, $\tau_s=G_s/2\pi$ where G_s= shear modulus.						
UTS[2] (MPa)	83	140-195	224	210	180-215	100	12

* Key: Impenetrable Caps: Ni, Pt, Pd; Penetrable Caps: Cr, Cu, Pb; Debatable: Au
[2] Values from Mathematica's Element Data function.

This simple mechanical analysis is complicated by several factors. The chief shortcoming is that the shear strength values reported in Table 49 are measured for pure forms of the cap metals, under the assumption that diffusion between substrate and film is absent and/or no intermetallic compounds form. This is clearly not the case for the metal caps investigated here. RBS and AES show substantial diffusion of the underlying Sn into the metal caps, even at room temperature. This means that τ_s will be different from the pure elemental values and, in most cases, a more accurate analysis requires the shear strength of intermetallic compound caps, not pure elemental caps. However, there are few experimental measurements of the shear strength of either intermetallic compounds or metals containing second element diffusion profiles.

The RBS/AES diffusion results are displayed in Table 50 in a simple yes/no format. As a technique, RBS yields a nondestructive depth profile of materials by measuring the backscattered energies of incident 2MeV He^+ ions from target elements in the film stack. By comparison of RBS spectrum taken immediately after deposition to

after incubation, intermixing of Sn and cap metal over time is observed for many cases. For example, after ~3 months, Sn mixes into all Cr and Au films (except for the 3000 Å Au film) and the thinnest Pt (325 Å) and Ni (350 Å) films. For the case of Ni, Sn mixing is found in all film thicknesses after ~ 1.3 years of incubation.

Table 50: Sn/Cap Metal Mixing vs.Time

Capping Metal	**Film Thickness (Å)**	**Sn/Cap Film Mixing**		
		2 Months	**3 Months**	**16 Months**
Au	875		Yes	
	1750		Yes	
	3000		No	
Cr	250		Yes	
	700		Yes	
	1400		Yes	
Pt	325		Yes	
	685		No	
	1360		No	
Ni	350	Yes		Yes
	700	No		Yes
	1500	No		Yes
	3100	No		Yes

Figure 91 shows Auger elemental compositions with depth for some of the capping films. The trend of each element vs. depth into the film is the significant feature rather than the accuracy of the compositions, which is only ~ 20% for Auger spectroscopy. Diffusion between Sn and cap films is observed in the thinnest Au, Cr and Pt cap films studied, which agrees with RBS. Generally speaking, the Au and Pt films

are very clean with low amounts (< 5 at %) of O and C, owing to the purity of the Sn sputter target and the cleanliness of our turbo-pumped magnetron sputtering system. In contrast, the Cr film contains a comparatively large amount (~ 10-20 at %) of incorporated O. Since the metal depositions were all carried out at the same base pressure, using the same procedural steps and sputtering system, the incorporated oxygen most likely originates from the partial pressure of oxygen-containing background gases in the sputtering chamber. The oxygen is incorporated into the Cr film (and not the other films) due to the large, negative Gibbs free energy of Cr oxide formation [106]. The existence of a substantially *oxidized* Cr film may explain why Cr cap films exhibit whisker penetration despite having large shear strengths.

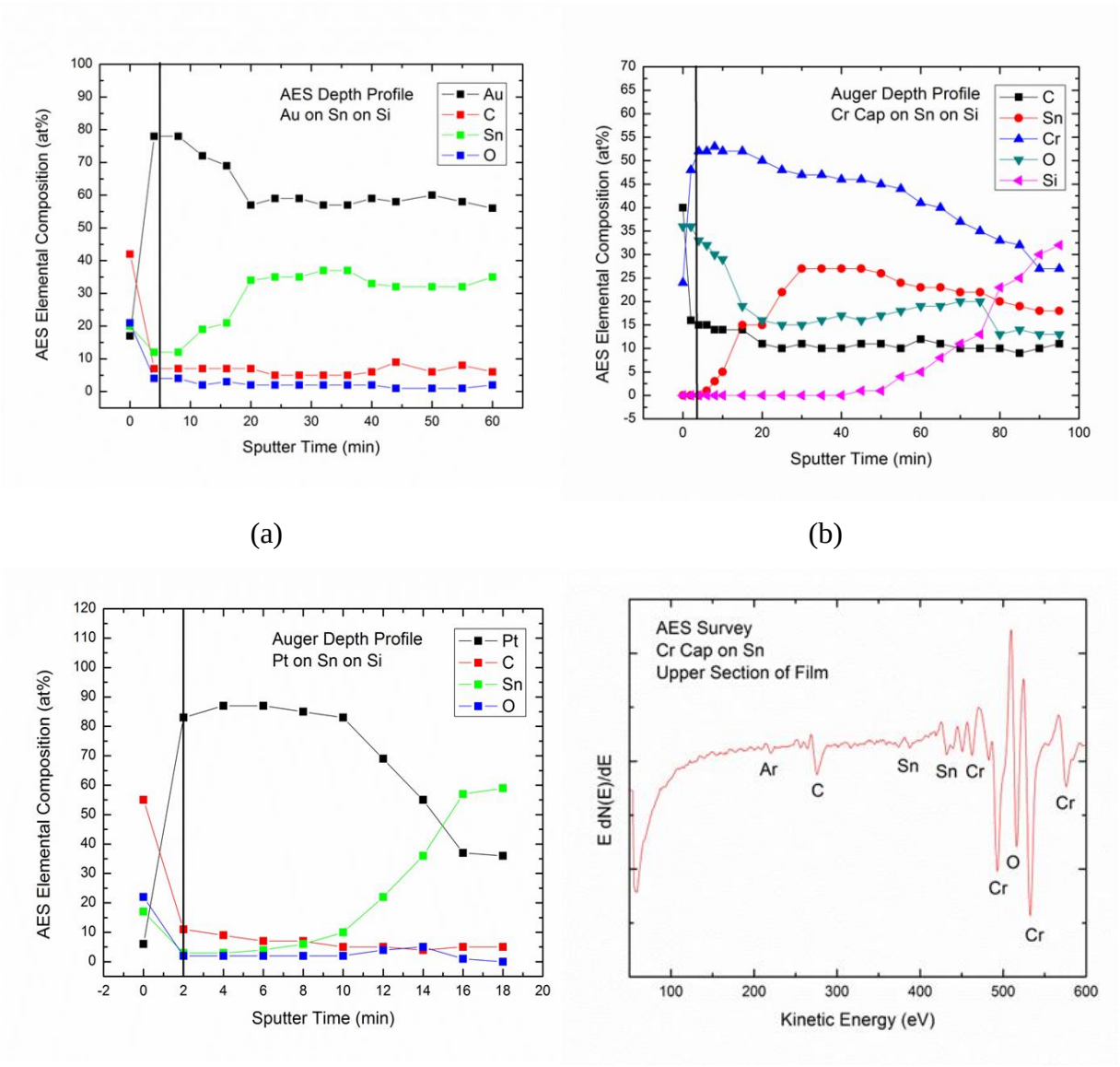

Figure 91: AES elemental composition with depth into the capping layers for the cases (a) 875 Å Au film; (b) 250 Å Cr film; (c) 325 Å Pt film; and (d) AES survey spectra from upper section of 250 Å Cr film, showing the large O(KLL) Auger feature within the film.

In conclusion, for compressively stressed Sn films, Ni and Pt metal cap films successfully blocked all Sn whiskers over long incubation times, with the exception of a lone whisker which penetrated the thinnest (350Å) Ni film. In contrast, all Au films were penetrated after ~ 1 month and all Cr films were penetrated after ~ 2 months of incubation.

Penetrating whiskers which carry up a fractured piece of the metal cap layer during the puncture process helps to explain why only certain metal caps block whiskers. Cap metals with high shear moduli are likely to block whiskers since cap penetration appears to be a metal punching process. Shear modulus values for the pure elemental cap films approximately follows the trend for whisker prevention metals, with the exception of Cr. The true situation is more complex owing to the formation of intermetallic compounds in the cap films and/or diffusion of Sn into the cap.

Our observation of Au penetration by Sn whiskers differs substantially from Kim et al. [121] of Osaka University, who reported that a 50 nm Au film prevented whisker growth for five years. On the other hand, our results agree with Kim in the case of Ni caps – both groups have found Ni to be essentially impenetrable over months and years. This suggests that Ni caps and the selective hard Ni cap method of Landman, Davy, and Fritz [122] offers a potential method of whisker prevention.

RBS and AES depth profiling show that most of the cap films react with the underlying Sn at room temperature over time. After ~ 3 months of incubation, diffusion between the cap/Sn films was found in all Au and Cr samples except the thicker, 3000 Å Au film. In addition, a significant amount of incorporated O was observed in Cr cap films due to the low and negative Gibbs free energy of formation of Cr oxides. Only the

thinnest, 325 Å Pt and 350 Å Ni films experienced any cap/Sn film mixing at 3 months of incubation. Sn mixing in all Ni films was detected after an extended incubation period of ~16 months. Accurate measurements of shear moduli for the case of intermetallic compounds and further studies of film diffusion at room temperature are necessary for additional insight on why only a few cap metals prevent whisker penetration.

CHAPTER 5

CONCLUSIONS

"The distance is nothing; it is only the first step that is difficult."

-Madame Marie Du Deffand

Summary of Results

This research was designed to clarify and control the mechanisms that govern whisker formation. While tin whisker growth is believed to be largely mechanical, there is currently no general agreement on the mechanism governing the growth of tin whiskers. In whiskering, multiple material and processing variables interact to create whiskers, which makes it difficult to develop a comprehensive picture of whisker growth. By studying whisker production through controlled laboratory experiments a more optimum model system can be designed and utilized. One of our goals was to generate a broad experimental whisker database to contribute to evolving efforts that describe whiskering, by studying several important factors involved with whisker growth and clarifying some of the key mechanisms.

Many previous investigations of whiskers involve electroplated thin film systems on brass or copper which, although complying with industry practice, introduce several uncontrolled variables into the whiskering event. Also, archival, industrial, and/or anecdotal specimens have very unpredictable incubation periods (ranging from days to years). All experiments conducted here have used a reliable method of growing whiskers in a reasonable (weeks) time by using magnetron sputtering techniques rather than electrochemical deposition. By depositing films with magnetron sputtering we produced

tailor-made films with known "dialed-in" intrinsic compressive film stress. Since deposition is conducted in vacuum, many of the uncontrolled variables that come into play when electroplating are eliminated. In this manner we have studied several important factors that are known to govern whisker growth and come to these conclusions:

1) Since we observe uniform film thicknesses decreases during the whisker growth period and do not observing local Sn depletion immediately surrounding the whisker root (from a variety of Sn film/substrate combinations where IMC's do and do not exist), a reasonable conclusion is that the Sn used to grow whiskers originates from a large range of proximity on the film. Woodruff [74] also reported data using tracer elements and secondary ion mass spectroscopy (SIMS) showing that Sn can migrate over large distances within the film. That we see the Sn pond draining uniformly additionally supports the notion of long-range Sn migration during whisker growth.

2) By studying micron-dimensional patterned Sn deposits, we observe significantly lower whisker numbers than we count on un-patterned (~ 1 cm^2) Sn films deposited under similar stress conditions and incubation times. The very low whisker numbers from the smallest deposited features leads to the notion that a minimum lateral size/volume of Sn may be necessary for optimum whisker growth. Further, we do not observe depletion zones around the whisker roots or within the patterned Sn features, nor do we observe (at least from microscopy images) any gross lateral Sn diffusion between the Sn features. The sluggish whisker growth from small, micron-dimensional patterned Sn deposits implies that large lateral films of tin are optimum for whisker growth.

3) We generally find that, for Sn on unpolished brass, thinner Sn films produce the highest whisker densities (the exception is the thinnest, 375 Å film). On polished brass, thicker Sn films produce higher whisker densities, with an optimum film thickness of 3000 Å. The case of polished brass is different from a wide variety of other whisker growth experiments reported in this thesis, which characteristically show that thinner films produce more whiskers. It is not clear at the moment what is causing this variation, except to note that brass suffers from the complication of the Su-Cu intermetallic compound at the interface which, for the thin films studied here, may be dominating the interfacial mechanics. We also find that polished substrates and thinner films tend to grow the longest whiskers (up to 577 μm long on the thinnest, 375 Å film), while the thickest films grew the shortest whiskers. This is in agreement with Oberndorff et al. [69].

4) Sn whiskers grow readily on thin, sputter-deposited Sn films (1600 Å) on semiconductor and insulator substrates under internal compressive film stress conditions where intermetallic layers are absent. The highest whisker density after 116 days of incubation occurred for the Si and Ge substrates, with over 22X the whisker density of 1500 Å Sn on brass after similar incubation periods . The fact that Sn on semiconductor surfaces grows copious amounts of whiskers is consistent with our earlier work on surface roughness, which showed that atomically smoother surfaces grow more whiskers [80]. Semiconductor surfaces are the smoothest surfaces that can be technologically manufactured. Though Sn on Ag produced significantly higher whisker numbers (the thinner, 1200 Å Sn film on Ag, grew over one million whiskers/cm^2) than on Si or Ge, it is clear that an IMC is not necessary to produce large numbers of whiskers.

5) By "dialing-in" various degrees of intrinsic thin film stress (tensile, none, compressive), it is evident that whisker growth from sputter-deposited Sn films under both compression and tension is possible. While there are questions about how the film stress evolves over time since deposition, the curvature results give some level of confidence that the initial "dialed" up stress states still existed three months later. At that time, the films under compressive and tensile stress produced whiskers (~ 15,000 whiskers/cm^2 and ~ 12,000 whiskers/cm^2 respectively). In contrast, the "unstressed" film had generated only a fraction (~ 4,000 whiskers/cm^2) of the whisker growth seen in compressive and tensile states. The lower whisker numbers on the unstressed film is better understood after verifying that the actual stress in the "unstressed" Sn film had a comparatively low, but nonzero, (tensile) value (9.83×10^8 dyn/cm^2), which was an order of magnitude lower than the stressed films. The stress values calculated using Stoney's equation were in the expected range for Si substrates and in accordance with the desired compressive film state (negative stress value) and tensile film state (positive stress value). While films under compression produced the largest whisker densities, the films under tension grew the longest whiskers (with whiskers reaching 338 μm). Although rare, the literature shows that whiskers can be produced under tensile stress, as seen in studies by Xu et al. [19] and previously in our laboratory [83] using sputtered Sn on brass (where whisker densities increased as the magnitude of the extrinsic tensile and compressive forces increased).

6) Whisker growth can occur on Sn alloyed deposits such as SAC and even SnPb under the right conditions. After over a year of incubation, we finally see whisker growth (albeit, near-zero) from the 1200 Å Sn-37Pb film (524 whiskers/cm^2),

corresponding to only 5 whiskers for every square millimeter of surface. The thinner 750 Å Sn-37Pb film has modest whisker numbers after a year, while SAC has produced over 147,000 whiskers/cm^2. The data highlights the ability of incorporated Pb to suppress whiskers and shows that, under specific stress conditions, both Sn-37Pb and SAC305 will form whiskers. In fact, Chason et al. [89] observed whiskering from electrodeposited Sn-10%Pb alloy films, and found that the stress developed in the SnPb film was much less than that in the pure Sn films, which is in agreement with results of the stress test and whisker statistics observed on the Sn-37Pb film.

7) In oxygen/humidity environments it is established that oxygen and humidity play a significant role on whisker production, but a *surface* oxide layer is not a necessary condition for whisker growth. Pure O_2 exposed samples produced ~ 9X more whiskers than similar thicknesses of Sn on brass incubated at ambient room temperature/humidity (RT/RH) conditions over similar incubation times. However, the average whisker length under O_2 exposure is less than half compared to atmospheric-exposure. Here it is found that the pure O_2 exposed Sn film has a larger fraction (1.5) of SnO/SnO_2 than the atmospheric-exposed sample (0.3). XPS and AES depth profiling found that the oxide thickness from O_2 exposure is similar to the native Sn oxide from RT/RH exposure (thinner than 50 Å after ~ 150 days of incubation). The fact that Sn in the elemental state is observed in the high resolution XPS spectra shows that the Sn oxides formed are thinner than 50 Å for both oxygen exposures. We infer this from the information volume probed by XPS, which is from 0 – 50 Å below the surface. Sn on brass and Si were also exposed to a full range of humidity environments, 33-98% RH. The highest whisker growth rate is for 85% RH, which agrees with previous studies

concerning the effect of humidity on whiskering, where it was found that ~ 85-93% RH produces the higher whisker densities [97]. After ~140 days of incubation, corrosion features/products are observed on all the exposed specimens and, in many cases, whiskers were found protruding from the corroded surface.

To further understand SnOx products and their growth, Sn on Si and bulk Sn was exposed to dry O_2 and H_20 steam at various elevated temperatures, where we conclude that grain size and wet/dry environments make a substantial difference in Sn oxidation. Under wet conditions, oxidation is possible through larger volumes of Sn, regardless of whether the Sn is in bulk or thin film form. Under dry conditions, oxidation does not turn-on until temperatures near the Sn melting point. In either case, one begins to wonder about the true role of oxidation in whiskering, since it is clear from this study that pure oxygen is not getting into the Sn bulk at temperatures near the standard operating temperature of most electronic circuitry. By studying ~ 1000 Å compressively stressed sputtered Au films on Si, Au whisker growth was observed after one month of incubation under both vacuum and air conditions, verified by high resolution AES on the whisker structures. Generating Au whisker growth from films which clearly contain no native and/or surface oxide shows that a surface oxide layer is not a necessary requisite for whisker production.

8) Whisker growth is accelerated by using field-enhanced, high current density methods (by exposing a 1 μm Sn film pattern to 0.2 A of current), where whiskers grow in hours rather than weeks and months. After only 10 hrs of steady 0.2 A current, a small number of whiskers are found on the 0.004 and 0.00267 A/μm^2 sections of the Sn pattern (and on the 0.002 A/μm^2 section after another 10 hrs exposure). After a

total of 115 hrs of current exposure, multiple voids were found in the 0.002 A/μm^2 section along with hillocks in the 0.002 and 0.00267 A/μm^2 sections together with the onset of voids is the 0.004 A/μm^2 section. A noticeable increase in whiskers in the 0.004 A/μm^2 section is also observed. In a similar study of Sn electromigration [112], whiskers are formed after 1 hour at 0.0036 A/μm^2 and after10 hrs at 0.0018 A/μm^2. No whisker growth occurred at current densities < 0.00045 A/μm^2, even after 100 hrs of current stress. S. H. Liu et al. [60] investigated Sn whisker growth in pure Sn due to the electromigration behavior in Sn, where only one whisker grew at 0.00075 A/μm^2 after 20 hrs of current stress. Current densities of 0.0015 A/μm^2 produced multiple whiskers and hillocks. Both works show there is a threshold current density/time for whiskering, which broadly agrees with our study.

9) Ease to implement, POSS spray offers a potentially viable solution to the whisker problem if applied properly. POSS coated on compressively stressed Sn on glass specimens completely blocked whiskers up to 2.3 years of incubation. Over the same incubation time, whiskers grew > 225 μm long on a control specimen without POSS coating.

10) A Ni under layer is a promising whisker mitigation method for sputtered Sn films (2000 and 1000 Å respectively). After ~ 250 days (> 8 months) of incubation, no whisker growth was observed on either brass or Si substrate specimens. In less than half the incubation period, ~ 1600 Å of Sn on Si sputtered under the same conditions produced ~ 38,500 whiskers/cm^2 and ~ 1500 Å of Sn on polished brass grew ~ 1,700 whiskers/cm^2 after 140 days of RT/RH incubation. The general consensus currently seems to be that if the Ni layer is “good” it works effectively as a whisker prevention

method, but if the Ni layer is “bad”; not so fast. What defines a “good” vs. a “bad” deposited film include the uniformity and conformality of the Ni film, film purity, the matte/bright nature of the electrodeposits, plating bath mixture, temperature during deposition, etc. Since all our films were deposited in clean, vacuum (~ 10^{-7} torr) conditions, our deposited films contain low to minimal contamination.

11) Some topside metal films (Ni, Pt) appear to prevent whisker growth while others (Cu, Pb) do not. Ideally, it is desirable to mitigate and/or prevent whisker growth failures before they occur. Here we have shown that whisker prevention is possible by a variety of impenetrable topside hard metal films, which prevent Sn whiskers from penetrating the capping barriers. In particular, Ni (700 Å or thicker) was found to successfully block all Sn whiskers for time periods of greater than one year. Pt films (325-1360 Å) also appear to be successful, preventing whisker penetration for over three months. In contrast, Au (875-3000 Å) and Cr (250-1400 Å) cap films are penetrated by Sn whiskers within a couple of months. The observation of Au penetration by Sn whiskers differs substantially from Kim et al. [121], who reported that a 50 nm Au film prevented whisker growth for five years. On the other hand, our results agree with Kim in the case of Ni caps – both groups have found Ni to be essentially impenetrable over months and years.

112) Penetrating whiskers have been observed to carry up a fractured piece of the metal cap layer during the puncture process, which helps explain why only certain metal caps block whiskers while others do not. Cap metals with high shear moduli are likely to block whiskers since cap penetration appears to be a metal punching process. Shear modulus values for the pure elemental cap films approximately follows the trend

for whisker prevention by metals, with the exception of Cr, which oxidizes considerably during thin film formation. The true situation is more complex than this simple mechanical picture, however, owing to the formation of intermetallic compounds and/or diffusion between the Sn and cap film layers.

Continuing Studies

As periodically mentioned throughout this work, there is still much to study and contribute further in the understanding of Sn whiskers and the mechanisms that govern whisker growth. From this work, some continuing investigations to consider include:

1) An additional stress measurement study, periodically monitoring the stress evolution in time, through stylus profilometry, during whisker growth. By initially depositing Sn films under compressive, tensile, and "no stress" states, followed by immediate film stress measurements, along with periodic whisker statistics count and stress measurements in time, the film's stress can be monitored for any change due to stress relaxation during whisker production. In this manner, the initial stress states due to film deposition can also be verified and observed during incubation.

2) The role of Sn oxide growth in whiskering is still ambiguous. Understanding the details of Sn oxidation will also be a fruitful line of inquiry for the next thesis student. There is a requirement for both high and low lateral resolution techniques to identify SnO and SnO_2 in whisker systems. By studying Sn oxides under a wider base of temperatures (including near standard operating conditions) through wet and dry oxidation) and observing Sn oxide products, compositions and oxide thicknesses

(by AES, XPS, RBS, EDX and Raman spectroscopy) a better understanding of the role of oxides can be accomplished.

3) As a corollary to the investigation of oxygen and oxide effects on whisker growth, it would also useful to investigate hydrogen effects since Sn produces hydroxides as well. Since hydrogen is difficult to detect by most analytical methods, this could be done by Sn film deposition, followed by hydrogen bombardment onto one Sn film (test) but not the other (control) and comparing the produced whisker statistics as a result.

4) Whiskering during electromigration was found to offer several advantages including a simple test vehicle by which to produce whiskers, direct observation of film migration, and accelerated whisker growth (whiskering within hours compared to weeks and months) in a controlled manner. Being able to produce whisker growth in such short periods of time allows for a simple, fast growing whisker model, which can be repeated with a variety of metals, substrates and current driving densities for future studies.

5) Many studies imply that Sn whisker growth can be affected by impurities introduced during deposition and different environments. One largely investigated "impurity" is oxygen, since Sn oxidizes readily in air. However, whisker growth has also occurred out in space where there is vacuum (as the case for the HS601 satellites [124]). Since Sn is fairly mobile at room temperatures, it would be interesting to study how whisker growth may be effected by energetic radiated particles. Can alpha, beta and/or gamma particles influence whisker production and if so, how significant are these effects? Also, since it was shown using Sn/Si that whiskers can be grown in a matter of days when exposed to an electric field, what about magnetic fields (steady and/or alternating)?

6) It is further desirable to explore other portions of the structure zone scheme for sputtered films by depositing films at various temperatures and stress conditions. The temperature conditions are known to alter the microstructure of the deposited films, which produces a suite of films with distinct microstructural character. In this fashion, Sn film microstructure can be investigated (using RBS, AES, XPS and SEM) for its impact on whisker growth.

7) As important as the understanding of whisker growth mechanisms is, it is ideal to find a way to prevent whisker growth in our electronic systems. It has been shown that a capping metal is a promising method to preventing whisker growth, but to know which metals would make a good whisker prevention capping film, a better understanding of the physical material properties of IMCs need to be accomplished. Since the effectiveness of cap metals in whisker penetration appears to depend on the shear moduli of the capping film, accurate measurements of shear moduli for the case of intermetallic compounds and further studies of film diffusion at room temperature are necessary for additional insight on why only a few cap metals prevent whisker penetration.

References

1 H. L. Cobb, *Cadmium Whiskers*, Monthly Rev. Am. Electroplaters Soc. 33, No. 28 (1946) 28-30.

2 K. G. Compton, A. Mendizza, and S. M. Arnold, *Filamentary Growths on Metal Surfaces—Whiskers*, Corrosion 7, No. 10 (1951) 327-334.

3 S. M. Arnold, *The Growth of Metal Whiskers on Electrical Components*, Proc. IEEE Electronic Components Technology Conf. (1959) 75-82.

4 C. H. Pitt and R. G. Henning, *Pressure-Induced Growth of Metal Whiskers*, J. Appl. Phys. 35 (1964) 459-460.

5 S. C. Britton, *Spontaneous Growth of Whiskers on Tin Coatings: 20 Years of Observation*, Trans. Inst. Metal Finishing 52 (1974) 95-102.

6 B. D. Dunn, *Metallurgy and Reliability in Spacecraft Electronics*, Metals and Materials 34 (1975) 32-40.

7 B. D. Dunn, *Whisker Formation on Electronic Materials*, Circuit World 2, No. 4 (1976) 32-40.

8 B. D. Nordwall, *Air Force Links Radar Problems to Growth of Tin Whiskers*, Aviation Week & Space Technology (1986) 65-68.

9 J. Capitano and J. Devaney, *Reliability Improvement by Removing Electrical Interrupts in Equipment Which Result in Retest--OK, Can't Duplicate, No Defect Found*, Proc. National Aerospace and Electronics Conf. (NAECON) (1986) 1110-1114.

10 L. Corbid, *Constraints on the Use of Tin Plate in Miniature Electronic Packages*, Proc. 3rd Int. Electronics Conf., SAMPE (1989) 773-778.

11 K. Cunningham and M. Donahue, *Tin Whiskers: Mechanism of Growth and Prevention*, Proc. 4th Int. Electronics Conf., SAMPE (1990) 569-575.

12 R. Diehl, *Significant Characteristics of Tin and Tin-Lead Contact Electrodeposits for Electronic Connectors*, Metal Finishing (1993) 37-42.

13 M. Ishii, T. Kataoka, and H. Kruihara, *Whisker Problem in Ultra-Fine Pitch Circuits*, Proc. 12th Eur. Microelectronics and Packaging Conf. (1999) 379-385.

14 General Electric Service Bulletin. Document no. MOD10 SB-100.03.27, (2000); http://www.geindustrial.com/pm/support/dls/dlssb01.pdf

15 C. Stevens, *Relay Failures Induced by the Growth of Tin Whiskers: A Case Study*, Proc. 38th Ann. Spring Reliability Symposium, IEEE Boston Chapter (2001) 1-6.

16 J. Khuri, *Agency Action Notice*, Government-Industry Data Exchange Program (GIDEP), (2002).

17 National Measurement Office (NMO); http://www.bis.gov.uk/nmo/enforcement.

18 M. Warwick, *Implementing Lead Free Soldering - European Consortium Research*, SMTA, J. Surf. Mount Tech. 12, Issue 4 (1999), 1-12.

19 C. Xu, Y. Zhang, C. Fan, and J. A. Abys, *Understanding Whisker Phenomenon, The Driving Force for Whisker Formation,* Circuit Tree (2002) 94-104.

20 J. H. Richardson and B. R. Lasley, *Tin Whisker Initiated Vacuum Metal Arcing in Spacecraft Electronics*, Government Microcircuit Applications Conference, XVIII (1992) 119-122.

21 J. Brusse, QSS Group, Inc @ NASA Goddard, *A Discussion of the Significance of Metal Whisker Formation to the High Reliability Community* (2003); *http://nepp.nasa.gov/whisker/reference/tech_papers/brusse2003-metal-whisker-discussion.pdf*

22 G. T. Galyon, C. Xu, S. Lal, B. Notohardjono, A. Frye, ECTC2005 iNEMI Tin Whisker Modeling Committee, iNEMI Tin Whisker Workshop, IEEE Elec. Comp. & Tech. Conf., Lake Buena Vista, FL, (2005).

23 B. Z. Lee and D. N. Lee, *Spontaneous Growth Mechanism of Tin Whiskers*, Acta Metallurgica 46, No. 10 (1998) 3701-3714.

24 S. Madra, *Thermo-Mechanical Characterization of Lead-Free Tin Plating: X-ray Diffraction Measurements and Correlation with Analytical and Numerical Models*, IPC/JEDEC Meeting, Frankfurt, Germany (2003) 115-120.

25 J. Smetana and iNEMI Tin Whisker User Group, *iNEMI Recommendations on Lead-Free Finishes for Components Used in High-Reliability Products*, IPC/APEX (2006).

26 W. J. Boettinger, C. E. Johnson, L. A. Bendersky, K. W. Moon, M. E. Williams, G. R. Stafford, *Whisker & Hillock Formation on Sn, Sn-Cu and Sn-Pb Electrodeposits,* Acta Met. 53 (2005) 5033-5050.

27 P. Harris, *The Growth of Tin Whiskers*, International Tin Research Institute Publication, 734 (1994) 1-19.

28 J. H. Zhao, P. Su, M. Ding, S. Chopin, and P. S. Ho, *Microstructure-Based Stress Modeling of Tin Whisker Growth*, IEEE Transactions on Electronics Packaging Manufacturing, 29 (2006) 265-273.

29 W. J. Choi, G. Galyon, K. N. Tu, and T. Y. Lee, *The Structure and Kinetics of Tin-Whisker Formation and Growth on High Tin Content Finishes*, Handbook of Lead-Free Solder Technology for Microelectronic Assemblies, Chapter 21 (2004).

30 JEDIC/IPC Joint Publication No. 002

31 P. T. Vianco and J. A. Rejent, *Dynamic Recrystallization (DRX) as the Mechanism for Sn Whisker Development. Part I: A Model*, Journal of Electronic Materials, 38 (2009) 1815-1825.

32 N. Hannay, W. Kaiser, and C. Thurmond, *The Solid State*, Annu. Rev. Phys. Chem. 11 (1960) 407-426.

33 I. Boguslavsky and P. Bush, *Recrystallization Principles Applied to Whisker Growth in Tin*, Proc. APEX Conf., Anaheim, CA (2003) S12-4-1 – S12-4-10.

34 A. T. Wu and Y. C. Ding, *The Suppression of Tin Whisker Growth by the Coating of Tin Oxide Nano Particles and Surface Treatment*, Microelectronics Reliability, 49 (2009) 318-322.

35 J. Smetana, *Theory of Tin Whisker Growth: "The End Game"*, IEEE Transactions on Electronics Packaging Manufacturing 30, No. 1 (2007) 11-22.

36 S. W. Han, K. S. Kim, C. H. Yu, M. Osterman and M. Pecht, *Observations of the Spontaneous Growth of Tin Whiskers in Various Reliability Conditions*, IEEE Electronic Components and Technology Conference (2008) 1484-1490.

37 K. Suganuma, A. Baated, K. S. Kim, K. Hamasaki, N. Nemoto, T. Nakagawa, and T. Yamada, *Sn Whisker Growth During Thermal Cycling*, Acta materialia 59 (2011) 7255-7267.

38 K. N. Tu, *Electronic Thin-Film Reliability*, Cambridge University Press, New York (2011).

39 K. W. Moon, C. E. Johnson, M. E. Williams, O. Kongstein, G. R. Stafford, C. A. Handwerker, and W. J. Boettinger, *Observed Correlation of Sn Oxide Film to Sn Whisker Growth in Sn-Cu Electrodeposit for Pb-Free Solders*, J. Elect. Mat. 34 (2005) L31-L33.

40 P. Oberndorff, J. Klerk, M. Dittes, and P. Crema, *Whisker Formation on Sn-Plated Components*, in Proc. Conf. Electron. Goes Green 2004+, Berlin, Germany, Sep. 6-8 (2004) 347-352.

41 R. J. Fields, S. R. Low III, and G. K. Lucey Jr. In: M. J Cieslak, J. H. Perepezko, S. Kang, M. E. Glicksman, editors. *The Metal Science of Joining*, Warrendale, PA: The Minerals, Metals & Materials Society (1992) 165-173.

42 N. Saunders and A. P. Miodownik, *The Cu-Sn (Copper-Tin) System*, Journal of Phase Equilibria, 11 (1990) 278-278.

43 Y. Zhang, C. Fan, C. Xu, O. Khaselev, and J. A. Abys, *Tin Whisker Growth – Substrate Effect Understanding CTE Mismatch and IMC Formation*, CircuiTree 7 (2004) 70-82.

44 J. A. Brusse, *Tin Whisker Observations on Pure Tin-plated Ceramic Chip Capacitors*, AESF SUR/FIN Proceedings, Orland (2002) 45-61.

45 J. A. Brusse, G.. Ewell, and J. P. Siplon, *Tin Whiskers: Attributes and Mitigation*, Proceedings of 22nd Capacitor and Resistor Technology Symposium, March 25-29 (2002) 67-80.

46 M. Dittes, P. Oberndorff and L. Petit, *Tin Whisker Formation – Results, Test Methods and Countermeasures*, Proc. 53rd Electronic Components & Technology Conference (2003), 822-826.

47 P. Oberndorff, M. Dittes, L. Petit, *Intermetallic Formation in Relation to Tin Whiskers*, Proc. Of the IPC/Soldertec International Conference "Towards Implementation of the RHS Directive," Brussels, Belgium (2003) 170-178.

48 P. Oberndorff, M. Dittes, P. Crema, *Whisker Formation on Sn Plating*, Proc. IPC/JEDEC 5th International Conference on Pb-Free Electronic Assemblies and Components, San Jose (2004) 34-34.

49 V. D. Glazunova and N. T. Kurdryavtsev, *An Investigation of the Conditions of Spontaneous Growth of Filiform Crystals on Electrolytic Coatings*, translated from Zhurnal Prikladnoi Khimii 36, 3 (1963) 543-550.

50 J. Osenbach, R. Shook, B. Vaccaro, B. Pottieger, A. Amin, P. Ruengsinsub, and K. Hooghan, *The Effects of Board Assembly Reflow Processing on Sn Whisker Formation*, Proc. IPC/JEDEC Pb-Free Conference (2004).

51 B. Rickett, G. Flowers, S. Gale, and J. Suhling, *Potential for Whisker Formation in Lead-Free Electroplated Connector Finishes*, Proceedings SMTA International Conference, Chicago, IL (2004) 707-716.

52 P. Su, J. Howell, and S. Chopin, *A Statistical Study of Sn Whisker Population and Growth during Elevated Temperature and Humidity Storage Tests*, IEEE Trans. Electronics Packaging Manufacturing, 55th ECTC Workshop 29 (2006) 246.

53 P. Oberndorff, M. Dittes, P. Crema, P. Su, and E. Yu, *Humidity Effects on Sn Whisker Formation*, IEEE Trans.Elect. Packag. Manuf. 29 (2006), 239-245.

54 P. Oberndorff, M. Dittes, P. Crema, and S. Chopin, *Whisker Formation on Matte Sn Influencing of High Humidity*, in Proc. 55th Electronic Components and Technology Conf. 1 (2005) 429-433.

55 M. W. Barsoum, E. N. Hoffman, R. D. Doherty, S. Gupta and A. Zavaliangos, *Driving Force and Mechanism for Spontaneous Metal Whisker Formation*, Phys. Rev. Lett. 93, 20 (2004) 206104-1 - 206104-4.

56 P. Su, M. Ding, and S. Chopin, *Effects of Reflow on the Microstructure and Whisker Growth Propensity of Sn Finish*, Proceedings of the 55th ECTC (2006) 434-440.

57 J. Osenbach, R. Shook, B. Vaccaro, B. Potteiger, A. Amin, and P. Ruengsinub, *Lead Free Packaging and Sn-Whiskers*, 54th Electronic Components and Technology Conference (2004) 1314-1324.

58 B. Hilty, N. Corman, F. Herrmann, *Electrostatic Fields and Current Flow Impact on Whisker Growth*, IEEE Transactions on Electronic Packaging Manufacturing 28, 1 (2005) 75-84.

59 M. Sampson, H. Leidecker, J. Kadesch, and J. Brusse, *Demonstration of the Bending of a Tin Whisker Caused by Electrostatic Attraction*, GSFC experiment #4 (2005). http://nepp.nasa.gov/whisker/experiment/exp4/index.html

60 S. H. Liu, C. Chen, P. C. Liu, and T. Chou, *Tin Whisker Growth Driven by Electrical Currents*, J. Appl. Phys. 95, 12 (2004) 7742-7747.

61 iNEMI Tin Whisker User Group, *Tin Whisker Acceptance Test Requirements*, (2004).

62 NASA, *Basic Info on Tin Whiskers*, http://nepp.nasa.gov/whisker/background/

63 R. M. Fisher, L. S. Darken, and K. G. Carroll, *Accelerated Growth of Tin Whiskers*, Acta Metallurgica. 2, No. 3 (1954) 368-372.

64 G. T. Galyon, *Annotated Tin Whisker Bibliography and Anthology*, IEEE Transactions on Electronics Packaging Manufacturing, 28, No. 1 (2005) 94-122.

65 J. A. Thornton and D. W. Hoffman, *Stress-Related Effects in Thin Films*, Thin Solid Films 171 (1989) 5.

66 JESD22-A121A, *Measuring Whisker Growth on Tin and Tin Alloy Surface Finishes* (2008).

67 L. Panashchenko, *Evaluation of Environmental Tests for Tin Whisker Assessment*, Masters of Science Thesis Defense at University of Maryland (2009).

68 Y. Fukuda, M Osterman, and M. Pecht, *Length Distribution Analysis of Tin Whisker Growth*, IEEE Transactions on Electronics Packaging Manufacturing, 30 (2007).

69 P. Oberndorff, M. Dittes, L. Petit, C.C. Chen, J. Klerk and E.E. de Kluizenaar, *Tin Whiskers on Lead-free Platings*, Semiconductor Technology Symp., Advanced packaging Technology II (2002) 51-55.

70 P. Oberndorff, M. Dittes, P. Crema, *Whisker Testing: Reality or Fiction?*, Proceedings of the IPC/Soldertec 2nd International Conference on Lead Free Electronics, Amsterdam (2004) CD-ROM.

71 Purchased from Goodfellow Cambridge Limited, Ermine Business Park, Huntingdon, PE29 6WR, Units C1 &C2, England.

72 J. A. Thornton and D. W. Hoffman, *Internal Stresses in Titanium, Nickel, Molybdenum, and Tantalum Films Deposited by Cylindrical Magnetron Sputtering*, J. Vac. Sci. Technol. 14, No. 1 (1977) 166.

73 Bozack, M.J. Crandall, E.R. Rodekohr, C.L. Dean, R.N. Flowers, G.T. Suhling, J.C., *High Lateral Resolution Auger Electron Spectroscopic (AES) Measurements on High-Aspect Ratio Sn Whiskers on Brass*, IEEE Transactions on Electronics Packaging Manufacturing 33, Issue 3 (2010) 198-204.

74 T. A. Woodrow, *Tracer Diffusion in Whisker-Prone Tin Platings*, Proceeding of STMA International Conference, Rosemont, IL Sept. 24-28 (2006).

75 Purchased from Ted Pella, Inc., P. O. Box 492477, Redding, CA 96049-2477.

76 Purchased from Electron Microscopy Sciences, 1560 Industry Rd., Box 550 Hatfield, PA 19440.

77 C. Xu, Y.Zhang, C. Fan and J. Abys, *Understanding Whisker Phenomenon – Part II, Competitive Mechanisms*, Proceedings of the APEX Meeting, San Diego (2002).

78 Semiconductors on NSM, http://www.ioffe.ru/SVA/NSM/Semicond/index.html

79 The Engineering ToolBox, http://www.engineeringtoolbox.com/linear-expansion-coefficients-d_95.html

80 C. L. Rodekohr, M. J. Bozack, G. T. Flowers, and J. C. Suhling, *Influence of Substrate Surface Roughness on Sn Whisker Growth*, Proceedings of the 54th IEEE Holm Conference on Electrical Contacts, October, 2008, 245.

81 M. Zecchino and T. Cunningham, *Thin Film Stress Measurement Using Dektak Stylus Profilers*, Veeco Instruments Inc. (2004).

82 T. Chudoba, N. Schwarzer, F. Richter, *Determination of Elastic Properties of Thin Films by Indentation Measurements with a Spherical Indenter*, Surf. Coat. Technol. 127 (2000) 9.

83 C. L. Rodekohr, G. T. Flowers, M. J. Bozack, R. N. Dean, R. L. Jackson, P. Lall, *Influence of Quantifiable Extrinsic Stresses on Tin Whisker Growth*, Proceedings of the ASME International Design Engineering Technical Conferences & Computers and Information in Engineering Conference, IDETC/CIE, San Diego (2009).

84 M. E. Thomas, M. P. Hartnett, J. E. McKay, *The Use of Surface Profilometers for the Measurement of Wafer Curvature*, J. Vac. Sci. Tech. A 6 (1988) 2570.

85 C. A. Handwerker, *Tin Whisker and Surface Defect Formation of Electrolplated Films and Reflowed* Joints, CALCE Symposium on Part Reprocessing, Tin Whisker Mitigation, and Assembly Rework/Repair (2008).

86 P. Bush, SUNY Buffalo from J. Brusse/Perot Systems, *Some Examples of "Whiskers" from Tin-Based Alloys* (2009). http://www.hlinstruments.com/RoHS_articles/Tin%20whiskers%20from%20tin%20alloy%20coatings.pdf

87 SWATCH Petition to EU TAC for RoHS Exemption (2006).

88 N. Asrar, O. Vancauwenberghe, and S. Prangere, *Whiskers from SnAg Eutectic Solder, Tin Whiskers Formation on an Electronic Product: A Case Study*, ASM International (2007).

89 E. Chason, N. Jadhav, W. L. Chan, L Reinbold, and K. S. Kumar, *Whisker formation in Sn and Pb-Sn Coatings: Role of Intermetallic Growth, Stress Evolution, and Plastic Deformation Processes*, App. Phys. Letters, 92 (2008) 171901.

90 H. Leidecker, C. Greenwell, and J. Brusse, *Whiskers of Tin-Lead (Sn-Pb) on REFLOWED Die Attach Solder Used in the Manufacture of a Laser Diode Array*, NASA Goddard Space Flight Center and QSS Group, Inc. (2003). http://nepp.nasa.gov/whisker

91 J. Liang, N. Dariavach, and D. Shangguan, *Tin Whisker Nucleation and Growth on Sn-Pb Eutectic Coating Layer Inside Plated Through Holes With Press-Fit Pins*, IEEE Comp. and Pack. Tech. 31 (2008), 1.

92 W. Zhangz and F. Schwager, *Effects of Lead on Tin Whisker Elimination Efforts Toward Lead-Free and Whisker-Free Electrodeposition of Tin*, J. Electrochem. Soc. 153 (2006) 5.

93 J. W. Osenbach, J. M. DeLucca, B. D. Potteiger, A. Amin, R. L. Shook, and F. A. Baiocchi, *Sn Corrosion and Its Influence on Whisker Growth*, IEEE Trans. Electron. Packag. Manuf., 30 (2007) 23-35.

94 P. Villars and L. D. Calvert, *Pearson's Handbook of Crystallographic Data for Intermetallic Phases*, ASM International, Metals Park, OH (1991).

95 Standard Practice for Maintaining Constant Relative Humidity by Means of Aqueous Solutions, ASTM International, E 104-51 (2002).

96 L. Panashchenko and M. Osterman, *Examination of Nickel Underlayer as a Tin Whisker Mitigator*, 59th ECTC Conference, San Diego (2009) 8.

97 H. L. Reynolds, J. W. Osenbach, G. Henshall, R. D. Parker, and P. Su, *Tin Whisker Test Development – Temperature and Humidity Effects, Part I: Experimental Design, Observations, and Data Collection*, IEEE Tans. Electron. Packaging Manufacturing 33 (2010) 1.

98 K. N. Tu, *Irreversible Processes of Spontaneous Whisker Growth in Bimetallic Cu-Sn Thin Film Reactions*, Phys. Rev. B49, (1994) 2030-2034.

99 C. Y. Chang and R. W. Vook, *The Effect of Surface Aluminum Oxide Films on Thermally Induced Hillock Formation*, Tin Solid Films 228, (1993) 205-209.

100 R. K. Hart, *The Thermal Oxidation of Tin*, Proc. Phys. Soc., 65, PT. 12-B, (1952) 955.

101 N. Jadhav, E. Buchovecky, E. Chason, and A. Bower, *Real-Time SEM/FIB Studies of Whisker Growth and Surface Modification*, J. of Metals 62 (2010) 30-37.

102 W. J. Choi, T. Y. Lee, and K. N. Tu, *Structure and Kinetics of Sn Whisker Growth on Pb-free Solder Finish*, IEEE Electronic Components and Technology Conference (2002) 628-633.

103 Y. Nakadaira, S. Jeong, J. Shim, J. Seo, S. Min, T. Cho, S. Kang, and S. Oh, *Growth of Tin Whiskers for Lead-Free Plated Leadframe Packages in High Humid Environments and During Thermal Cycling*, Microelectronics Reliability 48 (2008) 83-104.

104 S. S. Brenner, *Strength of Gold Whiskers*, J. Appl. Phys. 30 (1959) 226-267.

105 S. S. Brenner, *Tensile Strength of Whiskers*, J. Appl. Phys. 27 (1956) 1484.

106 C. E. Wicks and F. E. Block, *Thermodynamic Properties of 65 Elements – Their Oxides, Halides, Carbides, and Nitrides*, Washington, U.S. Govt. Printing Office (1963).

107 A. Maekawa and F. Okuyama, *Nano and Microcrystallites of Gold Grown by Argon-Ion Bombardment*, Surf. Sci. 481 (2001) L427-L432.

108 A. Teverovsky, *Introducing a New Member to the Family: Gold Whiskers*, Internal Memorandum, NASA Goddard Flight Center, April 2003.

109 C. Y. Liu, C. Chen, and K. N. Tu, *Electromigration in Sn-Pb Solder Strips as a Function of Alloy Composition*, J. Appl. Phys. 88 (2000) 5703.

110 A. Khosla and H. B. Huntington, *Electromigration in Tin Single Crystals*, J. Phys. Chem. Solids, 36, Issue 5 (1975) 395-399.

111 Y. C. Hu, S. W. Wan and C. R. Kao, *Electromigration in Tin Thin Film*, Int'l Symposium on Electronic Materials and Packaging, IEEE Xplore (2002) 463-467.

112 Y. W. Lin, Y. S. Lai, Y. L. Lin, C. T. Tu and C. R. Kao, *Tin Whisker Growth Induced by High Electron Current Density*, J. Elect. Mat. 37 (2008) 17-22.

113 J. S. Kadesch and H. Leidecker, *Effects of Conformal Coat on Tin Whisker Growth*, EEE links, 6, No. 1, 20-22. http:/ / nepp.nasa.gov/ whisker/

114 J. S. Kadesch and J. Brusse, *The Continuing Dangers of Tin Whiskers and Attempts to Control Them with Conformal Coat*, NASA's EEE Links Newsletter (2001).

115 T. A. Woodrow and E. A. Ledbury, *Evaluation of Conformal Coatings as a Tin Whisker Mitigation Strategy*, IPC/JEDEC 8th International Conference on Lead-Free Electronic Components and Assemblies, San Jose, CA, April 18-20 (2005).

116 R. Schetty, *Minimization of Tin whisker Formation for Lead-Free Electronics Finishing*, Circuit World, 27 (2001) 17-20.

117 C. Xu, Y. Zhang, C. Fan, and J. A. Abys, *Whisker Prevention*, APEX, proceedings of the technical conference, S-18-3-1, California (2003).

118 S. C. Hsu, S. J. Wang, and C. Y. Liu, *Effect of Cu content on Interfacial Reactions Between Sn(Cu) Alloys and Ni/Ti Thin-Film Metallization*, J. Electron Mater. 32 (2003) 1214-1221.

119 Q. Sun, *Understanding and Minimization of Tin Whiskers*, in partial fulfillments of requirements for course MatE 234, 800-14-0839 (2003).

120 B. Hampshire and L. Hymes, *Shaving Tin Whiskers*, Circuits Assembly, (2000) 50-53.

121 K. S. Kim, S. S. Kim, S. J. Kim, K. Suganuma, *Prevention of Sn Whisker Formation by Surface Treatment of Sn Plating Part II*, ISIR, Osaka University, Masanobu Tsujimoto, Isamu Yanad, C. Uyemura & Co., Ltd., TMS Annual Meeting (2008).

122 R. J. Landman, G. Davy, and D. D. Fritz, *Whisker-Impenetrable Metal Cap Process for Electronic Assemblies*, Reliability Society Annual Technical Report (2010). (gdavy@ldfcoatings.com)

123 L. Reinbold, N. Jadhav, E. Chason, and K. Sharvan Kumar, *Relation of Sn Whisker Formation to Intermetallic Growth: Results from a Novel Sn-Cu "Bimetal Ledge Specimen",* J. Mater. Res., 24, 12 (2009) 3583-3589.

124 http://www.boeing.com/defense-space/space/bss/hsc_pressreleases/98_08_11_601ok.html